



Michigan Technological University
Create the Future Digital Commons @ Michigan Tech

Dissertations, Master's Theses and Master's
Reports - Open

Dissertations, Master's Theses and Master's
Reports

2012

Evaluation of flood risk in response to climate variability

Casey E. Fritsch
Michigan Technological University

Follow this and additional works at: <https://digitalcommons.mtu.edu/etds>



Part of the [Civil and Environmental Engineering Commons](#)

Copyright 2012 Casey E. Fritsch

Recommended Citation

Fritsch, Casey E., "Evaluation of flood risk in response to climate variability", Master's Thesis, Michigan Technological University, 2012.

<https://doi.org/10.37099/mtu.dc.etds/237>

Follow this and additional works at: <https://digitalcommons.mtu.edu/etds>



Part of the [Civil and Environmental Engineering Commons](#)

EVALUATION OF FLOOD RISK IN RESPONSE TO CLIMATE VARIABILITY

By

Casey E. Fritsch

A THESIS

Submitted in partial fulfillment of the requirements for the degree of

MASTER OF SCIENCE

(Civil Engineering)

MICHIGAN TECHNOLOGICAL UNIVERSITY

2012

Copyright © Casey E. Fritsch 2012

This thesis, "Evaluation of Flood Risk in Response to Climate Variability," is hereby approved in partial fulfillment of the requirements for the Degree of MASTER OF SCIENCE IN CIVIL ENGINEERING.

Department of Civil and Environmental Engineering

Signatures:

Thesis Advisor

Dr. Veronica W. Griffis

Department Chair

Dr. David Hand

Date

TABLE OF CONTENTS

CHAPTER 1 Introduction.....	1
1.1 Research Motivation	2
1.2 Research Objectives.....	12
CHAPTER 2 Identification of Nonstationarity in Hydroclimatic Data Series	13
2.1 Methods for Assessing Nonstationarity	13
2.1.1 Mann-Kendall Trend Test.....	15
2.1.2 Pettit Change-Point Test	16
2.1.3 Hurst's Exponent	18
2.2 Nonstationarity in Annual Maximum Flood Series	19
2.2.1 Data	20
2.2.2 Trends in Magnitude of Annual Maximum Flood Series	21
2.2.3 Change-Points in Magnitude of Annual Maximum Flood Series.....	23
2.2.4 Long-Term Persistence in AMF Series.....	28
2.2.5 Nonstationarity in the Timing of Flood Peaks.....	29
2.3 Nonstationarity in Flood Generating Meteorological Series	31
2.3.1 Trends in Flood Generating Precipitation Series	33

2.3.2 Change-Points in Flood Generating Precipitation Series.....	35
2.3.3 Trends in Flood Generating Temperature Series	37
2.3.4 Change-Points in Flood Generating Temperature Series.....	40
CHAPTER 3 Sources of Nonstationarity in Annual Maximum Flood Series.....	43
3.1 Methods for Evaluating Correlation	43
3.1.1 Pearson’s Correlation.....	44
3.1.2 Kendall’s Tau Correlation.....	45
3.1.3 Spearman’s Rho Correlation.....	47
3.2 Climatic Causes of Nonstationarity	48
3.2.1 Frequency of Annual Maximum Discharge.....	50
3.2.2 Evaluation of Teleconnections with Flood Flows	53
3.2.3 Common Shifts between Flood Flows and Climatic Phases	60
3.3 Meteorological Connections to Flood Peaks	63
3.3.1 Association among Precipitation and AMF Series	64
3.3.2 Association among Temperature and AMF Series	69
3.4 Physical Causes of Nonstationarity	76
CHAPTER 4 Climate Informed Flood Risk Projections	83
4.1 Current Procedures.....	83
4.2 Proposed Modification to Bulletin 17B	88

4.3 Climate Informed Flood Risk Projection.....	90
4.4 Model Limitations and Future Work	96
CHAPTER 5 Conclusions.....	99
REFERENCES	103
APPENDIX A Results of Nonstationarity Tests on Series of Flood Magnitude.....	113
APPENDIX B Trend and Change-Point Results for Timing of Flood Peaks.....	125
APPENDIX C Trend and Change-Point Results for Flood Generating Precipitation Series	129
C.1 Results for Precipitation Series Based on 1/8-Degree Gridded Data.....	130
C.2 Results for Precipitation Series Based on 1/4-Degree Gridded Data.....	135
APPENDIX D Trend and Change-Point Results for Flood Generating Temperature Series	141
D.1 Results for Minimum Temperature Series	142
D.2 Results for Maximum Temperature Series	147
APPENDIX E Correlation Analysis Results Between 10 Year Moving Average of Logs of Flood Flows and Climate Anomalies	153
E.1 AMO Correlation Results.....	154
E.2 MEI Correlation Results.....	164
E.3 NAO Correlation Results	171
E.4 NINO 3.4 Correlation Results	180

E.5 PDO Correlation Results	184
APPENDIX F Correlation Analysis Results Between 10 Year Moving Standard deviation of Logs of Flood Flows and Climate Anomalies	195
F.1 AMO Correlation Results	196
F.2 MEI Correlation Results	206
F.3 NAO Correlation Results.....	212
F.4 NINO 3.4 Correlation Results	219
F.5 PDO Correlation Results	223
APPENDIX G Correlation Analysis Results Between Annual Maximum Flood Series and Flood Generating Hydroclimatic Series.....	233

LIST OF FIGURES

Figure 2.1 Example graph illustrating nonstationarity in an AMF series in the form of a linear trend and an abrupt shift in the mean (USGS Station No. 05340500).....	14
Figure 2.2 Water-resources regions (gray-scale polygons) and major rivers (blue lines) of the continental U.S as defined by the USGS.	20
Figure 2.3 Location of 569 unimpaired USGS streamflow gauging stations within the continental U.S. selected from the HCDN having at minimum a continuous annual maximum flow record from 1940-2005.	21
Figure 2.4 Results of traditional Mann-Kendall trend tests on magnitude of AMF series (neglecting possible autocorrelation). Upright (inverted) triangles represent sites with a positive/increasing (negative/decreasing) trend.	22
Figure 2.5 Results of modified Mann-Kendall trend tests on magnitude of AMF series (accounting for autocorrelation). Upright (inverted) triangles represent sites with a positive/increasing (negative/decreasing) trend.	23
Figure 2.6 Locations of sites with a change-point in the mean annual maximum flood magnitude significant at 5% and 10% levels.	24
Figure 2.7 Time period in which a change-point in the mean annual maximum flood magnitude was identified by the Pettitt test (10% significance level).	25
Figure 2.8 Results of Mann-Kendall trend tests on annual maximum flood subseries before identified change-point in mean flood magnitude.	27
Figure 2.9 Results of Mann-Kendall trend tests on annual maximum flood subseries after identified change-point in mean flood magnitude.	27
Figure 2.10 Magnitude of Hurst exponent for annual maximum flood series in the contiguous U.S. with continuous record lengths of at least 66 years.	28
Figure 2.11 Results of Mann-Kendall trend tests on the day of occurrence of annual maximum flood peaks.	29
Figure 2.12 Locations of sites with a significant change-point in the mean day of occurrence of the annual maximum flood peak.	30

Figure 2.13 Time period of change-points in the mean day of occurrence of flood peaks as identified by the Pettitt test (10% significance level).....	31
Figure 2.14 Locations of 235 streamflow gauging stations used to create flood associated precipitation and temperature series.	32
Figure 2.15 Results of Mann-Kendall trend tests on flood generating precipitation series with 5-day lead time constructed using 1/8-degree gridded data.	35
Figure 2.16 Results of Pettitt tests on flood generating precipitation series with a 5-day lead constructed using 1/8-degree gridded data.....	36
Figure 2.17 Results of Mann-Kendall tests on flood generating maximum temperature series with a 4-day lead time.....	39
Figure 2.18 Results of Mann-Kendall tests on flood generating minimum temperature series with a 4-day lead time.....	39
Figure 2.19 Results of Pettitt tests on flood generating maximum temperature series with a 4-day lead time.....	41
Figure 2.20 Results of Pettitt tests on flood generating minimum temperature series with a 4-day lead time.....	41
Figure 3.1 Location of 14,835 USGS stations with a minimum 12 years of AMF record.	51
Figure 3.2 Most common (mode) month of occurrence of AMF peaks.	51
Figure 3.3 Frequency of occurrence of AMF peaks in identified mode month.....	51
Figure 3.4 Combined frequency of occurrence of AMF peaks in three month seasons (A. Dec-Jan-Feb, B. Mar-Apr-May, C. Jun-July-Aug, D. Sep-Oct-Nov).....	52
Figure 3.5 Locations of sites with significant correlation between 10-year moving average of log-transformed flood flows and 3-month average AMO anomalies with 6-month lead.	55
Figure 3.6 Locations of sites with significant correlation between 10-year moving average of log-transformed flood flows and 3-month average MEI anomalies with 9-month lead.	55

Figure 3.7 Locations of sites with significant correlation between 10-year moving average of log-transformed flood flows and 3-month average NAO anomalies with 3-month lead.	56
Figure 3.8 Locations of sites with significant correlation between 10-year moving average of log-transformed flood flows and 3-month average PDO anomalies with 9-month lead.	56
Figure 3.9 Locations of sites with significant correlation between 10-year moving standard deviation of log-transformed flood flows and 3-month average AMO anomalies with 3-month lead.	58
Figure 3.10 Locations of sites with significant correlation between 10-year moving standard deviation of log-transformed flood flows and 3-month average MEI anomalies with 9-month lead.	58
Figure 3.11 Locations of sites with significant correlation between 10-year moving standard deviation of log-transformed flood flows and 3-month average NAO anomalies with 3-month lead.	59
Figure 3.12 Locations of sites with significant correlation between 10-year moving standard deviation of log-transformed flood flows and 3-month average PDO anomalies with 9-month lead.	59
Figure 3.13 X-day lead time yielding most significant Pearson's correlation coefficient between AMF series and the associated flood generating precipitation series constructed using 1/8-degree gridded data.	65
Figure 3.14 Location of sites with trends in both the AMF series and the best X-day flood generating precipitation series constructed using 1/8-degree gridded data.	66
Figure 3.15 Location of sites with shifts in both the AMF series and the best X-day flood generating precipitation series constructed using 1/8-degree gridded data.	66
Figure 3.16 X-day lead time yielding the most significant Pearson's correlation coefficient between the AMF peaks and associated minimum temperature series.	69
Figure 3.17 X-day lead time yielding the most significant Pearson's correlation coefficient between the AMF peaks and associated maximum temperature series.	70

Figure 3.18 Location of sites with trends in both the best X-day flood generating minimum temperature and the AMF series.	71
Figure 3.19 Location of sites with trends in both the best X-day flood generating maximum temperature and the AMF series.	71
Figure 3.20 Location of sites with change-points in both the best X-day flood generating minimum temperature series and the AMF series.	73
Figure 3.21 Location of sites with change-points in both the best X-day flood generating maximum temperature series and the AMF series.	73
Figure 3.22 X-day lead time yielding the most significant Pearson's correlation coefficient between the day of occurrence of AMF peaks and associated minimum temperature series.	75
Figure 3.23 X-day lead time yielding the most significant Pearson's correlation coefficient between the day of occurrence of AMF peaks and associated maximum temperature series.	76
Figure 4.1 Location of six USGS stations used to compare current flood risk projection procedures to proposed climate informed flood risk projection model.	91
Figure 4.2 One-year ahead forecast of flood risk for Sheepscot River at North Whitefield, Maine (USGS Station No. 01038000) obtained using the <i>Bulletin 17B</i> LP3 model and the proposed modification to incorporate climate variability.	93
Figure 4.3 One-year ahead forecast of flood risk for Swift River near Roxbury, Maine (USGS Station No. 01055000) obtained using the <i>Bulletin 17B</i> LP3 model and the proposed modification to incorporate climate variability.	94
Figure 4.4 One-year ahead forecast of flood risk for Saco River near Conway, NH (USGS Station No. 01064500) obtained using the <i>Bulletin 17B</i> LP3 model and the proposed modification to incorporate climate variability.	94
Figure 4.5 One-year ahead forecast of flood risk for Oyster River near Durham, NH (USGS Station No. 01073000) obtained using the <i>Bulletin 17B</i> LP3 model and the proposed modification to incorporate climate variability.	95
Figure 4.6 One-year ahead forecast of flood risk for Smith River near Bristol, NH (USGS Station No. 01078000) obtained using the <i>Bulletin 17B</i> LP3 model and the proposed modification to incorporate climate variability.	95

Figure 4.7 One-year ahead forecast of flood risk for Ammonoosuc River at Bethlehem Junction, NH (USGS Station No. 01137500) obtained using the Bulletin 17B LP3 model and the proposed modification to incorporate climate variability.	96
Figure C.1 Results of Mann-Kendall trend tests on flood generating precipitation series with 2-day lead constructed using 1/8-degree gridded data.....	130
Figure C.2 Results of Pettitt tests on flood generating precipitation series with 2-day lead constructed using 1/8-degree gridded data.	130
Figure C.3 Results of Mann-Kendall trend tests on flood generating precipitation series with 3-day lead constructed using 1/8-degree gridded data.....	131
Figure C.4 Results of Pettitt tests on flood generating precipitation series with 3-day lead constructed using 1/8-degree gridded data.	131
Figure C.5 Results of Mann-Kendall trend tests on flood generating precipitation series with 4-day lead constructed using 1/8-degree gridded data.....	132
Figure C.6 Results of Pettitt tests on flood generating precipitation series with 4-day lead constructed using 1/8-degree gridded data.	132
Figure C.7 Results of Mann-Kendall trend tests on flood generating precipitation series with 6-day lead constructed using 1/8-degree gridded data.....	133
Figure C.8 Results of Pettitt tests on flood generating precipitation series with 6-day lead constructed using 1/8-degree gridded data.	133
Figure C.9 Results of Mann-Kendall trend tests on flood generating precipitation series with 7-day lead constructed using 1/8-degree gridded data.....	134
Figure C.10 Results of Pettitt tests on flood generating precipitation series with 7-day lead constructed using 1/8-degree gridded data.....	134
Figure C.11 Results of Mann-Kendall trend tests on flood generating precipitation series with 2-day lead constructed using 1/4-degree gridded data.....	135
Figure C.12 Results of Pettitt tests on flood generating precipitation series with 2-day lead constructed using 1/4-degree gridded data.....	135
Figure C.13 Results of Mann-Kendall trend tests on flood generating precipitation series with 3-day lead constructed using 1/4-degree gridded data.....	136

Figure C.14 Results of Pettitt tests on flood generating precipitation series with 3-day lead constructed using 1/4-degree gridded data.....	136
Figure C.15 Results of Mann-Kendall trend tests on flood generating precipitation series with 4-day lead constructed using 1/4-degree gridded data.....	137
Figure C.16 Results of Pettitt tests on flood generating precipitation series with 4-day lead constructed using 1/4-degree gridded data.....	137
Figure C.17 Results of Mann-Kendall trend tests on flood generating precipitation series with 5-day lead constructed using 1/4-degree gridded data.....	138
Figure C.18 Results of Pettitt tests on flood generating precipitation series with 5-day lead constructed using 1/4-degree gridded data.....	138
Figure C.19 Results of Mann-Kendall trend tests on flood generating precipitation series with 6-day lead constructed using 1/4-degree gridded data.....	139
Figure C.20 Results of Pettitt tests on flood generating precipitation series with 6-day lead constructed using 1/4-degree gridded data.....	139
Figure C.21 Results of Mann-Kendall trend tests on flood generating precipitation series with 7-day lead constructed using 1/4-degree gridded data.....	140
Figure C.22 Results of Pettitt tests on flood generating precipitation series with 7-day lead constructed using 1/4-degree gridded data.....	140
Figure D.1 Results of Mann-Kendall tests on flood generating minimum temperature series with 2-day lead.....	142
Figure D.2 Results of Pettitt tests on flood generating minimum temperature series with 2-day lead.....	142
Figure D.3 Results of Mann-Kendall tests on flood generating minimum temperature series with 3-day lead.....	143
Figure D.4 Results of Pettitt tests on flood generating minimum temperature series with 3-day lead.....	143
Figure D.5 Results of Mann-Kendall tests on flood generating minimum temperature series with 5-day lead.....	144

Figure D.6 Results of Pettitt tests on flood generating minimum temperature series with 5-day lead.....	144
Figure D.7 Results of Mann-Kendall tests on flood generating minimum temperature series with 6-day lead.....	145
Figure D.8 Results of Pettitt tests on flood generating minimum temperature series with 6-day lead.....	145
Figure D.9 Results of Mann-Kendall tests on flood generating minimum temperature series with 7-day lead.....	146
Figure D.10 Results of Pettitt tests on flood generating minimum temperature series with 7-day lead.....	146
Figure D.11 Results of Mann-Kendall tests on flood generating maximum temperature series with 2-day lead.....	147
Figure D.12 Results of Pettitt tests on flood generating maximum temperature series with 2-day lead.....	147
Figure D.13 Results of Mann-Kendall tests on flood generating maximum temperature series with 3-day lead.....	148
Figure D.14 Results of Pettitt tests on flood generating maximum temperature series with 3-day lead.....	148
Figure D.15 Results of Mann-Kendall tests on flood generating maximum temperature series with 5-day lead.....	149
Figure D.16 Results of Pettitt tests on flood generating maximum temperature series with 5-day lead.....	149
Figure D.17 Results of Mann-Kendall tests on flood generating maximum temperature series with 6-day lead.....	150
Figure D.18 Results of Pettitt tests on flood generating maximum temperature series with 6-day lead.....	150
Figure D.19 Results of Mann-Kendall tests on flood generating maximum temperature series with 7-day lead.....	151

Figure D.20 Results of Pettitt tests on flood generating maximum temperature series with 7-day lead.....	151
Figure E.1 Locations of sites with significant Kendall's tau correlation between 10-year moving average of log-transformed flood flows and 3-month average AMO anomalies with 3-month lead.....	162
Figure E.2 Locations of sites with significant Kendall's tau correlation between 10-year moving average of log-transformed flood flows and 3-month average AMO anomalies with 9-month lead.....	162
Figure E.1 Locations of sites with significant Pearson's r correlation between 10-year moving average of log-transformed flood flows and 3-month average AMO anomalies with 6-month lead.....	163
Figure E.2 Locations of sites with significant Spearman's rho correlation between 10-year moving average of log-transformed flood flows and 3-month average AMO anomalies with 6-month lead.....	163
Figure E.3 Locations of sites with significant Kendall's tau correlation between 10-year moving average of log-transformed flood flows and 3-month average MEI anomalies with 3-month lead.....	169
Figure E.4 Locations of sites with significant Kendall's tau correlation between 10-year moving average of log-transformed flood flows and 3-month average MEI anomalies with 6-month lead.....	170
Figure E.5 Locations of sites with significant Pearson's r correlation between 10-year moving average of log-transformed flood flows and 3-month average MEI anomalies with 9-month lead.....	170
Figure E.6 Locations of sites with significant Spearman's rho correlation between 10-year moving average of log-transformed flood flows and 3-month average MEI anomalies with 9-month lead.....	171
Figure E.9 Locations of sites with significant Pearson's r correlation between 10-year moving average of log-transformed flood flows and 3-month average NAO anomalies with 3-month lead.....	179

Figure E.10 Locations of sites with significant Spearman's rho correlation between 10-year moving average of log-transformed flood flows and 3-month average NAO anomalies with 3-month lead.	179
Figure E.11 Locations of sites with significant Kendall's tau correlation between 10-year moving average of log-transformed flood flows and 3-month average Nino3.4 anomalies with 3-month lead.	182
Figure E.12 Locations of sites with significant Kendall's tau correlation between 10-year moving average of log-transformed flood flows and 3-month average Nino3.4 anomalies with 6-month lead.	182
Figure E.13 Locations of sites with significant Kendall's tau correlation between 10-year moving average of log-transformed flood flows and 3-month average Nino3.4 anomalies with 9-month lead.	183
Figure E.14 Locations of sites with significant Pearson's r correlation between 10-year moving average of log-transformed flood flows and 3-month average Nino3.4 anomalies with 9-month lead.	183
Figure E.15 Locations of sites with significant Spearman's rho correlation between 10-year moving average of log-transformed flood flows and 3-month average Nino3.4 anomalies with 9-month lead.	184
Figure E.16 Locations of sites with significant Kendall's tau correlation between 10-year moving average of log-transformed flood flows and 3-month average PDO anomalies with 3-month lead.	193
Figure E.17 Locations of sites with significant Kendall's tau correlation between 10-year moving average of log-transformed flood flows and 3-month average PDO anomalies with 6-month lead.	193
Figure E.18 Locations of sites with significant Pearson's r correlation between 10-year moving average of log-transformed flood flows and 3-month average PDO anomalies with 9-month lead.	194
Figure E.19 Locations of sites with significant Spearman's rho correlation between 10-year moving average of log-transformed flood flows and 3-month average PDO anomalies with 9-month lead.	194

Figure F.1 Locations of sites with significant Kendall's tau correlation between 10-year moving standard deviation of log-transformed flood flows and 3-month average AMO anomalies with 6-month lead.....	204
Figure F.2 Locations of sites with significant Kendall's tau correlation between 10-year moving standard deviation of log-transformed flood flows and 3-month average AMO anomalies with 9-month lead.....	204
Figure F.3 Locations of sites with significant Pearson's r correlation between 10-year moving standard deviation of log-transformed flood flows and 3-month average AMO anomalies with 6-month lead.....	205
Figure F.4 Locations of sites with significant Spearman's rho correlation between 10-year moving standard deviation of log-transformed flood flows and 3-month average AMO anomalies with 3-month lead.....	205
Figure F.5 Locations of sites with significant Kendall's tau correlation between 10-year moving standard deviation of log-transformed flood flows and 3-month average MEI anomalies with 3-month lead.....	210
Figure F.6 Locations of sites with significant Kendall's tau correlation between 10-year moving standard deviation of log-transformed flood flows and 3-month average MEI anomalies with 6-month lead.....	211
Figure F.7 Locations of sites with significant Pearson's r correlation between 10-year moving standard deviation of log-transformed flood flows and 3-month average MEI anomalies with 9-month lead.....	211
Figure F.8 Locations of sites with significant Spearman's rho correlation between 10-year moving standard deviation of log-transformed flood flows and 3-month average MEI anomalies with 9-month lead.....	212
Figure F.11 Locations of sites with significant Pearson's r correlation between 10-year moving standard deviation of log-transformed flood flows and 3-month average NAO anomalies with 3-month lead.	218
Figure F.12 Locations of sites with significant Spearman's rho correlation between 10-year moving standard deviation of log-transformed flood flows and 3-month average NAO anomalies with 3-month lead.	219

Figure F.16 Locations of sites with significant Pearson's r correlation between 10-year moving standard deviation of log-transformed flood flows and 3-month average Nino3.4 anomalies with 9-month lead.	222
Figure F.17 Locations of sites with significant Spearman's ρ correlation between 10-year moving standard deviation of log-transformed flood flows and 3-month average Nino3.4 anomalies with 9-month lead.....	223
Figure F.20 Locations of sites with significant Pearson's r correlation between 10-year moving standard deviation of log-transformed flood flows and 3-month average PDO anomalies with 9-month lead.	232
Figure F.21 Locations of sites with significant Spearman's ρ correlation between 10-year moving standard deviation of log-transformed flood flows and 3-month average PDO anomalies with 9-month lead.....	232

LIST OF TABLES

Table 2.1	Number of trends identified in the complete record and/or subseries with respect to identified change-points in mean flood magnitude.	26
Table 2.2	Number of sites with significant negative and positive trends in flood generating precipitation series identified using Mann-Kendall trend tests.....	34
Table 2.3	Number of sites with significant change-points in the mean of flood generating precipitation identified using the Pettitt test with 5% and 10% significance levels.	36
Table 2.4	Number of sites with significant trends (negative or positive) in flood generating maximum and minimum temperature series with X-days lead times identified using Mann-Kendall tests.	38
Table 2.5	Number of sites with change-points in the mean of flood associated minimum and maximum temperature series identified using the Pettitt test with 5% and 10% significance levels.	40
Table 3.1	Sources of climatic indices used to identify teleconnections with flood flows.	49
Table 3.2	Number of sites with significant Kendall's tau correlation (5 and 10% levels) between 10-year moving average of log-transformed flood peaks and AMO, MEI, NINO 3.4, NAO, and PDO indices with specified lead times.	53
Table 3.3	Number of sites with significant Kendall's tau correlation (5 and 10% levels) between 10-year moving standard deviation of log-transformed flood peaks and AMO, MEI, NINO 3.4, NAO, and PDO indices with specified lead times.	54
Table 3.4	Timing of Cold/Negative and Warm/Positive phases of AMO, PDO, and NAO.....	60
Table 3.5	Coincidental timing of AMO phase changes and identified change-points in the mean of AMF series; including respective Kendall's tau values and associated p-values for correlation between the 10-year moving average of AMF series and AMO climate anomalies with 6-month lead.	61
Table 3.6	Coincidental timing of PDO phase changes and identified change-points in the mean of AMF series; including respective Kendall's tau values and associated p-	

values for correlation between the 10-year moving average of AMF series and PDO climate anomalies with 9-month lead.	62
Table 3.7 Coincidental timing of NAO phase changes and identified change-points in the mean of AMF series; including respective Kendall's tau values and associated p-values for correlation between the 10-year moving average of AMF series and NAO climate anomalies with 3-month lead.....	62
Table 3.8 Number of sites yielding significant Pearson's correlation coefficients for AMF series relative to precipitation series with X-day lead times constructed using 1/8 and 1/4 degree gridded data.	64
Table 3.9 Summary results for sites with trends in both the magnitude of AMF series and the best X-day flood generating precipitation series.....	67
Table 3.10 Summary results for sites with significant shifts in both the magnitude of AMF series and the best X-day flood generating precipitation series.	68
Table 3.11 Summary results for sites with trends in both the magnitude of AMF series and the best X-day flood generating minimum and maximum temperature series.	72
Table 3.12 Summary results for sites with significant shifts in both the magnitude of AMF series and the best X-day flood generating minimum/maximum temperature series.	74
Table 3.13 Summary results for sites with significant shifts in AMF magnitude for which water report remarks pertinent to hydrologic modifications exist within <i>Falcone et al.</i> [2011].....	78
Table 3.14 Summary results for sites with shifts in the magnitude of AMF series and corresponding changes in amount of storage (megaliters total storage per square km) in each basin.	80
Table 4.1 Three-month averaged values of climate indices with specified lead time relative to April flood peak used in regression models to obtain one-year ahead forecasts $\mu(2009)$ and $\sigma(2009)$: observed values for 2009 and extreme scenario. 91	
Table 4.2 Regression coefficients obtained for the model of the log space mean at six sample sites. Coefficients reported are all significant at the 10% level.....	92

Table 4.3	Regression coefficients obtained for the model of the log space standard deviation at six sample sites. Coefficients reported are all significant on the 10% level.....	92
Table 4.4	Moments of the log-transformed flood peaks based on stationary P3 model through 2008, proposed model with observed climate indices for 2009 and hypothetical extreme climate indices.....	92
Table A.1	Results of Pettitt and Mann-Kendall tests on flood magnitude (significant on the 10% level), including the year of the identified shift in the mean, and the direction of significant trends, either positive (+) and negative (-).	113
Table A.2	Results of Mann-Kendall tests (10% significance level) on AMF subseries for sites exhibiting a significant change-point in the mean flood magnitude at the 10% level. The mean flood magnitude in the complete series, and each subseries are also reported.....	119
Table A.3	Hurst exponents for AMF series for all 569 sites considered. Values in red indicate sites characterized by a random walk or anti-persistence.	120
Table B.1	Mann-Kendall results for sites exhibiting a significant trend whether positive (+) or negative (-), in the day of occurrence of flood peaks on the 10% level. ..	125
Table B.2	Change-point results indicating year of identified shift in the day of occurrence of flood peaks and associated p-value.	126
Table E.1	Number of sites with significant Pearson's r and Spearman's rho correlations (5 and 10% levels) between 10-yr moving mean of log-transformed flood peaks and for AMO, MEI, NINO 3.4, NAO, and PDO indices with specified lead times.	153
Table E.2	Results of Kendall's tau analyses (significant 10% level) between 10-year moving average of log-transformed flood flows and 3-month average AMO anomalies with 3-, 6-, and 9-month leads.	154
Table E.3	Results of Kendall's tau analyses (significant 10% level) between 10-year moving average of log-transformed flood flows and 3-month average MEI anomalies with 3-, 6-, and 9-month leads.	164

Table E.4 Results of Kendall's tau analyses (significant 10% level) between 10-year moving average of log-transformed flood flows and 3-month average NAO anomalies with 3-, 6-, and 9-month leads.	171
Table E.5 Results of Kendall's tau analyses (significant at 10% level) between 10-year moving average of log-transformed flood flows and 3-month average Nino3.4 anomalies with 3-, 6-, and 9-month leads.	180
Table E.6 Results of Kendall's tau analyses (significant 10% level) between 10-year moving average of log-transformed flood flows and 3-month average PDO anomalies with 3-, 6-, 9-month leads.	184
Table F.1 Number of sites with significant Pearson's r and Spearman's rho correlations (5 and 10% levels) between 10-yr moving standard deviation of log-transformed flood peaks and for AMO, MEI, NINO 3.4, NAO, and PDO indices with specified lead times.	195
Table F.2 Results of Kendall's tau analyses (significant 10% level) between 10-year moving standard deviation of log-transformed flood flows and 3-month average AMO anomalies with 3-, 6-, and 9-month leads.	196
Table F.3 Results of Kendall's tau analyses (significant at 10% level) between 10-year moving standard deviation of log-transformed flood flows and 3-month average MEI anomalies with 3-, 6-, and 9-month leads.	206
Table F.4 Results of Kendall's tau analyses (significant at 10% level) between 10-year moving standard deviation of log-transformed flood flows and 3-month average NAO anomalies with 3-, 6-, and 9-month leads.	212
Table F.5 Results of Kendall's tau analyses (significant at 10% level) between 10-year moving standard deviation of log-transformed flood flows and 3-month average Nino3.4 anomalies with 3-, 6-, and 9-month leads.	219
Table F.6 Results of Kendall's tau analyses (significant at 10% level) between 10-year moving standard deviation of log-transformed flood flows and 3-month average PDO anomalies with 3-, 6-, and 9-month leads.	223
Table G.1 Results of Pearson's correlation analyses between magnitude of AMF peaks and associated flood generating hydroclimatic series with best lead times.	233
Table G.2 Results of Pearson's correlation analyses between timing of AMF peaks and associated flood generating temperature (minimum and maximum) series with best lead times.	239

ACKNOWLEDGEMENTS

Foremost, I would like to express my sincere gratitude to Dr. Veronica Griffis for her immense patience, constructive advice, and her willingness to allow me to get involved with her research as an undergraduate student. This project would never have been possible without her support, words of enthusiasm, and immense knowledge. The past year has been filled with up and downs or should I say “abrupt shifts,” but Dr. Griffis still supported me, and working with her as my advisor has been a rewarding experience.

My thanks also go to the members of my major committee Dr. Veronica Griffis, Dr. Ann Maclean and Dr. Watkins for their time and contribution to this research.

Further, I wish to thank Dr. Ann Maclean for her invaluable contributions and guidance with GIS, and her willingness to allow me to be a GIS teaching assistant.

I would like to thank my fellow classmate Karl Meingast, for the countless stimulating discussions in the duck blind about my research and how to get my MATLAB code to run, and for all the fun we have had in the last year in and out of class. On this note, I would also like to recognize my dog “Wigeon” who was always by my side whether on the water duck hunting or just taking a walk to “escape” the labs.

My parents, Denice and Joe, receive my deepest gratitude and love for their dedication and the many years of support during my undergraduate studies that provided the foundation for this work. Had it not been for them and their continuous words of encouragement, I would not be where I am today. Special thanks to my siblings, Jeremiah and Jonathan, who have been my true role models.

Last, but not least, I would like to thank my girlfriend Stephanie Mayer for her understanding and love during the past few years. Her support and encouragement was in the end what made this thesis possible.

ABSTRACT

Standard procedures for forecasting flood risk (*Bulletin 17B*) assume annual maximum flood (AMF) series are stationary, meaning the distribution of flood flows is not significantly affected by climatic trends/cycles, or anthropogenic activities within the watershed. Historical flood events are therefore considered representative of future flood occurrences, and the risk associated with a given flood magnitude is modeled as constant over time. However, in light of increasing evidence to the contrary, this assumption should be reconsidered, especially as the existence of nonstationarity in AMF series can have significant impacts on planning and management of water resources and relevant infrastructure. Research presented in this thesis quantifies the degree of nonstationarity evident in AMF series for unimpaired watersheds throughout the contiguous U.S., identifies meteorological, climatic, and anthropogenic causes of this nonstationarity, and proposes an extension of the *Bulletin 17B* methodology which yields forecasts of flood risk that reflect climatic influences on flood magnitude.

To appropriately forecast flood risk, it is necessary to consider the driving causes of nonstationarity in AMF series. Herein, large-scale climate patterns—including El Niño-Southern Oscillation (ENSO), Pacific Decadal Oscillation (PDO), North Atlantic Oscillation (NAO), and Atlantic Multidecadal Oscillation (AMO)—are identified as influencing factors on flood magnitude at numerous stations across the U.S. Strong relationships between flood magnitude and associated precipitation series were also observed for the majority of sites analyzed in the Upper Midwest and Northeastern regions of the U.S. Although relationships between flood magnitude and associated temperature series are not apparent, results do indicate that temperature is highly correlated with the timing of flood peaks. Despite consideration of watersheds classified as unimpaired, analyses also suggest that identified change-points in AMF series are due to dam construction, and other types of regulation and diversion. Although not explored herein, trends in AMF series are also likely to be partially explained by changes in land use and land cover over time.

Results obtained herein suggest that improved forecasts of flood risk may be obtained using a simple modification of the *Bulletin 17B* framework, wherein the mean and standard deviation of the log-transformed flows are modeled as functions of climate indices associated with oceanic-atmospheric patterns (e.g. AMO, ENSO, NAO, and PDO) with lead times between 3 and 9 months. Herein, one-year ahead forecasts of the mean and standard deviation, and subsequently flood risk, are obtained by applying site specific multivariate regression models, which reflect the phase and intensity of a given climate pattern, as well as possible impacts of coupling of the climate cycles. These forecasts of flood risk are compared with forecasts derived using the existing *Bulletin 17B* model; large differences in the one-year ahead forecasts are observed in some locations. The increased knowledge of the inherent structure of AMF series and an improved understanding of physical and/or climatic causes of nonstationarity gained from this research should serve as insight for the formulation of a physical-casual based statistical model, incorporating both climatic variations and human impacts, for flood risk over longer planning horizons (e.g., 10-, 50, 100-years) necessary for water resources design, planning, and management.

CHAPTER 1 INTRODUCTION

During the 2010 water year, within the United States alone, flood damages bolstered \$5.04 billion in accumulation—67% the cost of the previous thirty years' average (1980 – 2009), totaling \$7.56 billion [NOAA, 2011]. These figures, in themselves, raise reason for concern of attaining an accurate approach for flood frequency analysis and estimation of flood risk. Standard procedures for forecasting flood risk [LACWD, 1982] entail employing an assumed theoretical probability distribution to estimate the recurrence interval associated with observed annual maximum discharges. Hydraulic structures are then designed to withstand and/or accommodate the flood magnitude corresponding to a designated recurrence interval (e.g., the 100-year event). Similarly, the resulting magnitude of design events may be utilized in a variety of water resources applications (e.g., floodplain delineation, land-use planning/management, design/operation of water-use and water-control structures, and design of transportation infrastructure like bridges and roadways), thus indicating the importance of accurate flood risk estimation.

Current procedures presuppose instantaneous annual maximum flood (AMF) flow series as stationary, thereby assuming parameters of the fitted probability distribution as constant over time, and disregarding any possible influence of climatic cycles and/or trends [Olsen *et al.*, 1999; Hirschboeck *et al.*, 2000]. Otherwise stated, standard procedures assume historical events are representative of future flood events over any time horizon. This assumption, however, is increasingly being debated in the hydrologic literature; results of studies already executed suggest AMF series are nonstationary [e.g. National Research Council, 1998; Franks and Kuczera, 2002; Kashelikar and Griffiths, 2008; Petrow and Merz, 2009; Villarini *et al.*, 2009, 2011]. This thesis provides further evidence that AMF series in relatively unimpaired watersheds within the U.S. are nonstationary, and considers how to incorporate sources of nonstationarity in annual maximum flood flows into standard flood frequency analysis procedures to improve one-year ahead estimates of flood risk. This research provides the groundwork for needed advances in water resources planning and management, and stochastic hydrology.

1.1 Research Motivation

In light of natural climate variability and potential climate change, a vast amount of research has been dedicated to investigating nonstationarity in hydroclimatic data series. Results of previous studies reveal that trends and/or change-points are evident in multiple hydroclimatic data series including precipitation and streamflow [e.g., *Lettenmaier et al.*, 1994; *Lins and Slack*, 1999; *Olsen et al.*, 1999; *Perreault et al.*, 1999; *Rasmussen*, 2001; *Burn and Hag Elnur*, 2002; *McCabe and Wolock*, 2002; *Kalra et al.*, 2006, 2008; *Small et al.*, 2006; *Seidou and Ouarda*, 2007; *Ehsanzadeh et al.*, 2010; *Walter and Vogel*, 2010 and references therein]. With respect to streamflow series, the majority of these studies have considered annual and seasonal minimum, median, and average quantities. In the U.S., *Douglas et al.* [2000] and *Small et al.* [2006] considered nonstationarity in high flows defined as the annual maximum average daily streamflow. Only a few studies have considered existence of nonstationarity in instantaneous annual maximum flood (AMF) series within the U.S. [*Olsen et al.*, 1999; *Kashelkar and Griffis*, 2008; *Collins*, 2009; *Villarini et al.*, 2009, 2011], as are evaluated herein. Outside of the U.S., others have investigated trends in flood series comprised of peaks-over threshold and annual maximum events [e.g., *Petrow and Merz*, 2009; *Burn and Hag Elnur*, 2002; *Yue et al.*, 2002].

Nonstationarity in the form of trends has been investigated in annual average daily streamflow series (not AMF series) by means of a non-parametric Mann-Kendall trend test [e.g., *Small et al.*, 2006; *Lins and Slack*, 1999; *Douglas et al.*, 2000; *Hodgkins and Dudley*, 2005]. While the focus herein is on AMF series, results of these studies are discussed briefly as they illustrate what changes might be occurring within the hydrologic cycle over time, and indicate what trends might exist in AMF series. *Hodgkins and Dudley* [2005] analyzed trends in annual average daily streamflow series at 27 stations in New England. They did not identify any significant trends in annual average daily streamflows; however, significant increases were identified in various percentiles of annual streamflow (minimum, 25th percentile, median, 75th percentile, and maximum) at the majority of the stations analyzed. *Small et al.* [2006] analyzed annual average daily flow series of 218 basins across the eastern half of the U.S.; only a small portion of sites

were found to exhibit trends. *Lins and Slack* [1999] appraised trends in quantiles of annual average daily streamflows across the U.S. They observed upward trends in minimum and median quantiles, but relatively few in maximum quantiles, thereby indicating that “the U.S. is getting wetter, but less extreme” [*Lins and Slack*, 1999, p.227]. Results of *Douglas et al.* [2000] indicate that significant trends in maximum annual average daily flows do not exist when accounting for cross-correlation. Overall, these results suggest trends would not exist in AMF series, i.e. instantaneous annual maximum peak discharge series.

In the U.S., only a few studies have focused attention on identifying trends in AMF series [*Olsen et al.*, 1999; *Kashelikar and Griffis*, 2008; *Villarini et al.*, 2009, 2010, 2011]. *Olsen et al.* [1999] identified significant upward trends in flood series in the Upper Mississippi and Missouri Rivers by performing linear regression on AMF series over time; Spearman rank correlation tests further reinforced their findings. *Kashelikar and Griffis* [2008] performed Mann-Kendall trend tests on 396 relatively unimpaired basins across the U.S. Their results show most sites exhibiting a significant trend in flood flows are located in the North Pacific, the Midwest and the Eastern U.S. Several studies have identified significant trends (both positive and negative) in the Northeastern quadrant of the U.S. on a site-by-site basis [*Olsen et al.*, 1999; *Kashelikar and Griffis*, 2008; *Villarini et al.*, 2010]. Overall, results of trend analyses in flood series have been mixed in the U.S., as noted by *Walter and Vogel* [2010]. Discrepancies in the existence (or attained significance) of trends in peak flows are due to conflicting methodologies as well as record lengths employed [*Villarini et al.*, 2009].

A number of studies pertaining to nonstationarity in flood flows have been conducted outside the U.S. Across the UK, *Robson et al.* [1998] investigated two types of flood series—AMF and peaks-over-threshold (POT)—for trends by employing three standard statistical tests—linear regression, normal scores regression, and Spearman’s rho; no significant trends in flood behavior were identified. Others investigated trends in flood series using a Mann-Kendall test. In Germany, *Petrow and Merz* [2009] accounted for serial correlation when investigating trends in AMF and POT series, and observed that

basins exhibiting significant trends in flood series tended to be spatially clustered. In Canada, *Burn and Hag Elnur* [2002] identified spatial differences in both occurrence and direction of trends in AMF series. *Yue et al.* [2002] utilized both Mann-Kendall and Spearman's rho tests to detect trends in AMF series of 20 pristine basins in Ontario, Canada; they observed negative trends, or a general decrease in flood magnitudes. Though outside the U.S., these studies raise concern as to the validity of the assumption of nonstationarity in flood series.

Others have investigated nonstationarity in streamflows in the form of change-points (abrupt shifts) rather than gradual trends [e.g., *McCabe and Wolock*, 2002; *Kalra et al.*, 2006; *Seidou and Ouarda*, 2007; *Ehsanzadeh et al.*, 2010]. Results of these studies indicate the need to couple trend and change-point tests when investigating nonstationarity in hydroclimatic series to limit false detection of trends. *Ehsanzadeh et al.* [2010] investigated the presence of gradual and abrupt changes in Canadian low flows using a Mann-Kendall trend test combined with a Bayesian change-point detection methodology proposed by *Seidou and Ouarda* [2007]. *Kalra et al.* [2006] examined average annual and monthly streamflow quantities for trends using Spearman's rho, Mann-Kendall, and linear regression analyses. Their results indicate streamflow quantities are increasing in the Upper and Middle Mississippi regions. These results were corroborated using rank sum and student t tests to evaluate step changes in streamflow quantity [*Kalra et al.*, 2006]. *McCabe and Wolock* [2002] discovered a mixed pattern of increases and decreases in average annual daily maximum flows throughout the U.S. when using a Mann-Kendall trend test, but results of a standard departures test revealed that the apparent linear monotonic trends actually occur as abrupt shifts.

The importance of investigating nonstationarity in the form of both trends (gradual changes) and abrupt shifts is evident based on the studies discussed above; however, only a few studies have completed this type of analysis for AMF series [e.g., *Collins*, 2009; *Armstrong et al.*, 2011; *Villarini et al.*, 2009, 2010, 2011]. *Armstrong et al.* [2011] investigated changes in the number of peaks-over-threshold per water year in New England. They compared pre- and post-1970 records using the Wilcoxon Rank-Sum test,

and found a median increase of one flood per year for the post-1970 period. *Villarini et al.* [2009] investigated the presence of monotonic trends in AMF series by applying Mann-Kendall and Spearman's rho tests. Abrupt change-points in the mean and variance of AMF series were also investigated by means of the Pettitt change-point test [*Villarini et al.*, 2009, 2011]. Results throughout the Midwest and Northeastern U.S. indicate that observed increases in flood magnitude are due to an abrupt shift (change-point), the presence of which results in spurious results of the Mann-Kendall test when not accounted for [*Villarini et al.*, 2009, 2011]. Similarly, using a standard departures test, *Collins* [2009] identified increasing magnitudes of instantaneous peak flows in New England which occurred as abrupt shifts rather than gradual changes. These limited results for AMF series further illustrate the need to couple tests when trying to identify nonstationarity.

Not only have the methods employed for trend detection been under debate, but also whether the trends themselves will continue unabated into the future or if they are the result of long term persistence, and thus only part of a longer-term cycle not apparent in the available record [e.g., *Villarini et al.*, 2009; *Stedinger and Griffis*, 2011]. *Hurst* [1951] investigated dependence properties of water levels in the Nile River, and concluded that the data exhibited signs of long-term persistence or dependence that is beyond what one could explain by assuming independent and identically distributed observations. Others have since applied the Hurst phenomenon to a variety of hydrologic variables [e.g., *Sakalauskiene*, 2003; *Koutsoyiannis*, 2003]. In order to improve our understanding of nonstationarity in flood series, persistence in AMF series is investigated herein in addition to trends and change-points. Moreover, in the context of water resources applications, it is necessary to move beyond simply assessing the degree of nonstationarity in AMF series, and consider the driving causes, whether climatic and/or human-induced, of the observed changes in flood magnitude and the associated flood risk.

With respect to climatic influences on flood flows, *Robson et al.* [1998] observed strong year-to-year variations in UK floods (POT and AMF series), noting that the flows

displayed systematic behavior (fluctuations), with emergence of some possible cyclic tendencies when smoothed using locally weighted regression. The observed behavior suggests that fluctuations in flood flows are driven climatically. Climate variability and its relation to streamflows is often investigated through teleconnections—large and persistent oceanic-atmospheric patterns which occur over large areas, displaying causal effects on regional climate conditions in adjacent and often remote areas [*Piechota and Dracup, 1999*]. Examples of large scale oceanic patterns include the El Nino-Southern Oscillation (ENSO), North Atlantic Oscillation (NAO), and Pacific Decadal Oscillation (PDO). These large scale patterns have either inter-annual variations (2-10 years) or inter-decadal variations (10-50 years) [*Piechota and Dracup, 1999*]. Interannual climate variability occurs when large scale oceanic-atmospheric patterns result in extremely large climate anomalies, i.e. departures from a long-term average. Several studies have demonstrated how these well-organized spatial and temporal climatic patterns have high correlations with other hydroclimatic data series, such as precipitation and streamflows [e.g., *Dettinger et al., 2000; Chiew and McMahon, 2002; Twine et al., 2005*].

Others have attempted to explain natural variation and identified shifts in the magnitudes of floods by relating the timing of the shifts to phase changes in climatic patterns. *Jain and Lall [2000]* performed nonlinear regression on AMF records for a site on the Black Fork River in Utah; their results indicate ENSO and PDO could potentially explain 40% of the variation in AMF peaks at this one location. *Hamlet and Lettenmaier [2007]* investigated changes in flood risk in the western U.S. associated with both century-scale warming and interannual climate variations. Their results indicate climate variations associated with PDO and ENSO have strong effects on flood risk, especially when they are in phase with each other. In addition, they observe that a recent increase in flood risk in the western U.S. has resulted from changes in variability of cool season precipitation after 1973 [*Hamlet and Lettenmaier, 2007*]. Similarly, *Collins [2009]* observed that step increases in New England flood magnitudes occurred around 1970, in conjunction with a well-documented phase change in the low-frequency variability of NAO. Further, his results indicate a statistically significant, positive lagged correlation between indices of NAO and flood magnitudes.

In the context of water resources planning and management, these identified relationships have the potential to be incorporated into streamflow forecasting [e.g., *Dettinger et al.*, 2000; *Chiew and McMahon*, 2002; *Twine et al.*, 2005]. *Dettinger et al.* [2000] found strong correlations between average monthly streamflow series and winter averages (December-February) of SOI across North America. *Chiew and McMahon* [2002] investigated global ENSO-streamflow relationships to allude to the idea of using these identified relationships to potentially forecast monthly streamflow several months in advance. A number of papers provide examples of site specific applications of ENSO indicators in probabilistic streamflow forecasts [e.g., *Hamlet et al.*, 1999; *Piechota and Dracup*, 1999; *Grantz et al.*, 2005]. With respect to AMF peaks, knowledge of strong teleconnections has led to the use of climate anomalies to improve year-specific estimates of flood risk [e.g., *Kiem et al.*, 2003; *Kashelkar and Griffis*, 2008; *Kwon et al.*, 2008; *Kashelkar*, 2009].

In a similar fashion, the existence of trends in flood series could be due to trends in relevant climate variables such as precipitation. Several studies have investigated precipitation series for trends [e.g., *Knight and Karl*, 1998; *Kunkel et al.*, 1999; *Groisman et al.*, 2001; *Balling and Goodrich*, 2010]. *Knight and Karl* [1998] explored trends in precipitation by employing a variety of methods to fully characterize changes in quantity, frequency, and intensity of precipitation in the U.S. Their results indicate precipitation has increased by 10% across the continental U.S. since 1910. The driving force behind this observed increase in annual precipitation depth is due to identified trends in extreme precipitation series, resulting from an increase in heavy and intense rain events [*Knight and Karl*, 1998; *Kunkel et al.*, 1999; *Groisman et al.*, 2001]. However, mixed results are identified in Canada; the frequency of rare extreme events has not increased, but less extreme events have become more regular [*Kunkel et al.*, 1999]. *Balling and Goodrich* [2010] investigated trends and variations in precipitation intensity over the contiguous U.S. Only two regions within the U.S. exhibited a spatially coherent change in intensity—an increase in the Northeastern quadrant of the U.S., and a decrease in the center portion of the Western U.S.—while the rest of the U.S. exhibits high spatial entropy (disorder) [*Balling and Goodrich*, 2010].

Beyond investigating nonstationarity in precipitation series as discussed above, it is necessary to understand how changes in precipitation series could partially or fully explain identified gradual and/or abrupt changes in streamflow series. *Small et al.* [2006] associated trends in annual average and 7-day low flows with trends in average fall precipitation in basins within the Upper Mississippi and Great Lakes regions. Further, they note that spring precipitation series in the Eastern U.S. do not exhibit strong increasing trends, thereby providing evidence to the lack of identified trends in AMF series in that region. *Lettenmaier et al.* [1994] identified strong trends in average monthly precipitation across the U.S. using a seasonal Kendall's test, and applied a bivariate test to evaluate changes in streamflow relative to precipitation and temperature series. Their results indicate observed trends in average monthly streamflow are not completely consistent with trends in climatic variables, implying that observed trends in streamflow quantities are caused by a mixture of climatic and anthropogenic effects.

The recent increased understanding of climate variability and its connections to streamflows and flood flows as discussed above holds promise for improved estimation of flood risk, and will thereby have a significant impact on the design of water resources infrastructure, as well as water resources management. However, to improve flood frequency forecasts for long-term planning and management, it is also necessary to quantify the impacts of anthropogenic activities relative to those of natural climate variability [e.g., *Juckem et al.*, 2008]. Changes in the mean or variance of hydroclimatic time series can be caused by several mechanisms, including land cover changes (e.g., fire, urbanization, deforestation and changing agricultural practices), channel modifications (e.g., construction of dams and levees), and water withdrawals [*Ehsanzadeh et al.*, 2010].

Many of the aforementioned studies considered unimpaired watersheds in an attempt to isolate the impacts of climate variability on streamflow. The term unimpaired is used to describe a watershed relatively free of anthropogenic influences such as water source regulation, diversion, water withdrawals and land use changes [*Slack and Landwehr*, 1992]. For example, *Kashelkar* [2009] used unimpaired flood series for sites contained in the Hydro-Climatic Data Network (HCDN) Streamflow Dataset [*Slack et al.*, 1993].

For a site to be included in the HCDN, unimpaired basin conditions were defined as follows:

“At least with respect to the computation of a monthly mean discharge value -- There should be no overt adjustment of "natural" streamflow, such as flow diversion or augmentation, regulation of the streamflow by some containment structure, or reduction of base flow by extreme ground-water pumping, nor should the degree of human activity in the watershed, such as changes in land use during the period of record, be so large as to significantly affect the value of monthly mean discharge (computed on the basis of the daily mean discharge) at the station.”

[*Slack et al.*, 1993]

In addition, sites could be included in the HCDN if a river was regulated by a low-head hydropower dam which only produced temporary effects on high and low streamflows.

Records for sites contained within the HCDN should be used with caution, because not all sites included were considered unimpaired for the entire time period analyzed [*Slack et al.*, 1993]. Moreover, the status quo of an “unimpaired” watershed could have been jeopardized at any time since 1988 when it was originally classified. For example, abrupt or gradual land use/land cover changes can affect streamflow; if a basin has undergone changes from forest to agriculture to urban, it would no longer be considered unimpaired, and thus would not be included in the HCDN at present.

Prior to 2010, when the Geospatial Attributes of Gages for Evaluating Streamflow (GAGES) was published, no updates to the 1988 HCDN had been made and an alternative large scale database containing basins which represent hydrologic conditions least disturbed by human influences ("reference gages") did not exist [*Falcone et al.*, 2010]. In 2011, GAGES II (updated version of GAGES) was published. The dataset was created to provide users with a comprehensive set of geospatial characteristics for a large number of gaged watersheds, and to provide reference watersheds representative of hydrologic conditions which are least affected by anthropogenic effects [*Falcone et al.*, 2010]. A total of 9,322 sites were analyzed, and 2,057 are classified as reference sites. The dataset also includes a new “HCDN-2009” consisting of 743 sites defined as having potential for hydro-climatic studies following criteria based on continuous flow record

length and activity, and basin characteristics (<5% imperviousness). Additional details are provided by *Falcone et al.* [2011].

Undoubtedly, the U.S. has become more urbanized in the last century. The removal of vegetation and soil, grading of the land surface, and construction of drainage networks typically results in an increased magnitude and frequency of floods [Konrad, 2003]. Significant river engineering projects have also been related to observed trends in flooding [Pinter et al., 2008; Villiarini et al., 2009, 2011]. Villiarini et al. [2009, 2011] related change-points in the mean of AMF series to USGS qualification code “6”—“discharge affected by regulation or diversion.” Pinter et al. [2008] explored the effects of river engineering on the Mississippi River system with respect to observed trends in flood series. They concluded that climate and/or land use changes have played a role in observed increases in flood risk; however, these increases could also be associated with major engineering infrastructure (dikes, navigational structures, and levees).

Unimpaired watersheds predominantly consisting of forest cover can also experience increased flood risk by human effects. Storck et al. [1998] examined forest harvest effects on peak streamflows in the Pacific Northwest U.S. by employing a GIS-based distributed hydrologic model to simulate discrete (single storm) events for several watersheds. All results indicate clear-cutting can increase the magnitude of flows resulting from rain-on-snow events. Results of Jones and Grant [1996] reveal that the installation of logging roads increases streamflows to the same degree as clear-cutting.

Potter [1991] investigated a relatively unimpaired agricultural watershed in southwestern Wisconsin and related an observed decrease in the magnitude of flood flows to changing land management practices (i.e., adoption of conservation tillage and treatment of gullies) rather than climatic variations, reservoir construction, or major land use changes. However, Juckem et al. [2008] observe that changes in baseflows and stormflows in southwestern Wisconsin coincide with changes in precipitation in the 1970’s, and note that both were likely amplified by changing agricultural practices in the 1930’s.

Despite the cause, the existence of trends or change-points in AMF series can have a significant impact on the planning and management of water infrastructure. Several studies have proposed methods for coping with nonstationarity when forecasting flood risk. *Strupczewski et al.* [2001] and *Olsen et al.* [1999] incorporated hydrological nonstationarity into at-site flood frequency estimation by projecting observed trends in AMF series. *Sveinsson et al.* [2005] considered modeling variation in AMF series by incorporating shifting mean models that assume a constant long-term mean about which the stochastic model moves from one “stationary” state to another. For prediction of nonstationary hydrological time series, a dynamic recurrent neural network was proposed by *Coulibaly and Baldwin* [2005]. Generalized additive models have been proposed for modeling time series under nonstationary conditions by employing time-dependent parameters which take into account both trends and abrupt shifts [*Villarini et al.*, 2009, 2011]. The abilities of these models to forecast flood risk under changing climate and land use/land cover are limited, however, as they are merely a function of time.

On the contrary, *Kashelkar and Griffis* [2008] and *Kashelkar* [2009] propose a physical-causal model of flood risk which reflects observed nonstationarity in flood series. They used a regression model to incorporate effects of climate variability associated with ENSO events into updated estimates of the mean of AMF series to improve one-year ahead forecasts of flood risk. Their model appropriately increases/decreases expected flood risk relative to the phase and intensity of forecasted ENSO anomalies. Still, to be useful in the design of large-scale water control projects, models are needed which can provide accurate forecasts of flood risk over relevant planning/construction horizons of at least 50 years. Before these models can be developed, increased understanding of the prevalence of nonstationarity in flood series, and knowledge of the climatic, meteorologic, and anthropogenic causes of identified nonstationarity is needed.

1.2 Research Objectives

The objectives of this thesis are to identify causes of nonstationarity in AMF series, and to provide insight as to how traditional statistical models of flood risk can be adapted to better estimate flood risk by incorporating effects of nonstationary related to climate variability. To accomplish this, the thesis has been divided into three main tasks:

- (1) Identify hydroclimatic data series that exhibit nonstationarity in the form of gradual monotonic trends, abrupt shifts, and/or long-term persistence using standard statistical procedures.
- (2) Identify climatic, meteorologic, and/or human-induced causes of nonstationarity in AMF time series.
- (3) Develop site specific regression models to forecast flood risk one-year ahead as a function of forecasted climate anomalies.

Although the assumption of stationarity is considered “dead,” as inferred by *Milly et al.* [2008], there exists no need to reinvent the overall process for flood risk estimation; rather, traditional statistical models of flood risk may be adapted to incorporate sources of nonstationarity, and thereby allow for generation of more accurate flood risk estimates. It is imperative that we disregard all presuppositions that variables of flood frequency are unaffected over time, and transform our models to reflect identified causes of nonstationarity for which there exists a physical-causal basis for flood risk projection [*Stedinger and Griffis, 2011*].

CHAPTER 2 IDENTIFICATION OF NONSTATIONARITY IN HYDROCLIMATIC DATA SERIES

Previous studies have provided evidence of nonstationarity in hydroclimatic series, including precipitation, streamflow and temperature at various time scales. Results of studies already executed for various parts of the U.S. also suggest annual maximum flood (AMF) series are nonstationary [e.g. *National Research Council*, 1998; *Franks and Kuczera*, 2002; *Kashelkar and Griffis*, 2008; *Petrow and Merz*, 2009; *Villarini et al.*, 2009, 2011]. These findings provide motivation to challenge current flood frequency analysis procedures which presuppose AMF series as stationary, and thereby assume parameters of the fitted probability distribution are unassociated with time, and disregard any possible influence of climatic cycles and/or trends [*Olsen et al.*, 1999; *Hirschboeck et al.*, 2000]. This chapter presents results of an investigation of nonstationarity in AMF series at unimpaired sites throughout the contiguous U.S., as well as other associated hydroclimatic data series including flood-associated total daily precipitation series, and average daily maximum and minimum temperature series. Nonstationarity in the AMF series is considered with respect to both the magnitude of flood peaks and the day of occurrence. Sources of the nonstationarity identified in flood series will be investigated in Chapter 3.

2.1 Methods for Assessing Nonstationarity

The most common methods of investigating possible nonstationarity in hydroclimatic series are trend and change-point analyses. The existence of linear, temporal trends in annual maximum flood series is frequently evaluated using the non-parametric Mann-Kendall (MK) test [e.g., *Helsel and Hirsch*, 1993; *Douglas et al.*, 2000; *Kashelkar and Griffis*, 2008; *Villarini et al.*, 2009, 2011]. Change-point analyses are frequently used to test for abrupt shifts in either the mean or variance of the flood peaks [e.g., *Seidou and Ouarda*, 2007; *Kalra et al.*, 2008; *Villarini et al.*, 2009, 2011]. Per *Villarini et al.* [2009], AMF series and flood associated hydroclimatic series considered herein were first

checked for change-points in the mean using the non-parametric Pettitt test [Pettitt, 1979], and then checked for temporal trends using the Mann-Kendall test. In the instance a change-point is detected in an AMF series, the sub-series before and after the shift will be checked independently for temporal trends. Each flood series was also checked for autocorrelation, and appropriate modifications of the Mann-Kendall test were used to avoid spurious results [Hamad and Rao, 1998; Yue *et al.*, 2003; Cohn and Lins, 2005; Hamad, 2009]. Figure 2.1 shows the results of change-point and trend tests for a sample station's AMF series. The figure indicates a significant change-point in the mean occurred in 1940 and shows the series is better characterized by an abrupt shift rather than a linear monotonic trend. Further, as a trend identified as statistically significant could be part of a long-term cycle not apparent in the analyzed time series [Hamad, 2009], the Hurst exponent [Hurst, 1951] will be estimated to test for the presence of long-term persistence. Additional details of the methods used herein to identify nonstationarity are provided below.

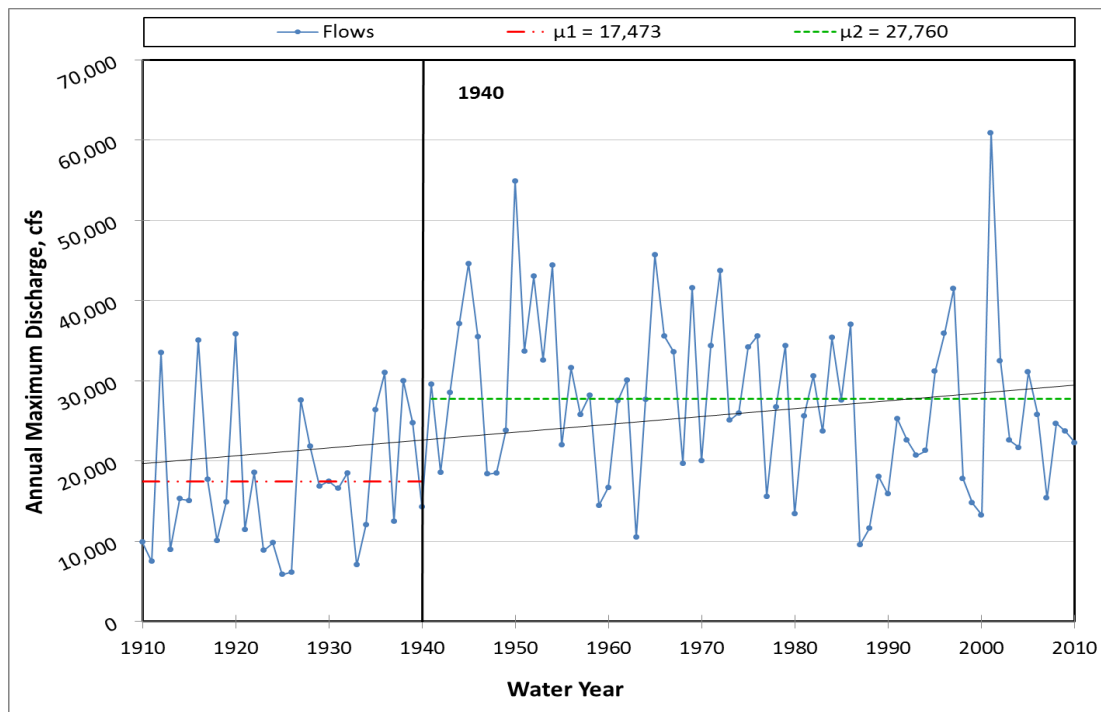


Figure 2.1 Example graph illustrating nonstationarity in an AMF series in the form of a linear trend and an abrupt shift in the mean (USGS Station No. 05340500).

2.1.1 Mann-Kendall Trend Test

Standard statistical trend tests used to identify monotonic trends include the Mann-Kendall test, Spearman's rho and linear regression with time as an independent variable. Several studies have investigated trends in streamflow quantities including annual and seasonal minimum, median, and averages by employing such tests [Lettenmaier *et al.*, 1994; Lins and Slack, 1999; Olsen *et al.*, 1999; Douglas *et al.*, 2000; Burn and Hag Elnur, 2002; McCabe and Wolock, 2002; Yue *et al.*, 2002; Hodgkins and Dudley, 2005; Small *et al.*, 2006; Collins, 2009; Petrow and Merz, 2009; Villarini *et al.*, 2009, 2011]. Yue *et al.* [2002] investigated the power of Mann-Kendall (MK) and Spearman's rho tests for detecting monotonic trends in time series data; their findings indicate both tests provide indistinguishable results when used in practice. They also note the power depends on the magnitude of the trend, sample size, and the amount of variation within the time series. Only the MK test will be utilized in this study to investigate trends in hydroclimatic series as it provides similar results as the Spearman's rho test, and it is routinely used to identify trends in hydroclimatic time series.

The MK test is a non-parametric, rank based method, therefore it is more robust given outliers in the data set, and is advantageous in that it does not assume an underlying distribution of the data (in particular, normality is not required). The MK test is used to detect monotonic trends by evaluating whether there is an increase or decrease in values with respect to time. The test is completed by considering each observation as its own datum, and differences between the datum and successive observations are computed across a triangular table. The test statistic S is computed by taking the difference between the number of positive (P) and negative differences (N):

$$S = P - N \quad (1)$$

To evaluate the significance of the trend, when the sample size (n) is greater than 10, the test statistic S is transformed to define a standard normal Z statistic as follows:

$$Z = \begin{cases} (S - 1)/\sigma_s & \text{If } S > 0 \\ 0 & \text{If } S = 0 \\ (S + 1)/\sigma_s & \text{If } S < 0 \end{cases} \quad (2)$$

where,

$$\sigma_s^2 = \frac{n(n-1)(2n+5)}{18} \quad (3)$$

in the instance that no ties are observed. When data values are tied, the following correction is applied to σ_s^2 :

$$\sigma_s^2 = \frac{n(n-1)(2n+5) - \sum_{i=1}^n t_i(i-1)(2i+5)}{18} \quad (4)$$

where t_i symbolizes the number of ties of extent i .

A trend is apparent in a time series when the absolute value of the Z-statistic computed in equation (2) is greater than $z_{\alpha/2} = \Phi^{-1}(1 - \alpha/2)$ for a defined significance level (α), and thus the null hypothesis (no trend) is rejected. A detailed discussion of the Mann-Kendall test and its application to evaluate hydrological time series is provided by *Douglas et al.* [2000].

2.1.2 Pettit Change-Point Test

Nonstationarity in time series can also be characterized by abrupt shifts in the mean or variance of the series. To identify possible shifts, standard change-point procedures have been applied to multiple time series in earth sciences including precipitation and temperature [*Tome et al.*, 2004]. One type of homogeneity (change-point) test is the Pettitt test [*Pettitt*, 1979], which is a non-parametric test—requiring no assumption of the underlying distribution.

The Pettitt test is a version of the Mann-Whitney two-sample test which allows for identification of the time t at which a possible abrupt shift may occur. Under the null hypothesis, the time series is composed of homogeneous variables which follow the same distribution (with same location parameter, but not necessarily equal variance). Under the alternative hypothesis, the mean of the subseries prior to time t is statistically different from the mean of the subseries after time t . In order to test for

shifts in the variance of the distribution, the data set is first transformed such that identified shifts are inferred from changes in average variance between the two subseries [e.g., *Villarini et al.*, 2009].

To perform the two-tailed hypothesis test on the location parameter (mean), the Pettitt test statistic is calculated as:

$$D_{ij} = \begin{cases} -1 & (x_i - x_j) < 0 \\ 0 & (x_i - x_j) = 0 \\ 1 & (x_i - x_j) > 0 \end{cases} \quad (5)$$

where x_i and x_j correspond to the magnitude of the hydroclimatic variable under consideration, and x_i precedes x_j in time. For evaluation over the entire sample (T years), these D statistics are combined as follows:

$$U_{t,T} = \sum_{i=1}^t \sum_{j=t+1}^T D_{ij} \quad (6)$$

The statistic $U_{t,T}$ is equivalent to a Mann-Whitney statistic for testing that the two samples X_1, \dots, X_t and X_{t+1}, \dots, X_T come from the same population. The test statistic $U_{t,T}$ is evaluated for all possible values of t ranging from 1 to T . The most probable year of a change-point occurring is evaluated using a two-tailed test on the following statistic:

$$K_T = \max_{1 \leq t < T} |U_{t,T}| \quad (7)$$

If the statistic K_T is significantly different from 0, then a change-point occurs in the year t corresponding to the point in time for which the absolute value of $U_{t,T}$ is obtained. To evaluate the significance of the test, a Monte Carlo resampling procedure within XLSTAT was applied to calculate corresponding p-values [XLSTAT, 2011]. The statistic K_T is significantly different from 0, and thus a change-point is said to occur, when the p-value is less than the desired level of significance (α).

2.1.3 Hurst's Exponent

The Hurst exponent, H , is a common indicator of long-term persistence in hydrologic data [Hurst, 1951]. Evaluation of the presence of long-term persistence is particularly important as gauged records are often relatively short, and thus identified trends could be part of a long-term cycle not apparent in the available record [Hamad, 2009]. The Hurst exponent is estimated using a rescaled range (R/S) analysis wherein the range of partial sums of departures of a time series from its mean is rescaled by its standard deviation [Sakalauskiene, 2003]. For a representative time series, $(X = X_1, X_2, \dots, X_n)$ and $[t = 1, 2, \dots, n]$, the R/S analysis is performed as follows. First, the mean (m) of the n observations in the total time series is computed:

$$m = \frac{1}{n} \sum_{i=1}^n X_i \quad (8)$$

The mean adjusted series, Y , is then obtained as

$$Y_t = X_t - m \quad (9)$$

Summing over the mean adjusted series through time t (for $t = 1, \dots, n$) yields the cumulative deviate series Z :

$$Z_t = \sum_{i=1}^t Y_i \quad (10)$$

The range series, R , is defined as

$$R_t = \max(Z_1, Z_2, \dots, Z_t) - \min(Z_1, Z_2, \dots, Z_t) \quad (11)$$

where $\max(Z_1, Z_2, \dots, Z_t)$ is the adjusted surplus and $\min(Z_1, Z_2, \dots, Z_t)$ is the adjusted deficit. The standard deviation, S , for observations through time t is calculated as

$$S_t = \sqrt{\frac{1}{t} \sum_{i=1}^t (X_i - u)^2} \quad (12)$$

where \bar{u} is the mean value of the observations $\{X_1, \dots, X_t\}$. The standard deviation for time t is then used to scale the corresponding sample range for time t to yield the rescaled range series (R/S) :

$$(R/S)_t = R_t/S_t \quad (13)$$

By analyzing long term storage requirements of the Nile River, *Hurst* [1951] found that (R/S) scales by the power-law as time increases:

$$(R/S)_t = (c)t^H \quad (14)$$

where c is a scaling constant. The expected value of the rescaled range, or $E \left[\frac{R_t}{S_t} \right]$, is determined over partial time series (subseries of the overall record) and converges on the Hurst exponent power function [*Bras and Rodriquez-Iturbe*, 1985]:

$$E \left[\frac{R_t}{S_t} \right] = cn^H \text{ as } n \rightarrow \infty \quad (15)$$

When the time series is truly random, i.e. representing a random walk, the expected value is described by the power $H = 0.5$ [*Sakalauskiene*, 2003]. If the Hurst exponent is between $0.5 < H \leq 1$, the time series shows signs of long-term persistence [*Sakalauskiene*, 2003]. For $0 \leq H < 0.5$, the time series exhibits signs of anti-persistent behavior, or a mean reverting system—the assumption that extremes within the data set are temporary, and that values will return to the average over time [*Sakalauskiene*, 2003].

2.2 Nonstationarity in Annual Maximum Flood Series

Identification of nonstationarity in both the magnitude and timing of AMF series is analyzed in the form of trends and abrupt shifts by means of standard statistical tests. In particular, Mann-Kendall trend and Pettitt change-point tests are employed as discussed above. The magnitude of AMF peaks are also analyzed for indications of long-term persistence using the Hurst exponent.

2.2.1 Data

Data used in this research includes AMF series for streamflow gauging stations throughout the continental United States selected from the USGS Hydro Climatological Data Network (HCDN) [Slack *et al.*, 1993]. The 1,659 sites included in the HCDN are scattered across 21 water resources regions of the U.S.; only the first 18 regions delineated for the continental U.S. are considered in this study (Figure 2.2). A total of 569 stations were used in this study, based on the criteria of having at least a continuous record for the period of 1940-2005 (Figure 2.3). As the HCDN only contains data through 1988, updated flood records were obtained from the U.S. Geological Survey (USGS) website (<http://nwis.waterdata.usgs.gov/usa/nwis/peak>). The minimum record length of 66 years is long enough to test for trends and other forms of nonstationarity in the flood series with reasonable certainty, as well as to identify physical and/or climatic causes of the nonstationarity as discussed in Chapter 3.

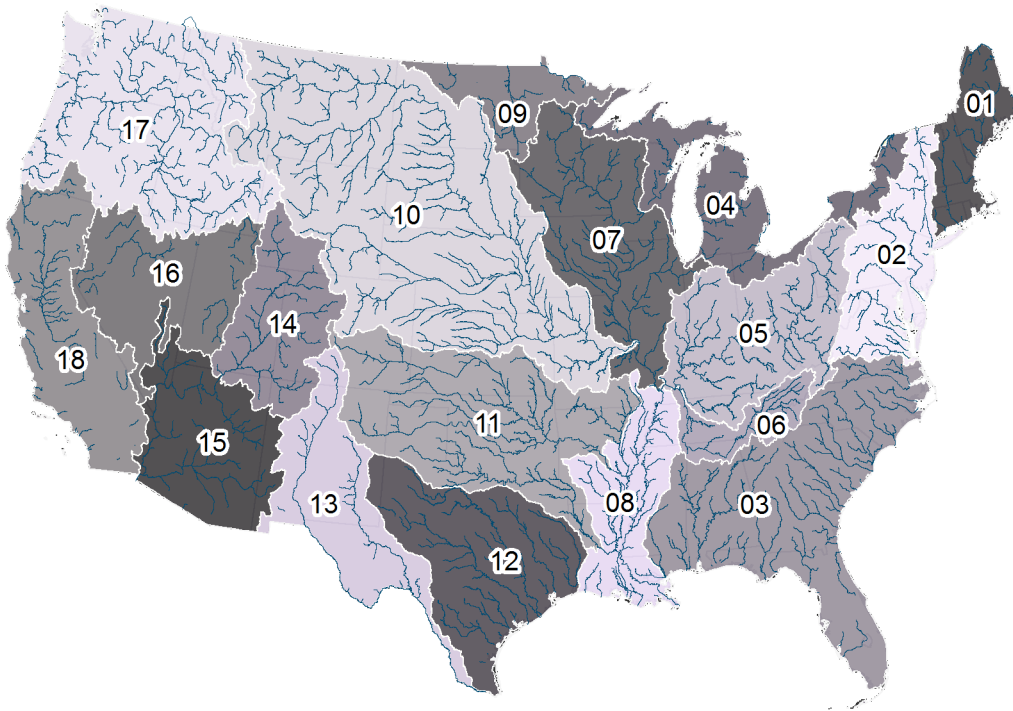


Figure 2.2 Water-resources regions (gray-scale polygons) and major rivers (blue lines) of the continental U.S as defined by the USGS.

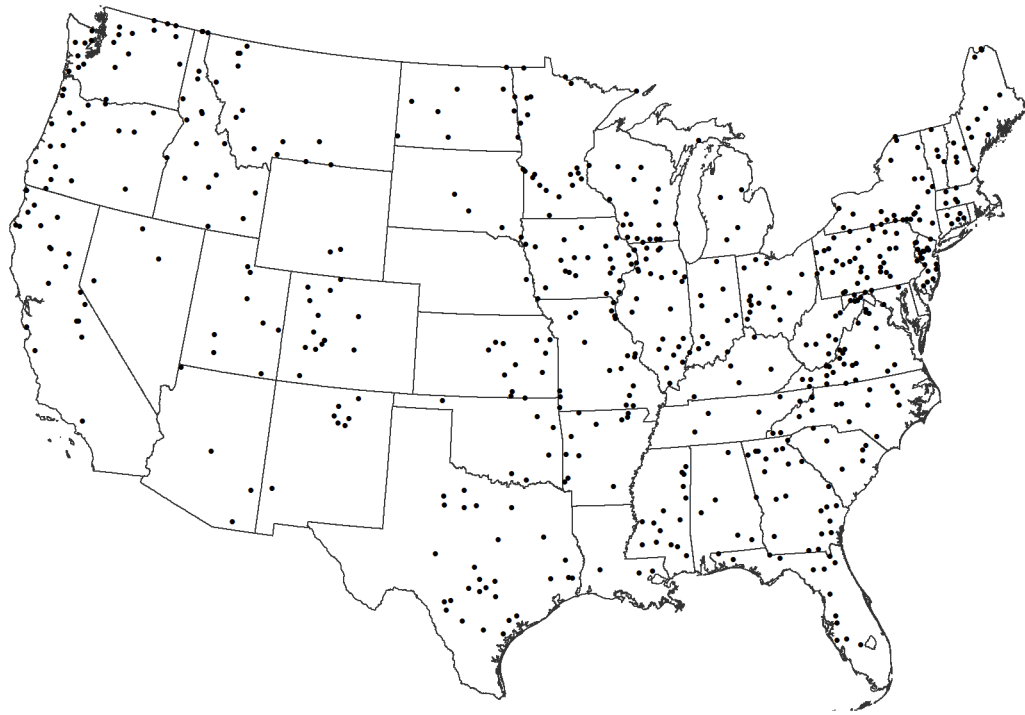


Figure 2.3 Location of 569 unimpaired USGS streamflow gauging stations within the continental U.S. selected from the HCDN having at minimum a continuous annual maximum flow record from 1940-2005.

2.2.2 Trends in Magnitude of Annual Maximum Flood Series

Trends in the magnitude of AMF series at each site in Figure 2.3 were identified by employing two versions of a standard MK test—both neglecting autocorrelation, and accounting for autocorrelation. In the latter case, each flood series was checked for autocorrelation, and appropriate modifications of the MK test were employed to avoid possible spurious results [Hamad and Rao, 1998; Yue *et al.*, 2002; Cohn and Lins, 2005; Hamad, 2009]. For significance levels of 5% and 10%, Figure 2.4 illustrates the location of sites for which significant trends were identified when autocorrelation is neglected; results of the MK tests when accounting for autocorrelation are shown in Figure 2.5. Herein, parenthesized values within figure legends correspond to the number of sites illustrated for their respective categories (e.g., (48) in Figure 2.4 indicates 48 stations were identified to have a negative trend significant on the 5% level). Considering results

at the 10% level, if possible autocorrelation is ignored (Figure 2.4), 59 of the 569 sites analyzed exhibit an upward trend indicating increasing flood risk over time; 70 sites exhibit a downward trend indicating decreasing flood risk over time. When accounting for the effects of autocorrelation using the procedure of *Yue and Wang* [2002, 2004], 53 sites exhibit a positive trend, and 58 sites exhibit a negative trend in the magnitude of flood peaks at the 10% level. A total of 129 significant trends (10% significance level) were identified when effects of autocorrelation were not accounted for, 111 trends were identified as significant when accounting for autocorrelation; only 69 of the trends identified in both analyses were found at common sites. These numbers exceed what would be expected due to random variability (i.e., 57 trends identified on 10% level), and thus the results do imply that trends exist in AMF series. After applying the Bonferroni correction to the results in Figure 2.4, 63 sites are still observed to exhibit a significant trend.

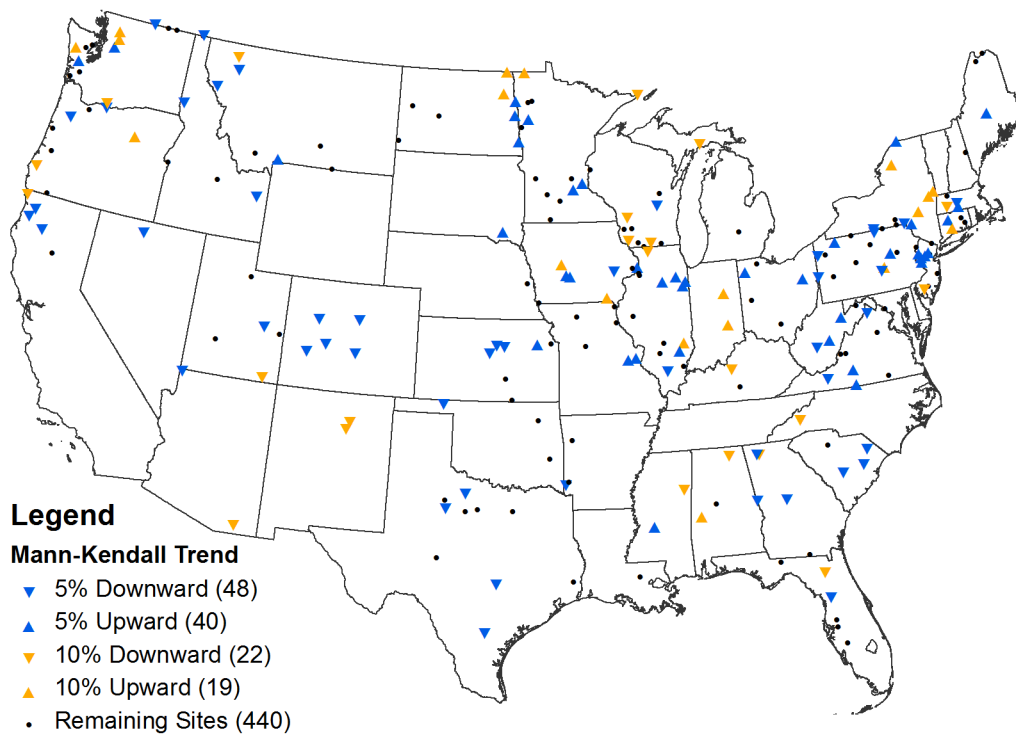


Figure 2.4 Results of traditional Mann-Kendall trend tests on magnitude of AMF series (neglecting possible autocorrelation). Upright (inverted) triangles represent sites with a positive/increasing (negative/decreasing) trend.

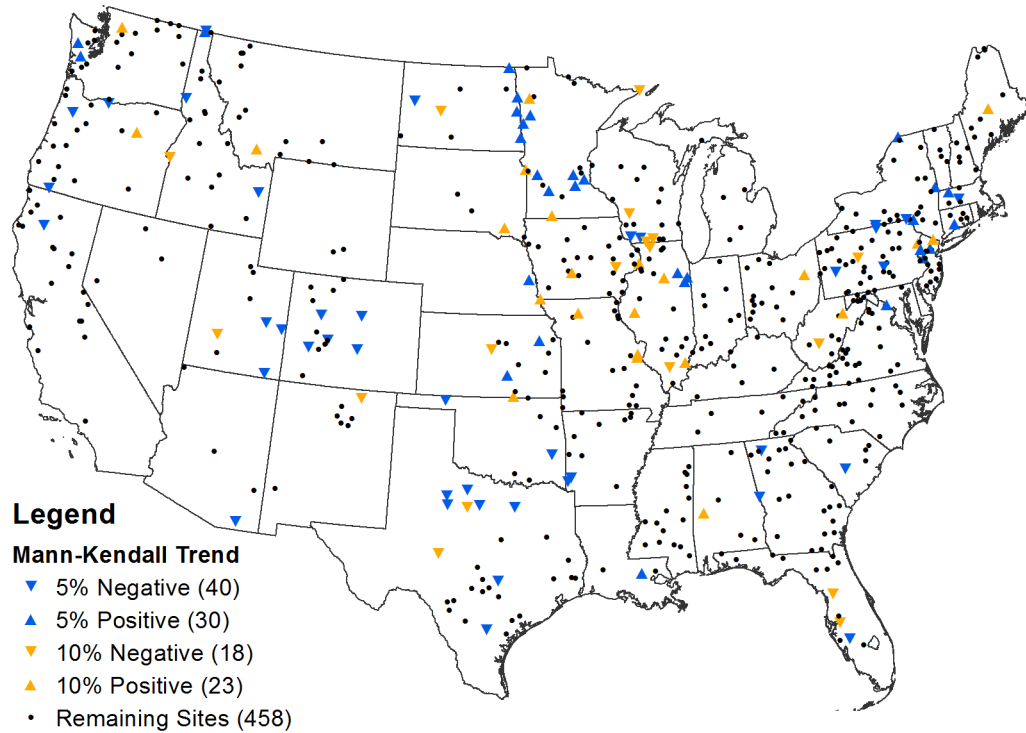


Figure 2.5 Results of modified Mann-Kendall trend tests on magnitude of AMF series (accounting for autocorrelation). Upright (inverted) triangles represent sites with a positive/increasing (negative/decreasing) trend.

Trends are evident across the U.S. both when neglecting and accounting for effects of autocorrelation in the magnitude of AMF series. Clusters of sites containing mixtures of negative and positive trends are found throughout areas of the U.S (Figure 2.4, Figure 2.5). Similar patterns of identified trends in the Eastern and Midwestern U.S. were reported in previous studies [e.g., *Villarini and Smith, 2010*; and *Villarini et al., 2011*]. APPENDIX A provides additional details of the trend analyses, reporting the direction of trends and corresponding p-values for sites with significant results at the 10% level.

2.2.3 Change-Points in Magnitude of Annual Maximum Flood Series

The Pettitt change-point test was used to identify potential shifts in the mean of the AMF series for each of the 569 sites in Figure 2.3. As illustrated in Figure 2.6, 202 stations were found to have a significant change-point in the mean of the AMF series at the 10% level. The years in which these abrupt shifts occurred are indicated in Figure 2.7. Sites

exhibiting a significant change-point in the mean flood magnitude tend to be scattered throughout the U.S., although sites in close proximity often show shifts around the same time period. The timing of these change-points is especially important when considering the causes of nonstationarity, whether human induced or due to natural climate variability, as is discussed in Chapter 3. In the Eastern and Midwestern U.S., identified patterns of change-points in the mean of AMF series support previous findings [e.g., Villarini and Smith, 2010; Villarini *et al.*, 2011]. APPENDIX A provides additional details of the change-point analyses, reporting the timing and corresponding p-values for sites with significant results at the 10% level.

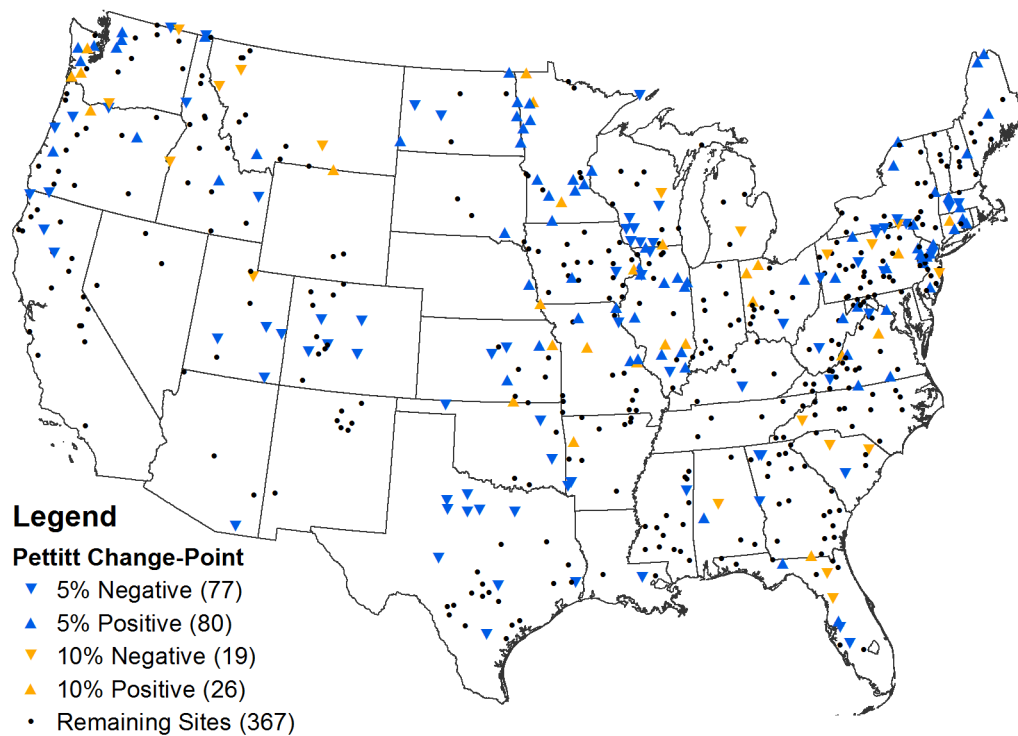


Figure 2.6 Locations of sites with a change-point in the mean annual maximum flood magnitude significant at 5% and 10% levels.

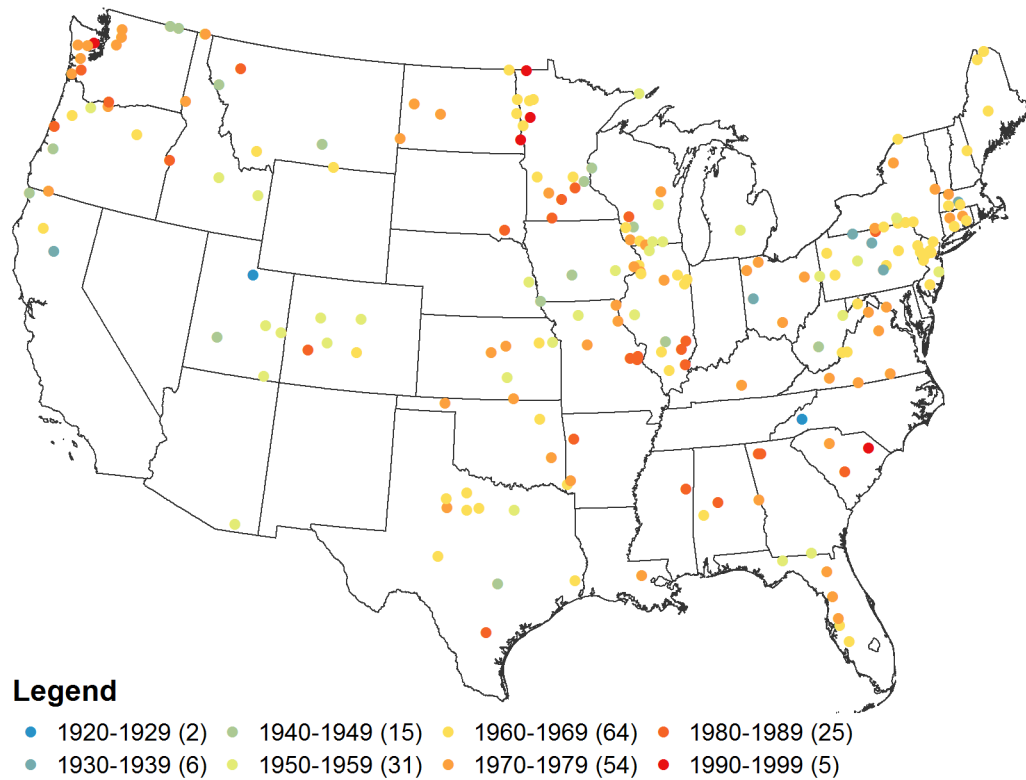


Figure 2.7 Time period in which a change-point in the mean annual maximum flood magnitude was identified by the Pettitt test (10% significance level).

Of the 202 sites identified to contain a change-point, 98 sites also exhibit a significant trend over the entire period of record; thus, of the 129 sites determined to exhibit a trend as shown in Figure 2.4, only 31 sites show signs of nonstationarity only in the form of trends. As the presence of change-points (abrupt shifts) in the mean of AMF series can produce spurious results of the MK trend test, the remaining 98 sites should be further investigated. Herein, for all 202 sites identified to have a significant change-point in the mean flood magnitude, the subseries before and after the shift were checked independently for temporal trends using Mann-Kendall tests. This type of analysis is in line with recommendations of others who indicate the need to couple trend and change-point tests when investigating nonstationarity in hydroclimatic series to limit false detection of trends [e.g., McCabe and Wolock, 2002; Kalra *et al.*, 2006; Seidou and Ouarda, 2007; Ehsanzadeh *et al.*, 2010].

The MK test results for each subseries of the 202 sites in question are illustrated in Figure 2.8 and Figure 2.9. A substantial reduction in the number of significant trends is observed when evaluating trends in subseries based on respective change-point dates. A breakdown of the results is provided in Table 2.1. Of the 98 sites observed to exhibit a trend in the complete record, 68 sites do not exhibit trends once the change-points are accounted for. Overall, significant trends were not identified in either subseries (before or after change-point) for 152 of the 202 sites analyzed. In addition to significant trends in the complete series, subseries at 15 sites were identified to exhibit a trend before the identified change-point, and 13 sites exhibit a trend in the subseries after the identified change-point. Only 2 sites exhibit trends in all series analyzed. These results are again consistent with findings of *Villarini and Smith* [2010], and *Villarini et al.* [2011]. APPENDIX A provides additional details of the trend analyses performed on the subseries, reporting the direction of trends and corresponding p-values.

Table 2.1
Number of trends identified in the complete record and/or subseries with respect to
identified change-points in mean flood magnitude.

Trend Identification	Count
Before, After, Complete	2
Before, Complete	15
After, Complete	13
Before	13
After	7
Complete	68
No Trend	84

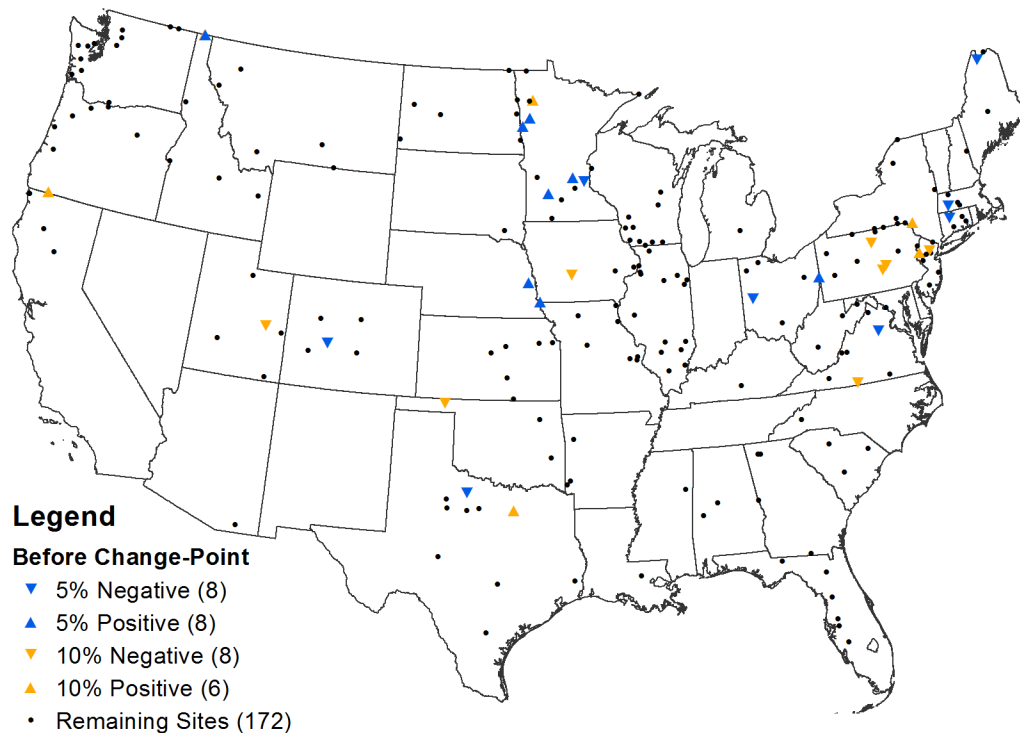


Figure 2.8 Results of Mann-Kendall trend tests on annual maximum flood subseries before identified change-point in mean flood magnitude.

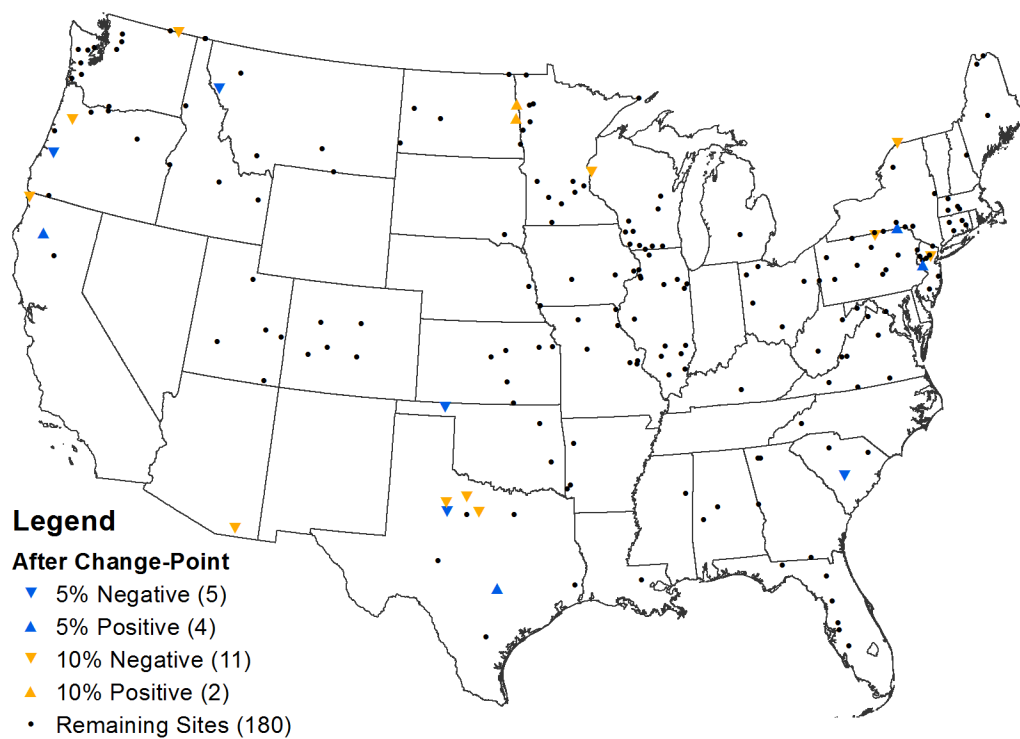


Figure 2.9 Results of Mann-Kendall trend tests on annual maximum flood subseries after identified change-point in mean flood magnitude.

2.2.4 Long-Term Persistence in AMF Series

As a trend and/or change-point identified as statistically significant could be part of a long-term cycle not apparent in the available record [Hamad, 2009], the Hurst exponent [Hurst, 1951] was used as an indicator of long-term persistence in AMF series. Of the 569 sites analyzed, 537 sites show signs of long-term persistence with H values greater than 0.5; the locations of these sites are illustrated in Figure 2.10. APPENDIX A includes tables of the estimated Hurst coefficients for all sites showing signs of long-term persistence at the 10% significance level. As the majority of the sites analyzed show signs of persistence, these results suggest that hydroclimatic time series may be affected by large-scale climatic patterns (e.g., PDO, AMO or NAO) with variations on decadal time scales, contrary to assumptions made in *Bulletin 17B*. Therefore, it is suggested that future work apply spectral analyses to identify the possible timing of cyclical oscillatory behavior in flood series [Baldwin and Lall, 1999].

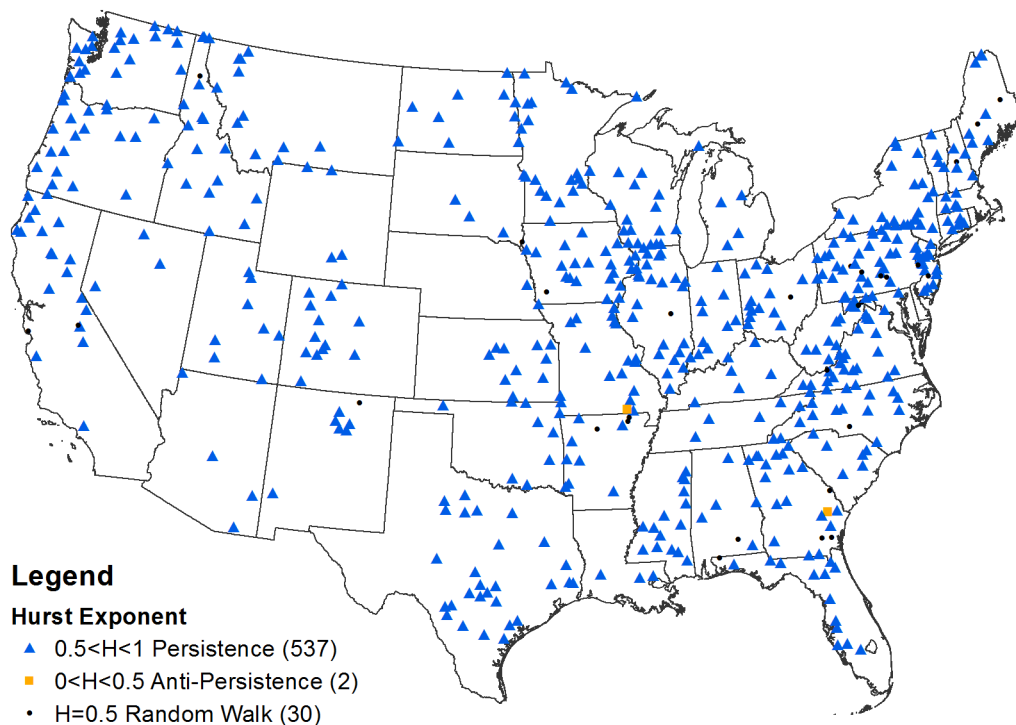


Figure 2.10 Magnitude of Hurst exponent for annual maximum flood series in the contiguous U.S. with continuous record lengths of at least 66 years.

2.2.5 Nonstationarity in the Timing of Flood Peaks

Nonstationarity in AMF series may also be exhibited in the form of changes in the timing of flood peaks, either as an abrupt shift (change-point) or a linear trend indicating, for instance, a steady change towards an earlier spring. Possible shifts in the timing of flood peaks in the form of linear trends were investigated at each station in Figure 2.3 by performing a MK test on the day of the water year the AMF peaks occurred (day 1 = October 1). The locations of sites with significant trends identified at both the 5% and 10% significance levels are shown in Figure 2.11. Of the 569 sites analyzed, only 29 stations exhibit an upward trend potentially indicating floods are occurring later in the water year; 43 stations exhibit a downward trend suggesting floods are occurring earlier in the water year. However, as the number of trends identified is less than what would be expected due to random variability, few conclusions can be made based on these results. Also, as no spatial patterns are evident in the data, it is unclear whether or not there are regional influences causing these trends.

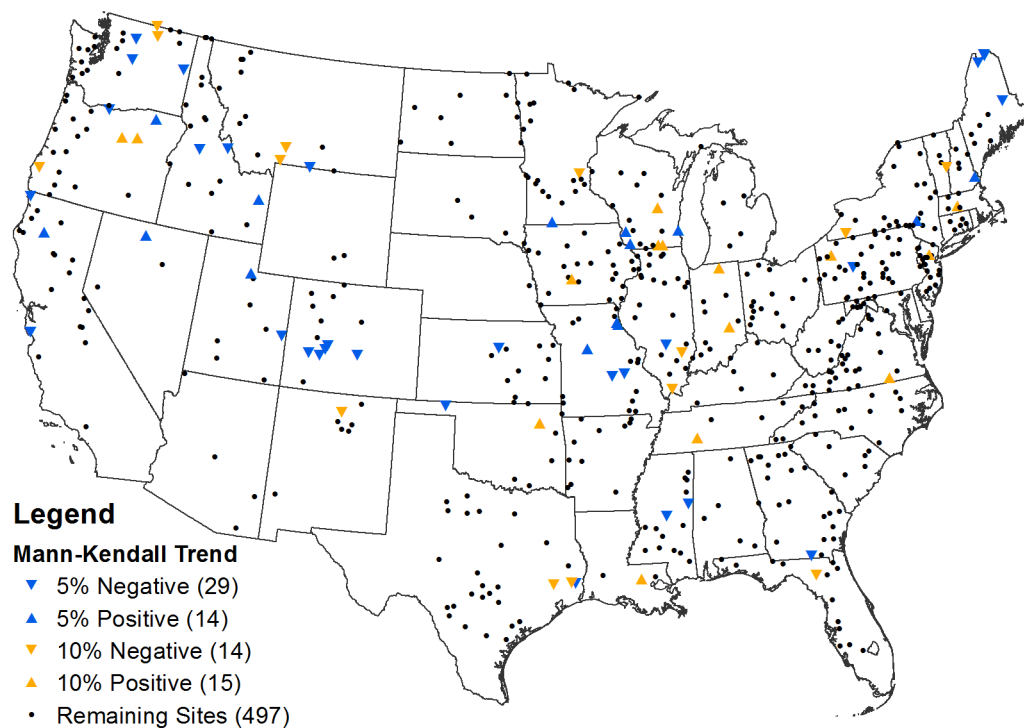


Figure 2.11 Results of Mann-Kendall trend tests on the day of occurrence of annual maximum flood peaks.

To confirm whether identified trends in the timing of flood peaks are truly gradual over time, or a spurious result due to an abrupt shift, the Pettitt change-point test was also applied to the day of occurrence series for each site in Figure 2.3. Of the 569 sites analyzed, 66 stations were identified to have a significant change-point in the mean day of occurrence of AMF peaks at the 10% level (Figure 2.12). The years in which these abrupt shifts occurred are indicated in Figure 2.13. Of the 66 stations, 33 had been identified to exhibit a trend in the complete record using the MK test; thus, nonstationarity in the time of occurrence at these sites may be better characterized by an abrupt shift rather than a gradual trend. However, the remaining 39 stations in Figure 2.11 only exhibit a gradual trend in the time of occurrence of flood peaks. Many of the trends and abrupt shifts identified in the time of occurrence of flood peaks occur in the Midwest and Western U.S., potentially due to dam installation in these areas (see CHAPTER 3). APPENDIX B provides additional results for the trend and change-point analyses on the time of occurrence of AMF peaks.

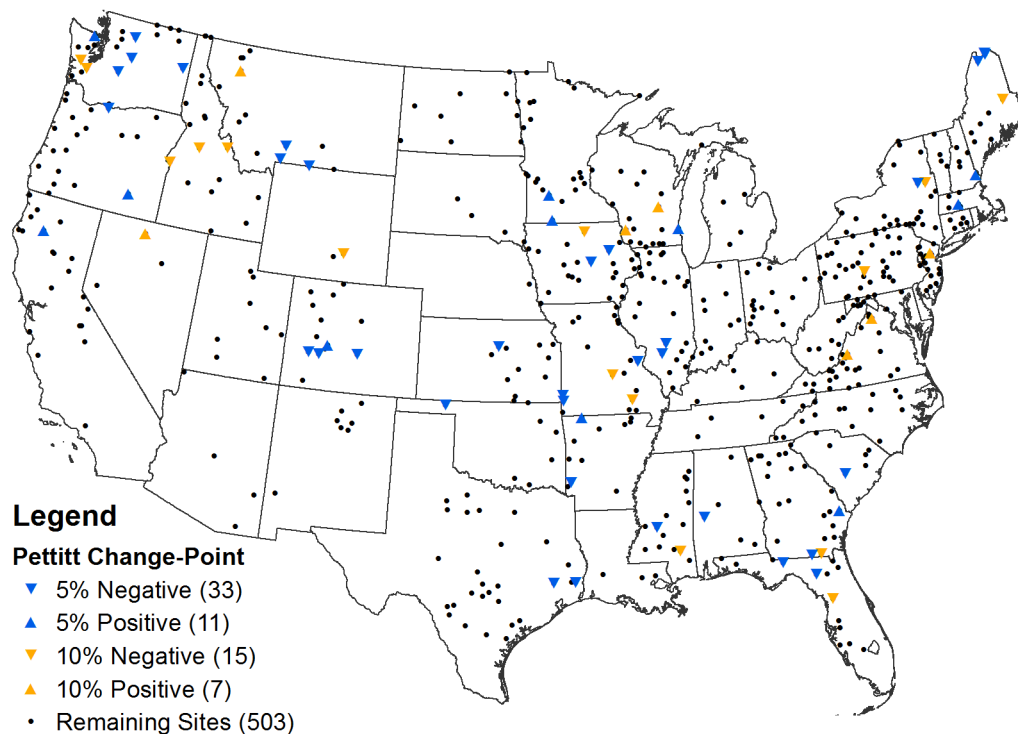


Figure 2.12 Locations of sites with a significant change-point in the mean day of occurrence of the annual maximum flood peak.

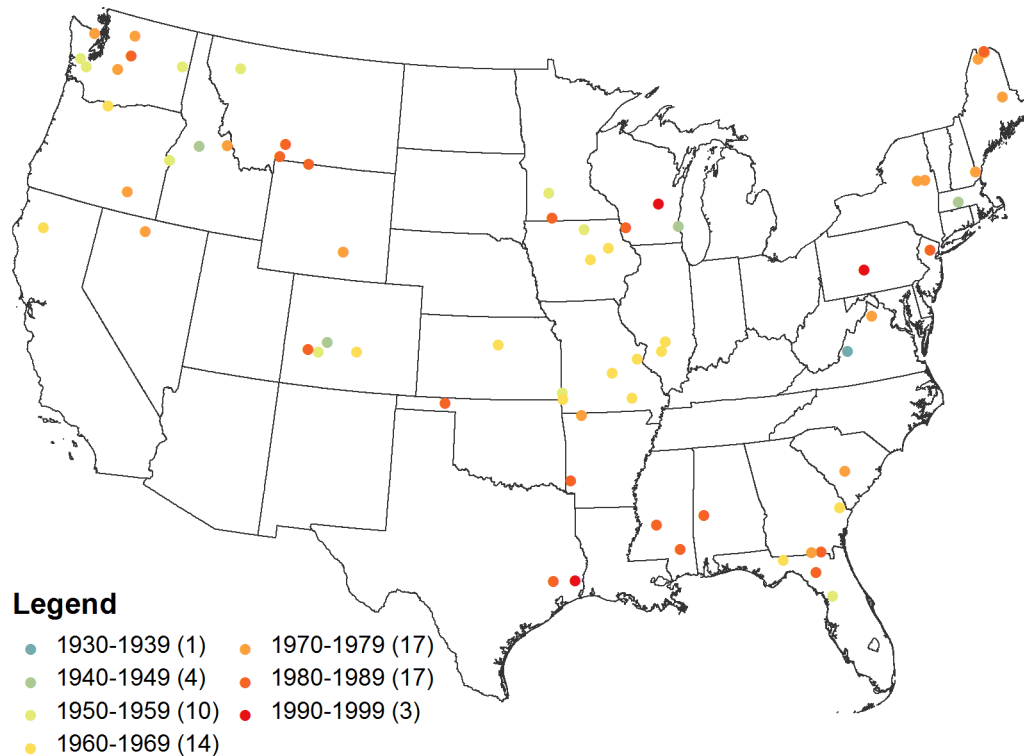


Figure 2.13 Time period of change-points in the mean day of occurrence of flood peaks as identified by the Pettitt test (10% significance level).

2.3 Nonstationarity in Flood Generating Meteorological Series

The results above indicate that flood series corresponding to relatively unimpaired watersheds throughout the U.S. are nonstationary in terms of both flood magnitude, exhibiting either a trend, abrupt shift, or long-term persistence. Possible sources of this nonstationarity will be investigated in Chapter 3. However, because the identified nonstationarity in flood series could be due to nonstationarity in associated precipitation and/or temperature series, the remainder of this chapter seeks to identify nonstationarity in relevant meteorological series. To this end, peak flood associated precipitation and annual temperature series were constructed using gridded daily precipitation and temperature data. Further, as significant effort will be required to identify sources of nonstationarity in the individual flood series, the remaining analyses will be conducted for a smaller region of the U.S. (see Figure 2.14).

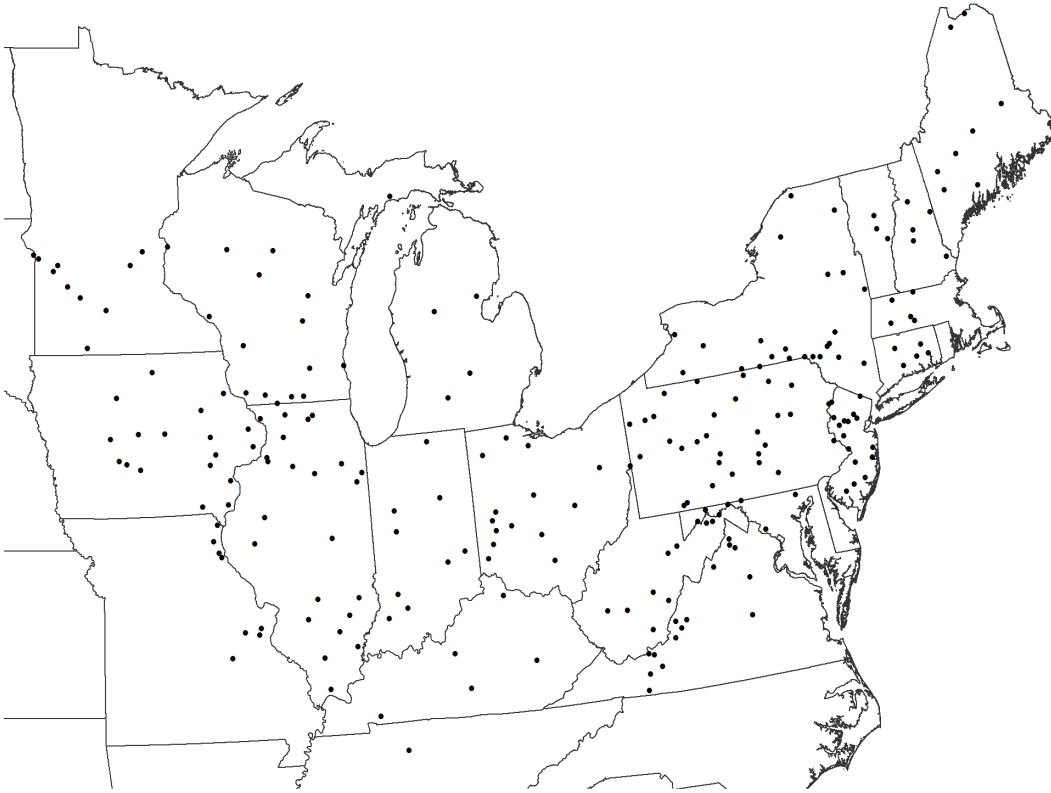


Figure 2.14 Locations of 235 streamflow gauging stations used to create flood associated precipitation and temperature series.

Based on the results of previous studies conducted in the Midwest [e.g., *Changnon and Kunkel*, 1995; *Changnon and Demissie*, 1996], flood generating precipitation series consisting of the total precipitation that occurred within X-days prior to the annual maximum flood peak were constructed for each of the 235 streamflow gauging stations in Figure 2.14. Similarly, flood generating temperature series consisting of the average daily maximum and minimum temperatures over X-days prior to the annual peak flow were constructed. For lead times of $X = 2, 3, 4, 5, 6$, and 7 days, 235 watershed specific precipitation and temperature series were constructed using 1/8 degree gridded daily precipitation (mm/day), and daily maximum and minimum temperatures (C) recorded from 1950 to 2006 (57 years) [*Maurer et al.*, 2002]. For each watershed, precipitation and temperature series were assembled by averaging the daily gridded data relative to the watershed boundary. The daily averages were then summed over the X-days to obtain a total precipitation depth prior to the flood peak, or averaged over the X-days to define the

temperature series. In addition, a coarser resolution precipitation dataset—.25x.25 Daily US UNIFIED Precipitation—was obtained from the National Oceanic & Atmospheric Administration Climate Prediction Center (NOAA CPC) website (<http://www.esrl.noaa.gov/psd/data/gridded/>), and used to construct a second set of flood generating precipitation series. Comparison of results using the 1/8-degree gridded data versus the 1/4-degree gridded data provides insight as to how the spatial resolution of data may influence analyses of nonstationarity.

2.3.1 Trends in Flood Generating Precipitation Series

Mann-Kendall trend tests were employed to investigate trends in the flood generating precipitation series corresponding to the streamflow gauging stations illustrated in Figure 2.14. A positive trend would indicate an increase in the total precipitation series over time, thus one would expect to see similar increases in the magnitude of AMF peaks. Conversely, a negative trend would indicate a decrease in the total precipitation series with respect to time, and thus a decrease in the corresponding flood magnitudes would be expected. The trend analyses for precipitation series were performed on two general categories of data to determine if the spatial scale of data used to construct precipitation series has an effect on trend results:

Category A: Flood generating precipitation series based on 1/8-degree gridded precipitation data.

Category B: Flood generating precipitation series based on 1/4-degree gridded precipitation data.

These analyses include a total of 6 data series (with 2-, 3-, 4-, 5-, 6-, and 7-day lead times) each for Category A and Category B. Table 2.2 provides a summary of the number of sites found to exhibit significant trends at both 5% and 10% significance levels for all series (lead times) considered.

Table 2.2
Number of sites with significant negative and positive trends in flood generating precipitation series identified using Mann-Kendall trend tests.

Lead Time (days)	5% Significance Level		10% Significance Level	
	Negative	Positive	Negative	Positive
<i>Category A: 1/8-degree generated precipitation series</i>				
2	5	20	6	36
3	0	21	0	32
4	0	25	0	43
5	0	21	1	45
6	0	25	1	43
7	2	28	3	49
<i>Category B: 1/4-degree generated precipitation series</i>				
2	8	16	10	32
3	7	17	10	34
4	8	15	9	29
5	3	16	11	33
6	2	18	7	35
7	3	18	5	36

The results in Table 2.2 indicate that both scales of data yield significantly more positive trends than negative trends in all precipitation series analyzed. In general, a greater number of negative trends are identified using coarser scale data (Category B), whereas more significant positive trends are identified with the finer scale data (Category A). Figure 2.15 illustrates the locations of the streamflow gauging stations for which the Mann-Kendall test identified significant trends in the flood generating precipitation series with a 5-day lead time constructed based on 1/8-degree gridded data. Of the 235 series analyzed, 45 sites exhibit an upward trend at the 10% level, indicating an increase in the flood associated precipitation depth; only 1 site exhibits a downward trend indicating a decrease in precipitation depth. The identified increases in flood generating precipitation series are consistent with the expectations of the IPCC [2007a, 2007b]: global warming is anticipated to result in increased precipitation and a higher frequency of heavy

precipitation events in many regions, including the northeastern quadrant of the U.S. The small number of negative trends in the flood generating precipitation series is inconsistent with the number of negative trends identified in AMF series (Figure 2.4); however, there are many other factors such as decreased snow pack or increased dam density/storage which could offset the effects of precipitation, as will be discussed in CHAPTER 3. For the remaining daily precipitation series considered in both categories, figures showing the location of sites with significant results are provided in APPENDIX C.

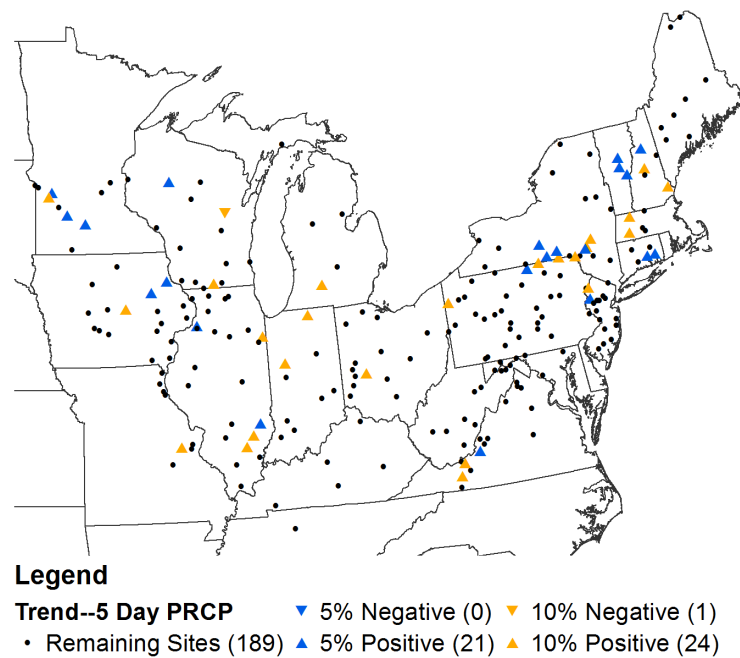


Figure 2.15 Results of Mann-Kendall trend tests on flood generating precipitation series with 5-day lead time constructed using 1/8-degree gridded data.

2.3.2 Change-Points in Flood Generating Precipitation Series

Pettitt change-point tests were conducted to investigate the possible presence of abrupt shifts in the mean of flood generating precipitation series with respect to time. Abrupt changes were investigated for both Categories A and B as previously described. Table 2.3 provides a summary of the number of sites where significant change-points were identified at both 5% and 10% significance levels for all flood generating precipitation series (2- to 7-day lead times) considered. Figure 2.16 shows results of the change-point

tests for precipitation series with a 5-day lead time based on 1/8-degree gridded data (Category A). Of the 235 series analyzed, a total of 62 sites exhibit a shift in the mean of their respective precipitation series. Figures showing the location of sites with significant results are provided in APPENDIX C for the remaining flood generating precipitation series considered in both categories.

Table 2.3
Number of sites with significant change-points in the mean of flood generating precipitation identified using the Pettitt test with 5% and 10% significance levels.

Lead Time (days)	Category A		Category B	
	5%	10%	5%	10%
2	38	53	26	40
3	27	40	27	48
4	32	55	24	47
5	35	62	28	49
6	40	62	28	48
7	45	65	27	52

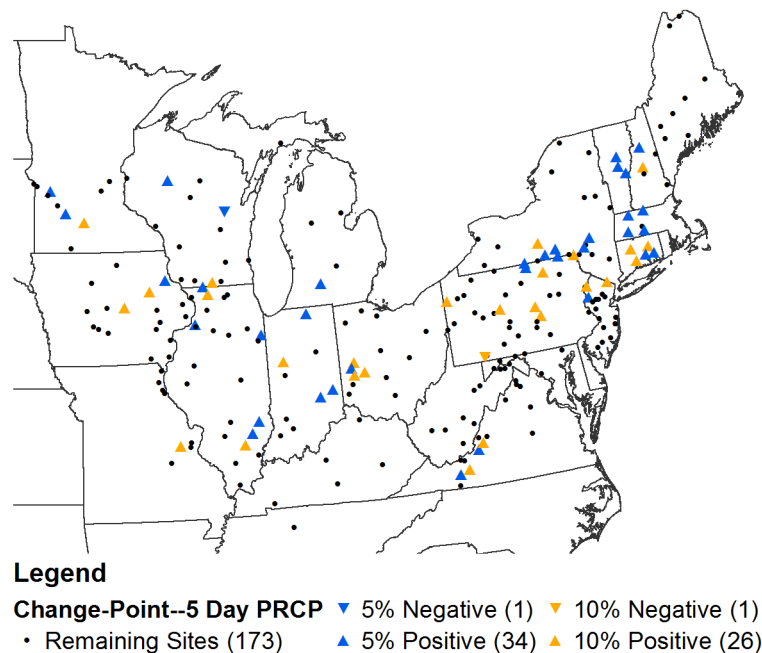


Figure 2.16 Results of Pettitt tests on flood generating precipitation series with a 5-day lead constructed using 1/8-degree gridded data.

The results in Table 2.3 indicate that more change-points were identified on both significance levels for flood generating precipitation series in Category A than those in Category B with the same lead time, except for series with a 3-day lead for which both resolutions of data yielded the same number of significant results at the 5% level. The precipitation series with a 7-day lead exhibit the most change-points on the 10% level compared to other X-day series considered. The increase in the number of identified shifts in the Category A series relative to Category B, as well as the differences observed in Table 2.3 with respect to trends, indicate the importance of the resolution of the data when considering nonstationarity in precipitation data.

2.3.3 Trends in Flood Generating Temperature Series

In response to climate change, future flood risk will likely be influenced by the potential changes in flood generating precipitation series as previously discussed, as well as possible changes in temperature. Projected increases in temperature could lead to decreased snow pack, earlier spring, and drier antecedent moisture conditions, all of which could lead to a decrease in AMF magnitude and/or a change in the timing of peak flood events. Therefore, this section summarizes results of Mann-Kendall tests conducted to investigate trends in flood-generating temperature series. Two types of temperature series (average daily maximum and average daily minimum) were constructed from 1/8-degree data with lead times of 2- to 7-days for the 235 previously described watersheds. Table 2.4 provides a summary of the number of sites where significant trends were identified at both 5% and 10% levels for all series considered. The results for average maximum temperature series indicate that the number of trends identified at the 10% level is relatively independent of the X-day lead time. On the other hand, average minimum temperature series exhibit fewer trends, both negative and positive, as X increases. Both average maximum and minimum temperature series show more increasing (positive) trends than decreasing (negative) trends; this is similar to the findings for trends in precipitation series. The identified increases (warming) in possible flood generating temperature is consistent with *IPCC* findings [2007a, 2007b]: in general

cold days, cold nights, and frost have become less frequent, while hot days, hot nights, and heat waves have become more frequent in the U.S.

Table 2.4
Number of sites with significant trends (negative or positive) in flood generating maximum and minimum temperature series with X-days lead times identified using Mann-Kendall tests.

Lead Time [days]	5%		10%	
	Negative	Positive	Negative	Positive
<i>Average Maximum Temperature</i>				
2	2	17	3	27
3	2	16	4	29
4	1	10	5	24
5	1	9	4	25
6	1	13	3	28
7	1	13	2	29
<i>Average Minimum Temperature</i>				
2	3	36	4	56
3	4	35	4	61
4	4	32	4	60
5	2	27	4	52
6	2	25	2	50
7	2	24	3	47

Figure 2.17 and Figure 2.18 show the locations of the streamflow gauging stations for which the Mann-Kendall test identified significant trends in the flood generating maximum and minimum temperature series with a 4-day lead time, respectively. Of the 235 series analyzed, 24 sites exhibit an upward trend in maximum temperature; only 5 sites exhibit a downward trend in maximum temperature. A greater portion of sites (60) exhibit an upward trend in minimum temperature; only 4 sites exhibit a downward trend. Overall, these results indicate a warming trend in this region, although no spatially coherent patterns or clustering of significant results are evident. Figures showing the location of sites with significant results for the remaining minimum and maximum temperatures series are provided in APPENDIX D.

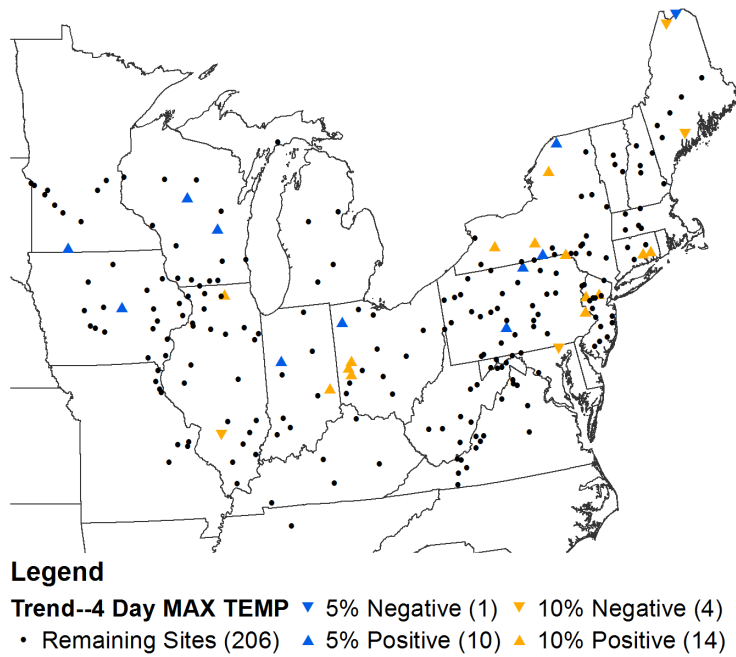


Figure 2.17 Results of Mann-Kendall tests on flood generating maximum temperature series with a 4-day lead time.

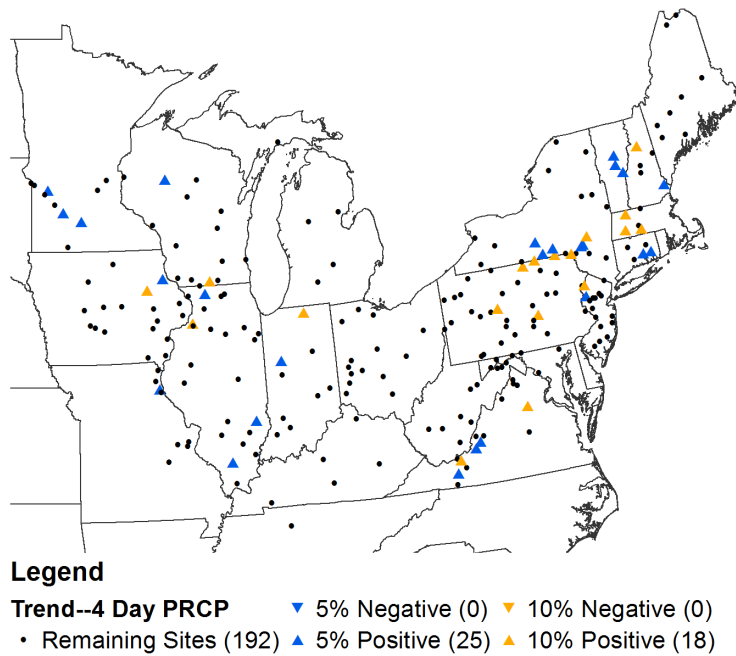


Figure 2.18 Results of Mann-Kendall tests on flood generating minimum temperature series with a 4-day lead time.

2.3.4 Change-Points in Flood Generating Temperature Series

Pettitt change-point tests were conducted to investigate abrupt shifts in temperature series. Identification of a change-point would indicate an abrupt shift in the mean of the flood associated temperature series with respect to time. Both average minimum and maximum temperature flood associated series were considered as previously described. Table 2.5 provides a summary of the number of sites where significant change-points were identified at both 5% and 10% levels for all series considered (lead times of 2- to 7-days). Overall, more change-points were identified for the minimum temperature series as compared to the maximum temperature series for each X-day lead time considered.

Table 2.5
Number of sites with change-points in the mean of flood associated minimum and maximum temperature series identified using the Pettitt test with 5% and 10% significance levels.

Lead Time (days)	Minimum Temperature		Maximum Temperature	
	5%	10%	5%	10%
2	33	51	22	29
3	31	58	20	29
4	29	49	13	28
5	27	48	12	26
6	29	48	17	33
7	28	51	17	38

Figure 2.19 and Figure 2.20 show the locations of the streamflow gauging stations where significant change-points were identified for the maximum and minimum temperature series with 4-day lead times, respectively. No spatial pattern is evident in these results. For the remaining lead times employed to define minimum and maximum temperatures series, figures showing the location of sites with significant results are provided in APPENDIX D.

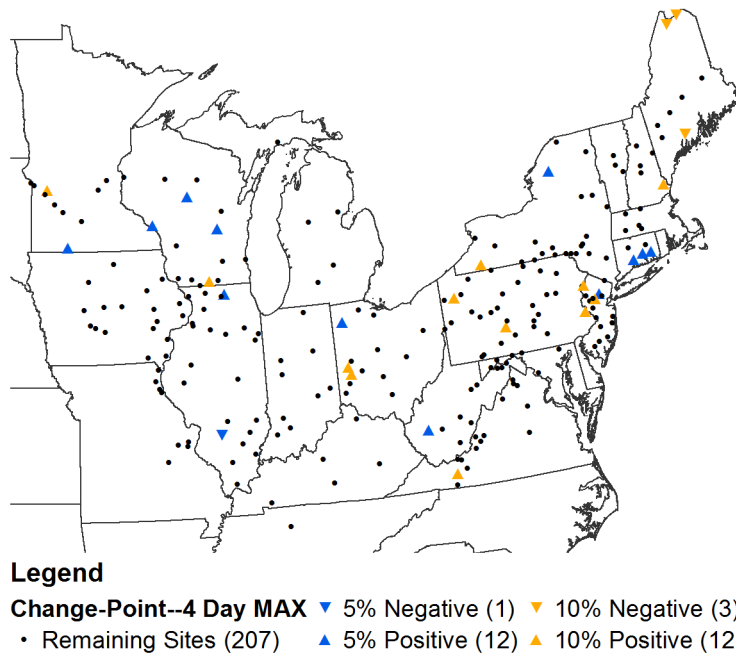


Figure 2.19 Results of Pettitt tests on flood generating maximum temperature series with a 4-day lead time.

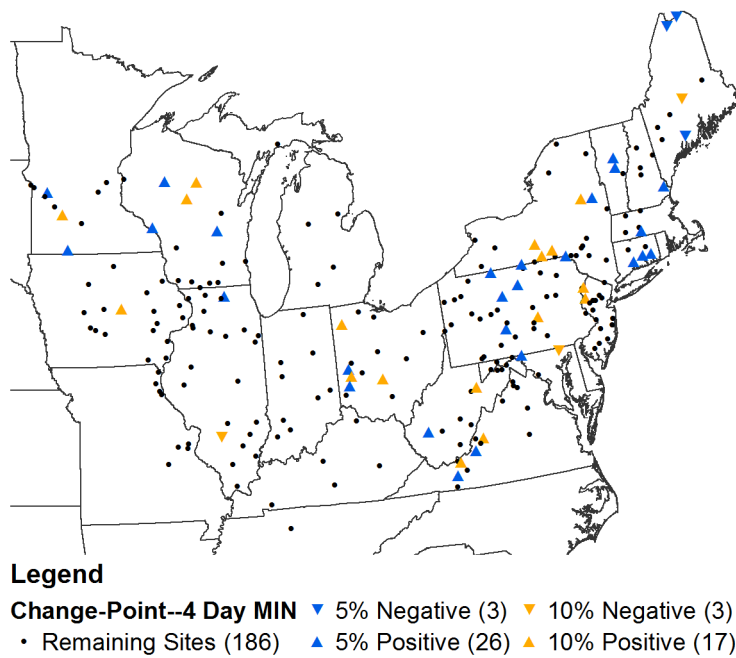


Figure 2.20 Results of Pettitt tests on flood generating minimum temperature series with a 4-day lead time.

CHAPTER 3 SOURCES OF NONSTATIONARITY IN ANNUAL MAXIMUM FLOOD SERIES

Results presented in CHAPTER 2 reveal that some annual maximum flood (AMF) series throughout the U.S. exhibit nonstationarity in the form of monotonic trends, change-points and/or long-term persistence. In the context of water resources applications, it is necessary to move beyond simply assessing the degree of nonstationarity in these series, to consider the driving causes of these observed changes in flood magnitude and the associated flood risk. Due to the variety of forms of nonstationarity exhibited in flood series and numerous possible climatic and human-induced causes of this nonstationarity, a mixture of statistical and inferential methods are employed herein to identify the causes of nonstationarity. Correlation analyses are used to assess the strength of association between flood series and climatic variables; correlation analyses are not conducted with respect to physical parameters (e.g., land cover and dam storage), due to the limited availability of relevant data over time. The influences of climatic shifts are assessed by comparing the timing of identified change-points in the AMF series to those of documented phase changes in oceanic-atmospheric patterns. Similar comparisons are made between the timing of change-points in AMF series and those in climatic series (precipitation and temperature), as well as documented modifications of the watershed and the channel. These results are indicative of the primary causes of nonstationarity in AMF series for unimpaired watersheds in the U.S.; however, more detailed analyses on a site specific basis are needed before this information could be used to increase the accuracy of forecasts of future flood risk.

3.1 Methods for Evaluating Correlation

Correlation analyses have been employed extensively in the hydrologic literature to increase understanding of the relationships between various streamflow quantities and climate parameters [e.g., *Jain and Lall, 2000; Stewart et al., 2005; Tootle et al., 2005; Kashelkar, 2009*]. Several studies have also investigated physical and/or climatic

relationships with streamflow quantities by means of linear regression analyses [Changnon and Kunkel, 1995; Changnon and Demissie, 1996; Olsen *et al.*, 1999; Regonda *et al.*, 2005], for which the significance of model coefficients is based on the strength of the correlation between the response variable and each independent variable. In general, these analyses reveal trends and patterns amongst climate/meteorological parameters common to those identified in streamflow series. To investigate the relationship between climate variables and flood magnitude, three common measures of correlation—Pearson’s r , Kendall’s tau, and Spearman’s rho—are employed herein to measure the strength of association between the variables. These methods are described in further detail below.

3.1.1 Pearson’s Correlation

The most common measure of dependence is Pearson’s correlation coefficient, ρ_{XY} , which measures the degree of linear correlation between two variables X and Y . The correlation coefficient ranges from -1 (strong negative correlation) to +1 (strong positive correlation); $\rho_{XY} = 0$ when no discernible linear relationship exists between the two variables. The equation describing the linear relationship between X and Y can be obtained by performing a regression analysis. The correlation coefficient is calculated as:

$$\rho_{XY} = \frac{cov(X, Y)}{\sigma_X \sigma_Y} \quad (16)$$

where $cov(X, Y)$ is the covariance between the two variables, and σ_X and σ_Y are the standard deviations of X and Y , respectively. Pearson’s correlation is a dimensionless value and is invariant to changes in units of either variable. However, this measure of correlation is sensitive to outliers, and is not robust if X and Y exhibit a nonlinear relationship [Helsel and Hirsch, 2002].

The Pearson product-moment correlation coefficient (r) is a maximum likelihood estimator of ρ_{XY} , and is calculated as:

$$r = \frac{\sum_{i=1}^n (x_i - \bar{x})(y_i - \bar{y})}{[\sum_{i=1}^n (x_i - \bar{x})^2 \sum_{i=1}^n (y_i - \bar{y})^2]^{1/2}} \quad (17)$$

where x_i and y_i are the values of the i^{th} observations, \bar{x} and \bar{y} are the sample means of X and Y, respectively, and n is the number of concurrent observations within the dataset. The significance of the observed correlation (pattern) is assessed by means of a two-tailed hypothesis test to determine if the correlation is statistically different from zero. The test assumes the data follows a bivariate normal distribution, and thus the test statistic follows a t-distribution with n-2 degrees of freedom. The test statistic is calculated as:

$$t^* = r \sqrt{\frac{n-2}{1-r^2}} \quad (18)$$

The null hypothesis that $\rho_{XY} = 0$ (no linear relationship between X and Y) is rejected if $|t^*| \geq t_{\frac{\alpha}{2}, n-2}$, or if the associated p-value is less than the desired significance level α . Additional details of the Pearson correlation test are provided by *Helsel and Hirsch* [2002].

3.1.2 Kendall's Tau Correlation

Kendall's tau (τ) is a non-parametric measure of the degree of monotonic correlation, whether linear or nonlinear, between two variables, X and Y. The Kendall τ coefficient depends only on the ranks of the data, not the actual observed values. As such, τ is resistant to the effects of outliers, and is not affected by power transformations of one or both variables. These properties of Kendall's tau make it more powerful than the Pearson's correlation coefficient for use in discerning the strength of relationships between two variables.

The τ coefficient is computed as a function of the degree of agreement/disagreement amongst pairs of observations (x_i, y_i) and (x_j, y_j) . Agreement, or concordance, among pairs is observed when the ranks of y increase (or decrease) with the ranks of x. Conversely, disagreement, or discordant pairs are those in which the ranks of y decrease as those of x increase, or vice versa. The test statistic S, which measures the monotonic dependence of

Y on X, and is computed by taking the difference between the number of discordant pairs (M) and the number of concordant pairs (P):

$$S = P - M \quad (19)$$

The τ coefficient is then calculated as follows:

$$\tau = \frac{S}{n(n-1)/2} \quad (20)$$

where n is the sample size, and the denominator represents the total number of pairs. As with Pearson's r , Kendall's τ must be in the range $(-1, +1)$ where $\tau = +1$ for perfect agreement, $\tau = -1$ for perfect disagreement, and $\tau = 0$ when X and Y are independent [Helsel and Hirsch, 2002].

The significance of τ is evaluated using a two-tailed hypothesis test to determine if S (and thus τ) is statistically different from zero. For n greater than 10, S is transformed to define a standard normal Z statistic as follows:

$$Z = \begin{cases} (S - 1)/\sigma_s & \text{if } S > 0 \\ 0 & \text{if } S = 0 \\ (S + 1)/\sigma_s & \text{if } S < 0 \end{cases} \quad (21)$$

where

$$\sigma_s^2 = \frac{n(n-1)(2n+5)}{18} \quad (22)$$

in the instance that no ties are observed. When data values are tied, the following correction is applied to σ_s^2 :

$$\sigma_s^2 = \frac{n(n-1)(2n+5) - \sum_{i=1}^n t_i(i-1)(2i+5)}{18} \quad (23)$$

where t_i symbolizes the number of ties of extent i .

A significant measure of correlation is apparent in a time series when the absolute value of Z computed using equation (21) is greater than $z_{\alpha/2} = \Phi^{-1}(1 - \alpha/2)$ for a desired significance level (α), and the null hypothesis that $S = 0$ is rejected. Additional details of the Kendall's correlation test are provided by *Helsel* and *Hirsch* [2002].

3.1.3 Spearman's Rho Correlation

An alternative non-parametric measure of correlation (linear or nonlinear) between two variables is Spearman's rho. As with Kendall's tau, Spearman's rho is a function of the ranks of the data, and thus is resistant to the effects of outliers. However, where Kendall's tau ignores the magnitude of differences between data pairs, Spearman's rho weights differences between data values ranked further apart more heavily. Ranks are assigned to the observations comprising each set of variables (X and Y) separately. Spearman's rho is then calculated as:

$$\text{rho} = \frac{\sum_{i=1}^n (Rx_i Ry_i) - n \left(\frac{n+1}{2} \right)^2}{n(n^2 - 1)/12} \quad (24)$$

where Rx_i and Ry_i are the ranks of observations x_i and y_i , respectively, $(n + 1)/2$ is the mean rank of both X and Y given a set of n concurrent observations, and the denominator reflects their variance.

Spearman's rho can be interpreted as Pearson's linear correlation coefficient computed based on the ranks of the data, instead of the data values themselves. As such, the significance of rho can be assessed using a two-tailed hypothesis test using the test statistic presented in equation (18) [*Helsel* and *Hirsch*, 2002]. Alternative formulations of the test statistic—exact and large sample approximations—for Spearman's rho are presented by *Bhattacharyya* and *Johnson* [1977]. Unfortunately, these approximations do not work well for small samples ($n < 20$), and thus use of Kendall's tau is typically preferred over Spearman's rho [*Helsel* and *Hirsch*, 2002]. As such, the discussions below focus on analysis of results using Kendall's tau correlations.

3.2 Climatic Causes of Nonstationarity

Cyclical patterns in flood series, whether evident in the historical flood record, or part of some unforeseen long-term persistence, could result from variation in the large-scale climate forcing of oceanic-atmospheric patterns, such as the Atlantic Multidecadal Oscillation (AMO), El Nino-Southern Oscillation (ENSO), North Atlantic Oscillation (NAO), or Pacific Decadal Oscillation (PDO). Correlation analyses, as described above, were performed herein to investigate these possible teleconnections with AMF series. These results provide insight as to how current methodologies for assessing flood risk could be updated in view of possible climate change, as discussed in greater detail in Chapter 4.

The strength of teleconnections with AMF series throughout the contiguous U.S. are assessed below using output of correlation analyses performed for two general categories of data:

Category A: 10-year moving averages of the log-transformed flood peaks and associated 3-month averaged climate indices representing AMO, ENSO, NAO, and PDO with 3-, 6-, and 9-month leads relative to the most common month of flood peak occurrence.

Category B: 10-year moving standard deviations of the log-transformed flood peaks and associated 3-month averaged climate indices representing AMO, ENSO, NAO, and PDO with 3-, 6-, and 9-month leads relative to the most common month of flood peak occurrence.

In both categories, moving windows are defined over the time period 1942 to 2010, such that the first 10-year window is computed using data from 1942 to 1951. The correlation analyses consider the relationship between the value of the mean or standard deviation computed using AMF peaks within the 10-year window ending in year t and the associated climate index with a lead time relative to year t . Sources for monthly climate index anomalies (available for the period 1950-2010) used herein are shown in Table 3.1. The smoothed time series resulting from use of a 10-year moving window reduces

(filters) the effects of random variations, thereby allowing for trends and/or cyclical patterns to be more easily distinguished. The 10-year interval in particular was chosen for two primary reasons: (1) shorter time intervals were not sufficient to clearly show trends or cyclical patterns, whereas longer windows result in too much dampening of the signal, and (2) the 10-year window is commensurate with climate patterns that follow cyclical patterns on decadal scales (e.g., AMO, PDO). Similarly, for each climate pattern, a three-month average of the relevant climate anomalies leading the AMF peak in year t was used to reduce effects of random monthly variations in respective indices.

Table 3.1
Sources of climatic indices used to identify teleconnections with flood flows.

Parameters	Source
AMO anomalies	NOAA Earth System Research Laboratory http://www.esrl.noaa.gov/psd/data/timeseries/AMO/
MEI anomalies	NOAA Earth System Research Laboratory http://www.esrl.noaa.gov/psd/enso/mei/table.html
NINO3.4 anomalies	NOAA Earth System Research Laboratory http://www.esrl.noaa.gov/psd/data/climateindices/list/
NAO anomalies	NOAA Earth System Research Laboratory Prediction http://www.cpc.ncep.noaa.gov/data/teledoc/nao.shtml
PDO anomalies	Joint Institute for the Study of the Atmosphere and Oceans, University of Washington http://www.atmos.washington.edu/~mantua/abst.PDO.html

Similar analyses were performed by *Kashelika* [2009], wherein relationships between oceanic-atmospheric patterns and flood series were assessed using Pearson's correlation coefficients computed using the observed magnitude of the flood peaks (real space), as well as the base-10 logarithmically transformed flood peaks (log space). The latter case is of interest as the standard guidelines employed for flood frequency analysis in the U.S. [IACWD, 1982] employ parameter values computed as a function of the log-transformed data. *Kashelika* [2009] observed that the tests in both real space and log space produce similar results, and thus herein, correlations are investigated using only the log-transformed flood flows. It should be noted that the results provided by *Kashelika* [2009] provide a more direct measure of how oceanic-atmospheric patterns influence flood risk in that she considered the correlation between the magnitude of flood peaks

and the associated climate indices with lead times relative to the actual date of flood peak occurrence. Herein, lead times are relative to the most common month of flood peak occurrence at a given site so that results can be used to improve one-year ahead forecasts of flood risk, wherein the actual date on which the flood peak will occur is unknown. The subsection below provides additional details for the selection of the mode month of flood peak occurrence as the baseline.

3.2.1 Frequency of Annual Maximum Discharge

To broaden current understanding of the timing of AMF peaks, a total of 14,835 AMF series across the U.S. (Figure 3.1) with a minimum 12 years of record were used to construct general frequency maps indicating the probability of a flood peak occurring within a given month/season. Figure 3.2 shows the general distribution of the most common (mode) month of occurrence of AMF peaks across the U.S. upon which lead times of climate indices for correlation analyses presented below, and subsequent models to forecast flood risk (CHAPTER 4), will be based. Figure 3.3 shows the frequency with which AMF peaks occur during the identified mode month of occurrence. Comparison of Figure 3.2 and Figure 3.3 suggests that the mode month of occurrence may not be the most appropriate baseline throughout the Eastern and South Central portions of the U.S. This may be due to the presence of a bimodal distribution in the time of occurrence (i.e., AMF peaks caused by multiple flood generating mechanisms).

To determine the extent to which bimodality exists, the frequencies of AMF peaks occurring within three-month seasons (Dec-Jan-Feb, Mar-Apr-May, Jun-July-Aug, Sep-Oct-Nov) were evaluated (Figure 3.4). Comparison of results across the four seasons suggests that the distribution for the time of flood peak occurrence is reasonably unimodal in many areas of the U.S. Although future floods may occur one month prior to or following the identified mode month, it is anticipated that use of a three-month average climate index as an indicator of flood risk would help offset these discrepancies. However, in the Eastern U.S. where floods tend to be generated by spring rains and fall hurricanes with relatively equal frequency, basing correlation analyses on the mode month of occurrence may not be the most appropriate procedure to follow. Future

developments of the flood risk forecasting framework proposed in CHAPTER 4 should include methods to account for this bimodality.

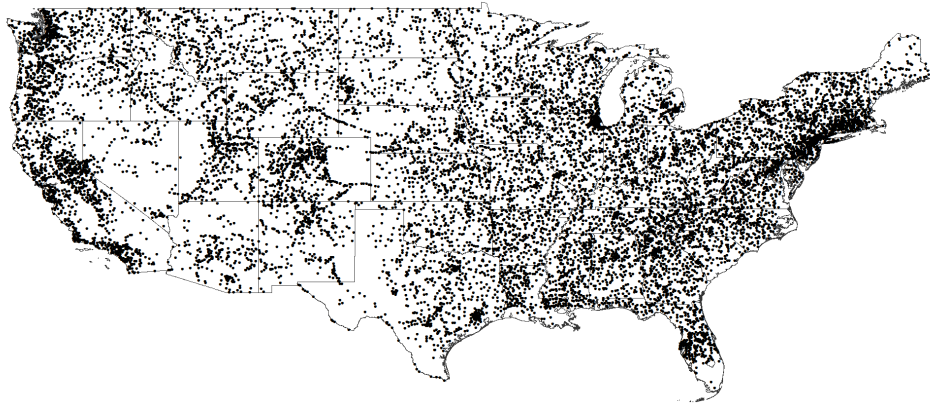


Figure 3.1 Location of 14,835 USGS stations with a minimum 12 years of AMF record.

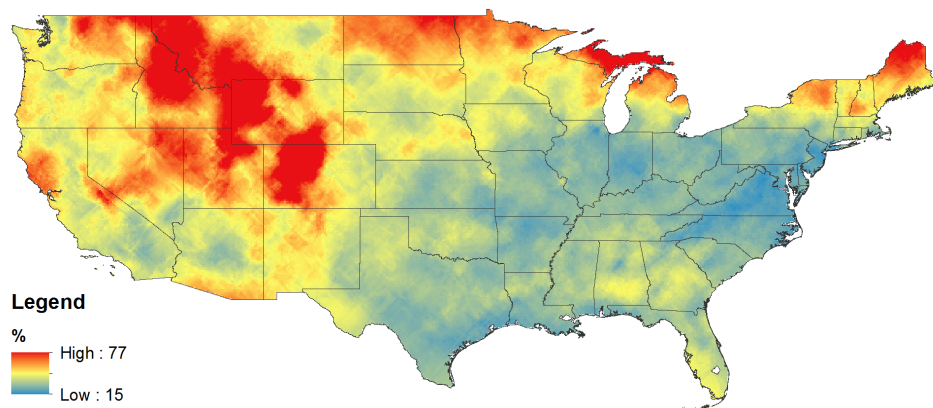


Figure 3.2 Most common (mode) month of occurrence of AMF peaks.

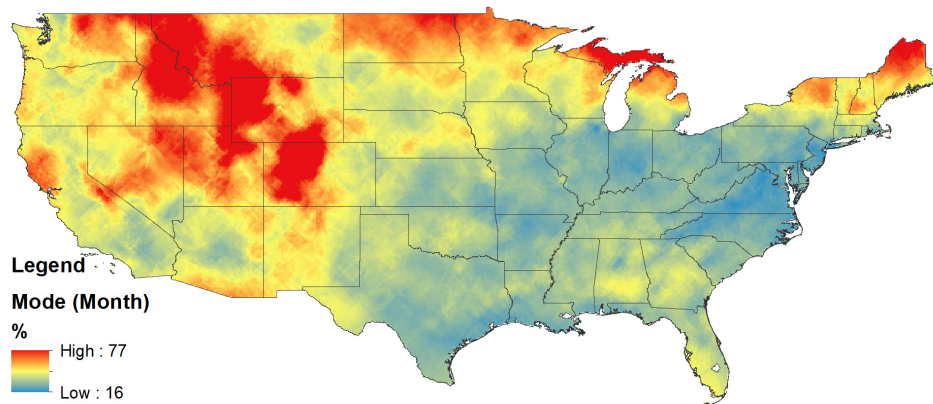


Figure 3.3 Frequency of occurrence of AMF peaks in identified mode month.

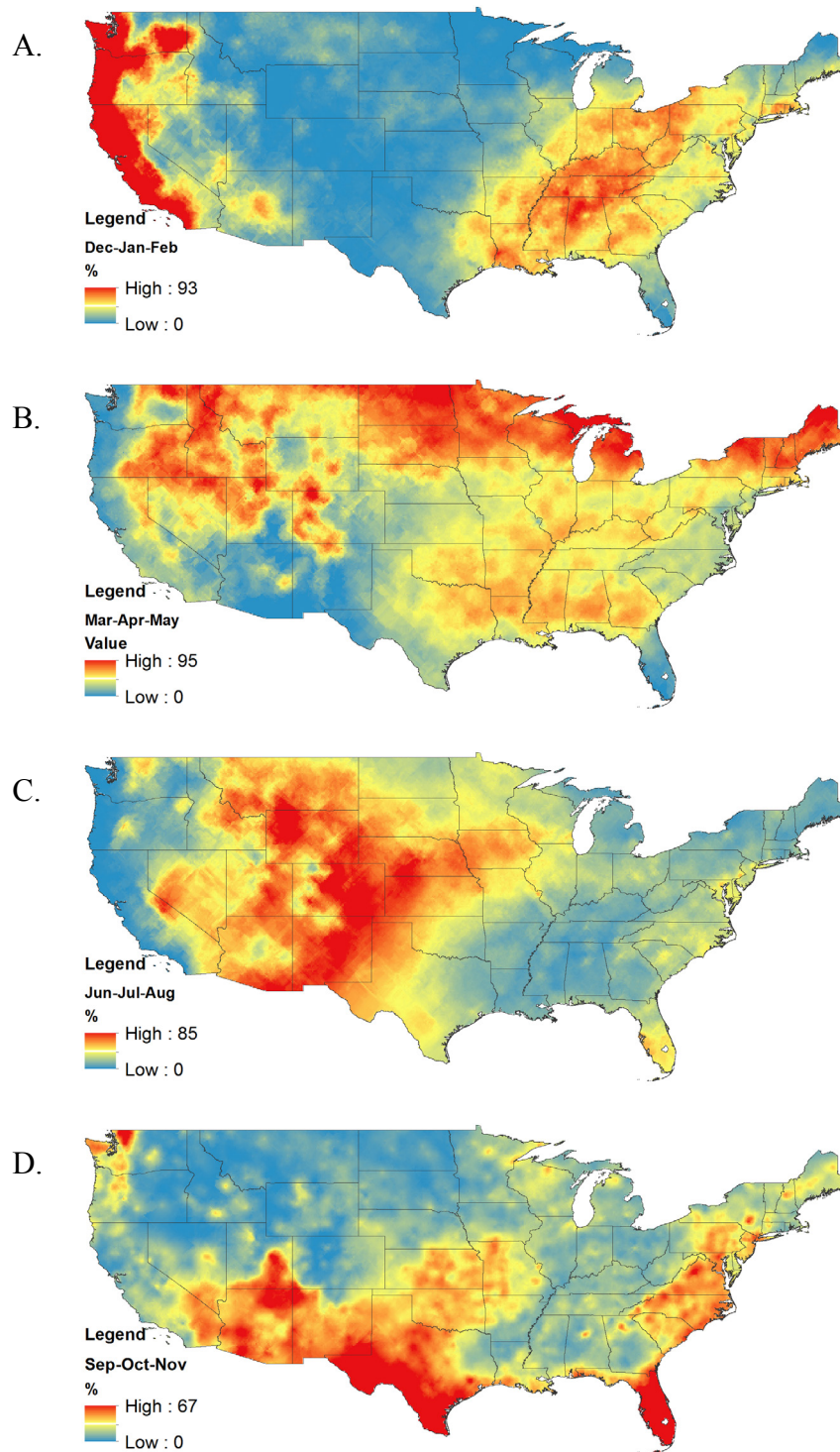


Figure 3.4 Combined frequency of occurrence of AMF peaks in three month seasons (A. Dec-Jan-Feb, B. Mar-Apr-May, C. Jun-July-Aug, D. Sep-Oct-Nov).

3.2.2 Evaluation of Teleconnections with Flood Flows

Overall, fifteen cases were considered within each category (A and B), resulting from use of three lead times (3-, 6-, and 9-months) for each of the five climatic indices used in this study: AMO, NAO, PDO, MEI, and NINO 3.4. The latter two indices are both indicators of ENSO. All three common measures of correlation—Pearson’s r , Kendall’s tau, and Spearman’s rho—were applied for each of the 569 sites in Figure 2.3. However, only results for Kendall’s tau are discussed herein, as it is generally considered more robust than Spearman’s rho, and is more powerful than Pearson’s r . Table 3.2 and Table 3.3 summarize the number of sites where significant results were obtained using Kendall’s tau at both 5% and 10% levels for all cases under consideration in Categories A and B, respectively. These results reveal that strong relationships between AMF series and Nino3.4 anomalies are nonexistent; however, MEI shows a much stronger relationship with AMF series. Results of the Kendall’s tau tests for each category are discussed in more detail below. Additional results for Kendall’s tau, as well as those for the Spearman’s rho and Pearson’s r tests, are provided in APPENDIX E and APPENDIX F for Categories A and B, respectively. Caution should be used when viewing these results as the correlation coefficient is a quality measure of the direction of the relationships between variables under consideration; however, by no means does it indicate a causal relationship.

Table 3.2
Number of sites with significant Kendall’s tau correlation (5 and 10% levels) between 10-year moving average of log-transformed flood peaks and AMO, MEI, NINO 3.4, NAO, and PDO indices with specified lead times.

Lead Time (months)	AMO		MEI		Nino 3.4		NAO		PDO	
	5%	10%	5%	10%	5%	10%	5%	10%	5%	10%
3	226	265	43	87	1	7	97	135	175	230
6	224	271	64	130	8	24	39	83	192	253
9	184	243	126	186	11	43	51	80	232	286

Table 3.3
Number of sites with significant Kendall's tau correlation (5 and 10% levels) between
10-year moving standard deviation of log-transformed flood peaks and AMO, MEI,
NINO 3.4, NAO, and PDO indices with specified lead times.

Lead Time (months)	AMO		MEI		Nino 3.4		NAO		PDO	
	5%	10%	5%	10%	5%	10%	5%	10%	5%	10%
3	228	285	40	72	3	8	75	102	153	198
6	232	280	46	94	6	18	26	47	174	220
9	198	246	100	148	16	36	38	77	198	246

The results in Table 3.2 suggest that the mean of the log-transformed flood peaks (Category A) could be modeled as variable over time, expressed as functions of the 3-month averaged AMO, MEI, NAO, and PDO indices with 6-, 9-, 3-, and 9-month lead times, respectively. For these four cases, the spatial representation of sites for which significant correlations were obtained are illustrated in the figures below. Figures illustrating results for other cases (lead times) considered, as well as with the Nino3.4 anomalies, are provided in APPENDIX E. Both AMO and PDO anomalies show significant relationships with AMF peaks across the U.S., as illustrated in Figure 3.5 and Figure 3.8, respectively. Significant relationships between the MEI anomalies and AMF peaks are also evident throughout the U.S. (Figure 3.6), although the teleconnections with ENSO are not as strong as for AMO and PDO, with fewer sites overall exhibiting significant correlations with MEI. Figure 3.7 suggests more regionally coherent teleconnections exist with NAO in the Pacific Northwest, South Central, and New England portions of the U.S. In general, these results suggest that teleconnections could be used to at least partially explain observed trends and/or possible cyclical behavior in AMF series.

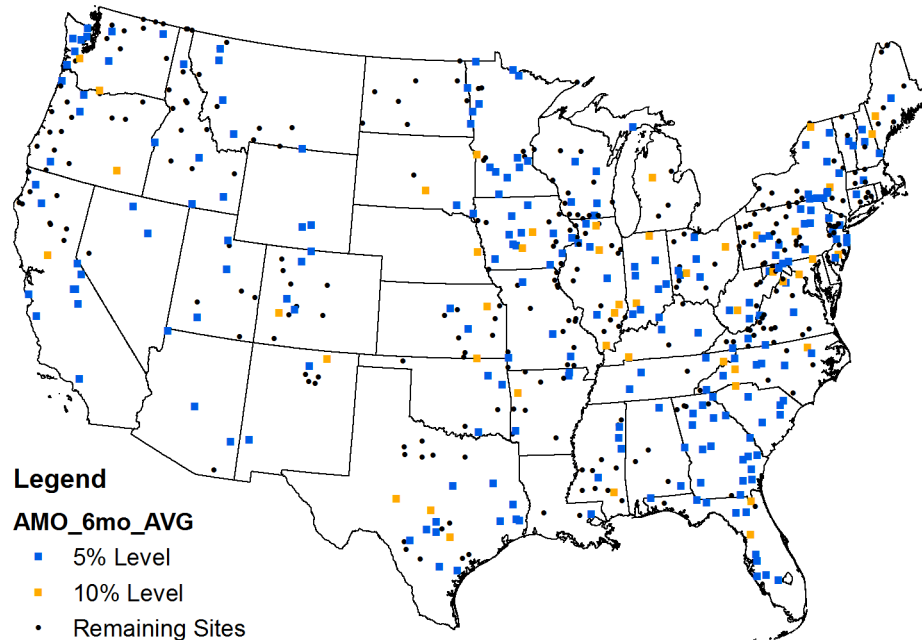


Figure 3.5 Locations of sites with significant correlation between 10-year moving average of log-transformed flood flows and 3-month average **AMO** anomalies with **6-month** lead.

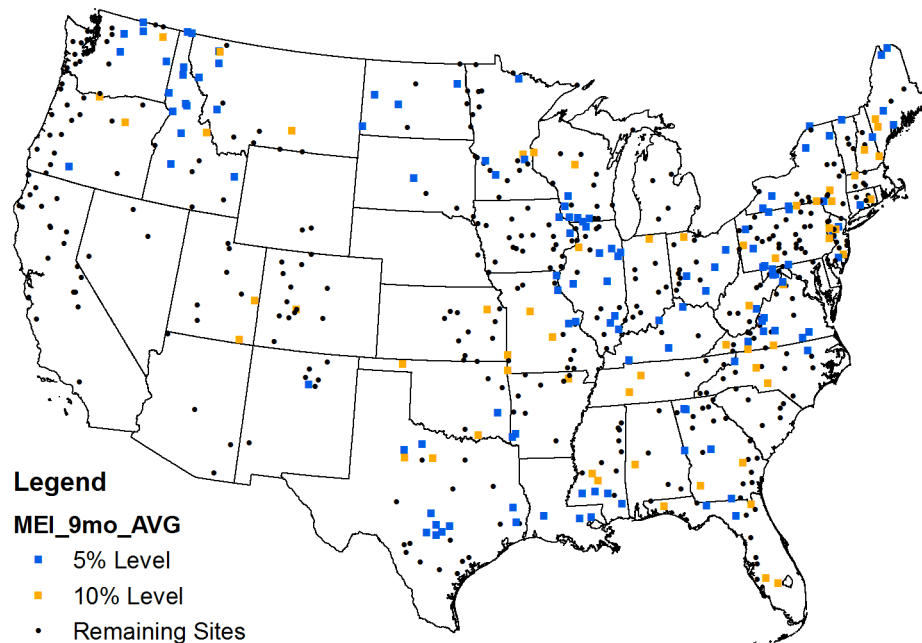


Figure 3.6 Locations of sites with significant correlation between 10-year moving average of log-transformed flood flows and 3-month average **MEI** anomalies with **9-month** lead.

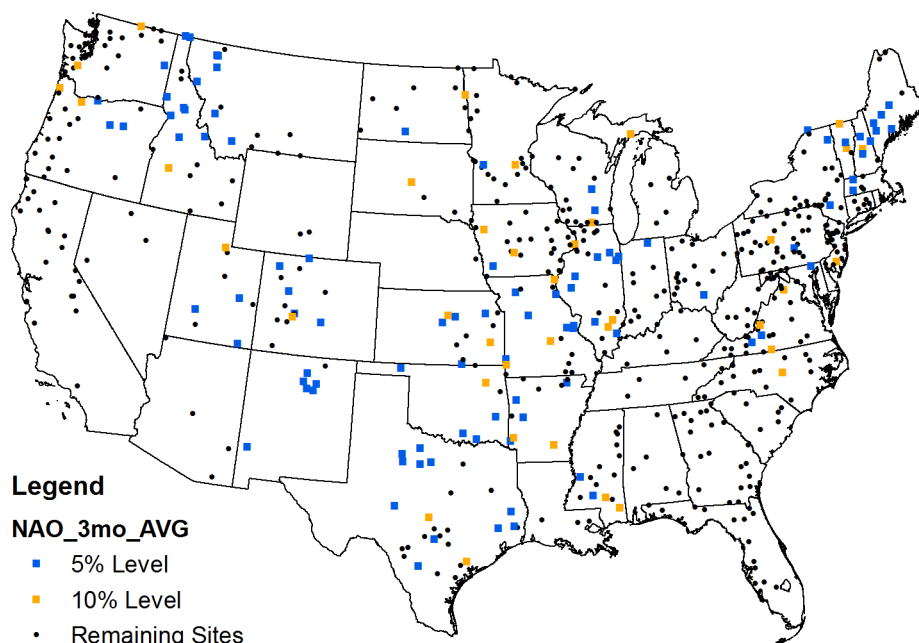


Figure 3.7 Locations of sites with significant correlation between 10-year moving average of log-transformed flood flows and 3-month average **NAO** anomalies with **3-month** lead.

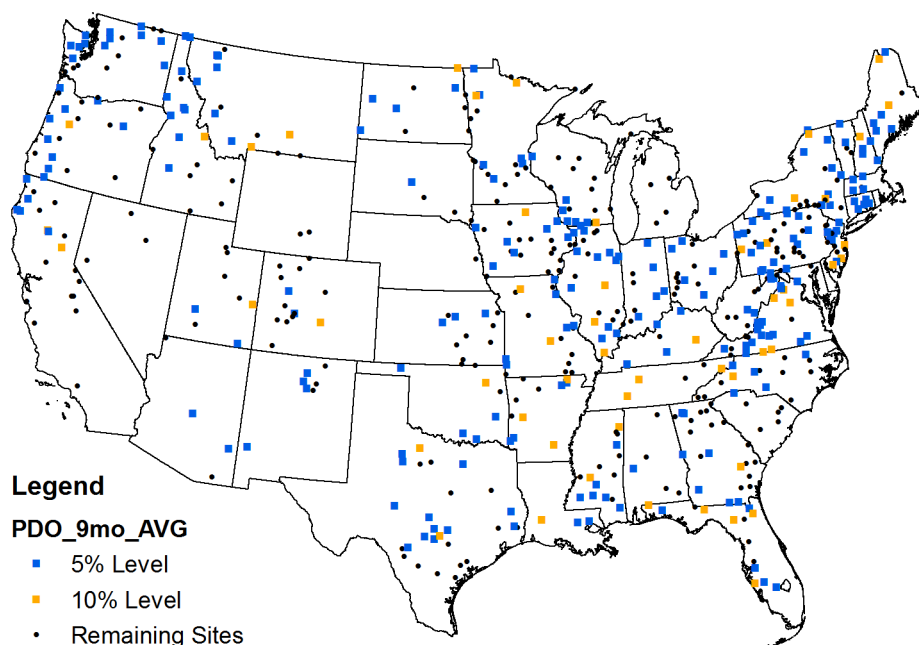


Figure 3.8 Locations of sites with significant correlation between 10-year moving average of log-transformed flood flows and 3-month average **PDO** anomalies with **9-month** lead.

With respect to Category B, the results in Table 3.2 suggest that the standard deviation of the log-transformed flows could be modeled as variable over time, expressed as a function of the 3-month averaged AMO, MEI, NAO, and PDO indices with 3-, 9-, 3-, and 9-month lead times, respectively. Except for AMO, the selected lead times are consistent with those for the 10-year moving averages. For these four cases, the spatial representation of sites for which significant correlations were obtained are illustrated in the figures below. Figures illustrating results for other cases (lead times) considered, as well as with the Nino3.4 anomalies, are provided in APPENDIX F. As was observed for the mean, both AMO and PDO anomalies show significant relationships with the variability in AMF series for sites across the U.S., as shown in Figure 3.9 and Figure 3.12, respectively. Significant relationships between the MEI anomalies and AMF peaks are also evident throughout the U.S. (Figure 3.10), although again, the teleconnections with ENSO are not as strong as for AMO and PDO, with fewer sites overall exhibiting significant correlations. Overall, the strength of teleconnections between NAO and the standard deviation (Figure 3.11) do not appear to be as strong, and certainly not as regionally coherent, as the results for the mean (Figure 3.7).

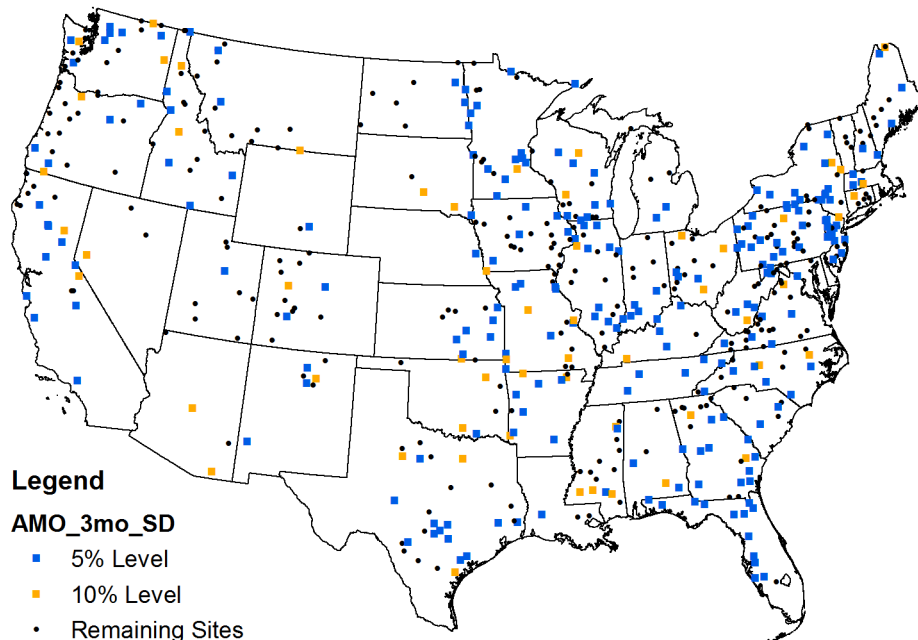


Figure 3.9 Locations of sites with significant correlation between 10-year moving standard deviation of log-transformed flood flows and 3-month average **AMO** anomalies with **3-month** lead.

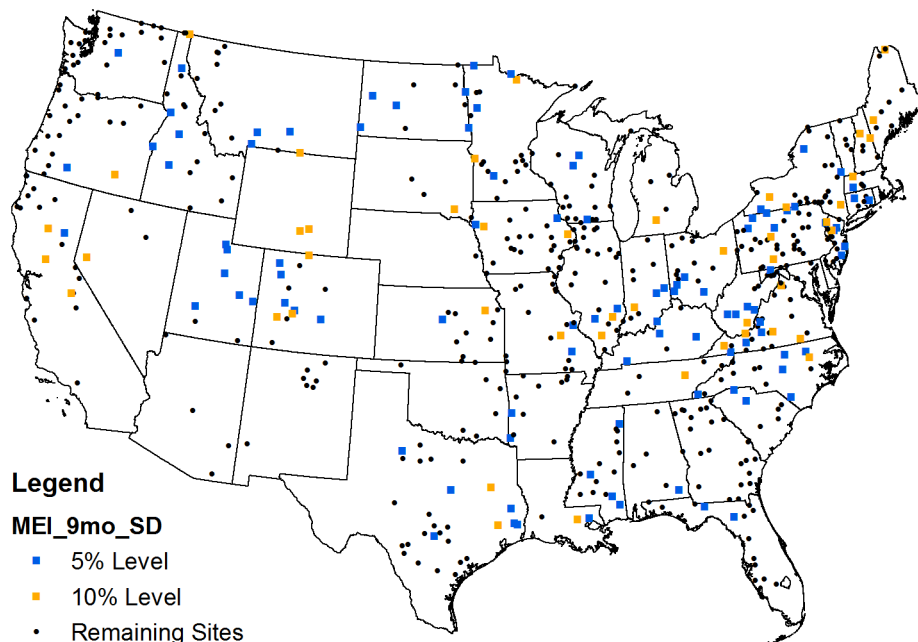


Figure 3.10 Locations of sites with significant correlation between 10-year moving standard deviation of log-transformed flood flows and 3-month average **MEI** anomalies with **9-month** lead.

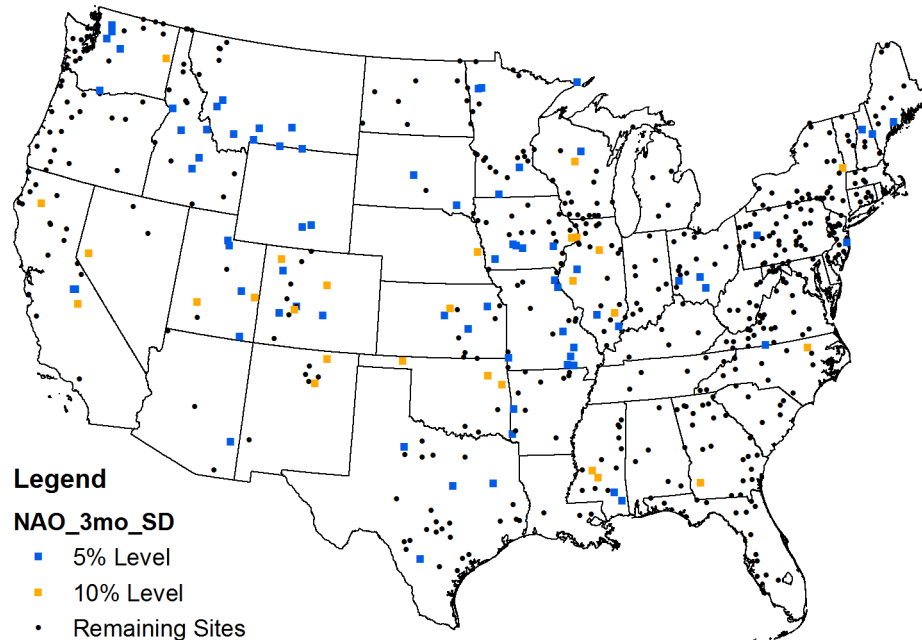


Figure 3.11 Locations of sites with significant correlation between 10-year moving standard deviation of log-transformed flood flows and 3-month average **NAO** anomalies with **3-month** lead.

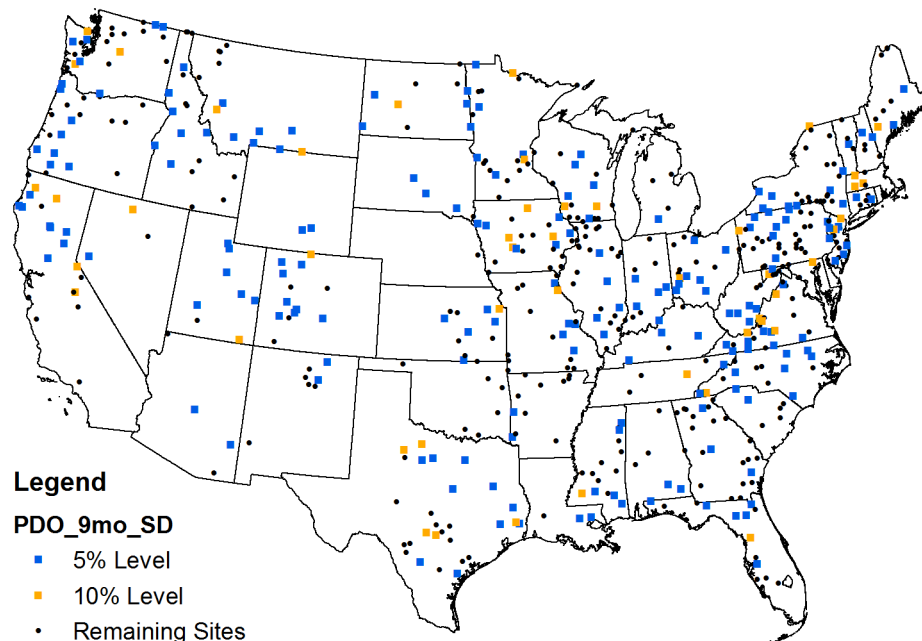


Figure 3.12 Locations of sites with significant correlation between 10-year moving standard deviation of log-transformed flood flows and 3-month average **PDO** anomalies with **9-month** lead.

3.2.3 Common Shifts between Flood Flows and Climatic Phases

Abrupt shifts (change-points) in the mean of AMF series could occur in response to abrupt shifts in the climate. The possible influence of climatic shifts was assessed by comparing the timing of identified change-points in AMF series (CHAPTER 2) to that of documented phase changes in oceanic-atmospheric patterns, such as AMO, NAO, and PDO [e.g., *Tootle et al.*, 2005]. Phases of AMO and NAO were classified as per *Tootle et al.* [2005]; phases of PDO were classified using information obtained from the Climate Impacts Group of the University of Washington (<http://cses.washington.edu/cig/pnw-c/compensopdo.shtml>). Table 3.4 summarizes the warm/cold phases of the three climate cycles on an annual time scale.

Table 3.4
Timing of Cold/Negative and Warm/Positive phases of AMO, PDO, and NAO.

	AMO	PDO	NAO
Cold (Negative)	1964-1994	1900-1924	1952-1972
		1947-1976	1977-1980
		1999-2002	
		2006-2009	
Warm (Positive)	1950-1963	1925-1946	1950-1951
	1995-2001	1977-1998	1973-1976
		2003-2005	1981-2001

Of the 569 sites analyzed for change-points in the mean of respective AMF series, 202 sites were identified to contain a significant change-point at the 10% level (Figure 2.6). To determine if these change-points were induced by shifts in climate, the timing of change-points in AMF series were related to the respective years when a climate pattern switched phases. For example, AMO switched from the warm phase to the cold phase in 1963. As the climatic shift should lead the shift in the mean of the AMF series for a causal relationship to exist, sites with change-points occurring in 1963, 1964, or 1965 are noted for further consideration. A total of 12 stations were identified to have common shifts with AMO; as shown in Table 3.5, of the 12 stations, only 5 had significant measures of correlation between the AMO climate anomalies and the 10-year moving

average of the AMF series at the 10% level. Similarly, Table 3.6 provides results for common shifts between flood series and PDO; 12 stations exhibit a common shift, and only 6 show significant measures of correlation. Identified common shifts between flood series and NAO are shown in Table 3.7. Results indicate a total of 55 stations have a common time of shift with NAO, but the number reduces to 22 stations when considering only stations with significant correlations. Overall, only 31 stations identified to have an abrupt shift in the mean flood magnitude were observed to have a common shift with at least one of the climate patterns considered. Two stations exhibit common shifts with both NAO and PDO (USGS Stations 05555300 and 13342500). As such, these results provide possible explanations of the observed shifts in relatively few AMF series, thereby giving reason to investigate other meteorological and physical causes of nonstationarity in AMF series.

Table 3.5

Coincidental timing of AMO phase changes and identified change-points in the mean of AMF series; including respective Kendall's tau values and associated p-values for correlation between the 10-year moving average of AMF series and AMO climate anomalies with 6-month lead.

Site Number	Change-Point		Correlation		Site Number	Change-Point		Correlation	
	Year	p-value	tau	p-value		Year	p-value	tau	p-value
01426500	1963	0.000	0.221	0.013	05280000	1964	0.012	0.276	0.002
01503000	1964	0.066	0.328	0.000	05304500	1964	0.005	0.116	0.193
01531000	1964	0.024	0.118	0.185	05420500	1964	0.003	0.097	0.278
05066500	1964	0.000	0.106	0.235	05520500	1965	0.000	0.049	0.588
05082500	1964	0.000	0.179	0.044	05597000	1964	0.003	0.142	0.111
05100000	1964	0.017	0.145	0.103	08128000	1964	0.010	0.167	0.060

Table 3.6

Coincidental timing of PDO phase changes and identified change-points in the mean of AMF series; including respective Kendall's tau values and associated p-values for correlation between the 10-year moving average of AMF series and PDO climate anomalies with 9-month lead.

Site Number	Change-Point		Correlation		Site Number	Change-Point		Correlation	
	Year	p-value	tau	p-value		Year	p-value	tau	p-value
03167000	1978	0.010	-0.274	0.002	12010000	1977	0.087	0.084	0.348
04079000	1976	0.076	-0.068	0.452	12035000	1978	0.006	0.327	0.000
05407000	1946	0.017	0.062	0.492	12354500	1946	0.082	-0.225	0.011
05555300	1978	0.011	0.266	0.003	12401500	1947	0.030	0.110	0.218
06335500	1978	0.011	-0.383	0.000	12404500	1947	0.067	0.046	0.605
06810000	1946	0.053	0.051	0.570	13342500	1976	0.000	-0.261	0.003

Table 3.7

Coincidental timing of NAO phase changes and identified change-points in the mean of AMF series; including respective Kendall's tau values and associated p-values for correlation between the 10-year moving average of AMF series and NAO climate anomalies with 3-month lead.

Site Number	Change-Point		Correlation		Site Number	Change-Point		Correlation	
	Year	p-value	tau	p-value		Year	p-value	tau	p-value
01169000	1972	0.000	0.275	0.002	05495000	1972	0.036	0.164	0.064
01334500	1972	0.000	0.077	0.386	05501000	1972	0.011	0.321	0.000
01518000	1980	0.000	0.079	0.379	05555300	1978	0.011	0.176	0.048
02173500	1980	0.001	0.033	0.716	06335500	1978	0.011	0.022	0.808
02321500	1973	0.100	0.053	0.553	06337000	1972	0.000	0.039	0.664
02383500	1980	0.000	0.016	0.858	06340500	1972	0.050	0.109	0.221
02387500	1980	0.010	-0.001	1.000	06478500	1982	0.010	0.146	0.101
03118500	1974	0.022	0.080	0.368	06908000	1972	0.073	0.227	0.011
03167000	1978	0.010	-0.046	0.610	07016500	1980	0.011	0.225	0.011
03234500	1972	0.034	-0.247	0.006	07018500	1981	0.058	0.225	0.011
03307000	1973	0.006	-0.031	0.734	07019000	1980	0.010	0.204	0.022
03345500	1981	0.078	-0.099	0.267	07146500	1972	0.065	0.216	0.015
03379500	1981	0.036	0.152	0.087	07234000	1973	0.000	-0.304	0.001

Table 3.7, continued

Site Number	Change- Point		Correlation		Site Number	Change-Point		Correlation	
	Year	p-value	tau	p-value		Year	p-value	tau	p-value
03381500	1981	0.040	0.257	0.004	07247500	1974	0.000	-0.251	0.005
04073500	1953	0.021	0.187	0.037	07252000	1981	0.073	0.199	0.025
04079000	1976	0.076	-0.060	0.509	07340500	1974	0.000	-0.151	0.089
04191500	1973	0.063	0.028	0.759	08080500	1972	0.000	-0.278	0.002
04193500	1973	0.078	-0.017	0.853	12010000	1977	0.087	-0.013	0.888
04262500	1973	0.048	0.140	0.117	12035000	1978	0.006	-0.024	0.794
05316500	1974	0.003	0.031	0.731	12134500	1973	0.040	0.044	0.628
05317000	1982	0.094	-0.005	0.959	12186000	1973	0.031	-0.004	0.969
05330000	1982	0.005	0.110	0.216	12189500	1973	0.016	0.073	0.414
05422000	1972	0.053	-0.050	0.575	12321500	1952	0.007	0.066	0.463
05431486	1953	0.092	0.145	0.103	12322000	1972	0.000	-0.331	0.000
05435500	1953	0.006	-0.012	0.898	13342500	1976	0.000	-0.289	0.001
05436500	1953	0.014	0.009	0.922	14105700	1972	0.000	-0.369	0.000
05454500	1953	0.004	0.083	0.355	14137000	1952	0.075	0.159	0.074
05476000	1982	0.046	0.091	0.307					

3.3 Meteorological Connections to Flood Peaks

Observed trends in flood series could be due to trends in associated precipitation and/or temperature series. Previous studies have documented the influence of temperature changes on shifts in the timing of spring snowmelt and corresponding runoff events in the western U.S. [e.g., *Cayan et al.*, 2001; *Stewart et al.*, 2005; *Moore et al.*, 2007]. For the 235 sites under consideration in the Northeastern quadrant of the U.S. (Figure 2.14), the presence of common trends between the AMF series and the flood generating precipitation and temperature series were investigated using Pearson's correlation analyses. In addition, relationships between temperature series and timing of flood peaks were analyzed. These analyses only consider the Pearson's correlation coefficient as the interest herein is to determine the extent to which changes in the AMF series over time are explained by changes in associated meteorological series. The Pearson's correlation coefficient appropriately describes the direction and degree to which one variable is

linearly related to another, and thus will indicate the proportion of variability within the AMF series explained by either precipitation or temperature. Conversely, Kendall's tau represents the probability that the observed data are similarly ranked (agreement) versus the probability that the observed data are not in agreement with respect to rank [*Bolboaca and Jantschi, 2006*]. The presence of coincidental shifts in the meteorologic and AMF series are also investigated.

3.3.1 Association among Precipitation and AMF Series

Flood generating precipitation series consisting of the total precipitation that occurred within X-days prior to the annual maximum flow were constructed for each of the 235 streamflow gauging stations. For lead times of $X = 2, 3, 4, 5, 6$, and 7 days, these watershed specific precipitation series were constructed for 1950-2006 (57 years) using two different spatial scales of gridded data—1/8 and 1/4 degree. (See CHAPTER 2 for details.) Correlation analyses were performed between the AMF peaks and X-day precipitation totals for both spatial scales of data. Table 3.8 provides a summary of the number of sites where significant measures of correlation (Pearson's r) were identified on both 5% and 10% levels for all cases considered. Overall, a large portion of the 235 AMF series considered exhibit a significant degree of correlation with associated precipitation series. The discussion below pertains to results obtained using the finer scale precipitation data (1/8-degree). Additional results are provided in Appendix G.

Table 3.8

Number of sites yielding significant Pearson's correlation coefficients for AMF series relative to precipitation series with X-day lead times constructed using 1/8 and 1/4 degree gridded data.

Lead Time (days)	1/8 Degree Gridded Data		1/4 Degree Gridded Data	
	5% Level	10% Level	5% Level	10% Level
2	165	181	186	190
3	186	200	188	198
4	195	203	195	199
5	199	206	189	199
6	195	205	192	200
7	198	204	193	200

For a given site, only the precipitation series constructed using the X-day lead time (1/8-degree gridded data) which exhibited the highest measure of correlation with the AMF peaks was used to evaluate the presence of common trends and/or shifts between the two respective series. The most significant (best) X-day lead time chosen for each site, provided Pearson's r was significant at the 10% significance level, is presented in Figure 3.13. Of the 235 sites analyzed, 221 sites exhibit a significant measure of correlation between flood magnitude and the associated precipitation depth. The locations of sites where the best X-day precipitation series and the AMF series both exhibit trends and shifts (as identified in CHAPTER 2) are illustrated in Figure 3.14 and Figure 3.15, respectively. In the latter case, it should be noted that both the precipitation and AMF series were observed to contain a significant change-point, but they do not necessarily occur at the same time.

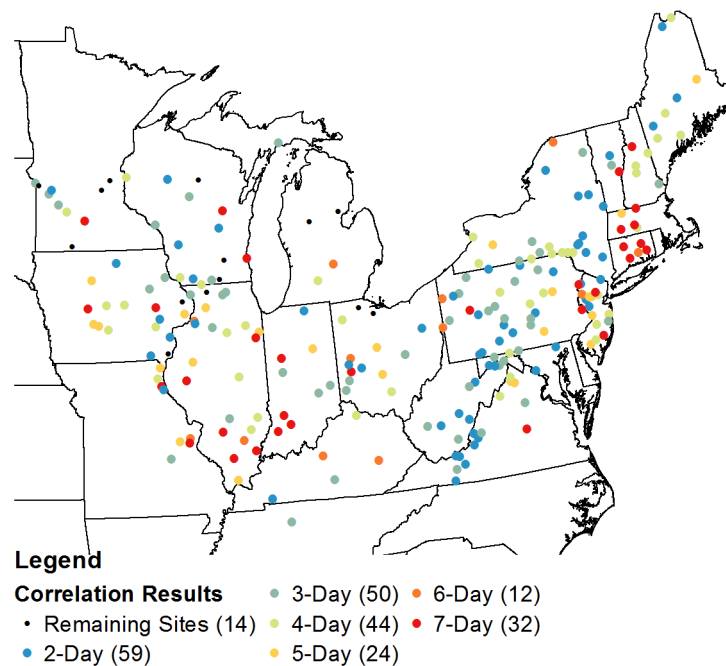


Figure 3.13 X-day lead time yielding most significant Pearson's correlation coefficient between AMF series and the associated flood generating precipitation series constructed using 1/8-degree gridded data.

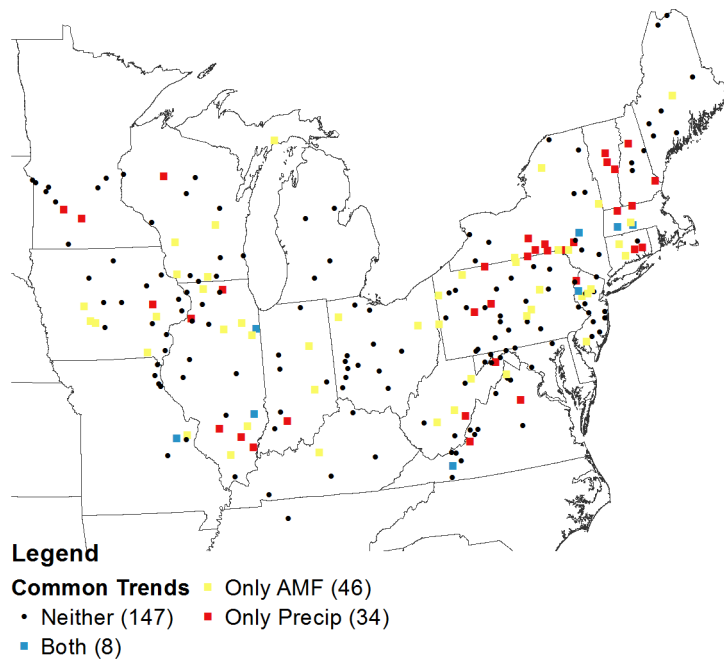


Figure 3.14 Location of sites with trends in both the AMF series and the best X-day flood generating precipitation series constructed using 1/8-degree gridded data.

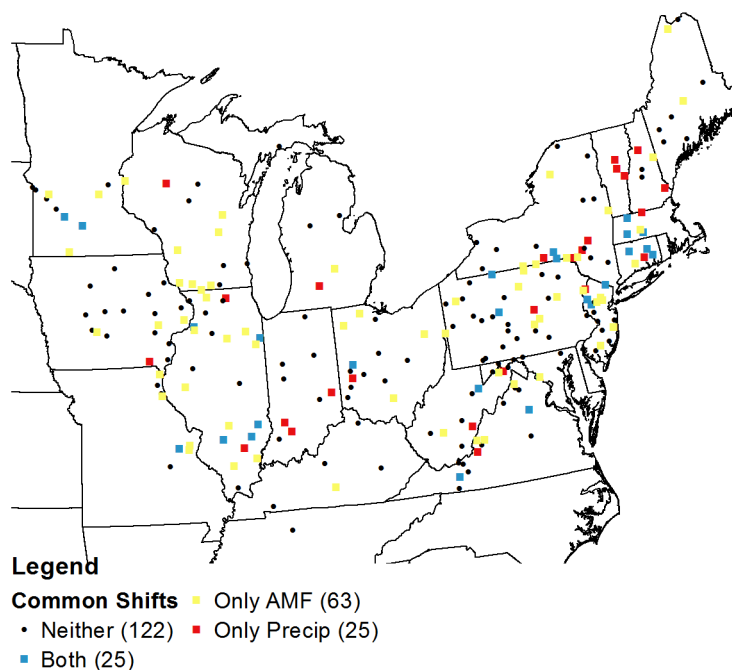


Figure 3.15 Location of sites with shifts in both the AMF series and the best X-day flood generating precipitation series constructed using 1/8-degree gridded data.

Table 3.9 summarizes the trend results in both precipitation and AMF series for the 8 sites in Figure 3.14 determined to have a common trend. Of the 8 sites, two exhibit decreasing trends in the magnitude of AMF series, and increasing trends in flood generating precipitation series. As such, the significant Pearson's correlation is actually indicative of a strong inverse relationship between precipitation and flood magnitude, and thus a causal relationship does not exist.

Table 3.10 summarizes the change-point results for the 25 sites in Figure 3.15 which exhibit shifts in both the X-day precipitation and AMF series, though not necessarily at the same time. The last column in the table reports the difference between the year in which the shift in the AMF series occurs and the year in which the shift in the precipitation series occurs. Thus, a positive difference indicates that the shift in the precipitation series leads the shift in flood magnitude. Further, a small difference would indicate a possible causative effect of the shift in precipitation on flood magnitude. Sites for which further analysis is warranted are indicated in bold font. Overall, relatively few sites are identified; however, this analysis may be limited by the robustness of the Pettitt test, as well as the inability of the test to identify multiple shifts which may occur if the time series exhibits cyclical behavior.

Table 3.9
Summary results for sites with trends in both the magnitude of AMF series and the best X-day flood generating precipitation series.

Station Number	AMF Trend Results		Pearson's r Correlation		Precipitation Trend Results	
	tau	p-value	Lead Time (days)	p-value	tau	p-value
01176000	0.193	0.010	4	0.000	0.167	0.068
01181000	-0.192	0.092	7	0.000	0.183	0.045
01350000	0.177	0.069	2	0.000	0.169	0.064
01445500	0.353	0.000	6	0.000	0.216	0.018
03167000	-0.267	0.004	3	0.000	0.219	0.016
03345500	0.143	0.058	4	0.000	0.229	0.012
05520500	0.415	0.000	5	0.049	0.155	0.089
07016500	0.166	0.034	5	0.000	0.174	0.057

Table 3.10
Summary results for sites with significant shifts in both the magnitude of AMF series and
the best X-day flood generating precipitation series.

Station Number	AMF Series		Precipitation Series		Difference
	Year	p-value	Year	p-value	
01119500	1971	0.038	1972	0.0551	-1
01127500	1967	0.020	1977	0.0298	-10
01169000	1972	0.000	1967	0.0184	5
01176000	1967	0.036	1973	0.0132	-6
01181000	1968	0.018	1968	0.0149	0
01188000	1971	0.069	1970	0.0584	1
01387500	1967	0.003	1967	0.0987	0
01396500	1969	0.002	1966	0.0953	3
01445500	1966	0.000	1966	0.0429	0
01503000	1964	0.066	1971	0.0497	-7
01512500	1950	0.031	1974	0.0296	-24
01541500	1956	0.017	1982	0.0743	-26
01667500	1971	0.056	1970	0.0116	1
03010500	1939	0.003	1960	0.015	-21
03069500	1954	0.002	1970	0.0934	-16
03167000	1978	0.010	1971	0.0116	7
03262000	1930	0.064	1986	0.0491	-56
03345500	1981	0.078	1982	0.002	-1
03379500	1981	0.036	1983	0.0582	-2
05316500	1974	0.003	1989	0.0249	-15
05317000	1982	0.094	1982	0.0169	0
05446500	1970	0.049	1969	0.0158	1
05520500	1965	0.000	1985	0.0289	-20
05593000	1962	0.003	1963	0.0288	-1
07016500	1980	0.011	1982	0.0554	-2

3.3.2 Association among Temperature and AMF Series

Flood generating temperature series consisting of the average daily maximum and minimum temperatures over X-days prior to the annual peak flow were constructed using 1/8-degree gridded data. (See CHAPTER 2 for details.) For a given site, only the minimum and maximum temperature series constructed using the X-day lead time which exhibited the highest measure of correlation with the magnitude of AMF peaks was used to evaluate the presence of common trends and/or shifts between the two respective series. The most significant (best) X-day lead times chosen for each site, provided Pearson's r was significant at the 10% significance level, are presented in Figure 3.16 and Figure 3.17 for the minimum and maximum temperature series, respectively. Only a few sites show a significant measure of correlation between flood magnitude and the temperature series analyzed. Additional results for the correlation analyses are provided in Appendix G.

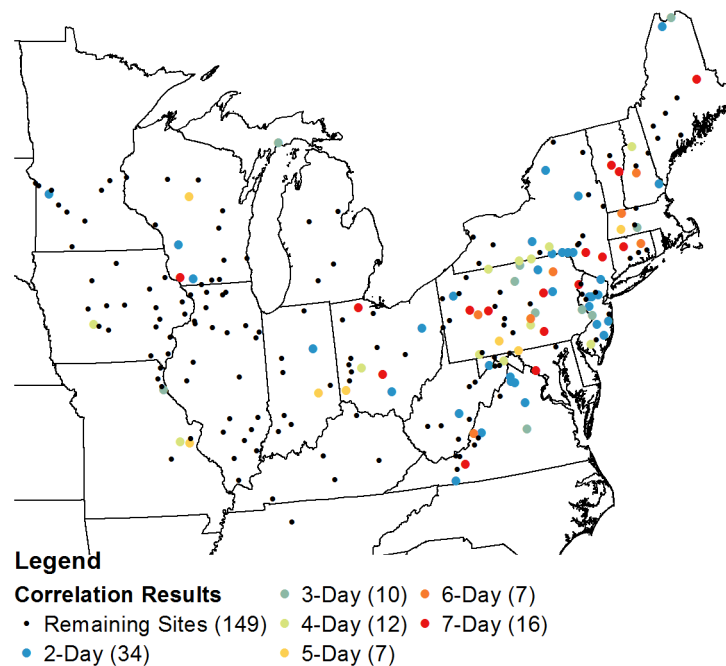


Figure 3.16 X-day lead time yielding the most significant Pearson's correlation coefficient between the AMF peaks and associated minimum temperature series.

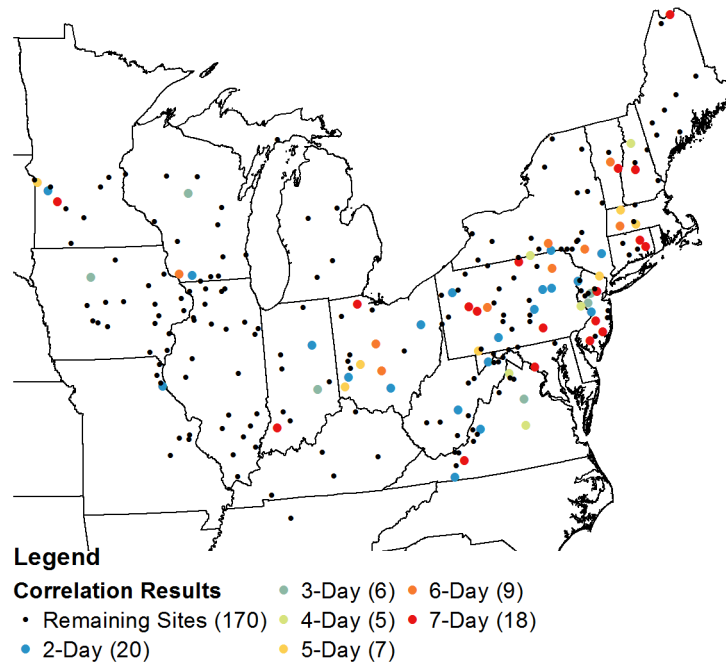


Figure 3.17 X-day lead time yielding the most significant Pearson's correlation coefficient between the AMF peaks and associated maximum temperature series.

Figure 3.18 and Figure 3.19 show sites at which trends were identified in both the AMF series and the best X-day minimum and maximum flood generating temperature series, respectively. Table 3.11 summarizes the trend results for the 6 sites in Figure 3.18 and the 2 sites in Figure 3.19 determined to have both a trend in the AMF series and the respective temperature series. For these 8 sites, each of the flood generating temperature (minimum/maximum) series show signs of increasing trends at the 10% level; however, 4 of the corresponding AMF series exhibit decreasing trends in the magnitude despite significant correlation with the respective temperature series. Therefore, the causative effects of temperature on flood magnitude are unclear.

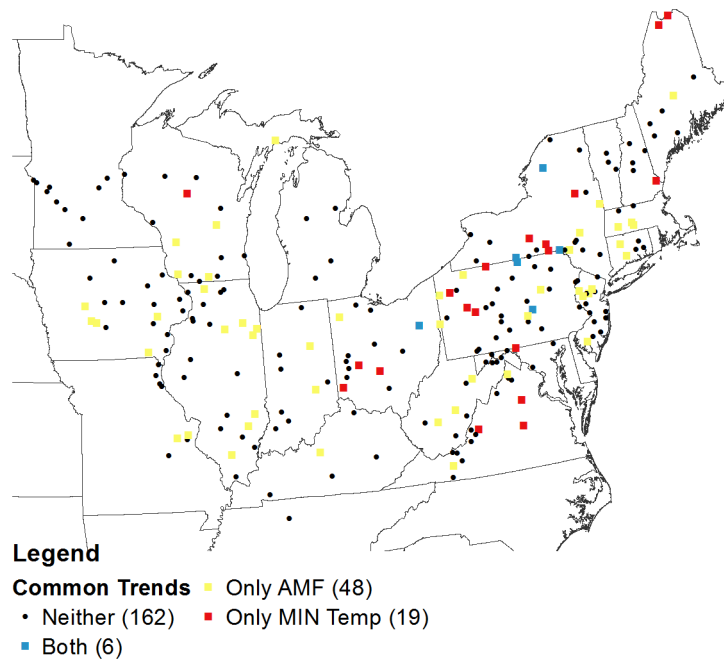


Figure 3.18 Location of sites with trends in both the best X-day flood generating minimum temperature and the AMF series.

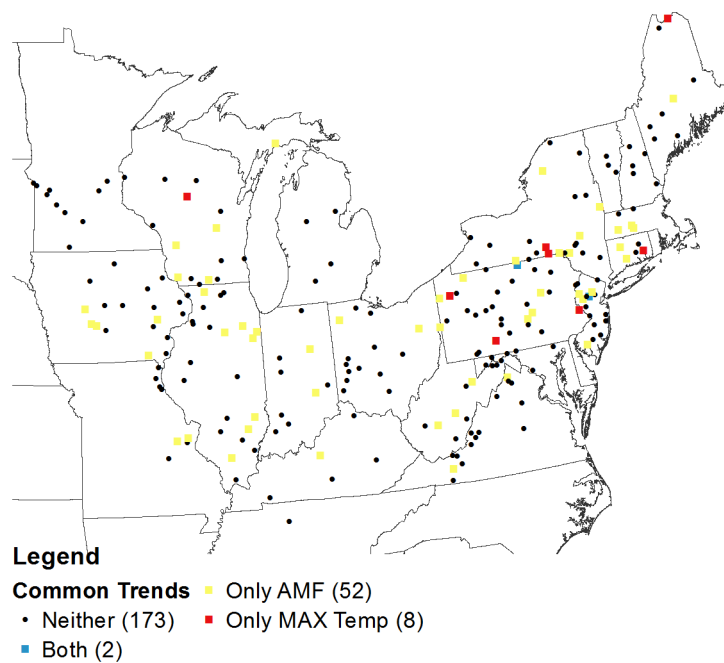


Figure 3.19 Location of sites with trends in both the best X-day flood generating maximum temperature and the AMF series.

Table 3.11

Summary results for sites with trends in both the magnitude of AMF series and the best X-day flood generating minimum and maximum temperature series.

Station Number	AMF Trend Results		Pearson's r Correlation		Temperature Trend Results	
	tau	p-value	Lead Time (days)	p-value	tau	p-value
<i>Minimum Temperature Series</i>						
01426500	-0.277	0.000	2	0.050	0.174	0.057
01518000	-0.313	0.011	3	0.030	0.187	0.041
01520500	-0.406	0.000	4	0.079	0.209	0.022
01555500	0.171	0.078	3	0.037	0.167	0.068
03118500	0.174	0.037	2	0.010	0.169	0.064
04262500	0.144	0.064	2	0.025	0.221	0.016
<i>Maximum Temperature Series</i>						
01398500	0.199	0.018	3	0.035	0.182	0.047
01518000	-0.313	0.011	7	0.070	0.237	0.009

Sites at which shifts are identified in both the AMF series and the minimum/maximum temperature series, though not necessarily at the same time, are shown in Figure 3.20 and Figure 3.21, respectively. Table 3.12 summarizes the change-point results for the 14 sites in Figure 3.20 and the 6 sites in Figure 3.21 which exhibit shifts in both the X-day minimum/maximum temperature series and AMF magnitude. The last column in the table reports the difference between the year in which the shift in the AMF series occurs and the year in which the shift in the temperature series occurs. Overall, the differences are large enough that it is unlikely that shifts in temperature alone would lead to the observed shifts in the AMF series. However, this analysis may be limited as discussed above with respect to the influence of precipitation series.

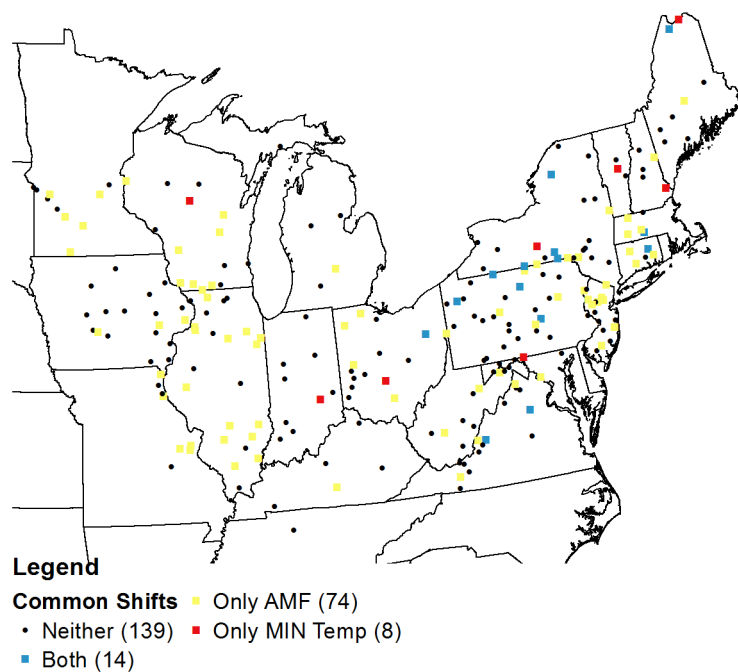


Figure 3.20 Location of sites with change-points in both the best X-day flood generating minimum temperature series and the AMF series.

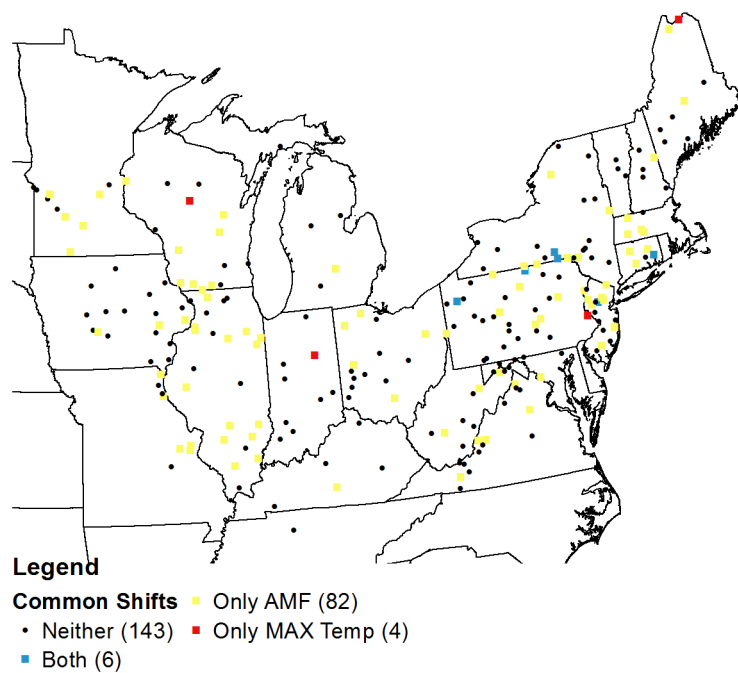


Figure 3.21 Location of sites with change-points in both the best X-day flood generating maximum temperature series and the AMF series.

Table 3.12

Summary results for sites with significant shifts in both the magnitude of AMF series and the best X-day flood generating minimum/maximum temperature series.

Table 3.12, continued

Table 6.12, continued

Station Number	AMF Series		Temperature Series		Difference
	Year	p-value	Year	p-value	
Minimum Temperature Series					
1011000	1968	0.040	1979	0.002	-11
1119500	1971	0.038	1979	0.089	-8
1176000	1967	0.036	1978	0.033	-11
1503000	1964	0.066	1970	0.007	-6
1512500	1950	0.031	1971	0.058	-21
1520500	1979	0.000	1971	0.01	8
1548500	1935	0.069	1968	0.014	-33
1555500	1969	0.007	1981	0.056	-12
1667500	1971	0.056	1978	0.077	-7
2016000	1968	0.040	1979	0.064	-11
3010500	1939	0.003	1971	0.002	-32
3024000	1969	0.057	1971	0.062	-2
3118500	1974	0.022	1968	0.099	6
4262500	1973	0.048	1968	0.023	5
Maximum Temperature Series					
1127500	1967	0.020	1979	0.004	-12
1398500	1969	0.002	1982	0.067	-13
1503000	1964	0.066	1987	0.018	-23
1512500	1950	0.031	1971	0.057	-21
1518000	1980	0.000	1970	0.079	10
3024000	1969	0.057	1981	0.016	-12

Moving past the few commonalities identified between temperature series and flood magnitude, relationships between temperature series and timing of flood flows, if any, would potentially be useful in improving forecasts of flood risk by considering when a future flood might occur. In particular, the ability to reasonably forecast the month in which a future flood was most likely to occur would be advantageous in areas of the U.S.

where timing of AMF peaks are better represented by a bimodal distribution. The strength of the relationship between temperature and the day of occurrence of AMF peaks for each site in Figure 2.14 was assessed using Pearson's correlation. The most significant (best) X-day lead times chosen for each site, provided Pearson's r was significant at the 10% significance level, for the minimum and maximum temperature series are presented in Figure 3.22 and Figure 3.23, respectively. These results in themselves illustrate the prevalence of significant relationships between temperature and timing of AMF peaks. Additional test results are provided in APPENDIX G.

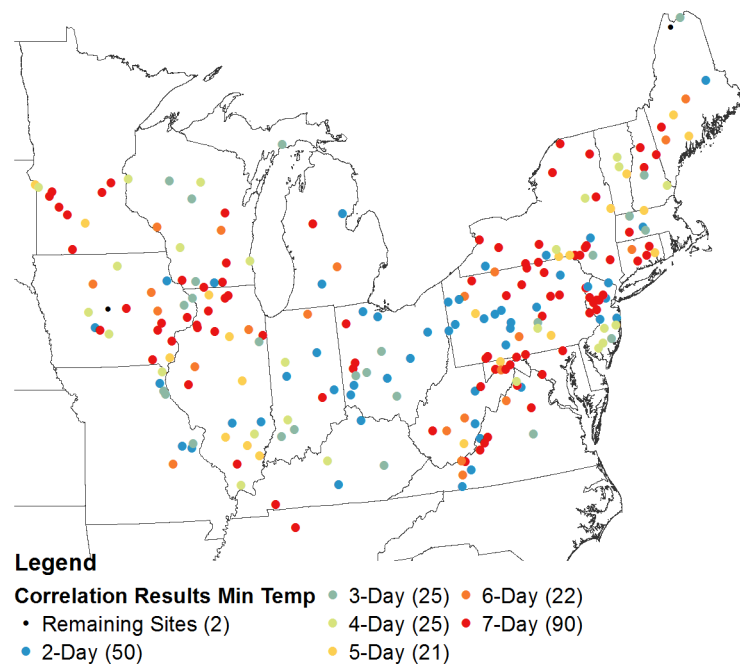


Figure 3.22 X-day lead time yielding the most significant Pearson's correlation coefficient between the day of occurrence of AMF peaks and associated minimum temperature series.

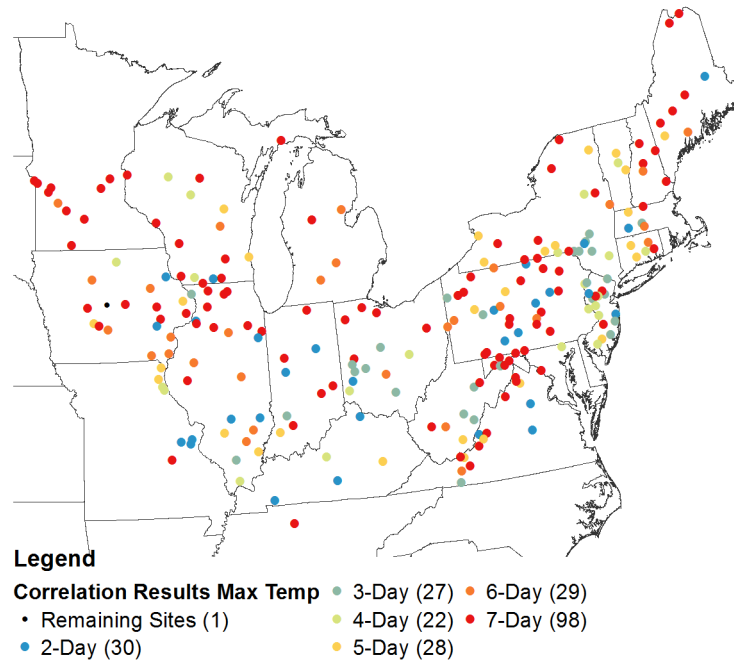


Figure 3.23 X-day lead time yielding the most significant Pearson's correlation coefficient between the day of occurrence of AMF peaks and associated maximum temperature series.

3.4 Physical Causes of Nonstationarity

An abrupt shift (change-point) in the mean or variance of annual maximum flood series could occur in response to a regime shift such as regulation, channelization, gauge movement, or land use change (e.g., wildfire or changing agricultural practices) [e.g., *Ehsanzadeh et al.*, 2010]. The correlation analyses discussed above work well to identify common patterns or trends between climate parameters and flood series; however, these analyses cannot be completed with respect to physical parameters due to the limited availability of relevant data over time. Thus, physical causes of nonstationarity are considered by relating identified trends and/or change-points to documented changes in land use/land cover, changes in agricultural practices, and the installation of major reservoirs. These analyses are conducted for the same 235 stations used to investigate precipitation/temperature relationships with flood series (see Figure 2.14).

The GAGES-II database, which identifies sites to be part of the 2009 HCDN, and reports water data remarks and hydraulic modifications on a site-by-site basis, was used to assess possible physical causes of nonstationarity. As the sites included in Figure 2.14 were chosen for their inclusion in the original HCDN [Slack *et al.*, 1993], an initial check was performed to see if they were also part of the 2009-HCDN. As for the original HCDN, the 2009-HCDN consists of sites defined as having potential for use in hydro-climatic studies following criteria based on continuous flow record length, activity within the watershed, and basin characteristics (<5% imperviousness); additional details are provided by *Falcone et al.* [2011]. Therefore, if the sites were included in the 2009-HCDN, this would suggest that anthropogenic effects on flood flows were minor over the duration of the record, and thus any nonstationarity in the flood series should be due to climate/meteorological influences, as previously discussed. Of the 235 sites under consideration, only 55 sites are contained within the 2009-HCDN. Of the 55 sites, 11 were identified to have a significant trend, and 15 have a significant change-point (see Chapter 2), which would presumably be due to climatic/meteorologic influences as discussed above.

For the remaining 180 sites under consideration, which are not included in the 2009-HCDN, the fore mentioned investigation of climatic/meteorologic causes does not explain all of the identified trends and/or shifts in AMF peaks series, thus suggesting structural/anthropogenic effects may play a role in the observed nonstationarity. Table 3.13 reports summary results for 18 sites which were identified to contain a significant shift in the magnitude of AMF series, and for which water report remarks pertinent to hydrologic modifications were obtained from the Annual Data Report [*Falcone et al.*, 2011]. The last column in the table reports the difference between the year in which the Water Report remark was made and the year in which the shift in the AMF series occurs. Thus, a negative difference indicates that the hydrologic modification leads the shift in flood magnitude. Further, a small difference would indicate a possible causative effect on flood magnitude. Sites for which further analysis is warranted are indicated in bold font. For example, USGS #03193000 was identified to have a shift in the mean of the AMF series in 1939, which was consistent with a water resources remark indicating that

flow has been regulated since 1939 by Claytor Lake [Falcone *et al.*, 2011]. This method was used because the water report remarks are more specific to the timing of the hydrologic modification than alternative informational databases, such as the USGS qualification codes indicating the degree of regulation or diversion previously employed by others for similar assessments of anthropogenic influences [e.g., Villiarini *et al.*, 2009, Villarini *et al.*, 2011].

Table 3.13

Summary results for sites with significant shifts in AMF magnitude for which water report remarks pertinent to hydrologic modifications exist within Falcone *et al.* [2011].

Table 3.13, continued

Station Number	Mann-Kendall Trend Results		Pettitt Change-Point Results		Water Report Remarks	
	Direction of Trend	p-value	p-value	Year	Year	Difference
01011000			0.040	1968	1969	1
01175500	-	0.004	0.000	1939	1939	0
01176000	+	0.010	0.036	1967	1965	-2
01408500			0.081	1957	1990	33
01426500	-	0.000	0.000	1963	1963	0
01512500			0.031	1950	1942	-8
01518000	-	0.011	0.000	1980	1979	-1
01520500	-	0.000	0.000	1979	1979	0
01541500			0.017	1956	1960	4
01567000	-	0.001	0.006	1937	1973	36
03024000			0.057	1969	1970	1
03193000	-	0.002	0.003	1940	1939	-1
03262000			0.064	1930	1921	-9
04112500			0.051	1957	1975	18
04262500	+	0.064	0.048	1973	1985	12
05592500			0.069	1942	1969	27
05593000			0.003	1962	1967	5
05597000	-	0.021	0.003	1964	1970	6

Change in dam storage could also cause changes in the magnitude of AMF peaks. Estimates of dam storage (megaliters total storage per square km) for each watershed pre-

1940, -1950, -1960, -1970, -1980 and -1990 were obtained from the GAGES II database ([*Falcone et al.*, 2011 and references therein]). For relevant sites, the decade within which the largest change in storage was observed is reported in Table 3.14. The year reported is the last year of the decade in which the largest change occurred. For instance, for USGS Station No. 01011000, the largest change occurred in the period 1961 to 1970. The table also reports results of the Pettitt tests performed on the AMF series as discussed in CHAPTER 2. For each site, the last column of the table reports the difference between the end year of the decade in which the largest change in storage was observed and the year in which the shift in the AMF series occurs. Thus, positive differences on the order of 0-10 years and small negative differences would suggest a possible causative effect of the change in storage on flood magnitude. Based on this cursory analysis, a number of the AMF series could be influenced by change in dam storage. However, as the change in storage is computed on a decadal time scale, further analyses should be conducted to link increasing dam storage over time with the gradual trends observed in AMF series, or perhaps step changes therein which could be identified using an alternative homogeneity test, such as the Bayesian change-point test proposed by *Seidou and Ouarda* [2007].

The analysis of anthropogenic effects presented herein provides a general direction for future research, as more detailed analyses are needed on a site-by-site basis. In addition, to improve flood frequency forecasts for long-term planning and management, it will be necessary to quantify the impacts of anthropogenic activities relative to those of natural climate variability [e.g., *Juckem et al.*, 2008]. To quantify the impacts of nonstationarity due to anthropogenic effects, AMF series could be regressed on their respective flood generating hydroclimatic series to determine the amount of flow individually explained by precipitation and temperature. The residual flow values after removing the effects of precipitation and temperature could then be tested for trends; any remaining trends could be attributed to land use changes, or other anthropogenic influences.

Table 3.14

Summary results for sites with shifts in the magnitude of AMF series and corresponding changes in amount of storage (megaliters total storage per square km) in each basin.

Station Number	Year	p-value	Year	Max Change	Difference
01011000	1968	0.040	1970	38.3	2
01031500	1966	0.022	1960	5.75	-6
01064500	1966	0.035	1980	1.54	14
01119500	1971	0.038	1970	44.5	-1
01127500	1967	0.020	1970	0.29	3
01169000	1972	0.000	1980	1.63	8
01175500	1939	0.000	1980	0.20	41
01176000	1967	0.036	1970	12.2	3
01181000	1968	0.018	1970	13.5	2
01196500	1968	0.000	1960	7.77	-8
01334500	1972	0.000	1990	1.96	18
01379500	1966	0.010	1950	0.58	-16
01387500	1967	0.003	1960	3.13	-7
01396500	1969	0.002	1980	0.47	11
01398500	1969	0.002	1950	1.09	-19
01408500	1957	0.081	1960	2.14	3
01411000	1966	0.027	1960	2.17	-6
01420500	1968	0.000	1950	1.24	-18
01426500	1963	0.000	1970	360.9	7
01439500	1967	0.014	1960	14.6	-7
01445500	1966	0.000	1980	6.59	14
01503000	1964	0.066	1960	12.9	-4
01512500	1950	0.031	1950	56.7	0
01518000	1980	0.000	1980	243.9	0
01520500	1979	0.000	1980	173.5	1
01531000	1964	0.024	1980	53.8	16
01541500	1956	0.017	1970	87.6	14
01548500	1935	0.069	1970	3.82	35
01567000	1937	0.006	1980	125.3	43
01604500	1967	0.039	1970	58.1	3
01634500	1970	0.000	1980	1.79	10
01645000	1970	0.000	1990	116.7	20
01667500	1971	0.056	1970	4.32	-1
02016000	1968	0.040	1980	1.08	12
03010500	1939	0.003	1970	0.05	31
03024000	1969	0.057	1980	60.1	11
03069500	1954	0.002	1960	0.55	6
03109500	1959	0.002	1960	6.91	1
03167000	1978	0.010	1970	4.50	-8

Table 3.14, continued

Station Number	Year	p-value	Year	Max Change	Difference
03193000	1940	0.003	1950	35.9	10
03234500	1972	0.034	1980	26.8	8
03262000	1930	0.064	1980	0.30	50
03307000	1973	0.006	1970	0.35	-3
03345500	1981	0.078	1990	3.39	9
03379500	1981	0.036	1980	21.4	-1
03381500	1981	0.040	1980	11.6	-1
04073500	1953	0.021	1970	9.43	17
04079000	1976	0.076	1970	5.12	-6
04112500	1957	0.051	1980	0.50	23
04191500	1973	0.063	1980	7.76	7
04193500	1973	0.078	1980	3.49	7
05280000	1964	0.012	1950	12.7	-14
05304500	1964	0.005	1970	52.7	6
05316500	1974	0.003	1990	0.46	16
05317000	1982	0.094	1950	1.09	-32
05340500	1940	0.000	1970	5.03	30
05408000	1984	0.012	1980	4.38	-4
05414000	1979	0.000	1980	0.20	1
05422000	1972	0.053	1970	0.56	-2
05432500	1969	0.001	1980	2.04	11
05434500	1975	0.008	1960	2.95	-15
05435500	1953	0.006	1960	2.66	7
05436500	1953	0.014	1960	0.27	7
05446500	1970	0.049	1970	2.38	0
05447500	1968	0.001	1960	0.36	-8
05454500	1953	0.004	1960	61.6	7
05476000	1982	0.046	1950	2.21	-32
05484500	1943	0.006	1970	10.1	27
05495000	1972	0.036	1990	2.84	18
05501000	1972	0.011	1960	3.83	-12
05520500	1965	0.000	1980	2.21	15
05526000	1967	0.002	1960	3.17	-7
05527500	1967	0.000	1980	4.24	13
05555300	1978	0.011	1970	0.17	-8
05585000	1958	0.019	1950	1.84	-8
05592500	1942	0.069	1980	252.2	38
05593000	1962	0.003	1980	179.5	18
05597000	1964	0.003	1980	367.4	16
07016500	1980	0.011	1970	8.69	-10
07018500	1981	0.058	1970	39.8	-11
07019000	1980	0.010	1970	13.8	-10

CHAPTER 4 CLIMATE INFORMED FLOOD RISK PROJECTIONS

Standard procedures for forecasting flood risk (e.g., *Bulletin 17B*) assume AMF series are stationary, meaning the distribution of flood flows is not significantly affected by climatic trends or cycles. However, in light of surmounting evidence to the contrary [e.g. *Olsen et al.*, 1999; *Kashelikar and Griffis*, 2008; *Collins*, 2009; *Villarini et al.*, 2009, 2011], including results presented in Chapters 2 and 3 herein, this assumption deserves reconsideration. This chapter provides an overview of the current procedures for flood frequency analysis within the U.S. as outlined in *Bulletin 17B* [IACWD, 1982], and recommends an extension of those procedures to account for nonstationarity in flood peaks caused by large-scale oceanic-atmospheric patterns (AMO, PDO, and ENSO). The proposed extension is a modified version of the model proposed by *Kashelikar and Griffis* [2008] and *Kashelikar* [2009] for improved one-year ahead forecasts of flood risk. Their model only incorporated effects of ENSO on flood risk, and was based on the assumption that flood peaks throughout the U.S. tend to occur in April.

4.1 Current Procedures

Water resources planning and management requires coordination between various levels of government (e.g., local, state and federal), as well as the private sector. Thus, a set of uniform flood frequency analysis procedures for use across agencies has been sought after since the U.S. Water Resources Council published their first attempt, *Bulletin 15* in 1967 [WRC, 1967]. Several updates were published thereafter to create a more unified and accurate set of guidelines, culminating with the publication of *Bulletin 17B* in 1982 [IACWD, 1982]. Despite recognized discrepancies within and limitations of those procedures [see *Thomas*, 1985], as well as subsequent advances in statistics and computing capabilities over the last 30 years [see *Griffis and Stedinger*, 2007a; *Stedinger and Griffis*, 2008], a new update to the *Bulletin* has yet to be published. *Griffis and Stedinger* [2007a] provide an in-depth review of the development/evolution of the *Bulletin*, an evaluation of its procedures, and recommendations for improvements.

A primary limitation of the procedures outlined in *Bulletin 17B* is that they are based on the assumption that AMF series are stationary, and thus the distribution of flood flows is assumed to be unaffected by climatic trends and/or cycles. Historical flood events are thus considered representative of future flood occurrences, and the flood risk associated with a given magnitude of flow is modeled as constant over time. In addition, *Bulletin 17B* procedures assume AMF series are composed of independent and identically distributed events. Thereby, it is inherently assumed that gradual land use/land cover changes have little to no effect on flood peaks despite evidence of anthropogenic-induced nonstationarity in flood peaks [e.g., *Potter*, 1991; *Pinter et al.*, 2008; *Villiarini et al.*, 2009, 2011]. Although evidence of both climatic and anthropogenic effects on AMF series is mounting, *Bulletin 17B* remains the standard for flood frequency analysis in the U.S. *Stedinger* and *Griffis* [2011] comment on the need to adapt the traditional B17 model to incorporate parameters which reflect climatic/physical causes of nonstationarity in AMF series. The use of parameters which reflect influences of oceanic-atmospheric patterns on flood magnitude is discussed herein.

Bulletin 17B procedures employ the log-Pearson type III (LP3) distribution to model the frequency associated with annual maximum flood peaks. The LP3 distribution is a three parameter distribution which describes a random variable whose logarithms are Pearson type III (P3) distributed with shape, scale, and location parameters α , β and ξ , respectively. The P3 distribution is defined by the probability density function:

$$f_x(x) = \frac{1}{|\beta|\Gamma(\alpha)} \left(\frac{x - \xi}{\beta} \right)^{\alpha-1} \exp \left(- \frac{x - \xi}{\beta} \right) \quad (25)$$

for $\alpha > 0$ and $(x - \xi)/\beta > 0$, where $\Gamma(\alpha)$ is the gamma function:

$$\Gamma(\alpha) = \int_0^{\infty} t^{\alpha-1} e^{-t} dt \quad (26)$$

Given a record of n years at an individual station, *Bulletin 17B* procedures involve fitting a LP3 distribution to the annual maximum flood series $\{Q_1, Q_2, \dots, Q_n\}$ by fitting a P3

distribution to the base-10 logarithms of the flood peaks $\{X_1, X_2, \dots, X_n\}$ using the method of moments (MOM). The population mean (μ_x), standard deviation (σ_x) and skew (γ_x) of the logarithms are estimated using traditional moment estimators:

$$\hat{\mu}_x = \frac{1}{n} \sum_{i=1}^n x_i \quad (27)$$

$$\hat{\sigma}_x = \sqrt{\frac{1}{n-1} \sum_{i=1}^n (x_i - \hat{\mu}_x)^2} \quad (28)$$

$$\hat{\gamma}_x = \frac{n}{(n-1)(n-2)} \sum_{i=1}^n \left(\frac{x_i - \hat{\mu}_x}{\hat{\sigma}_x} \right)^3 \quad (29)$$

Using MOM, the parameters of the P3 distribution (α, β, ξ) are then estimated using the following equations wherein the population moments are equated to the sample moments:

$$\hat{\alpha} = \frac{4}{\hat{\gamma}_x^2} \quad (30)$$

$$\hat{\beta} = \frac{\hat{\sigma}_x \hat{\gamma}_x}{2} \quad (31)$$

$$\hat{\xi} = \hat{\mu}_x - 2 \frac{\hat{\sigma}_x}{\hat{\gamma}_x} \quad (32)$$

The statistical reliability of $\hat{\alpha}$, $\hat{\beta}$, $\hat{\xi}$, and therefore, the accuracy of the fitted LP3 distribution and subsequent quantile estimators, are highly dependent on the accuracy of $\hat{\mu}_x$, $\hat{\sigma}_x$ and $\hat{\gamma}_x$. The traditional moment estimators are functions of at-site data, and due to limited record lengths, often less than 30 years, the skewness estimator can be unstable. Instability in the at-site skewness estimator is improved by using a regional skewness estimator which combines data from nearby sites [IACWD, 1982]. The use of the LP3 distribution in flood frequency analysis and the value of weighted skew estimators are discussed in detail by *Griffis and Stedinger* [2007b,c, 2009].

A closed-form expression for the cumulative distribution function (CDF) of the P3 distribution and its inverse are not available. To account for this, the p^{th} quantile of the fitted P3 distribution is computed as follows:

$$\hat{X}_p = \log(\hat{Q}_p) = \hat{\mu}_x + \hat{\sigma}_x K_p(\hat{\gamma}_x) \quad (33)$$

where the frequency factor $K_p(\hat{\gamma}_x)$ is the p^{th} quantile of a standard P3 distribution with mean zero, variance 1 and skew $\hat{\gamma}_x$ [IACWD, 1982; Chow *et al.*, 1988]. For $|\gamma_x| < 2$, $\gamma_x \neq 0$ and $0.01 < p < 0.99$, $K_p(\hat{\gamma}_x)$ is well approximated by the Wilson-Hilferty transformation [Kirby, 1972]:

$$K_p(\hat{\gamma}_x) = \frac{2}{\hat{\gamma}_x} \left\{ \left[\left(z_p - \frac{\hat{\gamma}_x}{6} \right) \frac{\hat{\gamma}_x}{6} + 1 \right]^3 - 1 \right\} \quad (34)$$

where z_p is the p^{th} quantile of a standard normal distribution. As γ_x goes to zero, the P3 distribution converges to the normal distribution. As a result, P3 quantiles for $|\gamma_x| < 0.01$ are given by:

$$\hat{X}_p = \hat{\mu}_x + \hat{\sigma}_x z_p = \hat{\mu}_x + \hat{\sigma}_x \Phi^{-1}(p) \quad (35)$$

where $\Phi()$ represents the CDF of the standard normal distribution. Quantiles obtained using equations (33) and (35) must subsequently be converted back to real space using a base-10 antilogarithmic transformation to yield the magnitude of discharge associated with the desired exceedance probability (i.e., magnitude of a design event).

Quantiles computed using the equations above, and the associated frequency curve, are only approximations of the population distribution/quantiles based on a limited sample of observations. To account for the presence of sampling variability, confidence intervals can be constructed to provide a measure of the uncertainty in the estimated discharge [design magnitude] at a selected exceedance probability (E). *Bulletin 17B* (Appendix 9) presents a procedure to approximate the uncertainty in the P3 quantile estimates [IACWD, 1982]. Confidence limits are computed as follows:

$$U_{E,C}(X) = \bar{X} + S(k_{E,C}^U) \quad (36)$$

$$L_{E,C}(X) = \bar{X} + S(k_{E,C}^L) \quad (37)$$

where \bar{X} and S are the log base-10 mean and standard deviation corresponding to the final estimated LP3 density function representing the AMF series. The upper and lower confidence coefficients $k_{E,C}^U$ and $k_{E,C}^L$ are based on a large sample approximation using the non-central t-distribution:

$$k_{E,C}^U = \frac{K_{G_W,E} + \sqrt{K_{G_W,E}^2 - ab}}{a} \quad (38)$$

$$k_{E,C}^L = \frac{K_{G_W,E} - \sqrt{K_{G_W,E}^2 - ab}}{a} \quad (39)$$

where

$$a = 1 - \frac{Z_c^2}{2(n-1)} \quad (40)$$

$$b = K_{G_W,E}^2 - \frac{Z_c^2}{n} \quad [41]$$

and Z_c is the standard normal deviate with cumulative probability, C. The value of C employed reflects the desired level of confidence with which the computed bounds should contain the true quantile of the P3 distribution. The record length, n, controls the statistical reliability (accuracy) of the estimated function [IACWD, 1982]. Thus, the accuracy of quantile estimates increases with the availability of additional flood peak occurrences.

4.2 Proposed Modification to Bulletin 17B

Several studies have proposed methods for coping with nonstationarity when forecasting flood risk. *Strupczewski et al.* [2001] and *Olsen et al.* [1999] incorporated hydrological nonstationarity into at-site flood frequency estimation by projecting observed trends in AMF series. Severe limitations arise with this proposed method; identified linear monotonic trends may be better characterized as an abrupt shift, or could be part of a larger cycle not evident in the period of record. Other methods which account for nonstationarity in flood frequency analysis by employing time-dependent distribution parameters have also been proposed [e.g., *Coulibaly and Baldwin*, 2005; *Sveinsson et al.*, 2005; *Villarini et al.*, 2009, 2011]. Unfortunately, the ability of models such as these, which consider variations in flood risk only as a function of time, to accurately forecast flood risk under changing climate and/or land use/land cover is questionable. On the contrary, *Kiem et al.* [2003], *Kashelikar and Griffiths* [2008], *Kwon et al.* [2008], and *Kashelikar* [2009] propose models of flood risk which reflect observed nonstationarity in flood series due to influences of oceanic-atmospheric patterns. *Stedinger and Griffiths* [2011] further comment on the need to adapt traditional flood frequency analysis procedures to incorporate parameters which can vary over time in response to climatic/physical causes of nonstationarity in AMF series.

A model is proposed herein which incorporates the coupled effects of multiple climate patterns on flood magnitude to provide one-year ahead forecasts of both the mean and standard deviation of the log-transformed flood peaks. This work extends the model proposed by *Kashelikar* [2009], wherein nonstationarity in flood peaks was accounted for by updating (shifting) the mean year to year in response to climate variability associated strictly with ENSO events. The model proposed herein also corrects a major limitation of that proposed by *Kashelikar* [2009]. Her forecasts (updates) of the mean were computed as a function of ENSO indices obtained with a specified lead time based on the assumption that flood peaks across the U.S. tend to occur in the month of April. Results provided in CHAPTER 3 herein demonstrate that this assumption is not valid for many areas of the U.S. (see Figure 3.2). Instead, model parameters based on climate indices relative to the mode month of flood peak occurrence for a given site would provide a

more appropriate framework for forecasting flood risk wherein the time occurrence of the future flood peak is unknown. The correlation analyses presented in CHAPTER 3 indicate that the mean of the log-transformed flows can be modeled as functions of the AMO, MEI, NAO, and PDO indices with 6-, 9-, 3-, and 9-month lead times, respectively, relative to the mode month of occurrence. Similarly, the standard deviation of the log-transformed flows can be modeled as functions of the AMO, MEI, NAO, and PDO indices with 3-, 9-, 3-, and 9-month lead times, respectively.

For each site in Figure 2.3, climate informed P3 parameters are obtained using a regression model of the following form:

$$\begin{aligned}\mu[t] &= \alpha_1 + \beta_{11}C_{t_AMO} + \beta_{12}C_{t_MEI} + \beta_{13}C_{t_NAO} + \beta_{14}C_{t_PDO} + \varepsilon_t \\ \sigma[t] &= \alpha_2 + \beta_{21}C_{t_AMO} + \beta_{22}C_{t_MEI} + \beta_{23}C_{t_NAO} + \beta_{24}C_{t_PDO} + \varepsilon_t\end{aligned}\quad (42)$$

where $\mu(t)$ and $\sigma(t)$ are the mean and standard deviation of the log-transformed flows computed using a 10-year moving window ending in time t , C_{t_i} is a three-month average of climate index i observed in time t with an appropriate lead time relative to the mode month of occurrence of AMF peaks at the site in question, α and β are regression parameters, and ε_t is the independent model error. The logarithms of the AMF peaks are subsequently modeled as:

$$X_t \sim P3[\mu_x(t), \sigma_x(t), \gamma] \quad (43)$$

in which the skew of the logarithms (γ) is independent of time (i.e., stationary). Year-specific quantile estimates (for year t) which reflect the influence of climate patterns can then be obtained using equation (33) or (35) as a function of the updated (or climate-informed) mean $\mu(t)$ and standard deviation $\sigma(t)$. The proposed model does not consider the skew estimator to be a function of time due to present challenges in the standard stationary procedure to estimate the skew well with limited data [Reis *et al.*, 2005; Gruber and Stedinger, 2008; Griffis and Stedinger, 2009]. In addition, *Bulletin 17B* procedures to improve quantile estimates by using regional skew information, accounting for low outliers, or the addition of historical flood data are not considered herein.

4.3 Climate Informed Flood Risk Projection

The extension of the *Bulletin 17B* framework proposed above can be used to obtain one-year ahead forecasts of flood risk which reflect the influence of large-scale climate patterns (AMO, NOA, ENSO, or PDO). To do so, the site specific regression models of the form in equation (42) would be used to forecast the mean and standard deviation one-year ahead in time ($t+1$) using forecasts of relevant climate indices obtained from (http://www.cpc.ncep.noaa.gov/products/analysis_monitoring/lanina/ensoforecast.shtml). To illustrate how accounting for nonstationarity due to climate variability impacts projected flood risk, one-year ahead estimates of flood risk corresponding to various cumulative probabilities were computed for six sample USGS gauging stations (Figure 4.1) using the proposed model and compared against estimates computed under the assumption of stationarity (i.e., the traditional *Bulletin 17B* model). The parameters of the regression models for $\mu(t)$ and $\sigma(t)$ for each station were obtained using the logarithms of annual maximum flood data through $t = 2008$. The values of the regression parameters obtained for the model of the mean and standard deviation at each site are reported in Table 4.2 and Table 4.3, respectively. One-year ahead forecasts of the mean and standard deviation for $t = 2009$ obtained for each of the stations are reported in Table 4.4; the parameters of the traditional (stationary) *Bulletin 17B* LP3 model obtained using all available data through 2008 are also provided. The mode month of occurrence was April for all sites considered; thus, respective climate indices used to forecast $\mu(2009)$ and $\sigma(2009)$ were the same. The historical (observed) three-month averaged climate indices with the appropriate lead times for 2009 are reported in Table 4.1. With the exception of PDO, the climate patterns were reasonably neutral in 2009, therefore, a hypothetical extreme scenario was also considered, assuming all climate indices were in the positive (warm) phase. For each climate pattern, the extreme value employed is the maximum value of the three-month averaged climate index with the appropriate lead observed over the period of record.

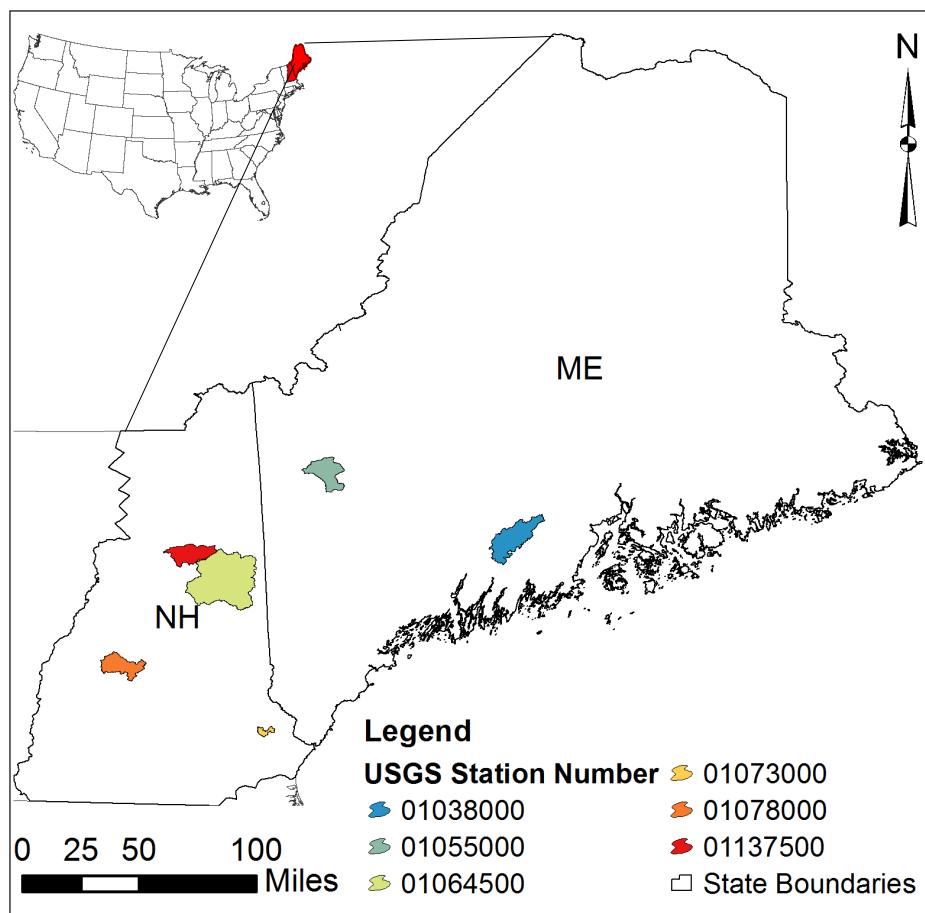


Figure 4.1 Location of six USGS stations used to compare current flood risk projection procedures to proposed climate informed flood risk projection model.

Table 4.1

Three-month averaged values of climate indices with specified lead time relative to April flood peak used in regression models to obtain one-year ahead forecasts $\mu(2009)$ and $\sigma(2009)$: observed values for 2009 and extreme scenario.

Parameters	AMO (6m lead)	MEI (9m lead)	NAO (3m lead)	PDO (9m lead)
Extreme Scenario	0.300	2.140	1.720	2.557
Observed	0.027	-0.104	-0.203	-1.460

Table 4.2

Regression coefficients obtained for the model of the log space mean at six sample sites. Coefficients reported are all significant at the 10% level.

Site Number	Intercept (α_1)	AMO (β_{11})	MEI (β_{12})	NAO (β_{13})	PDO (β_{14})	R ²
01038000	3.313	-0.073		0.020	0.023	0.330
01055000	3.793	0.075		0.035	0.019	0.359
01064500	4.245	0.068		0.041	0.026	0.467
01073000	2.482	0.125			0.028	0.447
01078000	3.226			0.021	0.017	0.322
01137500	3.651	0.141	-0.016	0.027	0.012	0.544

Table 4.3

Regression coefficients obtained for the model of the log space standard deviation at six sample sites. Coefficients reported are all significant on the 10% level.

Site Number	Intercept (α_2)	AMO (β_{21})	MEI (β_{22})	NAO (β_{23})	PDO (β_{24})	R ²
01038000	0.184	-0.097		0.014	0.012	0.376
01055000	0.252	0.053				0.169
01064500	0.235			-0.031	-0.013	0.234
01073000	0.235	0.068				0.146
01078000	0.175					0.203
01137500	0.189			-0.017	-0.010	0.204

Table 4.4

Moments of the log-transformed flood peaks based on stationary P3 model through 2008, proposed model with observed climate indices for 2009 and hypothetical extreme climate indices.

Site Number	Stationary P3 Model				Proposed Model (2009 Indices)		Proposed Model (Extreme Indices)	
	Years	μ	σ	γ	$\mu(t)$	$\sigma(t)$	$\mu(t)$	$\sigma(t)$
01038000	72	3.323	0.197	0.569	3.261	0.161	3.372	0.210
01055000	81	3.784	0.243	-0.280	3.773	0.253	3.938	0.268
01064500	81	4.231	0.225	-0.255	4.213	0.260	4.415	0.148
01073000	74	2.494	0.234	0.158	2.466	0.236	2.613	0.255
01078000	91	3.255	0.194	0.448	3.197	0.176	3.306	0.195
01137500	70	3.643	0.183	0.254	3.657	0.208	3.760	0.132

The sample moments (μ , σ , γ) of the log-transformed data through 2008 are reported in Table 4.4. These moments define the P3 distribution used to forecast flood risk under the assumption that flood series are stationary (i.e., *Bulletin 17B* model). The P3 distribution used to forecast flood risk under the proposed model is defined by the values of $\mu(2009)$ and $\sigma(2009)$ reported in Table 4.4, for either the historical (observed) indices or the extreme scenario, combined with the skew γ computed assuming stationarity. Figure 4.2 through Figure 4.7 show one-year ahead forecasts of flood risk obtained using these three models. Overall, these examples demonstrate that the modified (proposed) LP3 model can yield significantly different flood risk estimates than the traditional *Bulletin 17B* model. The proposed modification of the *Bulletin 17B* LP3 model yields one-year ahead forecasts of flood risk which are consistent with the phase and intensity of climate patterns, and thus the observed differences in flood risk forecasts are enhanced when climate indices are more extreme. Similar observations were made by *Kashelkar* [2009] who only considered the mean to be variable over time, modeled as a function of the Nino3.4 index. However, before the model can be adopted in practice, analyses must be performed to validate the model performance for projection of flood risk.

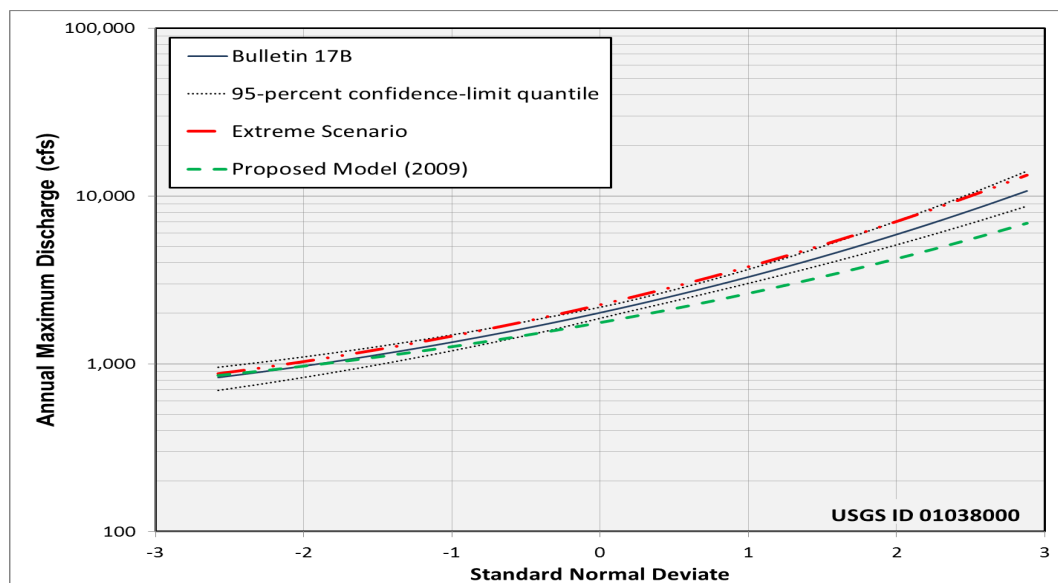


Figure 4.2 One-year ahead forecast of flood risk for Sheepscot River at North Whitefield, Maine (USGS Station No. 01038000) obtained using the *Bulletin 17B* LP3 model and the proposed modification to incorporate climate variability.

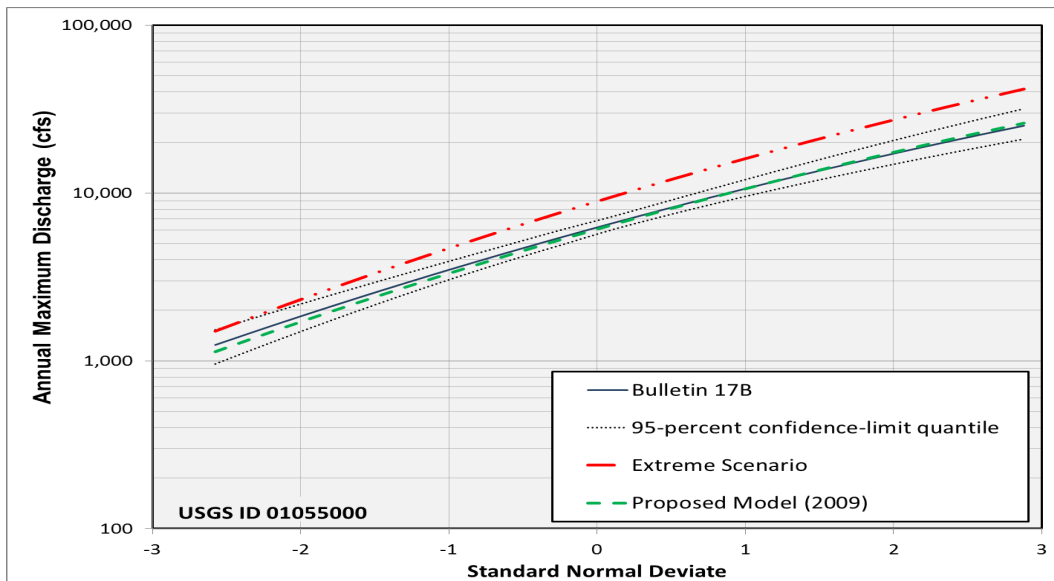


Figure 4.3 One-year ahead forecast of flood risk for Swift River near Roxbury, Maine (USGS Station No. 01055000) obtained using the Bulletin 17B LP3 model and the proposed modification to incorporate climate variability.

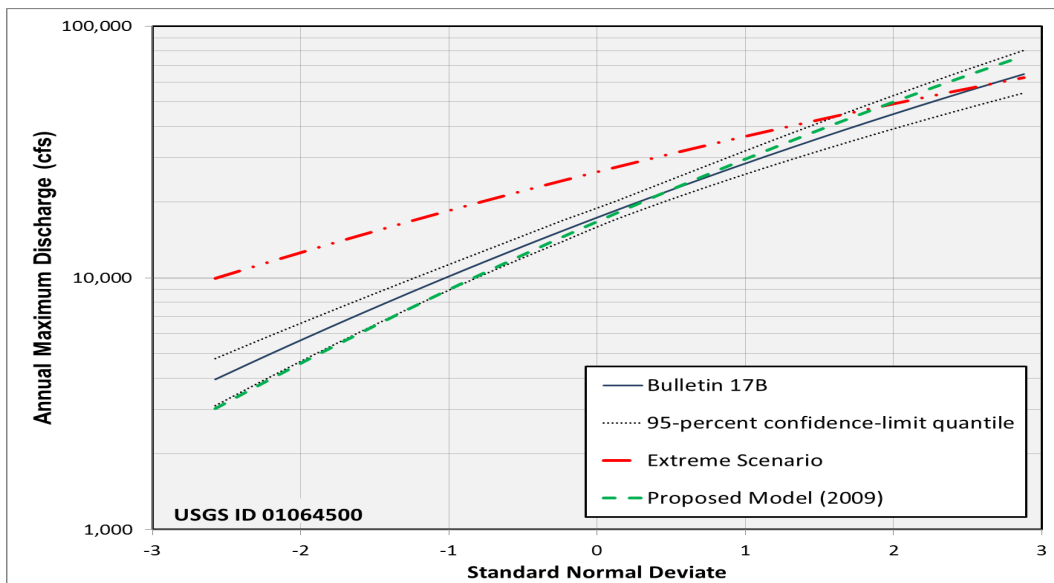


Figure 4.4 One-year ahead forecast of flood risk for Saco River near Conway, NH (USGS Station No. 01064500) obtained using the Bulletin 17B LP3 model and the proposed modification to incorporate climate variability.

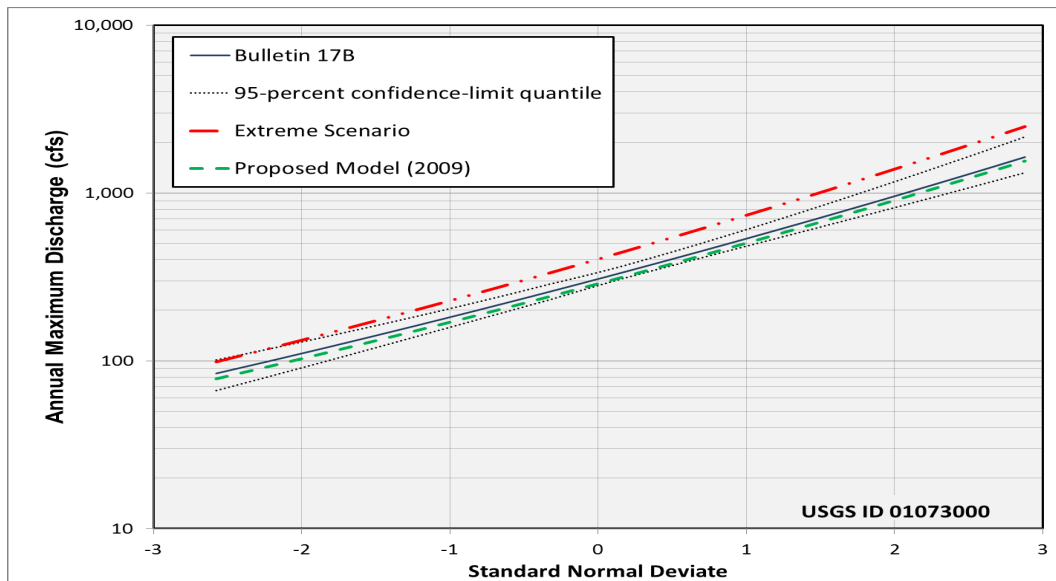


Figure 4.5 One-year ahead forecast of flood risk for Oyster River near Durham, NH (USGS Station No. 01073000) obtained using the Bulletin 17B LP3 model and the proposed modification to incorporate climate variability.

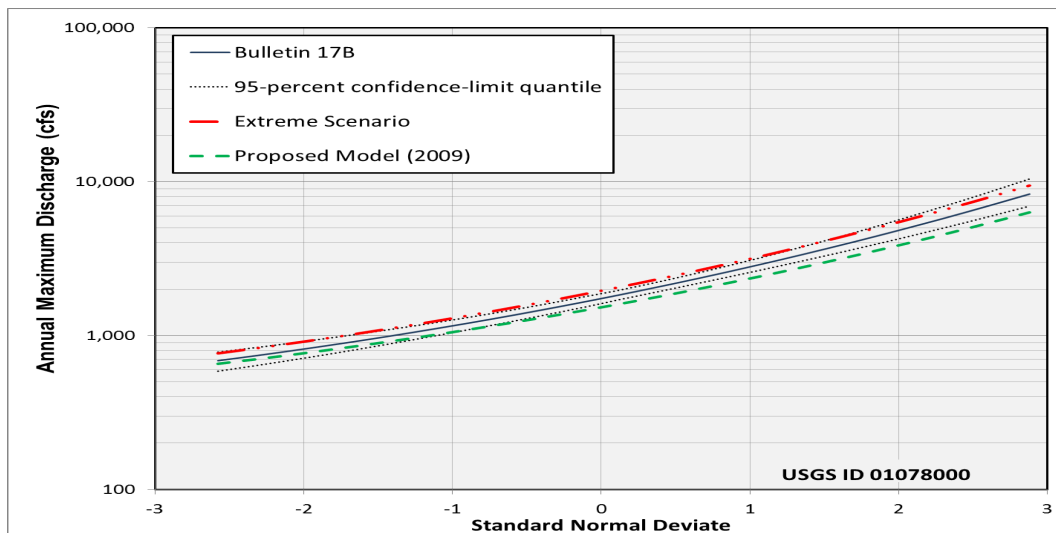


Figure 4.6 One-year ahead forecast of flood risk for Smith River near Bristol, NH (USGS Station No. 01078000) obtained using the Bulletin 17B LP3 model and the proposed modification to incorporate climate variability.

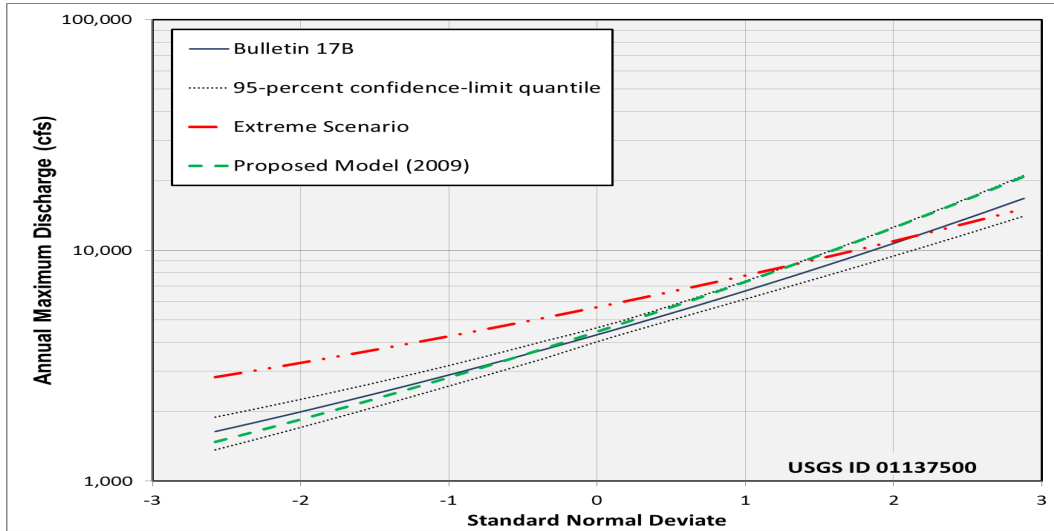


Figure 4.7 One-year ahead forecast of flood risk for Ammonoosuc River at Bethlehem Junction, NH (USGS Station No. 01137500) obtained using the Bulletin 17B LP3 model and the proposed modification to incorporate climate variability.

4.4 Model Limitations and Future Work

The proposed modification of *Bulletin 17B* procedures appropriately increases/decreases expected flood risk relative to the phase and intensity of forecasted anomalies indicative of climate indices (e.g., AMO, MEI, NAO and PDO) for the upcoming year. However, estimates of $\mu(t)$ and $\sigma(t)$ could possibly be improved by employing non-linear or non-parametric models instead of a multiple linear regression model as proposed in equation (42). Additionally, cyclical patterns in AMF series could be better understood by applying spectral analyses, thereby providing insight as to the appropriate model form for $\mu(t)$ and $\sigma(t)$.

The model proposed herein would be particularly useful for long-term planning and/or construction horizons (e.g., 10-, 50-, 100-years), but how to forecast the needed climate indices with sufficient accuracy is not clear at this time. One possible solution would be to model the log space mean, and perhaps the standard deviation, as a function of appropriately downscaled GCM outputs. Results presented in CHAPTER 3 indicate that strong relationships exist between the magnitude of AMF peaks and the associated flood generating precipitation series. Although flood generating series could not be obtained

directly, the use of the monthly precipitation forecasted within the mode month of flood peak occurrence could be investigated as a possible substitute. In addition, as the timing of flood peaks is highly correlated with temperature, GCM outputs could be used to forecast the timing of the flood peak in a future year instead of using the mode month of occurrence as a reference. The forecasted time (month) of occurrence could then be combined with a model of magnitude based on precipitation to indicate overall flood risk in the future. Along these lines, meteorological inputs such as quantity and timing of precipitation events, as well as storm type, should be further investigated to understand changes in hydrological extremes.

Beyond impacts of climate variability and potential climate change, the influence of human activities within the watershed on future flood risk must also be considered. Several USGS studies provide insight for modeling flood risk as a function of physical, observable watershed characteristics. Regional regression equations have been developed for the estimation of peak discharges with various recurrence intervals for rural watersheds as a function of characteristics, such as drainage area and percent forest cover [Jennings *et al.*, 1994]. A procedure is also available to estimate peak discharges in urban watersheds as a function of the rural equivalent peak discharge and physical characteristics including percent impervious surface and a basin development factor used to quantify manmade changes to the drainage system [Sauer *et al.*, 1983]. Although these procedures assume flood series are stationary, a recent extension by Moglen and Shivers [2006] accounts for nonstationarity in flood series resulting from urbanization via annual time series of percent impervious surface, or population density as a surrogate where data is limited [e.g., Stankowski, 1972]. A comprehensive analysis of how flood risk could be forecasted in the presence of both climatic and anthropogenic changes has yet to be conducted. But, the fore mentioned studies provide insight to how a physical-causal based statistical model for flood risk projection can be created based on knowledge of the inherent structure of AMF series, and the physical and/or climatic causes of nonstationarity therein. Thus:

“The issue is how to use all the information available to reliably forecast flood risk in the future: “Where do we go from here?”” [Stedinger and Griffis, 2011]

CHAPTER 5 CONCLUSIONS

Flooding is the most common occurring natural disaster, and a large portion of the U.S. population, infrastructure, and industry is located in flood prone areas. However, the structural and nonstructural strategies (e.g., the National Flood Insurance Program) used to reduce the economic, social and environmental impacts of floods continue to be based on static estimates of flood risk. The standard procedures for flood frequency analysis (i.e., *Bulletin 17B*) assume annual maximum flood (AMF) peaks are independent, identically distributed, and stationary over time; thus, AMF peaks are assumed to be unaffected by climate cycles and/or trends, or by human activities within the watershed. However, in light of surmounting evidence to the contrary, these assumptions deserve reconsideration.

The research presented herein investigated the presence of nonstationarity in AMF series for relatively unimpaired watersheds throughout the contiguous U.S. Standard statistical tests reveal AMF series exhibit nonstationarity in the form of monotonic trends, abrupt shifts, and/or long-term persistence in terms of flood magnitude. Sites exhibiting either positive or negative trends in AMF magnitude tend to be clustered throughout the U.S. However, half of these sites also contain a significant change-point, and thus, the nonstationarity in these AMF series would likely be better characterized by an abrupt shift, rather than a gradual monotonic change. Further, as the majority of the sites considered displayed signs of long-term persistence by means of the Hurst exponent, it is possible that the identified trend/change-points in the flood series are part of a long-term cycle not evident in the available record. Thus, future work should include a more in-depth analysis of the possible cyclical behavior of AMF series using methods such as spectral analysis. The time of occurrence of flood peaks was also investigated for signs of nonstationarity as an identified shift (change-point) or a linear trend could be indicative of a steady change towards an earlier/later spring; however, few sites yielded significant results.

Watersheds are deemed unimpaired when human activities have insignificant impacts on the distribution of flows; therefore, for the purposes of this study, any nonstationarity identified in corresponding flood series should be primarily due to meteorological and/or climatic forcing, although modest trends could be observed in response to land use/land cover changes over time. Driving causes of nonstationarity in AMF series were investigated herein by relating observed changes in flood magnitude and timing to that of associated flood generating hydroclimatic series (total precipitation and average temperature series prior to occurrence of flood peak), as well as climate anomalies indicative of the large-scale climate forcing of oceanic-atmospheric patterns. Climate patterns—including the El Niño-Southern Oscillation (ENSO), North Atlantic Oscillation (NAO), Pacific Decadal Oscillation (PDO), and Atlantic Multidecadal Oscillation (AMO)—were identified as influencing factors on AMF magnitudes at numerous unimpaired gauging stations throughout the contiguous U.S. Strong relationships between AMF magnitudes and flood generating precipitation series were observed for the majority of sites analyzed in the northeast quadrant of the U.S. Although significant relationships were not identified between flood magnitude and associated temperature series, results indicate that flood generating temperature series are highly correlated with the timing of AMF peaks.

Despite the fact that the watersheds considered were classified as unimpaired, analyses herein suggest possible anthropogenic causes (e.g., regulation, dams, land use/land cover changes) of nonstationarity in AMF series. However, more in-depth investigations on a site-by-site basis are needed. To move past qualitatively assessing physical causes of nonstationarity in AMF series, and to further quantify the relative impacts of climatic variation versus anthropogenic activities on flood risk, future work should involve the regression of AMF peaks on annual flood generating meteorological series to determine the amount of variability in flood peaks individually explained by precipitation and temperature. The residual flow values after removing the effects of these meteorological variables could then be tested for trends. Any remaining trends could then be attributed to land use/land cover changes or other human effects, which could be subsequently identified.

The existence of nonstationarity in AMF series can have a significant impact on the planning and management of water resources and relevant infrastructure; thus, the prevalence of nonstationarity in AMF series for unimpaired watersheds dictates that *Bulletin 17B* procedures be modified to produce forecasts of flood risk which reflect the meteorological/climatic influences on flood magnitude and timing. A modification is proposed herein which accounts for nonstationarity in AMF series due to the large-scale climatic forcing of ocean-atmospheric patterns. Site specific regression models were developed to forecast flood risk one-year ahead as a function of forecasted climate pattern anomalies, which reflect the phase and intensity of climate patterns. Large differences in the one-year ahead forecasts are obtained in some locations relative to estimates obtained using the standard *Bulletin 17B* procedures, which would potentially have significant impacts on water resources planning and management (e.g., reservoir operation). However, additional analyses to validate the proposed model are needed. A further extension of the proposed model would be particularly useful for long-term planning horizons (e.g., 10-, 50-, 100-years) and design, but how to forecast the needed indices is not particularly clear at this time. However, similar models could be derived which relate flood distribution parameters to meteorological variables, such as precipitation, for which future forecasts could be obtained using outputs of General Circulation Models. Overall, the increased knowledge of the inherent structure of AMF series and the improved understanding of physical and/or climatic causes of nonstationarity gained from this research should serve as insight for the future development of a statistical model for flood risk which incorporates impacts of both climate change (natural and/or anthropogenic) and human activities within the watershed.

REFERENCES

- Addinsoft (2011), XLSTAT (Time), Computer Software, New York, New York, retrieved May 2011, available from <http://www.xlstat.com/>.
- Armstrong, W. H., M.J. Collins, and N.P. Snyder (2011), Increased frequency of low-magnitude floods in New England, *Journal of the American Water Resources Association*, 1-15. doi:10.1111/j.1752-1688.2011.00613.x.
- Baldwin, C. K., and U. Lall (1999), Seasonality of streamflow: The upper Mississippi River, *Water Resouces Research*, 35, 1143–1154.
- Balling, R., and G. Goodrich (2010), Increasing frought in the American Southwest? A continental perspective using a spatial analytical evaluation of recent trends, *Physical Geography*, 31(4), 293-306.
- Bhattacharyya, G., and R. Johnson (1977), *Statistical Concepts and Methods*, John Wiley and Sons, New York, New York.
- Bolboaca S.D., and L. Jaˆntschi (2006), Pearson versus Spearman, Kendall’s Tau correlation analysis on structure–activity relationships of biologic active compounds, *Leonardo Journal of Science*, 9, 179–200.
- Bras, R. L., and I. Rodriquez-Iturbe (1985), *Random Functions and Hydrology*, Addison-Wesley, Reading, Massachusetts.
- Burn, D. H., and M.A. Hag Elnur (2002), Detection of hydrologic trends and variability. *Journal of Hydrology*, 255, 107-22.
- Cayan, D. R., S. A. Kammerdiener, M. D. Dettinger, J. M. Caprio, D. H. Peterson (2001), Changes in the onset of spring in the western United States, *American Meteorological Society*, 82(3).
- Changnon, S.A. and K.E. Kunkel (1995), Climate-related fluctuations in midwestern floods during 1921-1985, *Journal of Water Resources Planning and Management*, 121, 326-334.
- Changnon, S.A. and M. Demissie (1996), Detection of changes in streamflow and floods resulting from climate fluctuations and land use-drainage changes, *Climatic Change*, 32, 411-421.
- Chiew F.H.S., and T.A. McMahon (2002), Global ENSO-streamflow teleconnection, streamflow forecasting and interannual variability, *Hydrological Sciences Journal*, 47(3), 505-522.
- Chow, Ven Te, D.R. Maidment, and L.W. Mays (1988), *Applied Hydrology*, McGraw-Hill, Columbus, Ohio.

- Cohn T.A., and H.F. Lins (2005), Nature's style: Naturally trendy, *Geophysical Research Letters*, 32, doi:10.1029/2005GL024476.
- Collins, M. J. (2009), Evidence for changing flood risk in New England since the late 20th Century, *Journal of the American Water Resources Association*, 45(2), 279-90.
- Coulibaly, P. and C. K. Baldwin (2005), Nonstationary hydrological time series forecasting using nonlinear dynamic methods, *Journal of Hydrology*, 307, 164-174.
- Dettinger, M. D., D. R. Cayan, G.J. McCabe, and J.A. Marengo (2000), Multiscale hydrologic variability associated with El Niño/Southern Oscillation, in *El Niño and the Southern Oscillation--Multiscale Variability, Global and Regional Impacts*, edited by Diaz, H.F., and V. Markgraf, pp. 113-146, Cambridge University Press, United Kingdom, and New York, New York.
- Douglas, E. M., R. M. Vogel, and C. N. Kroll (2000), Trends in floods and low flows in the United States: Impact of spatial correlation, *Journal of Hydrology*, 240, 90-105.
- Ehsanzadeh, E., T. Ouarda, and H.M. Saley (2011), A simultaneous analysis of gradual and abrupt changes in Canadian low streamflows, *Hydrological Processes*, 25, 727-739.
- Falcone, J.A., D.M. Carlisle, D.M. Wolock, and M.R. Meador (2010), Gages: A stream gage database for evaluating natural and altered flow conditions in the conterminous United States, *Ecology*.
- Falcone, J.A., D.M. Carlisle, D.M. Wolock, and M.R. Meador (2011), Gages: A stream gage database for evaluating natural and altered flow conditions in the conterminous United States, *Ecology*, 91, 621.
- Franks, S. W., and G. Kuczera (2002), Flood frequency analysis: Evidence and implications of secular climate variability, New South Wales, *Water Resources Research*, 38(5), doi:10.1029/2001WR000232.
- Grantz, K., B. Rajagopalan, M. Clark, and E. Zagana (2005), A technique for incorporating large-scale climate information in basin-scale ensemble streamflow forecasts, *Water Resources Research*, 41, W10410, doi:10.1029/2004WR003467.
- Griffis V. W., and J. R. Stedinger (2007), Evolution of flood frequency analysis with Bulletin 17, *Journal of Hydrologic Engineering*, 12(3).
- Griffis, V. W. and J. R. Stedinger (2007b) The log-Pearson type 3 distribution and its application in flood frequency analysis, 1. Distribution characteristics. *Journal of Hydrologic Engineering*, 12(5), 482-491.

- Griffis, V. W. and J. R. Stedinger (2007c) The log-Pearson type 3 distribution and its application in flood frequency analysis, 2. Parameter estimation methods. *Journal of Hydrologic Engineering*, 12(5), 492-500.
- Griffis, V. W., and J. R. Stedinger (2009), The log-Pearson type 3 distribution and its application in flood frequency analysis, III: Sample skew and weighted skew estimators, *Journal of Hydrologic Engineering*, 14(2), 209-212.
- Groisman, P. Y., R. W. Knight, and T. R. Karl (2001), Heavy precipitation and high streamflow in the contiguous United States: Trends in the twentieth century, *Bulletin of the American Meteorological Society*, 82(2), 219-46.
- Gruber, A.M., and J.R. Stedinger (2008), Models of LP3 regional skew, data selection, and bayesian GLS regression, paper presented at World Environmental and Water Resources Conference, American Society of Civil Engineers, edited by Babcock, R.W., and R. Walton, Honolulu, Hawaii.
- Hamad, K.H.(2009), Trend detection in hydrologic data: The Mann-Kendall trend test under the scaling hypothesis, *Journal of Hydrology*, 349, 350-363.
- Hamad, K.H., and A.R. Rao (1998), A modified Mann-Kendall trend test for autocorrelated data, *Journal of Hydrology*, 204, 182-196.
- Hamlet, A.F., and D. P. Lettenmaier (1999), Columbia River forecasting based on ENSO and PDO climate signals, *Journal of Water Resources Planning. and Managment*, 125(6).
- Hamlet, A.F., and D.P. Lettenmaier (2007), Effects of 20th century warming and climate variability on flood risk in the western U.S., *Water Resources Research*, 43, W06427, doi:10.1029/2006WR005099.
- Helsel D.R., and R.M. Hirsch (1993), Statistical methods in water resources, *Elsevier*, 522.
- Helsel, D.R., and R.M. Hirsch (2002), Statistical methods in water resources, in *Techniques of Water-Resource Investigations of the United States Geological Survey, Book 4*, <http://pubs.usgs.gov/twri/>, accessed May 2010.
- Hirschboeck, K.K., L.L. Ely, and R.A. Maddox (2000), *Hydroclimatology of Meteorologic Foods, Inland Flood Hazards*, edited by E.E. Wohl, pp. 39-72, Cambridge University Press, United Kingdom, and New York, New York.
- Hodgkins, G. A., and R. W. Dudley (2005), Changes in the magnitude of annual and monthly streamflows in New England, 1902-2002, in *U.S. Geological Survey Scientific Investigations Report 44, Report 2005-5135*, U.S. Geological Survey, Washington, D.C.

- Hurst, H.E. (1951), Long-term storage capacity of reservoirs, *Transactions of the American Society of Civil Engineers*, 116, 770-779.
- Interagency Committee on Water Data (1982), Bulletin 17B (revised and corrected), in *Guidelines For Determining Flood Flow Frequency*, 28, Hydrologic Subcommittee, Washington, D.C.
- Intergovernmental Panel on Climate Change, *Climate Change 2007: The Physical Science Basis*, contribution of Working Group I to the Fourth Assessment Report of the IPCC (2007a), edited by Solomon, S., D. Qin, M. Manning, Z. Chen, M. Marquis, K.B. Averyt, M. Tignor, and H.L. Miller, Cambridge University Press, Cambridge, United Kingdom and New York, New York.
- Intergovernmental Panel on Climate Change, Summary for Policy Makers in: *Climate Change 2007: The Physical Science Basis*, contribution of Working Group I to the Fourth Assessment Report of the IPCC (2007b), edited by Solomon, S., D. Qin, M. Manning, Z. Chen, M. Marquis, K.B. Averyt, M. Tignor, and H.L. Miller, Cambridge University Press, Cambridge, United Kingdom and New York, New York.
- Jain S., and U. Lall (2000), Magnitude and timing of annual maximum floods: Trends and large-scale climate associations for the Blacksmith Fork River, Utah, *Water Resources Research*, 36(12), 3641-3651.
- Jennings, M.E., W.O. Thomas Jr., and H.C. Riggs (1994), Nationwide Summary of U.S. Geological Survey Regional Regression Equations for Estimating Magnitude and Frequency of Floods for Ungaged Sites, 1993, in *Water-Resources Investigations, Report 94-4002*, p. 196, superseded by WRIR 02-4168, U.S. Geological Survey, Washington, D.C.
- Jones J.A., and G.E. Grant (1996), Peak flow responses to clearcutting and roads in small and large basins, Western Cascades, Oregon, *Water Resources Research*, 32, 959-74.
- Juckem, P., R.J. Hunt, M.P. Anderson, and D.M. Robertson (2008), Effects of climate and land management change on streamflow in the driftless area of Wisconsin, *Journal of Hydrology*, 355, 123-130.
- Kalra, A., T.C. Piechota, R. Davies, and G.A. Tootle (2008), Changes in the U.S. streamflow and western U.S. snowpack, *Journal of Hydrological Engineering*, 13, 156-163.
- Kalra, A., T.C. Piechota, R. Davies, G. A. Tootle (2006), Is climate change evident in U.S. streamflow? Examining the confluence of environmental and water concerns, paper presented at World Environmental and Water Resources Congress, American Society of Civil Engineers, edited by R. Graham, Reston, Virginia.

- Karl T. R., and R. W. Knight (1998), Secular trends of precipitation amount, frequency, and intensity in the United States., *Bulletin of the American Meteorological Society*, 79, 231-241.
- Kashelikar, A.S. (2009), Identification of teleconnections and improved flood risk forecasts using Bulletin 17B, MS thesis, Department of Civil & Environmental Engineering, Michigan Technological University, Houghton, MI.
- Kashelikar, A.S. and V.W. Griffis (2008), Forecasting flood risk with Bulletin 17B LP3 model and climate variability, paper presented at World Water and Environmental Resources Congress, American Society of Civil Engineers, edited by Babcock, R.W., and R. Walton, Honolulu, Hawaii.
- Kiem, A.S., S.W. Franks, and G. Kuczera (2003), Multi-decadal variability of flood risk, *Geophysical Research Letters*, 30(2), 1035, doi:10.1029/2002GL015992.
- Kirby, W. (1972), Computer-oriented Wilson-Hilferty transformation that preserves the first three moments and the lower bound of the Pearson type 3 distribution, *Water Resources Research*, 8(5), 1251-1254.
- Konrad, C.P. (2003), *Effects of Urban Development on Floods: U.S. Geological Survey Fact Sheet 076-03*, 4, <http://pubs.usgs.gov/fs/fs07603/>, accessed March 8, 2011.
- Koutsoyiannis, D. (2003), Climate change, the Hurst phenomenon, and hydrological statistics, *Hydrological Sciences Journal*, 48(1), 3- 24.
- Kunkel, K.E., K. Andsager, and D.R. Easterling (1999), Long-term trends in extreme precipitation events over the coterminous United States and Canada, *Journal of Climate*, 12, 2515-2527.
- Kwon, H.H., C. Brown, and U. Lall (2008), Climate informed flood frequency analysis and prediction in Montana using hierarchical Bayesian modeling, *Geophysical Research Letters*, 35, L05404, doi:10.1029/2007GL032220.
- Lettenmaier, D. P., E. F. Wood, and J. R. Wallis (1994), Hydro-climatological trends in the continental United States, 1948–88, *Journal of Climate*, 7, 586–607.
- Lins, H.F., and J.R. Slack (1999), Streamflow trends in the United States, *Geophysical Research Letters*, 26(2), 227-230.
- Maurer, E.P., A.W. Wood, J.C. Adam, D.P. Lettenmaier, and B. Nijssen (2002), A long-term hydrologically-based data set of land surface fluxes and states for the conterminous United States, *Journal of Climate*, 15, 3237-3251.

- McCabe, G.J., and D.M. Wolock (2002), A step increase in streamflow in the conterminous United States, *Geophysical Research Letters* 29(24), 2185, doi:10.1029/2002GL015999.
- Milly, P. C. D., J. Betancourt, M. Falkenmark, R. M. Hirsch, Z. W. Kundzewicz, D. P. Lettenmaier, and R. J. Stouffer (2008), Stationarity is dead: Whiter water management?, *Science*, 319, 573– 574.
- Moglen, G.E., and D.E. Shivers (2006), Methods for adjusting U.S. Geological Survey rural regression peak discharges in an urban setting, in *U.S. Geological Survey Scientific Investigations Report 2006, Report 5270*, p. 55, U.S. Geological Survey, Washington, D.C.
- Moore, J. N., J. T. Harper, and M. C. Greenwood (2007), Significance of trends toward earlier snowmelt runoff, Columbia and Missouri Basin headwaters, western United States, *Geophysical Research Letters*, 34, L16402, doi:10.1029/2007GL031022.
- National Research Council (1998), Decade-to-Century-Scale Climate Variability and Change: A Science Strategy, in *Panel on Climate Variability on Decade-to-Century Time Scales*, National Academy Press, Washington, D.C.
- NOAA (2011), Hydrologic Information Center - Flood Loss Data, in *National Oceanic and Atmospheric Administration's, National Weather Service*, <http://www.nws.noaa.gov/oh/hic/>, accessed Dec 2011.
- Olsen, J. R., J. R. Stedinger, N. C. Matalas, and E.Z. Stakhiv (1999), Climate variability and flood frequency estimation for the Upper Mississippi and Lower Missouri Rivers, *Journal of the American Water Resources Association*, 35(6), 1509-1524.
- Perreault, L., M. Hache', M. Slivitsky, and B. Bobe'e (1999), Detection of changes in precipitation and runoff over eastern Canada and U.S. using a Bayesian approach, *Stochastic Research and Risk Assessment*, 13, 201– 216.
- Petrow, T., and B. Merz (2009), Trends in flood magnitude, frequency and seasonality in Germany in the period 1951–2002, *Journal of Hydrology*, 371, 129-41.
- Pettitt, A. N. (1979), A non-parametric approach to the change-point problem, *Journal of Applied Statistics*, 28, 126– 135.
- Piechota, T. C., and J. A. Dracup (1999), Long-range streamflow forecasting using El Niño-Southern Oscillation indicators, *Journal of Hydrologic Engineering*, 4(2), 144-151.

- Pinter, N., A. Jemberie, J.W.F. Remo, and R.A. Heine, (2008), Flood trends and river engineering on the Mississippi River system, *Geophysical Research Letters*, 35, L23404, doi: 10.1029/2008GL035987.
- Potter, K. W. (1991), Hydrological impacts of changing land management practices in a moderate-sized agricultural catchment, *Water Resources Research*, 27(5), 845–855.
- Rasmussen, P. (2001), Bayesian estimation of change points using general linear model, *Water Resources Research*, 37(11), 2723–2731.
- Regonda, S. K., B. Rajagopalan, M. Clark, and J. Pitlick (2005), Seasonal cycle shifts in hydroclimatology over the western United States, *Journal of Climate*, 18(2), 372-384.
- Reis, D.S. Jr., J.R. Stedinger, and E.S. Martins (2005), Bayesian GLS regression with application to LP3 regional skew estimation, *Water Resources Research*, 41, W10419, doi: 10.1029/2004WR00344.
- Robson, A. J., T. K. Jones, D. W. Reed, and A. C. Bayliss, (1998), A study of national trend and variation in UK floods, *International Journal of Climatology*, 18, 165-82.
- Sakalauskienė, G. (2003), The Hurst Phenomenon in hydrology, *Environmental Research, Engineering and Management*, 3(25), 16–20.
- Sauer, V. B., W. O. Thomas, V. A. Stricker, and K. V. Wilson (1983), Flood characteristics of urban watersheds in the United States, in *U.S. Geological Water Supply Paper*, 2207.
- Seidou, O., and T. B. M. J. Ouarda (2007), Recursion-based multiple changepoint detection in multiple linear regression and application to river streamflows, *Water Resources Research*, 43, W07404, doi:10.1029/2006WR005021.
- Slack, J. R., A. M. Lumb, and J. M. Landwehr, Hydro-Climactic Data Network (1993), *Water-Resource Investigations Report 93-4076*, U.S. Geological Survey, Washington, D.C.
- Slack, J.R., and J.M. Landwehr (1992), *Hydro-Climatic Data Network: A U.S. Geological Survey Streamflow Data Set for the United States for the study of Climate Variations, 1874-1988*, , *Open-File Report 2-129*, U.S. Geological Survey, Washington, D.C.
- Small, D., S. Islam, and R. M. Vogel (2006), Trends in precipitation and streamflow in the eastern U.S.: Paradox or perception?, *Geophysical Research Letters*, 33, L03403.

- Stankowski, S.J. (1972), *Population density as an indirect indicator of urban and suburban land-surface modification*, Rep. 800B, B219-B224, U.S. Geological Survey, Washington, D.C.
- Stedinger, J. R., and V. W. Griffis (2008), Flood frequency analysis in the United States: Time to update, *Journal of Hydrological Engineering*, 4, 199–204.
- Stedinger, J. R., and V.W. Griffis (2011), Getting from here to where? Flood frequency analysis and climate, *Journal of the American Water Resources Association*, 47, 506–513. doi: 10.1111/j.1752-1688.2011.00545.x
- Stewart, I.T., D.R. Cayan, and M.D. Dettinger (2005), Changes toward earlier streamflow timing across western North America, *Journal of Climate*, 18, 1136-1155.
- Storck, P., L. Bowling, P. Wetherbee, and D. Lettenmaier (1998), Application of a GIS-based distribution hydrology model for prediction of forest harvest effects on peak stream flow in the Pacific Northwest, *Hydrological Processes*, 12, 889-904.
- Strupczewski, W. G., V. P. Singh, and W. Feluch (2001), Non-stationary approach to at-site flood frequency modeling I. maximum likelihood estimation, *Journal of Hydrology*, 248, 123-142.
- Sveinsson, O. G. B., J. D. Salas, and D. C. Boes (2005), Prediction of extreme events in hydrologic processes that exhibit abrupt shifting patterns, *Journal of Hydrologic Engineering*, 10(4), 315-326.
- Thomas, W. O. Jr. (1985), A uniform technique for flood frequency analysis, *Journal of Water Resources Planning and Management*, 111(3), 321-337.
- Tomé, A. R., and P.M.A. Miranda (2004), Piecewise linear fitting and trend changing points of climate parameters, *Geophysical Research Letters*, 31, L02207, doi:10.1029/2003GL019100.
- Tootle, G. A., T. C. Piechota, and A. Singh (2005), Coupled oceanic-atmospheric variability and U.S. streamflow, *Water Resources Research*, 41, W12408, doi:10.1029/2005WR004381.
- Twine, T. E., C. J. Kucharik, and J. A. Foley (2005), Effects of El Niño-Southern Oscillation on the climate, water balance, and streamflow of the Mississippi River Basin, *Journal of Climate*, 18(22), 4840-4861.
- Villarini, G., and J.A. Smith (2010), Flood peak distributions for the eastern United States, *Water Resources Research*, 46, W06504, doi: 10.1029/2009WR008395.

- Villarini, G., F. Serinaldi, J. A. Smith, and W. F. Krajewski (2009), On the stationarity of annual flood peaks in the continental united states during the 20th century, *Water Resources Research*, 45, W08417.
- Villarini, G., G.A. Vecchi, and J.A. Smith (2010), Modeling of the dependence of tropical storm counts in the North Atlantic Basin on climate indices, *Monthly Weather Review*, 138, 2681-2705, doi:10.1175/2010MWR33151
- Villarini, G., G.A. Vecchi, T.R. Knutson, M. Zhao, and J.A. Smith (2011), North Atlantic tropical storm frequency response to anthropogenic forcing: Projections and sources of uncertainty, *Journal of Climate*, doi: 10.1175/2011JCLI3853.1, in press.
- Walter, M., and R.M. Vogel (2010), Increasing trends in peak flow in the northeastern United States and their impacts on design, paper presented at 2nd Joint Federal Interagency Conference, Las Vegas, Nevada.
- Water Resources Council (1967), A uniform technique for determining flood flow frequencies, in *Bulletin 15*, Hydrologic Commission., Washington, D.C.
- Yue, S., and C. Wang (2004), The Mann–Kendall test modified by effective sample size to detect trend in serially correlated hydrological series, *Water Resources Management*, 18(3), 201–218
- Yue, S., and C.Y. Wang (2002), The applicability of pre-whitening to eliminate the influence of serial correlation on the Mann-Kendall test, *Water Resources. Research*, 38(6), doi:10.1029/2001WR000861, 4–1–7.
- Yue, S., P. Pilon, and B. Phinney (2003), Canadian streamflow trend detection: impacts of serial and cross-correlation, *Hydrologic Science. Journal*, 48(1), 51–64.
- Yue, S., P. Pilon, and G. Cavadias (2002), Power of the Mann-Kendall and Spearman’s Rho tests for detecting monotonic trends in hydrological series, *Journal of Hydrology*, 259, 254–271.

APPENDIX A RESULTS OF NONSTATIONARITY TESTS ON SERIES OF FLOOD MAGNITUDE

This appendix contains tables of results for the tests for trends, change-points, and long-term persistence in annual maximum flood series as discussed in CHAPTER 2. Results are presented for both the traditional Mann-Kendall test (neglecting autocorrelation) and the modified Mann-Kendall test to account for autocorrelation. The length of continuous data (N) analyzed for each site is also reported. Only sites for which results are significant on the 10% level are included in the following tables (results significant on the 5% level are in **bold**). Results are omitted (blank spaces) when p-values greater than 10% obtained. A table of Hurst exponents computed for all 569 sites is provided.

Table A.1
Results of Pettitt and Mann-Kendall tests on flood magnitude (significant on the 10% level), including the year of the identified shift in the mean, and the direction of significant trends, either positive (+) and negative (-).

Station Number	Years of Record N	Pettitt Test		Traditional Mann-Kendall		Modified Mann-Kendall	
		Year	p-value	p-value	Trend	p-value	Trend
01011000	79	1968	0.040				
01014000	84	1967	0.014				
01031500	108	1966	0.022	0.038	+	0.077	+
01064500	81	1966	0.035				
01119500	78	1971	0.038				
01127500	79	1967	0.020				
01169000	70	1972	0.000			0.026	+
01175500	99	1939	0.000	0.004	-	0.008	-
01176000	97	1967	0.036	0.010	+		
01181000	74	1968	0.018	0.092	-		
01188000	78	1971	0.069	0.036	+		
01196500	79	1968	0.000	0.091	+	0.004	+
01334500	87	1972	0.000	0.053	+	0.049	+
01350000				0.069	+		
01357500				0.058	+		
01379500	73	1966	0.010				
01381500	89	1969	0.000	0.000	+	0.041	+
01387500	88	1967	0.003			0.077	+
01396500	91	1969	0.002	0.032	+		
01397500	74	1968	0.000	0.001	+	0.000	+

Table A.1, continued

Station Number	Years of Record N	Pettitt Test		Traditional Mann-Kendall		Modified Mann-Kendall	
		Year	p-value	p-value	Trend	p-value	Trend
01398500	89	1969	0.002	0.018	+		
01408500	82	1957	0.081				
01411000	85	1966	0.027				
01411500				0.092	-		
01420500	97	1968	0.000	0.001	+	0.003	+
01426500	98	1963	0.000	0.000	-	0.002	-
01439500	102	1967	0.014			0.084	+
01445500	89	1966	0.000	0.000	+	0.000	+
01503000	98	1964	0.066				
01512500	98	1950	0.031				
01518000	72	1980	0.000	0.011	-	0.001	-
01520500	81	1979	0.000	0.000	-	0.002	-
01531000	107	1964	0.024				
01538000	91	1969	0.065				
01539000				0.011	+		
01541500	97	1956	0.017			0.057	-
01548500	92	1935	0.069				
01555500	81	1969	0.007	0.078	+		
01567000	111	1937	0.006	0.001	-	0.023	-
01604500	72	1967	0.039				
01634500	73	1970	0.000	0.026	-		
01645000	81	1970	0.000			0.005	+
01667500	80	1971	0.056				
02013000	82	1968	0.096				
02016000	85	1968	0.040				
02051500	83	1971	0.039				
02059500				0.047	+		
02074500	81	1971	0.003	0.016	+		
02131000	72	1993	0.100	0.036	-		
02136000				0.021	-		
02156500	71	1979	0.090				
02173500	72	1980	0.001	0.002	-	0.021	-
02213500				0.017	-		
02296750	80	1960	0.001			0.031	-
02301500	79	1968	0.011			0.068	-
02303000	71	1970	0.044				
02313000	79	1971	0.054	0.015	-	0.065	-
02317500	83	1957	0.074				
02321500	79	1973	0.100	0.088	-		
02329000	85	1957	0.012				
02339500	110	1975	0.001	0.000	-	0.009	-
02383500	73	1980	0.000	0.069	-	0.006	-
02387500	110	1980	0.010	0.028	-		

Table A.1, continued

Station Number	Years of Record N	Pettitt Test		Traditional Mann-Kendall		Modified Mann-Kendall	
		Year	p-value	p-value	Trend	p-value	Trend
02424000	83	1984	0.057				
02441000	71	1985	0.025	0.077	-		
02467000	82	1969	0.002	0.067	+	0.058	+
02486000				0.047	+		
03010500	95	1939	0.003				
03015500				0.033	+		
03024000	78	1969	0.057				
03049500	72	1966	0.003			0.020	-
03069500	97	1954	0.002	0.008	+	0.076	+
03102500				0.040	-		
03109500	94	1959	0.002	0.009	-		
03118500	90	1974	0.022	0.037	+	0.099	+
03167000	84	1978	0.010	0.004	-		
03186500				0.046	+		
03193000	111	1940	0.003	0.002	-	0.052	-
03234500	79	1972	0.034				
03262000	94	1930	0.064				
03301500				0.083	-		
03307000	70	1973	0.006				
03326500				0.064	+		
03345500	97	1981	0.078	0.058	+		
03363500				0.085	+		
03379500	96	1981	0.036	0.010	+		
03381500	71	1981	0.040			0.096	+
03451500	111	1920	0.059	0.050	-		
03574500				0.083	-		
04010500	87	1954	0.018	0.065	-	0.079	-
04056500				0.057	-		
04073500	110	1953	0.021	0.025	-		
04079000	73	1976	0.076				
04112500	100	1957	0.051				
04191500	95	1973	0.063	0.044	+		
04193500	73	1973	0.078				
04262500	94	1973	0.048	0.064	+		
04264331	93	1968	0.000	0.001	+	0.002	+
05053000	78	1992	0.002	0.010	+	0.031	+
05062000	80	1961	0.007			0.008	+
05062500	80	1992	0.000	0.020	+	0.003	+
05066500	77	1964	0.000	0.042	+	0.003	+
05078000	72	1961	0.056				
05078500	76	1961	0.006			0.052	+
05082500	111	1964	0.000	0.000	+	0.006	+
05084000				0.064	+		

Table A.1, continued

Station Number	Years of Record N	Pettitt Test		Traditional Mann-Kendall		Modified Mann-Kendall	
		Year	p-value	p-value	Trend	p-value	Trend
05100000	91	1964	0.017	0.072	+	0.043	+
05112000	91	1991	0.050	0.087	+		
05280000	81	1964	0.012			0.014	+
05291000						0.096	+
05304500	74	1964	0.005			0.024	+
05316500	81	1974	0.003			0.011	+
05317000	80	1982	0.094				
05330000	76	1982	0.005	0.010	+	0.025	+
05331000	110	1942	0.000	0.001	+	0.018	+
05340500	101	1940	0.000				
05407000	96	1946	0.017				
05408000	72	1984	0.012	0.083	-	0.080	-
05410490	77	1967	0.024				
05414000	76	1979	0.000	0.086	-	0.005	-
05420500	111	1964	0.003	0.007	+	0.067	+
05422000	76	1972	0.053				
05431486	71	1953	0.092				
05432500	71	1969	0.001			0.021	-
05434500	71	1975	0.008			0.053	-
05435500	97	1953	0.006	0.051	-	0.062	-
05436500	96	1953	0.014	0.058	-	0.061	-
05446500	71	1970	0.049				
05447500	75	1968	0.001				
05454500	108	1953	0.004	0.014	-	0.083	-
05476000	80	1982	0.046			0.059	+
05482500				0.077	+		
05484000				0.032	+		
05484500	96	1943	0.006	0.018	+	0.092	+
05490500				0.088	+		
05495000	89	1972	0.036				
05501000	76	1972	0.011				
05520500	96	1965	0.000	0.000	+	0.001	+
05526000	87	1967	0.002	0.006	+	0.014	+
05527500	96	1967	0.000	0.000	+	0.003	+
05555300	80	1978	0.011	0.044	+	0.071	+
05585000	90	1958	0.019			0.073	+
05592500	95	1942	0.069				
05593000	81	1962	0.003				
05597000	96	1964	0.003	0.021	-	0.053	-
06019500	72	1966	0.010			0.079	+
06191500				0.010	+		
06214500	83	1941	0.096				
06289000	72	1962	0.095				

Table A.1, continued

Station Number	Years of Record N	Pettitt Test		Traditional Mann-Kendall		Modified Mann-Kendall	
		Year	p-value	p-value	Trend	p-value	Trend
06335500	72	1978	0.011				
06337000	76	1972	0.000			0.025	-
06340500	73	1972	0.050			0.096	-
06478500	82	1982	0.010	0.013	+	0.095	+
06710500	88	1958	0.000	0.034	-	0.024	-
06800500	82	1957	0.009			0.020	+
06810000	81	1946	0.053			0.058	+
06864500	84	1975	0.004	0.044	-	0.065	-
06869500				0.013	-		
06876900	93	1975	0.036	0.004	-		
06889500	82	1966	0.000	0.027	+	0.014	+
06892000	82	1957	0.085				
06899500	83	1958	0.006			0.059	+
06908000	73	1972	0.073				
07016500	94	1980	0.011	0.034	+		
07018500	88	1981	0.058			0.071	+
07019000	89	1980	0.010	0.030	+	0.070	+
07096000	111	1966	0.002	0.001	-	0.034	-
07144200	90	1956	0.009			0.036	+
07146500	89	1972	0.065			0.077	+
07176000	75	1961	0.000				
07203000						0.092	-
07218000				0.055	-		
07234000	73	1973	0.000	0.000	-	0.000	-
07247500	72	1974	0.000			0.014	-
07252000	72	1981	0.073				
07340000	81	1969	0.000	0.019	-	0.005	-
07340500	73	1974	0.000			0.000	-
07378500	73	1971	0.005			0.038	+
08041000	90	1962	0.006				
08055500	88	1950	0.000			0.031	-
08080500	73	1972	0.000	0.004	-	0.004	-
08082000	73	1961	0.000			0.001	-
08082500	88	1967	0.000	0.000	-	0.000	-
08085500	87	1962	0.020			0.059	-
08088000	73	1969	0.003			0.009	-
08128000	81	1964	0.010			0.090	-
08158000	111	1941	0.000	0.000	-	0.014	-
08210000	95	1983	0.000	0.001	-	0.041	-
08380500				0.073	-		
09085000	100	1959	0.000	0.000	-	0.001	-
09110000	102	1958	0.000	0.000	-	0.000	-
09147500	90	1987	0.013	0.032	-	0.047	-

Table A.1, continued

Station Number	Years of Record N	Pettitt Test		Traditional Mann-Kendall		Modified Mann-Kendall	
		Year	p-value	p-value	Trend	p-value	Trend
09180500	88	1958	0.001			0.009	-
09315000	104	1958	0.000	0.000	-	0.003	-
09379500	84	1958	0.000	0.093	-	0.010	-
09415000				0.026	-		
09471000	76	1959	0.001	0.088	-	0.002	-
10128500	102	1923	0.089				
10234500	97	1949	0.003			0.096	-
10329500				0.031	-		
11383500	90	1937	0.022				
11522500				0.035	-		
11525500	99	1960	0.000	0.000	-	0.013	-
11530000				0.024	-		
11532500	79	1949	0.031	0.059	-		
12010000	81	1977	0.087				
12020000	71	1985	0.055				
12035000	81	1978	0.006	0.021	+	0.013	+
12039500	85	1979	0.027	0.097	+	0.035	+
12054000	72	1993	0.015				
12056500	86	1979	0.082				
12134500	82	1973	0.040	0.027	+		
12186000	82	1973	0.031	0.069	+		
12189500	82	1973	0.016	0.097	+	0.060	+
12321500	82	1952	0.007			0.033	+
12322000	83	1972	0.000	0.000	-	0.004	-
12354500	82	1946	0.082	0.041	-		
12355500				0.071	-		
12370000	89	1986	0.086	0.031	-		
12401500	82	1947	0.030				
12404500	81	1947	0.067				
12442500				0.029	-		
13037500	100	1956	0.001	0.033	-	0.017	-
13120500	91	1950	0.031				
13269000	101	1986	0.056			0.086	-
13342500	87	1976	0.000	0.000	-	0.012	-
14044000	81	1969	0.020	0.087	+	0.097	+
14105700	110	1972	0.000	0.000	-	0.000	-
14113000	82	1983	0.091	0.083	-		
14137000	99	1952	0.075				
14191000	111	1966	0.000	0.000	-	0.000	-
14306500	71	1983	0.037				
14321000	103	1945	0.045				
14325000				0.093	-		
14362000	72	1975	0.001			0.030	-

Table A.2

Results of Mann-Kendall tests (10% significance level) on AMF subseries for sites exhibiting a significant change-point in the mean flood magnitude at the 10% level. The mean flood magnitude in the complete series, and each subseries are also reported.

Site Number	Complete Series	Before Change-Point			After Change-point		
	Mean	Mean	Trend	p-value	Mean	Trend	p-value
1011000	16,305	14,307	-	0.018			
1181000	6,926	5,947	-	0.030			
1188000	362	305	-	0.013			
1379500	1,370				1,506	-	0.080
1381500	1,048	851	-	0.064			
1397500	561				808	+	0.004
1420500	14,142	10,599	+	0.062			
1445500	997	780	+	0.051			
1503000	32,940				31,026	+	0.045
1518000	10,081				5,578	-	0.086
1548500	14,687	9,861	-	0.087			
1555500	6,368	4,534	-	0.056			
1567000	49,251	57,038	-	0.080			
1667500	13,812	11,724	-	0.033			
2074500	5,183	4,224	-	0.059			
2173500	2,632				2,023	-	0.010
3109500	10,123	11,824	+	0.026			
3262000	4,501	5,934	-	0.014			
4264331	282,581				306,977	-	0.090
5062000	2,567	1,431	+	0.002			
5062500	2,410	1,721	+	0.029			
5066500	2,570				3,432	+	0.081
5078000	1,709	1,334	+	0.092			
5082500	23,342				34,260	+	0.065
5280000	5,035	3,790	+	0.007			
5316500	2,576	2,282	+	0.020			
5331000	47,228	33,631	-	0.025			
5340500	24,603				27,571	-	0.094
5484500	17,783	12,197	-	0.069			
6800500	18,459	14,276	+	0.048			
6810000	18,573	12,210	+	0.015			
7234000	6,896	13,201	-	0.078	1,088	-	0.000
8055500	13,709	28,596	+	0.078			
8080500	16,792				10,706	-	0.016
8082000	11,057				6,908	-	0.069
8082500	22,685	33,227	-	0.020	12,613	-	0.077
8088000	21,664				16,907	-	0.082
8158000	39,858				15,819	+	0.015

Table A.2, continued

Site Number	Complete Series	Before Change-Point			After Change-point		
	Mean	Mean	Trend	p-value	Mean	Trend	p-value
9110000	1,451	1,878	-	0.002			
9315000	27,511	32,891	-	0.051			
9471000	6,934				5,594	-	0.066
11525500	11,132				4,139	+	0.003
11532500	82,656				88,773	-	0.054
12321500	2,116	1,732	+	0.057			
12322000	60,141	78,575	+	0.024			
12354500	36,243				38,240	-	0.002
12404500	21,313				22,145	-	0.088
14191000	148,611				111,416	-	0.053
14321000	101,671				110,761	-	0.017
14362000	6,400	8,977	+	0.074			

Table A.3

Hurst exponents for AMF series for all 569 sites considered. Values in red indicate sites characterized by a random walk or anti-persistence.

Station Number	H	Station Number	H	Station Number	H	Station Number	H
01011000	0.71	02317500	0.64	05293000	0.69	08041500	0.65
01013500	0.63	02320500	0.56	05300000	0.52	08055500	0.82
01014000	0.70	02321500	0.71	05304500	0.68	08070000	0.68
01030500	0.53	02329000	0.59	05313500	0.58	08080500	0.80
01031500	0.66	02331600	0.62	05316500	0.62	08082000	0.86
01038000	0.65	02333500	0.71	05317000	0.58	08082500	0.84
01047000	0.54	02337000	0.57	05330000	0.63	08085500	0.58
01055000	0.59	02339500	0.75	05331000	0.74	08088000	0.73
01057000	0.60	02347500	0.57	05340500	0.78	08095000	0.67
01064500	0.64	02353500	0.62	05362000	0.60	08128000	0.69
01073000	0.66	02358000	0.59	05379500	0.66	08151500	0.60
01076500	0.51	02361000	0.65	05394500	0.60	08153500	0.60
01078000	0.69	02369000	0.61	05399500	0.62	08158000	0.82
01119500	0.56	02371500	0.50	05407000	0.70	08164000	0.67
01127500	0.70	02375500	0.54	05408000	0.67	08167000	0.64
01137500	0.56	02383500	0.79	05410490	0.67	08167500	0.64
01142500	0.62	02387500	0.74	05412500	0.59	08171000	0.61
01144000	0.64	02392000	0.60	05414000	0.74	08172000	0.61
01162500	0.65	02398000	0.57	05418500	0.64	08176500	0.63
01169000	0.75	02424000	0.68	05419000	0.59	08189500	0.62
01175500	0.87	02431000	0.68	05420500	0.73	08190000	0.56
01176000	0.57	02436500	0.57	05421000	0.57	08192000	0.59
01181000	0.66	02437000	0.57	05422000	0.68	08195000	0.70

Table A.3, continued

Station Number	H	Station Number	H	Station Number	H	Station Number	H
01188000	0.62	02441000	0.73	05426000	0.57	08205500	0.58
01193500	0.69	02448000	0.67	05430500	0.67	08210000	0.70
01196500	0.80	02467000	0.75	05431486	0.60	08276500	0.68
01318500	0.60	02472500	0.59	05432500	0.72	08291000	0.70
01321000	0.59	02474500	0.62	05434500	0.74	08378500	0.66
01334500	0.63	02475500	0.61	05435500	0.72	08380500	0.64
01350000	0.58	02479000	0.67	05436500	0.73	09085000	0.83
01357500	0.60	02484500	0.72	05438500	0.68	09110000	0.84
01365000	0.63	02486000	0.63	05440000	0.67	09112500	0.55
01372500	0.59	02487500	0.61	05444000	0.60	09119000	0.64
01379500	0.73	02488500	0.72	05446500	0.70	09124500	0.61
01381500	0.80	03010500	0.69	05447500	0.77	09132500	0.57
01387500	0.68	03011020	0.62	05451500	0.57	09147500	0.71
01396500	0.75	03015500	0.62	05454500	0.74	09180500	0.78
01397500	0.86	03020500	0.58	05455500	0.61	09239500	0.63
01398000	0.62	03024000	0.73	05459500	0.59	09251000	0.62
01398500	0.73	03032500	0.70	05464500	0.62	09304500	0.59
01399500	0.68	03034500	0.55	05465500	0.65	09310500	0.69
01408000	0.57	03049500	0.77	05470000	0.61	09315000	0.79
01408500	0.63	03051000	0.61	05474000	0.64	09361500	0.67
01410000	0.69	03069500	0.69	05476000	0.60	09379500	0.76
01411000	0.58	03079000	0.60	05479000	0.59	09415000	0.56
01411500	0.61	03080000	0.67	05482500	0.66	09430500	0.69
01413500	0.63	03102500	0.73	05484000	0.61	09448500	0.69
01414500	0.72	03106000	0.55	05484500	0.70	09471000	0.71
01420500	0.77	03109500	0.78	05486490	0.58	09508500	0.64
01421000	0.72	03118500	0.64	05490500	0.63	10128500	0.69
01426500	0.86	03144000	0.54	05495000	0.63	10131000	0.65
01439500	0.58	03164000	0.64	05497000	0.62	10174500	0.59
01440000	0.63	03167000	0.68	05500000	0.64	10234500	0.72
01445500	0.87	03170000	0.55	05501000	0.72	10296000	0.69
01459500	0.48	03173000	0.59	05520500	0.82	10310000	0.63
01463500	0.69	03175500	0.52	05526000	0.73	10312000	0.61
01467000	0.54	03182500	0.64	05527500	0.79	10322500	0.65
01503000	0.70	03183500	0.69	05555300	0.70	10329500	0.60
01512500	0.69	03186500	0.73	05556500	0.66	10396000	0.62
01514000	0.61	03193000	0.78	05570000	0.58	11098000	0.59
01518000	0.78	03198500	0.61	05572000	0.53	11152000	0.59
01520500	0.82	03219500	0.57	05585000	0.74	11160500	0.55
01531000	0.72	03230500	0.67	05592500	0.62	11237500	0.60
01532000	0.67	03234500	0.75	05593000	0.80	11264500	0.57
01534000	0.55	03253500	0.65	05597000	0.70	11266500	0.55
01538000	0.69	03262000	0.75	06019500	0.72	11367500	0.64
01539000	0.62	03265000	0.60	06191500	0.67	11381500	0.61

Table A.3, continued

Station Number	H	Station Number	H	Station Number	H	Station Number	H
01541000	0.55	03266000	0.55	06192500	0.59	11383500	0.69
01541500	0.64	03269500	0.64	06207500	0.62	11402000	0.59
01543500	0.57	03272000	0.62	06214500	0.69	11413000	0.55
01548500	0.61	03274000	0.62	06289000	0.64	11425500	0.59
01555000	0.58	03275000	0.60	06335500	0.75	11477000	0.70
01555500	0.65	03281500	0.74	06337000	0.75	11478500	0.70
01556000	0.59	03294500	0.65	06340500	0.69	11501000	0.68
01558000	0.48	03301500	0.69	06354000	0.65	11522500	0.71
01560000	0.67	03307000	0.69	06441500	0.60	11525500	0.88
01564500	0.59	03326500	0.71	06452000	0.61	11530000	0.71
01567000	0.63	03335500	0.60	06478500	0.77	11532500	0.78
01568000	0.54	03339500	0.66	06485500	0.52	12010000	0.66
01570500	0.51	03345500	0.59	06600500	0.61	12020000	0.69
01574000	0.66	03360500	0.63	06606600	0.62	12027500	0.61
01580000	0.63	03363500	0.61	06620000	0.61	12035000	0.73
01599000	0.66	03373500	0.57	06630000	0.64	12039500	0.68
01601500	0.60	03374000	0.59	06635000	0.69	12048000	0.66
01604500	0.71	03377500	0.58	06710500	0.72	12054000	0.75
01608500	0.54	03379500	0.70	06800500	0.62	12056500	0.56
01610000	0.52	03380500	0.66	06809500	0.53	12134500	0.71
01613000	0.64	03381500	0.65	06810000	0.63	12186000	0.68
01614500	0.60	03434500	0.59	06864500	0.66	12189500	0.72
01631000	0.59	03438000	0.60	06869500	0.67	12306500	0.77
01632000	0.57	03451500	0.64	06876900	0.62	12321500	0.72
01634000	0.56	03465500	0.62	06889500	0.79	12322000	0.93
01634500	0.72	03473000	0.65	06892000	0.59	12330000	0.69
01645000	0.73	03479000	0.58	06897500	0.66	12332000	0.69
01667500	0.67	03488000	0.72	06899500	0.67	12354500	0.80
02013000	0.72	03504000	0.67	06908000	0.65	12355500	0.69
02016000	0.68	03524000	0.70	06913500	0.65	12358500	0.65
02017500	0.60	03528000	0.68	06933500	0.61	12370000	0.69
02018000	0.67	03540500	0.61	07013000	0.66	12401500	0.73
02035000	0.68	03550000	0.73	07016500	0.72	12404500	0.74
02045500	0.69	03574500	0.67	07018500	0.69	12409000	0.68
02051500	0.72	03604000	0.59	07019000	0.69	12413000	0.48
02055000	0.65	03612000	0.58	07050500	0.56	12414500	0.57
02059500	0.63	04010500	0.71	07056000	0.55	12422500	0.71
02061500	0.73	04056500	0.59	07061500	0.61	12442500	0.77
02070000	0.60	04073500	0.71	07067000	0.61	12445000	0.75
02074500	0.72	04079000	0.68	07068000	0.60	12451000	0.67
02083000	0.65	04087000	0.68	07069500	0.54	12459000	0.66
02083500	0.63	04100500	0.64	07071500	0.44	12488500	0.72
02085500	0.59	04105000	0.66	07072000	0.54	13037500	0.77
02091500	0.60	04112500	0.65	07074000	0.56	13073000	0.71

Table A.3, continued

Station Number	H	Station Number	H	Station Number	H	Station Number	H
02102000	0.56	04121500	0.67	07096000	0.74	13082500	0.70
02116500	0.57	04142000	0.60	07144200	0.70	13120500	0.72
02118000	0.57	04191500	0.65	07146500	0.68	13139510	0.64
02126000	0.51	04193500	0.68	07147800	0.60	13185000	0.58
02131000	0.60	04198000	0.66	07172000	0.60	13269000	0.65
02132000	0.57	04214500	0.66	07176000	0.80	13302500	0.68
02134500	0.64	04223000	0.56	07180500	0.61	13313000	0.64
02136000	0.56	04234000	0.55	07183000	0.65	13317000	0.73
02138500	0.60	04262500	0.75	07186000	0.62	13336500	0.75
02154500	0.63	04264331	0.89	07187000	0.69	13337000	0.74
02156500	0.62	04269000	0.62	07189000	0.61	13342500	0.81
02173500	0.71	04275000	0.63	07196500	0.67	14020000	0.69
02177000	0.57	04287000	0.62	07203000	0.52	14044000	0.68
02192000	0.69	04293500	0.71	07218000	0.61	14046500	0.62
02198000	0.54	05014500	0.61	07234000	0.84	14105700	0.86
02202500	0.60	05053000	0.75	07247000	0.65	14113000	0.59
02203000	0.45	05062000	0.71	07247500	0.77	14137000	0.73
02213500	0.59	05062500	0.75	07252000	0.66	14154500	0.58
02217500	0.73	05066500	0.75	07261500	0.62	14178000	0.56
02225500	0.58	05078000	0.70	07290000	0.65	14185000	0.69
02226000	0.63	05078500	0.72	07291000	0.70	14191000	0.80
02226500	0.45	05082500	0.81	07331000	0.64	14301000	0.56
02228000	0.50	05084000	0.64	07332500	0.59	14301500	0.57
02231000	0.67	05100000	0.73	07340000	0.83	14306500	0.75
02246000	0.60	05112000	0.73	07340500	0.86	14308000	0.66
02256500	0.72	05120500	0.57	07363500	0.69	14321000	0.78
02296750	0.72	05131500	0.73	07375500	0.68	14325000	0.68
02298830	0.63	05133500	0.64	07378500	0.76	14359000	0.70
02301500	0.71	05280000	0.66	08013500	0.58	14362000	0.80
02303000	0.65	05286000	0.70	08032000	0.66		
02313000	0.69	05288500	0.65	08033500	0.66		
02314500	0.64	05291000	0.68	08041000	0.77		

APPENDIX B TREND AND CHANGE-POINT RESULTS FOR TIMING OF FLOOD PEAKS

This appendix contains tables of results for the trend and change-point tests on series of the day of occurrence of flood peaks as discussed in CHAPTER 2. The length of continuous data (N) analyzed for each site is also reported. Only results significant on the 10% level are reported in the following tables (sites significant on the 5% level are in **bold**). Results are omitted (blank spaces) when p-values greater than 10% were obtained.

Table B.1

Mann-Kendall results for sites exhibiting a significant trend whether positive (+) or negative (-), in the day of occurrence of flood peaks on the 10% level.

Station Number	N	Trend	P-Value		Station Number	N	Trend	P-Value
01011000	79	-	0.013		06207500	89	-	0.003
01013500	81	-	0.007		06869500	92	-	0.044
01014000	84	-	0.002		06908000	73	+	0.020
01030500	108	-	0.004		06933500	88	-	0.041
01073000	75	+	0.038		07013000	94	-	0.020
01144000	94	-	0.065		07096000	111	-	0.000
01175500	99	+	0.054		07176000	75	+	0.071
01381500	89	+	0.082		07234000	73	-	0.041
01414500	74	+	0.037		07378500	73	+	0.094
01541000	97	-	0.047		08041000	90	-	0.039
02051500	83	+	0.057		08041500	71	-	0.096
02317500	83	-	0.008		08070000	72	-	0.086
02320500	79	-	0.080		08276500	85	-	0.074
02448000	72	-	0.019		09112500	77	-	0.000
02484500	73	-	0.048		09119000	73	-	0.018
03011020	107	-	0.087		09124500	73	-	0.002
03020500	101	+	0.096		09147500	90	-	0.022
03363500	80	+	0.083		09180500	88	-	0.013
03379500	96	-	0.085		10131000	84	+	0.011
03604000	90	+	0.050		10329500	76	+	0.039
03612000	87	-	0.088		11160500	73	-	0.015
04073500	110	+	0.100		11525500	99	+	0.001
04087000	96	+	0.005		11532500	79	-	0.025
04100500	79	+	0.088		12422500	111	-	0.005
05286000	81	-	0.068		12442500	82	-	0.075
05410490	77	+	0.042		12445000	82	-	0.084
05414000	76	+	0.039		12451000	84	-	0.009

Table B.1, continued

Station Number	N	Trend	P-Value		Station Number	N	Trend	P-Value
05430500	96	+	0.082		12459000	82	-	0.004
05431486	71	+	0.080		13037500	100	+	0.011
05476000	80	+	0.014		13302500	91	-	0.046
05484500	96	+	0.077		13313000	82	-	0.007
05500000	76	+	0.048		14020000	78	+	0.012
05501000	76	+	0.022		14044000	81	+	0.058
05592500	95	-	0.004		14046500	81	+	0.050
06191500	100	-	0.065		14105700	110	-	0.007
06192500	73	-	0.066		14325000	82	-	0.062

Table B.2

Change-point results indicating year of identified shift in the day of occurrence of flood peaks and associated p-value.

Station Number	N	Year	P-Value		Station Number	N	Year	P-Value
01011000	79	1975	0.000		06192500	73	1983	0.003
01013500	81	1975	0.050		06207500	89	1984	0.032
01014000	84	1982	0.002		06635000	71	1972	0.064
01030500	108	1975	0.063		06869500	92	1969	0.001
01073000	75	1979	0.033		06933500	88	1967	0.085
01175500	99	1942	0.000		07018500	88	1963	0.048
01318500	89	1979	0.070		07050500	72	1970	0.033
01321000	99	1972	0.028		07067000	98	1965	0.067
01381500	89	1982	0.091		07096000	111	1966	0.000
01558000	72	1990	0.063		07186000	87	1958	0.007
01631000	80	1972	0.064		07187000	87	1964	0.013
02016000	85	1939	0.078		07234000	73	1984	0.025
02173500	72	1976	0.005		07340500	73	1984	0.020
02202500	75	1964	0.009		08041000	90	1993	0.023
02313000	79	1955	0.085		08070000	72	1987	0.037
02314500	73	1985	0.089		09110000	102	1940	0.025
02317500	83	1976	0.007		09124500	73	1957	0.007
02320500	79	1985	0.006		09147500	90	1983	0.012
02329000	85	1962	0.009		10329500	76	1974	0.062
02467000	82	1983	0.020		10396000	73	1972	0.050
02474500	71	1981	0.083		11525500	99	1964	0.000
02486000	109	1983	0.046		12027500	82	1957	0.067
04073500	110	1992	0.072		12035000	81	1953	0.075
04087000	96	1948	0.001		12048000	73	1977	0.042
05316500	81	1955	0.015		12370000	89	1958	0.078
05410490	77	1989	0.076		12422500	111	1957	0.023
05421000	77	1966	0.027		12451000	84	1978	0.014
05451500	78	1965	0.002		12459000	82	1986	0.009

Table B.2, continued

Station Number	N	Year	P-Value		Station Number	N	Year	P-Value
05459500	78	1952	0.076		12488500	71	1972	0.019
05476000	80	1980	0.003		13269000	101	1959	0.085
05592500	95	1966	0.027		13302500	91	1978	0.088
05593000	81	1966	0.011		13313000	82	1949	0.098
06191500	100	1983	0.001		14105700	110	1968	0.006

APPENDIX C TREND AND CHANGE-POINT RESULTS FOR FLOOD GENERATING PRECIPITATION SERIES

This appendix contains figures presenting results of Mann-Kendall and Pettitt tests conducted on flood generating precipitation series with lead times of 2- to 7-days constructed based on both 1/8-degree and 1/4-degree gridded precipitation data as discussed in CHAPTER 2. Note that results for precipitation series with a 5-day lead time based on 1/8-degree gridded data are included in Chapter 2.

C.1 Results for Precipitation Series based on 1/8-Degree Gridded Data

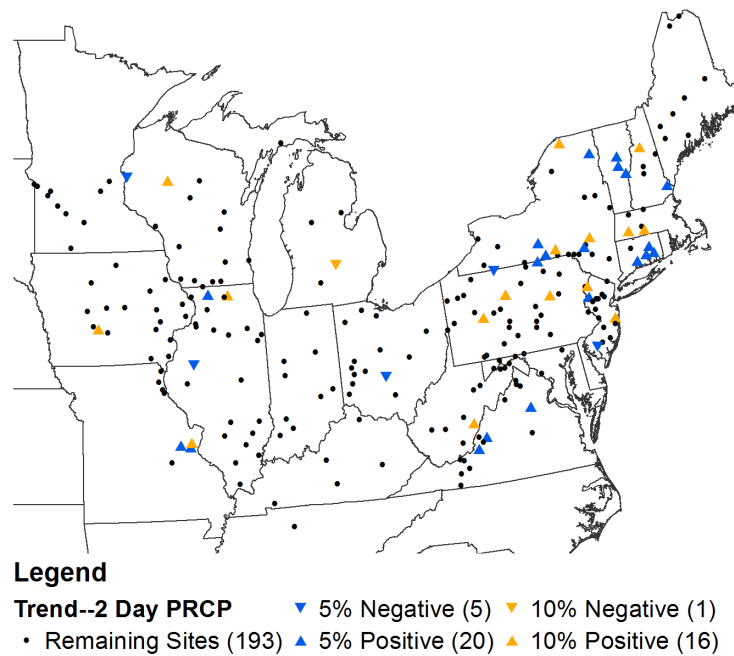


Figure C.1 Results of Mann-Kendall trend tests on flood generating precipitation series with 2-day lead constructed using 1/8-degree gridded data.

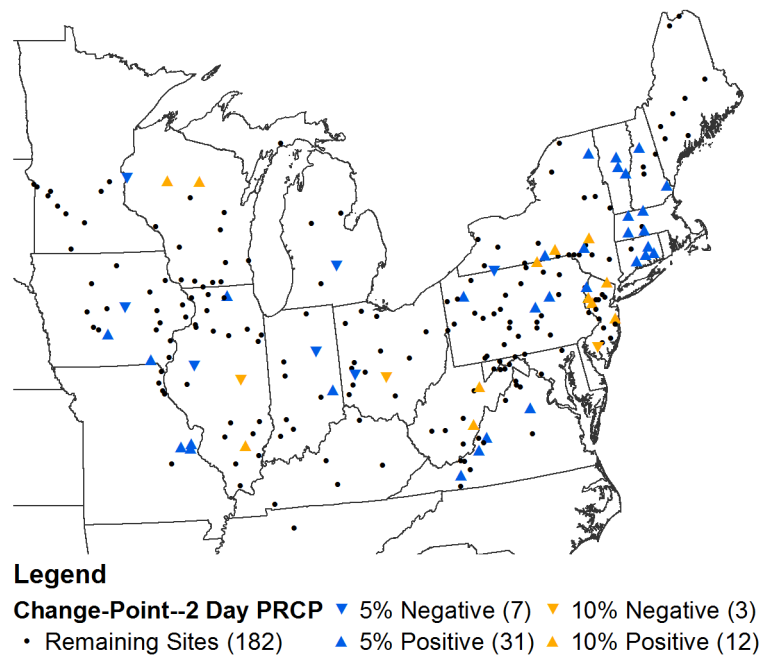


Figure C.2 Results of Pettitt tests on flood generating precipitation series with 2-day lead constructed using 1/8-degree gridded data.

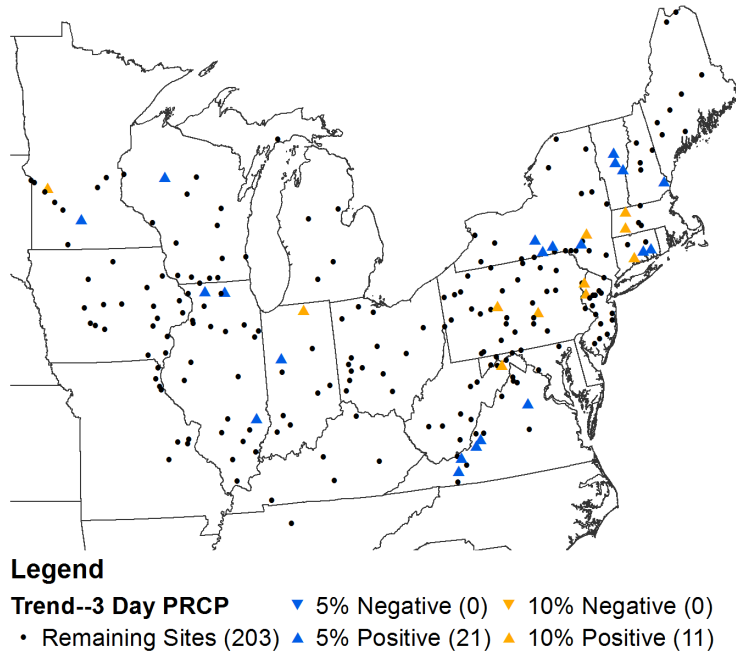


Figure C.3 Results of Mann-Kendall trend tests on flood generating precipitation series with 3-day lead constructed using 1/8-degree gridded data.

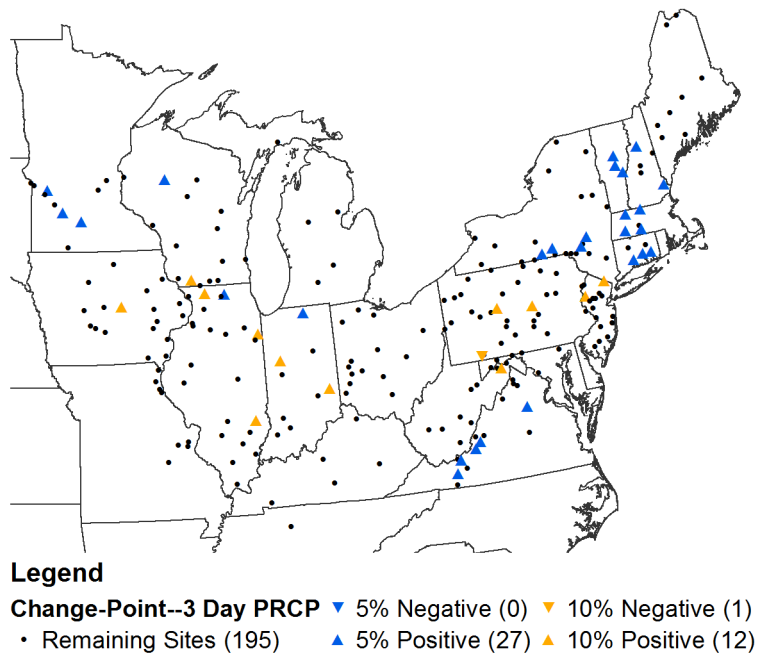


Figure C.4 Results of Pettitt tests on flood generating precipitation series with 3-day lead constructed using 1/8-degree gridded data.

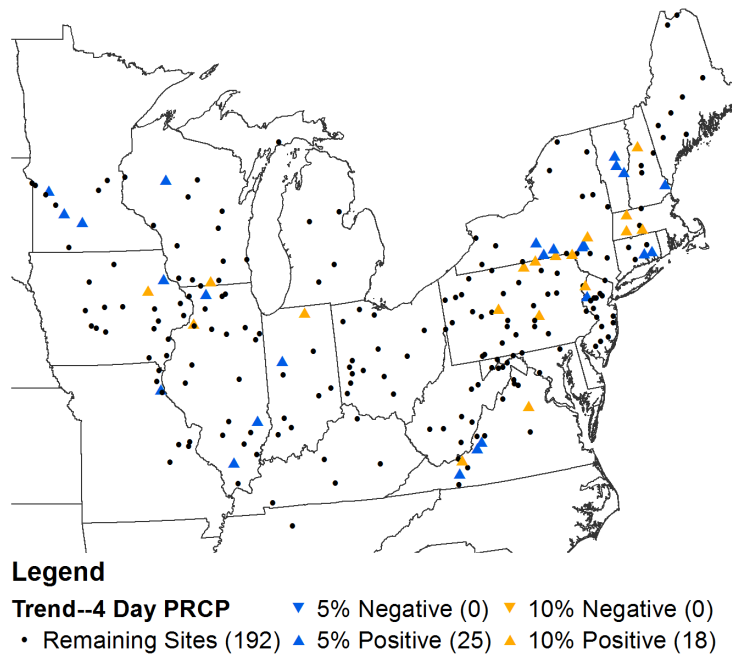


Figure C.5 Results of Mann-Kendall trend tests on flood generating precipitation series with 4-day lead constructed using 1/8-degree gridded data.

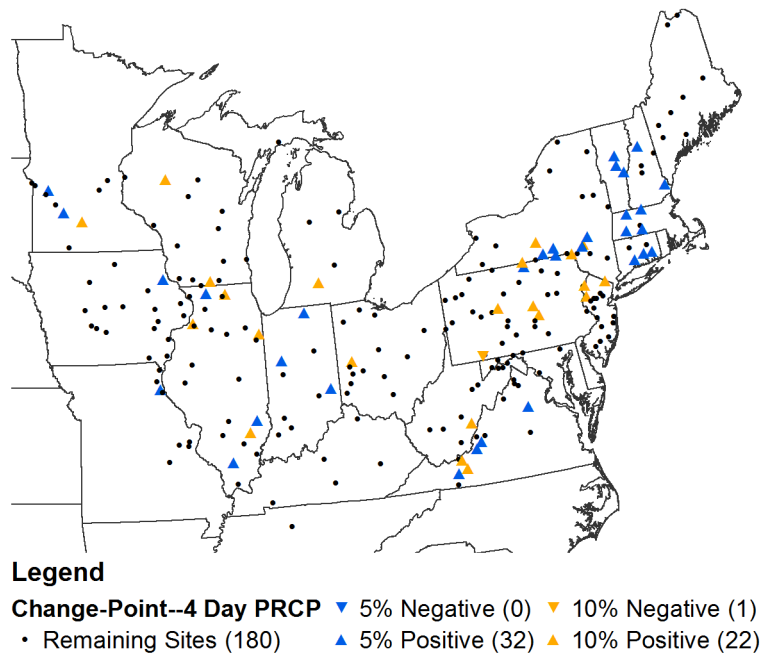


Figure C.6 Results of Pettitt tests on flood generating precipitation series with 4-day lead constructed using 1/8-degree gridded data.

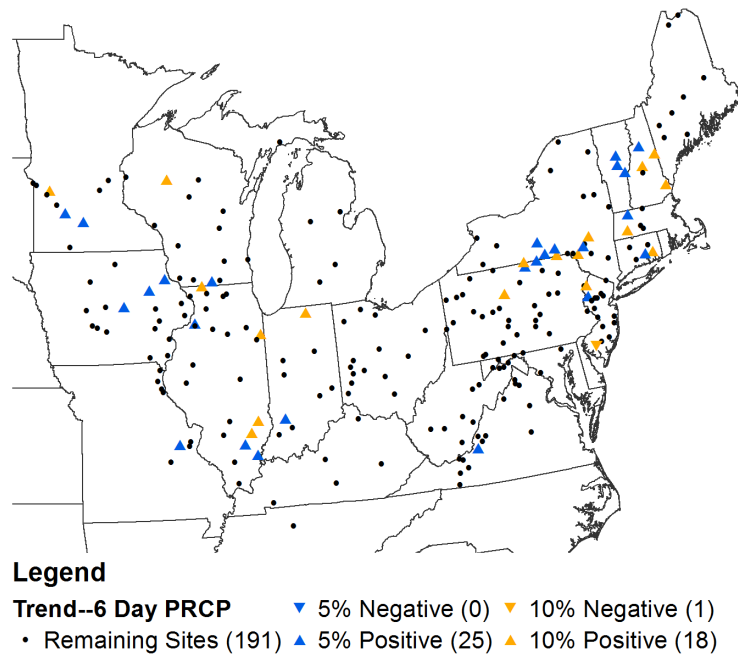


Figure C.7 Results of Mann-Kendall trend tests on flood generating precipitation series with 6-day lead constructed using 1/8-degree gridded data.

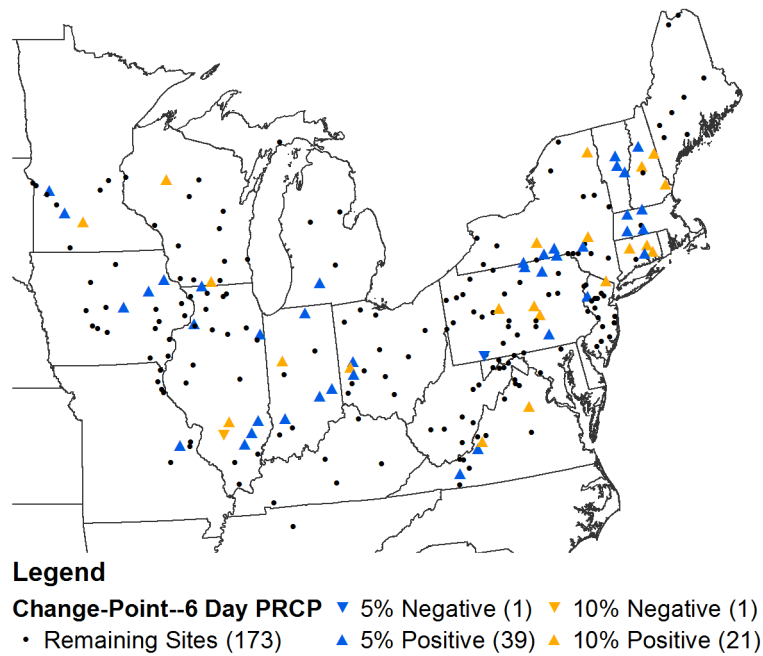


Figure C.8 Results of Pettitt tests on flood generating precipitation series with 6-day lead constructed using 1/8-degree gridded data.

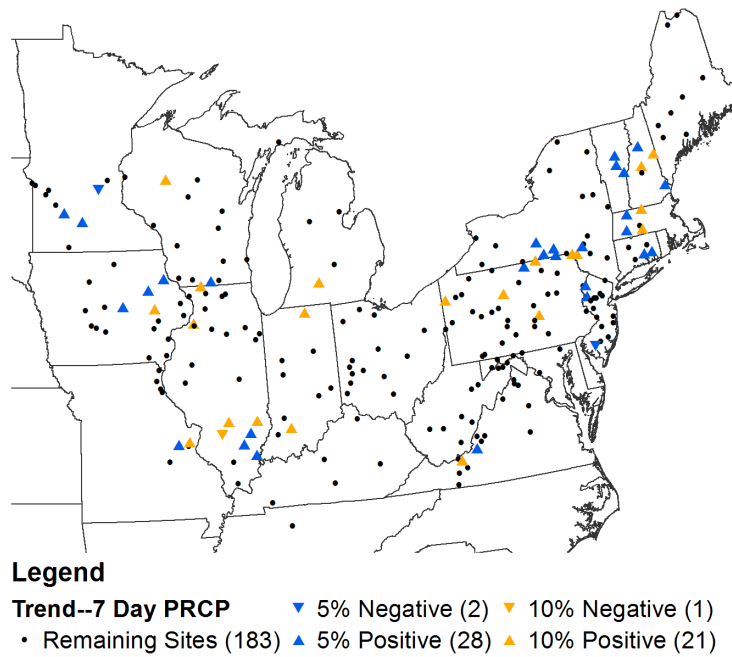


Figure C.9 Results of Mann-Kendall trend tests on flood generating precipitation series with 7-day lead constructed using 1/8-degree gridded data.

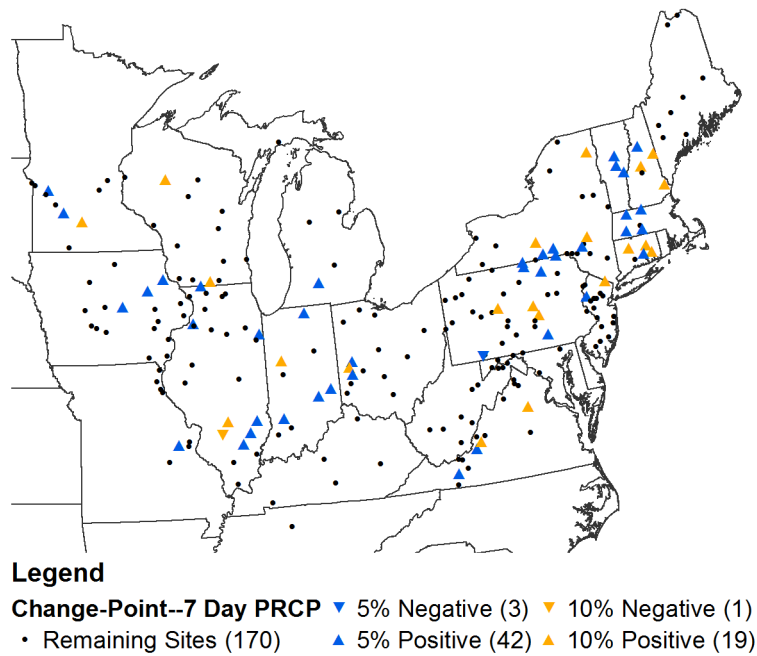


Figure C.10 Results of Pettitt tests on flood generating precipitation series with 7-day lead constructed using 1/8-degree gridded data.

C.2 Results for Precipitation Series Based on 1/4-Degree Gridded Data

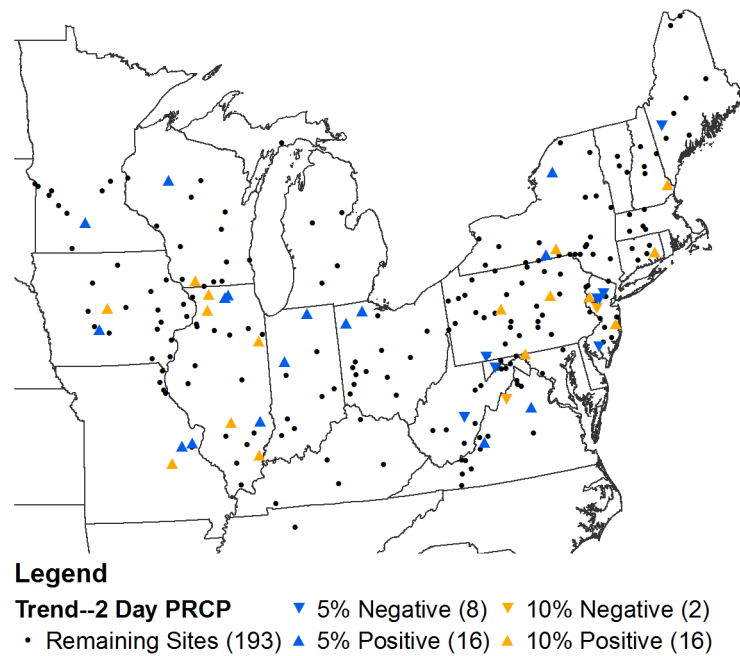


Figure C.11 Results of Mann-Kendall trend tests on flood generating precipitation series with 2-day lead constructed using 1/4-degree gridded data.

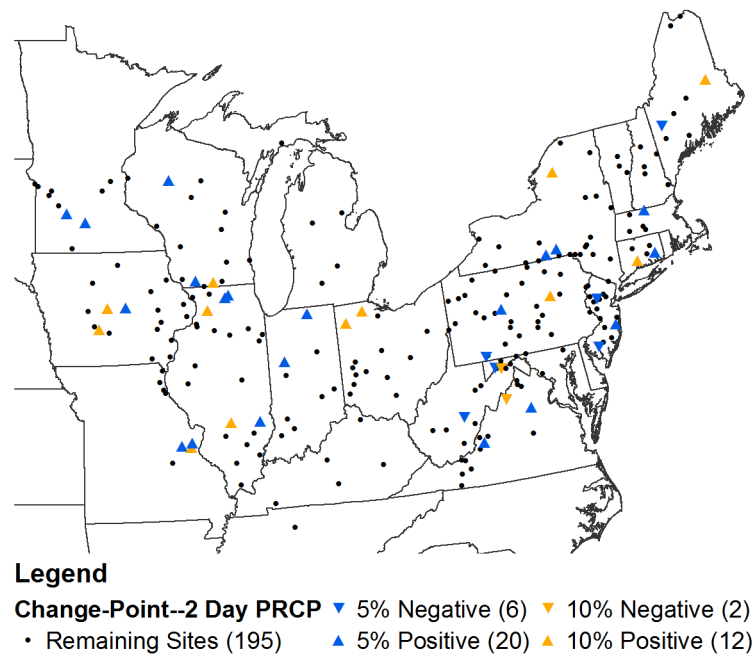


Figure C.12 Results of Pettitt tests on flood generating precipitation series with 2-day lead constructed using 1/4-degree gridded data.

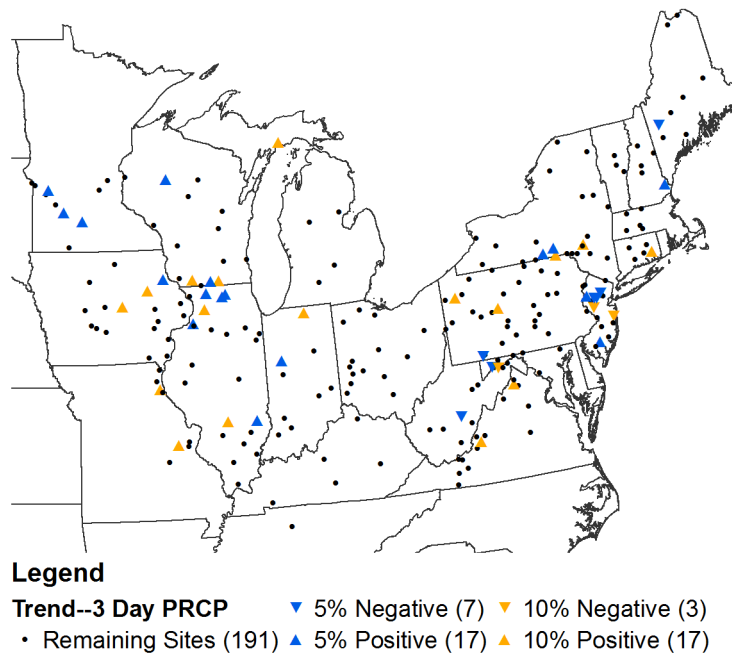


Figure C.13 Results of Mann-Kendall trend tests on flood generating precipitation series with 3-day lead constructed using 1/4-degree gridded data.

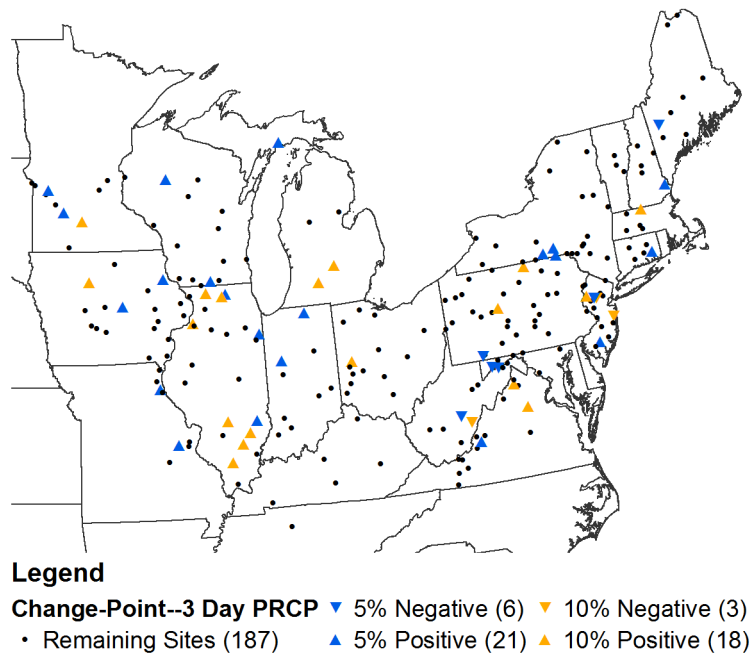


Figure C.14 Results of Pettitt tests on flood generating precipitation series with 3-day lead constructed using 1/4-degree gridded data.

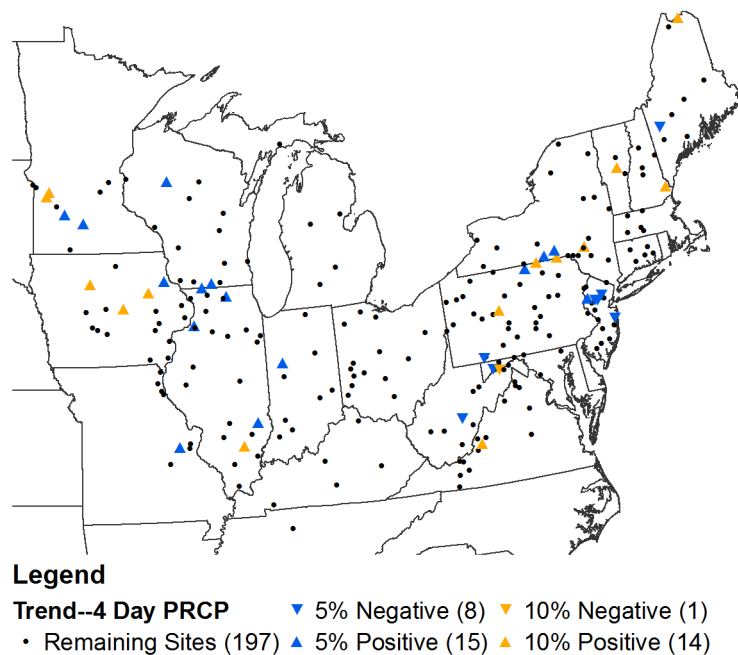


Figure C.15 Results of Mann-Kendall trend tests on flood generating precipitation series with 4-day lead constructed using 1/4-degree gridded data.

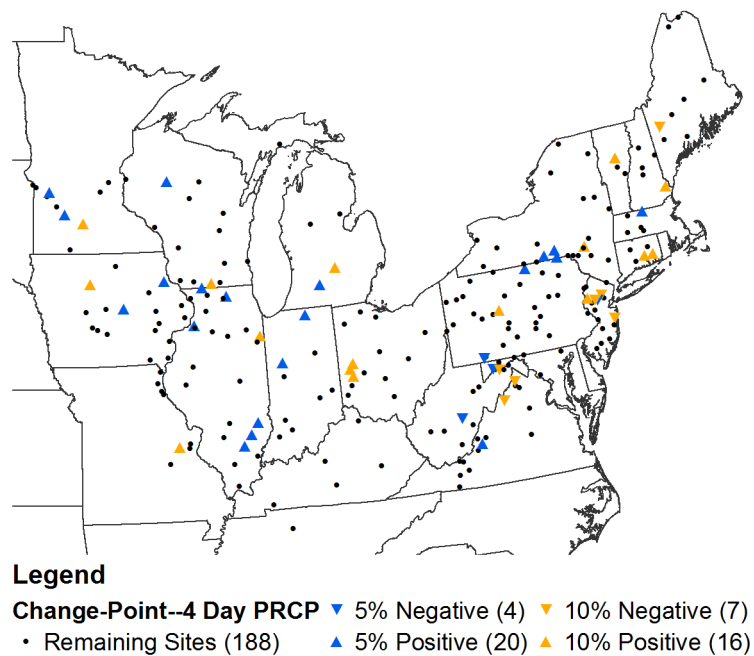


Figure C.16 Results of Pettitt tests on flood generating precipitation series with 4-day lead constructed using 1/4-degree gridded data.

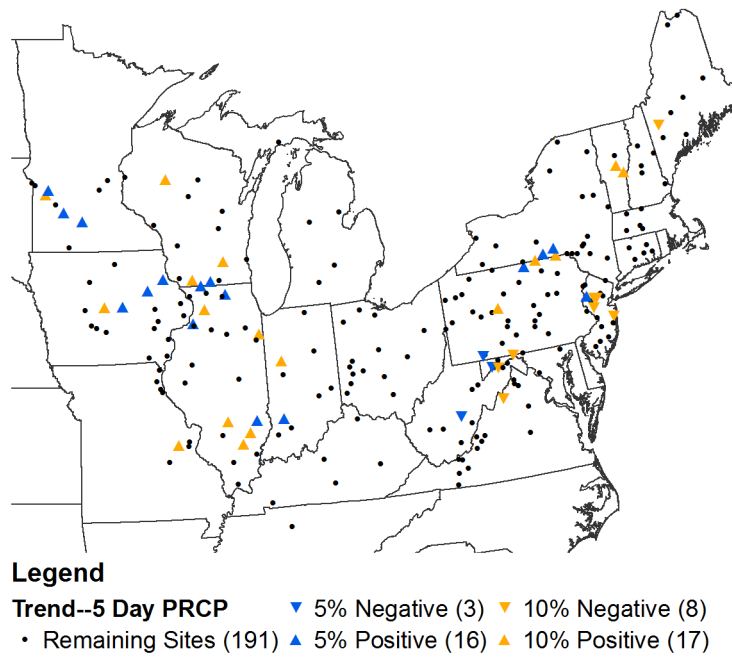


Figure C.17 Results of Mann-Kendall trend tests on flood generating precipitation series with 5-day lead constructed using 1/4-degree gridded data.

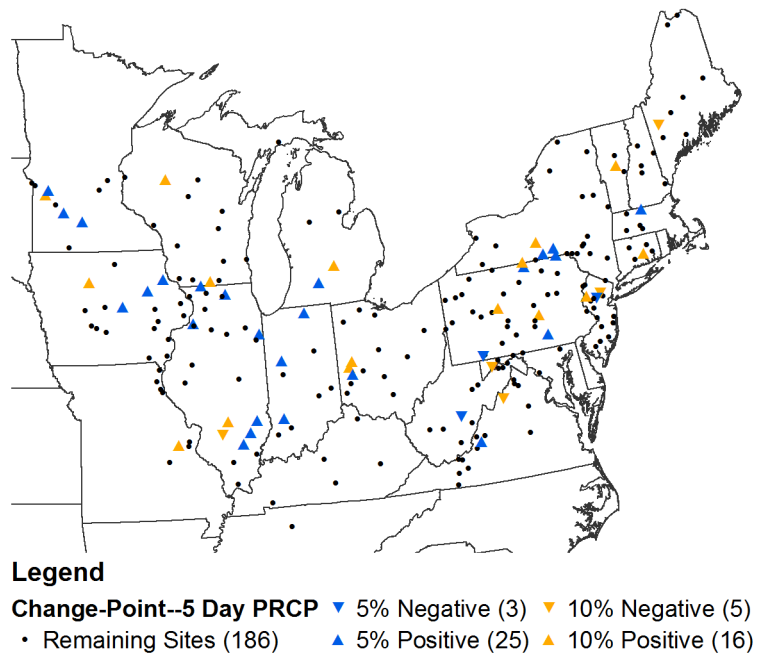


Figure C.18 Results of Pettitt tests on flood generating precipitation series with 5-day lead constructed using 1/4-degree gridded data.

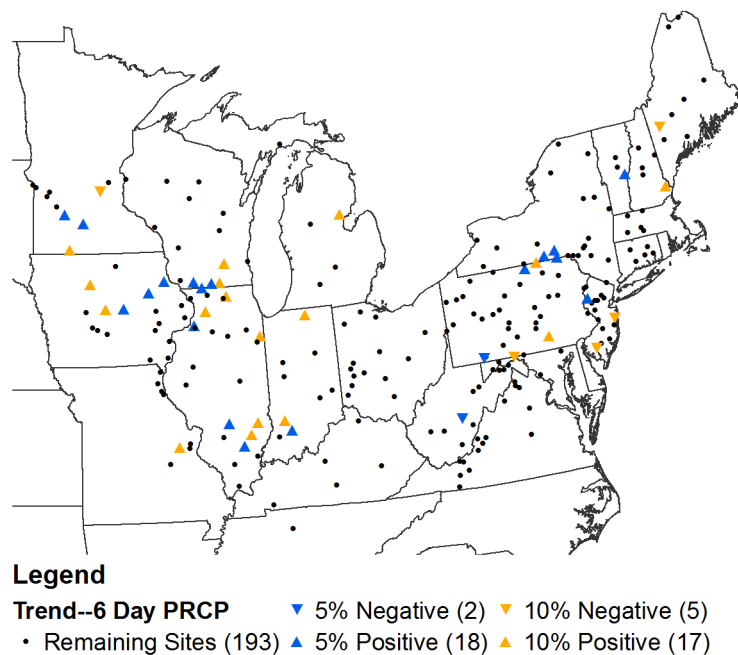


Figure C.19 Results of Mann-Kendall trend tests on flood generating precipitation series with 6-day lead constructed using 1/4-degree gridded data.

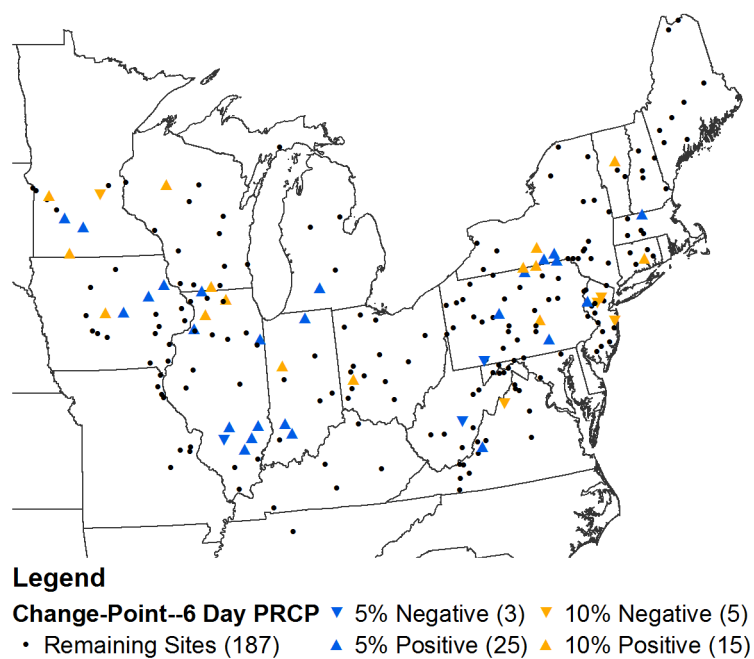


Figure C.20 Results of Pettitt tests on flood generating precipitation series with 6-day lead constructed using 1/4-degree gridded data.

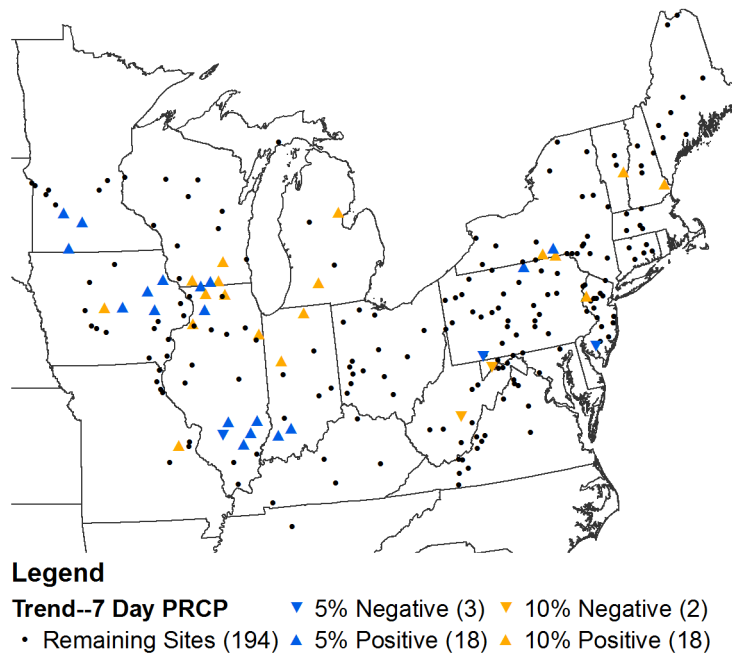


Figure C.21 Results of Mann-Kendall trend tests on flood generating precipitation series with 7-day lead constructed using 1/4-degree gridded data.

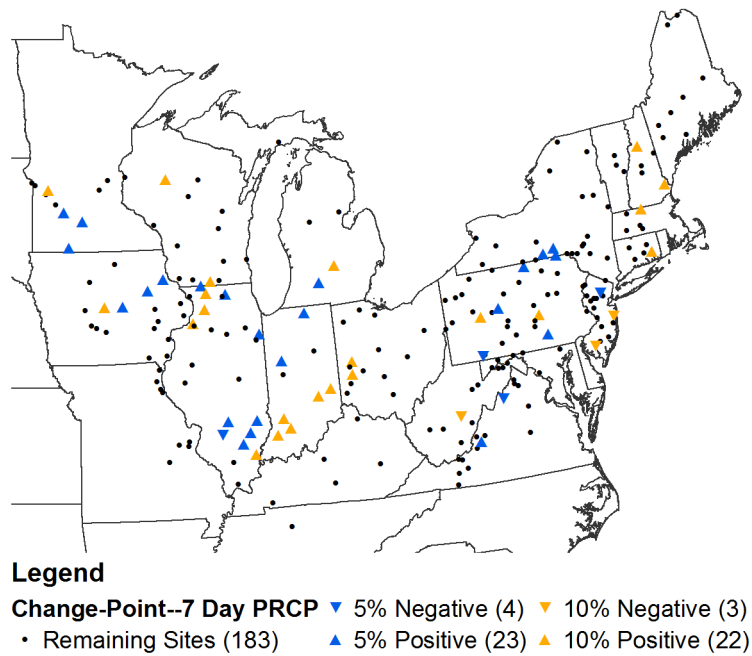


Figure C.22 Results of Pettitt tests on flood generating precipitation series with 7-day lead constructed using 1/4-degree gridded data.

APPENDIX D TREND AND CHANGE-POINT RESULTS FOR FLOOD GENERATING TEMPERATURE SERIES

This appendix contains figures presenting results of Mann-Kendall and Pettitt tests on flood generating minimum and maximum temperature series constructed with 2- to 7-day lead times based on 1/8-degree gridded data as discussed in CHAPTER 2. Note that results for both minimum and maximum temperature series with a 4-day lead time are included in Chapter 2.

D.1 Results for Minimum Temperature Series

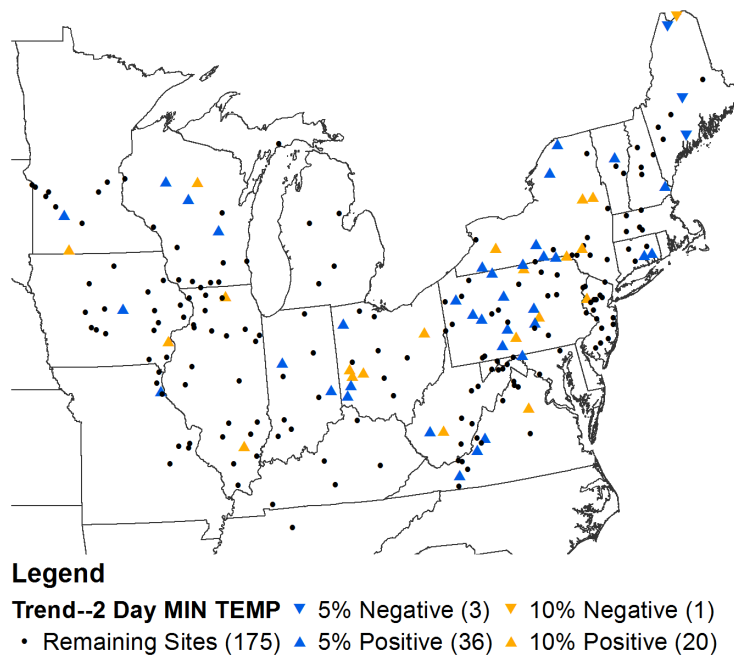


Figure D.1 Results of Mann-Kendall tests on flood generating minimum temperature series with 2-day lead.

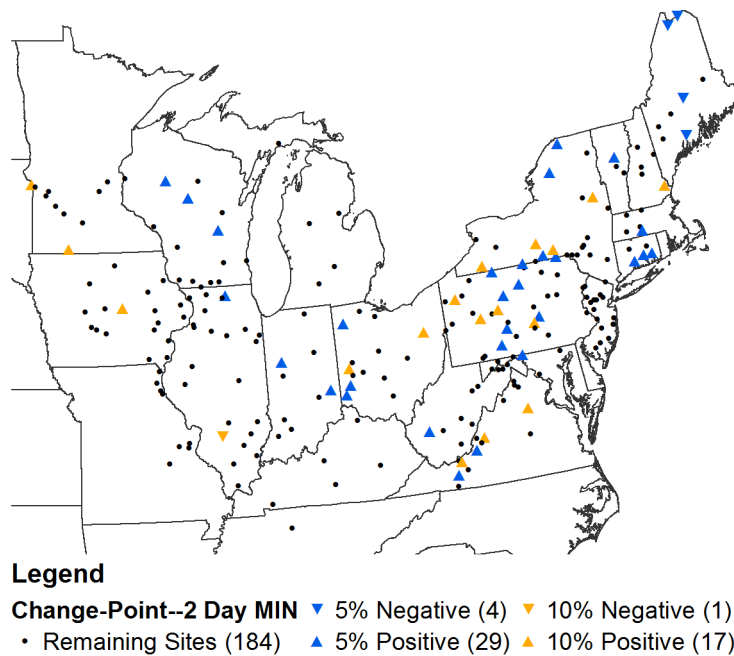


Figure D.2 Results of Pettitt tests on flood generating minimum temperature series with 2-day lead.

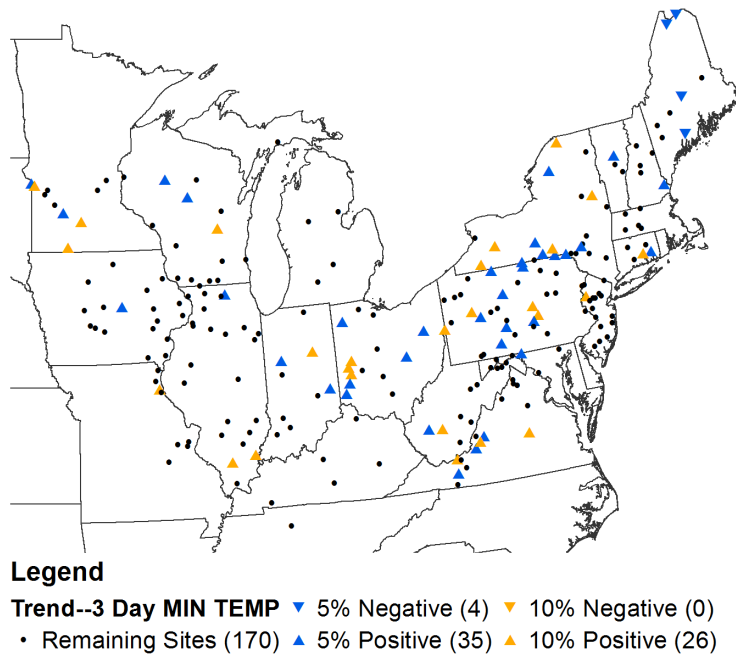


Figure D.3 Results of Mann-Kendall tests on flood generating minimum temperature series with 3-day lead.

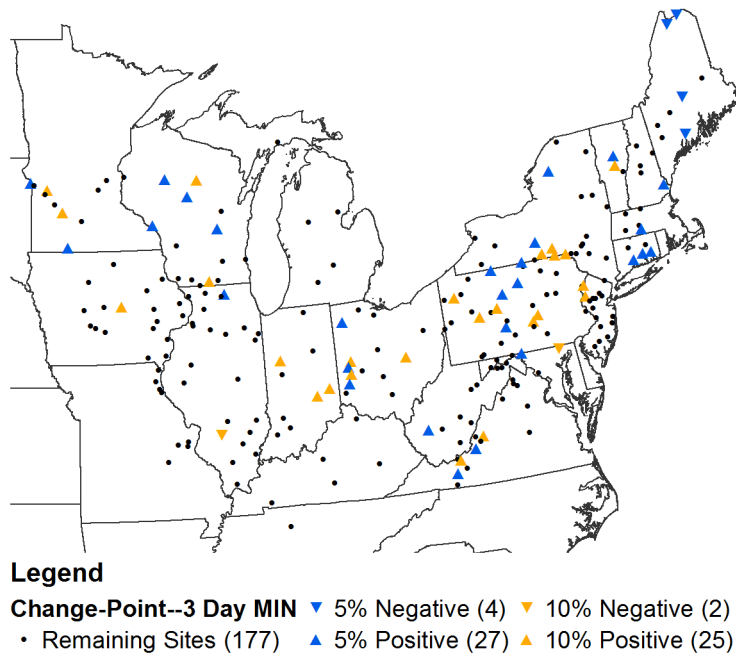


Figure D.4 Results of Pettitt tests on flood generating minimum temperature series with 3-day lead.

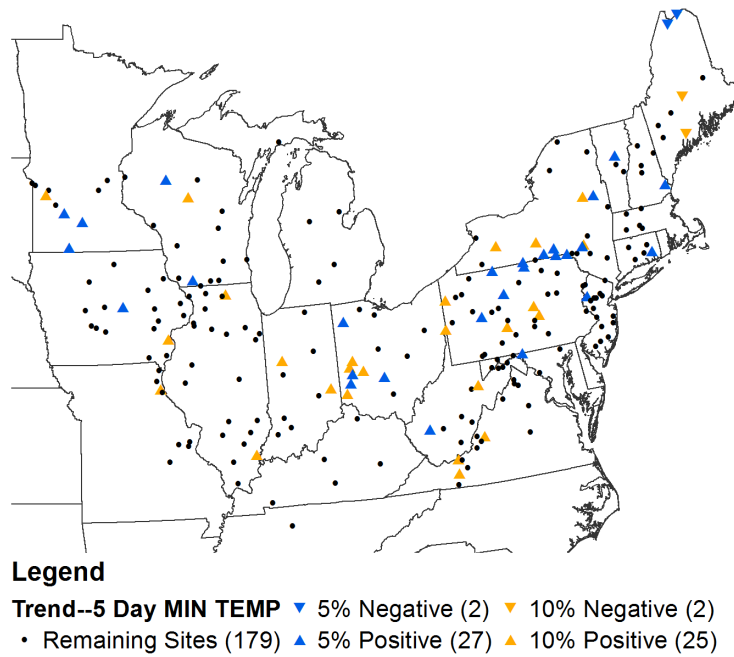


Figure D.5 Results of Mann-Kendall tests on flood generating minimum temperature series with 5-day lead.

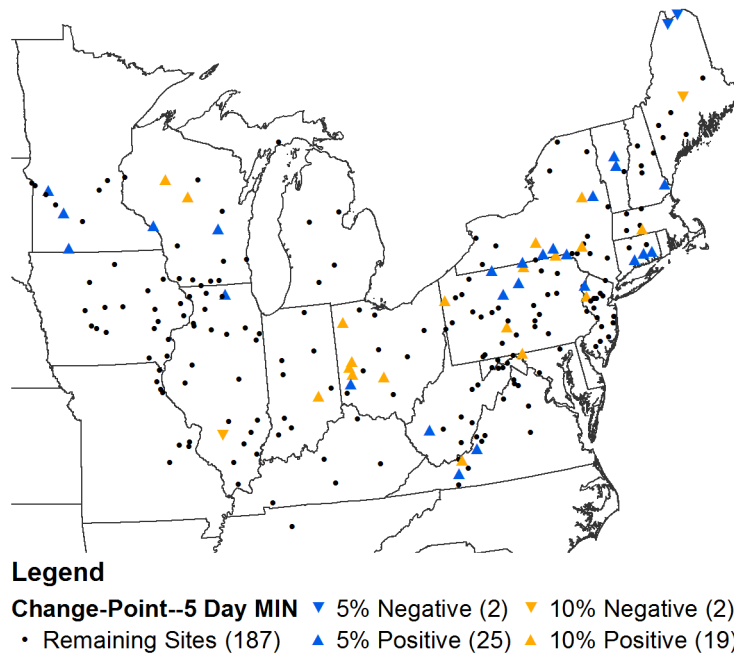


Figure D.6 Results of Pettitt tests on flood generating minimum temperature series with 5-day lead.

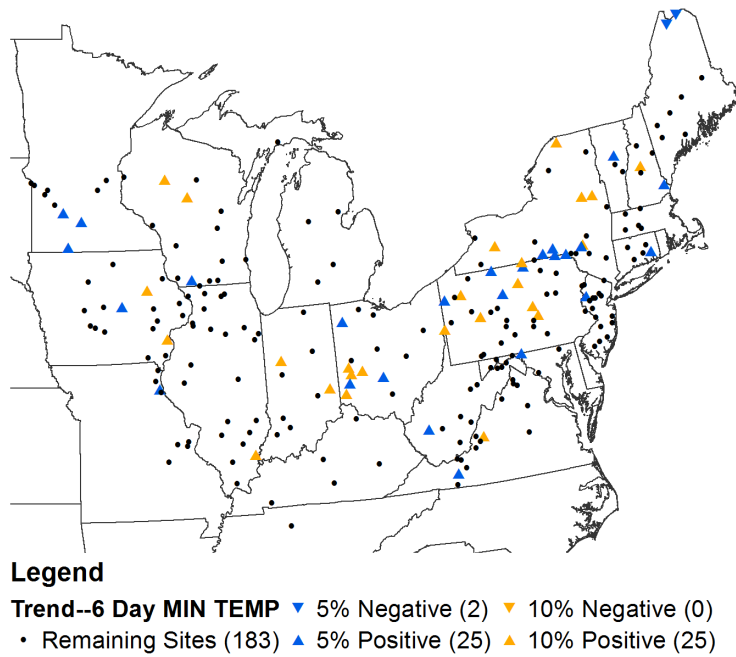


Figure D.7 Results of Mann-Kendall tests on flood generating minimum temperature series with 6-day lead.

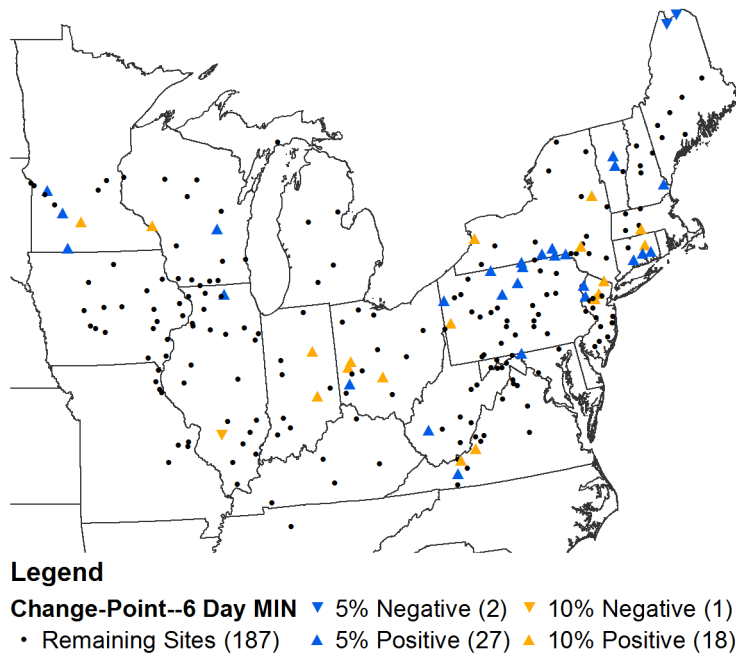


Figure D.8 Results of Pettitt tests on flood generating minimum temperature series with 6-day lead.

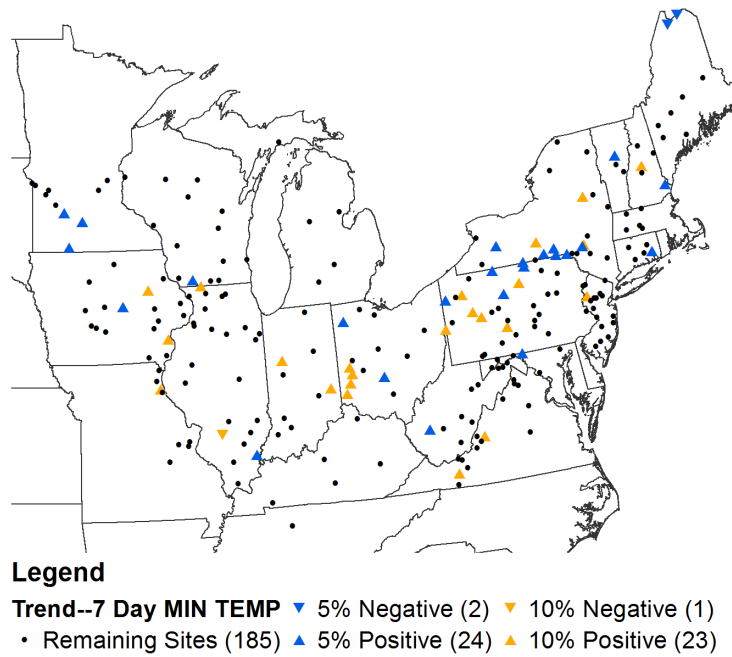


Figure D.9 Results of Mann-Kendall tests on flood generating minimum temperature series with 7-day lead.

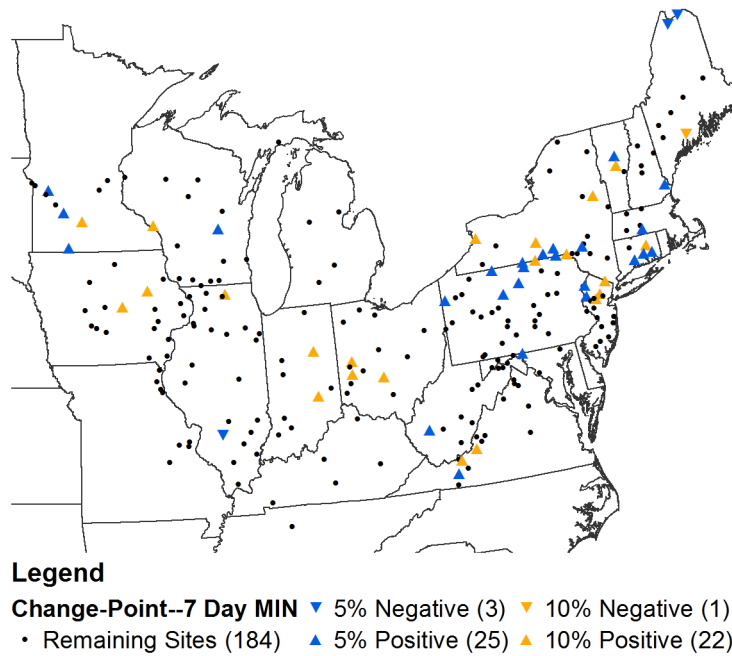


Figure D.10 Results of Pettitt tests on flood generating minimum temperature series with 7-day lead.

D.2 Results for Maximum Temperature Series

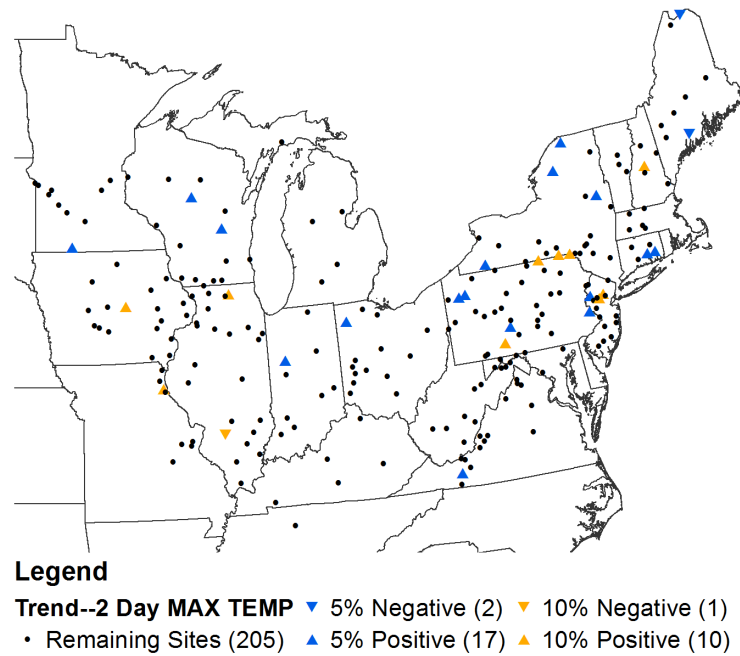


Figure D.11 Results of Mann-Kendall tests on flood generating maximum temperature series with 2-day lead.

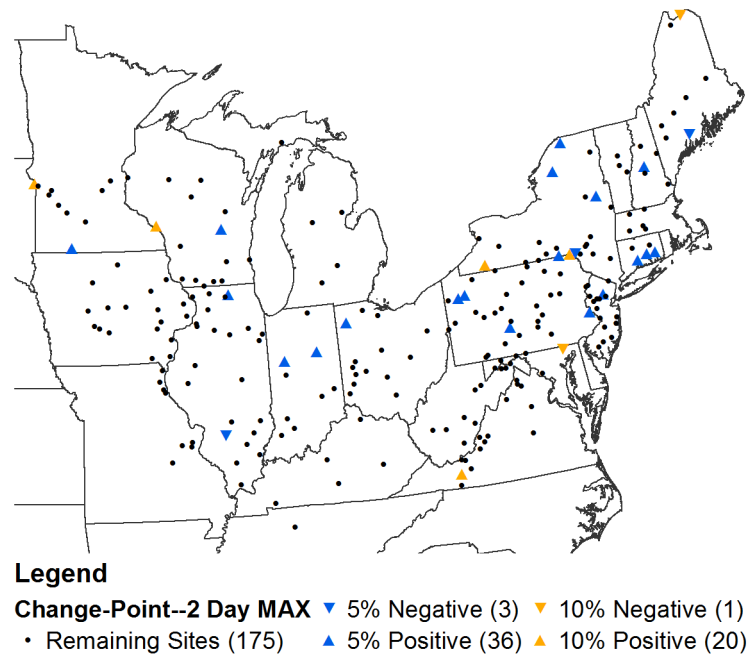


Figure D.12 Results of Pettitt tests on flood generating maximum temperature series with 2-day lead.

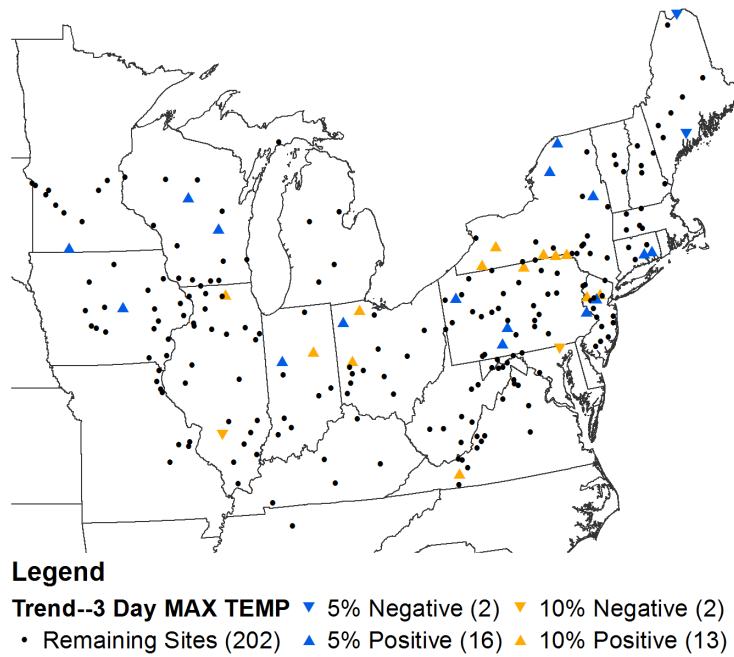


Figure D.13 Results of Mann-Kendall tests on flood generating maximum temperature series with 3-day lead.

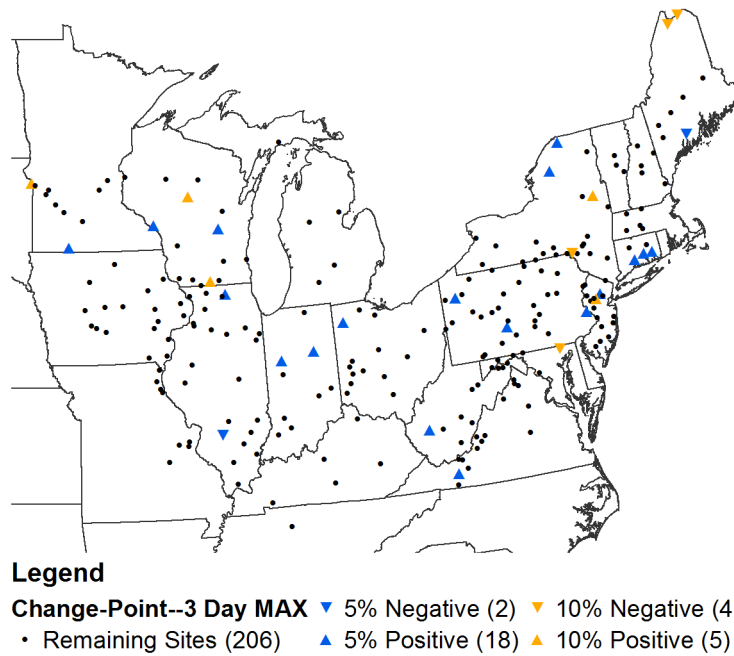


Figure D.14 Results of Pettitt tests on flood generating maximum temperature series with 3-day lead.

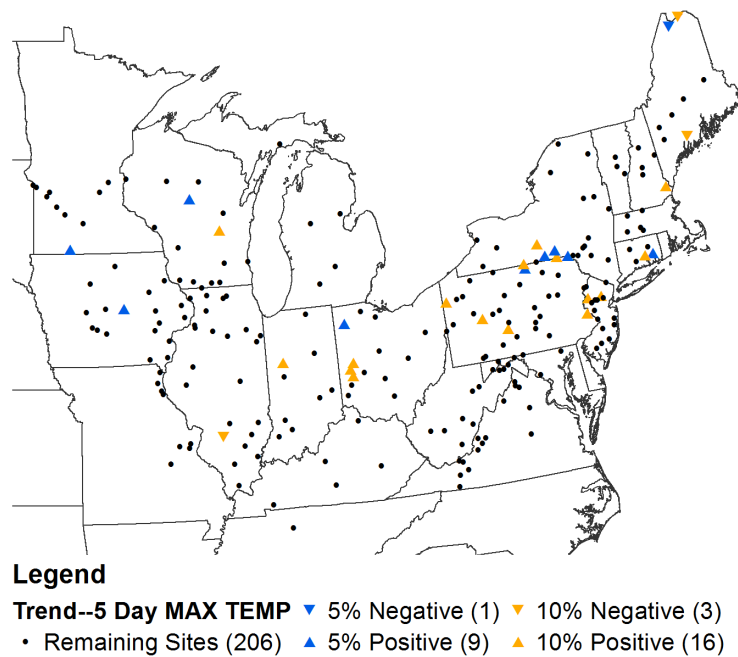


Figure D.15 Results of Mann-Kendall tests on flood generating maximum temperature series with 5-day lead.

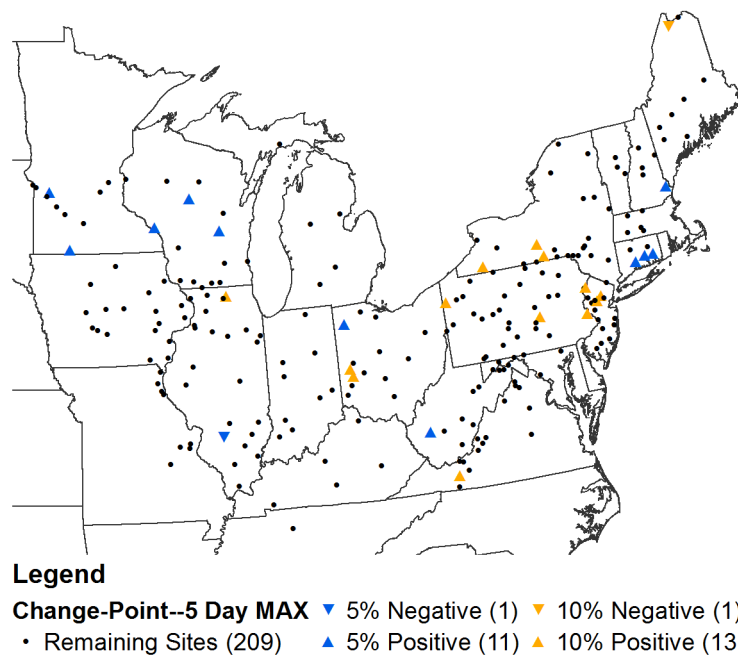


Figure D.16 Results of Pettitt tests on flood generating maximum temperature series with 5-day lead.

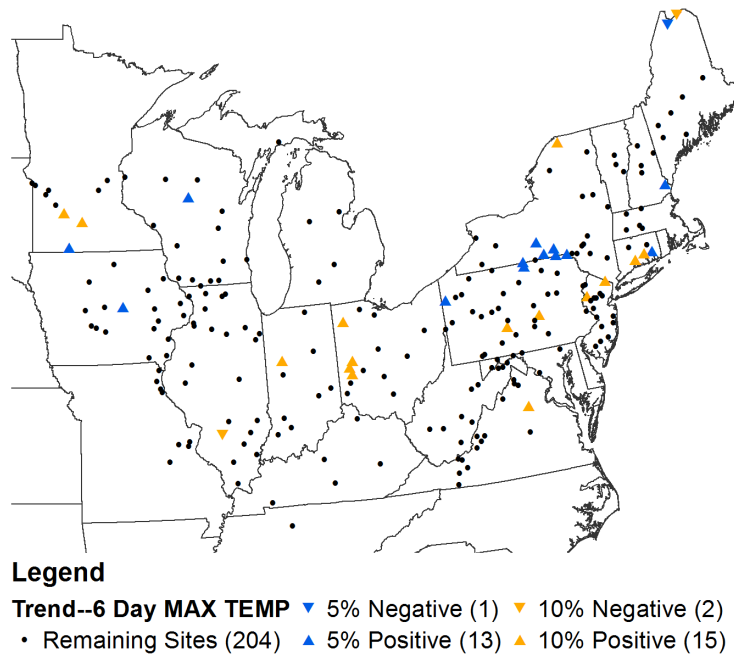


Figure D.17 Results of Mann-Kendall tests on flood generating maximum temperature series with 6-day lead.

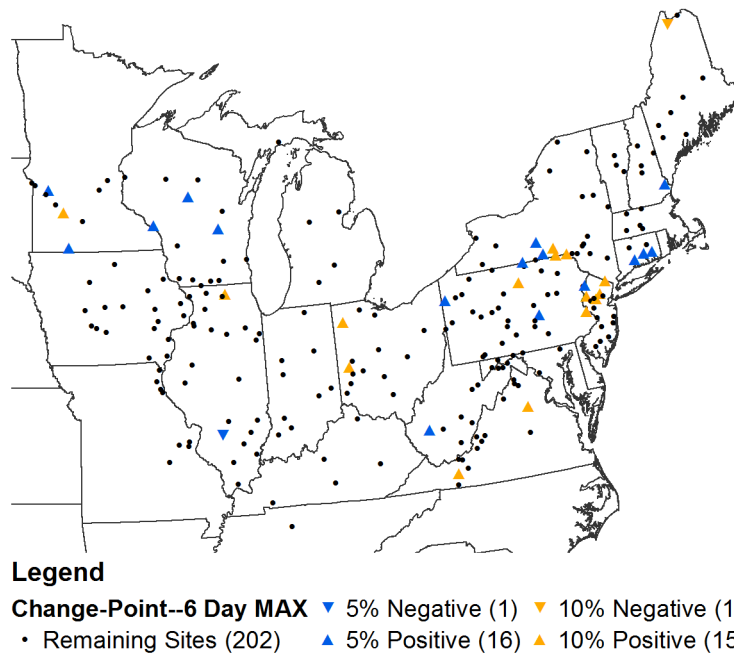


Figure D.18 Results of Pettitt tests on flood generating maximum temperature series with 6-day lead.

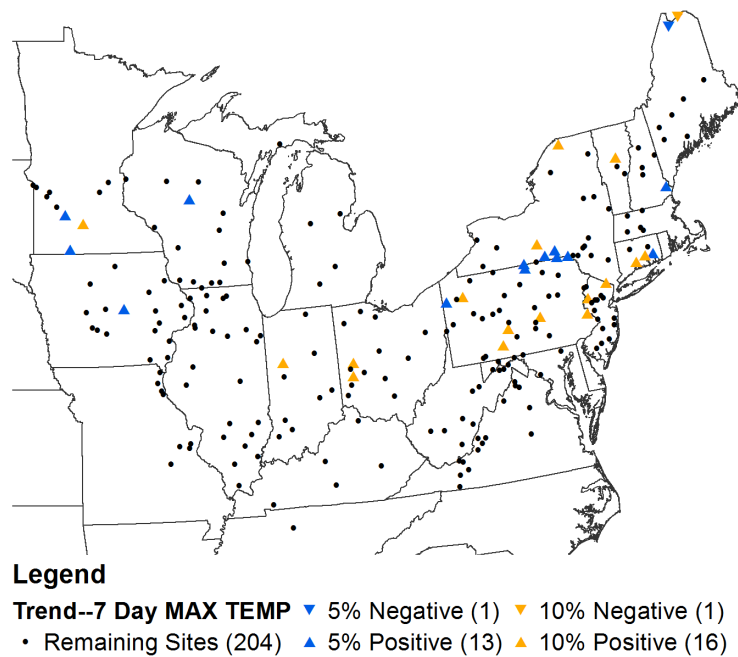


Figure D.19 Results of Mann-Kendall tests on flood generating maximum temperature series with 7-day lead.

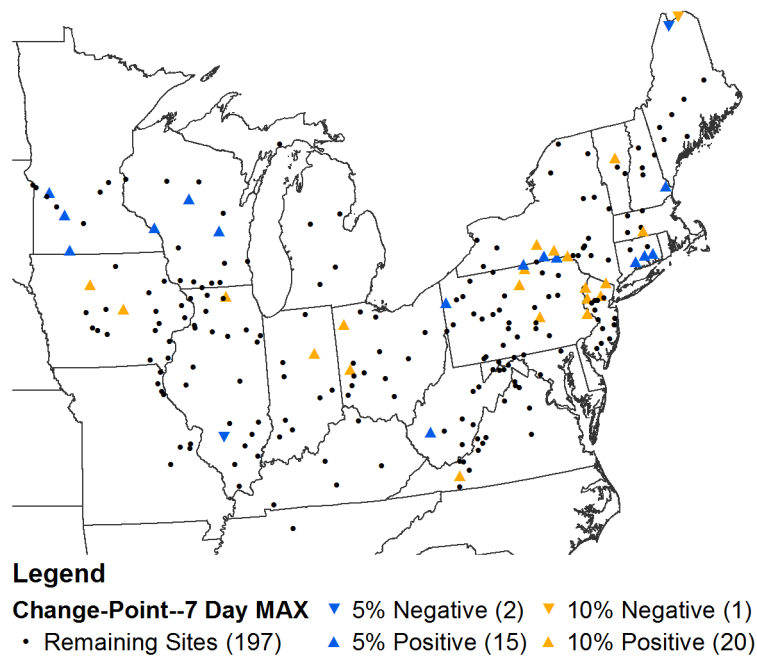


Figure D.20 Results of Pettitt tests on flood generating maximum temperature series with 7-day lead.

APPENDIX E CORRELATION ANALYSIS RESULTS

BETWEEN 10 YEAR MOVING AVERAGE OF LOGS OF FLOOD FLOWS AND CLIMATE ANOMALIES

This appendix contains tables and figures summarizing Kendall's tau correlation analyses between the 10-year moving average of log-transformed flood flows and 3-month average AMO, MEI, NAO, Nino3.4, and PDO anomalies with 3-, 6-, and 9-month leads. Tables include results only for sites with significant relationships on the 10% level (sites significant on the 5% level are in **bold**). Results are omitted (blank spaces) when p-values greater than 10% were obtained. Note that results of the Kendall's tau analyses for AMO, MEI, NAO, and PDO with lead times of 6-, 9-, 3-, and 9-months, respectively, are illustrated in Chapter 3. Figures for Pearson's r and Spearman's rho with the same lead times are included herein. The table below summarizes the number of sites where significant results were obtained using the Pearson's r and Spearman's rho analyses for all cases considered.

Table E.1

Number of sites with significant Pearson's r and Spearman's rho correlations (5 and 10% levels) between 10-yr moving mean of log-transformed flood peaks and for AMO, MEI, NINO 3.4, NAO, and PDO indices with specified lead times.

Lead Time (months)	AMO		MEI		Nino 3.4		NAO		PDO	
	5%	10%	5%	10%	5%	10%	5%	10%	5%	10%
<i>Pearson's r Correlation</i>										
3	233	282	48	107	1	6	110	144	174	235
6	247	297	90	162	4	16	48	81	204	254
9	213	265	159	214	14	35	48	85	251	296
<i>Spearman's rho Correlation</i>										
3	234	271	44	90	1	7	99	138	180	239
6	234	281	69	134	6	20	47	85	197	248
9	192	252	135	188	14	42	52	82	236	285

E.1 AMO Correlation Results

Table E.2

Results of Kendall's tau analyses (significant 10% level) between 10-year moving average of log-transformed flood flows and 3-month average **AMO** anomalies with 3-, 6-, and 9-month leads.

Station Number	3-Month Lead		6-Month Lead		9-Month Lead	
	tau	p-value	tau	p-value	tau	p-value
1011000	-0.185	0.038				
1014000	-0.196	0.027				
1031500	-0.274	0.002	-0.196	0.027		
1038000	-0.224	0.012				
1055000			0.166	0.062		
1064500			0.146	0.100		
1073000	0.220	0.014	0.353	0.000	0.344	0.000
1076500	0.173	0.054	0.254	0.005	0.202	0.024
1127500	-0.226	0.012				
1137500	0.353	0.000	0.452	0.000	0.349	0.000
1142500	0.355	0.000	0.436	0.000	0.337	0.000
1144000	0.178	0.047	0.222	0.013	0.173	0.054
1175500	0.379	0.000	0.360	0.000	0.363	0.000
1188000			0.255	0.004	0.195	0.029
1193500	-0.157	0.080				
1196500	-0.164	0.067				
1321000	0.361	0.000	0.381	0.000	0.366	0.000
1350000			0.160	0.072		
1357500	0.177	0.046	0.220	0.013	0.227	0.011
1379500	-0.417	0.000	-0.317	0.000	-0.386	0.000
1381500	-0.148	0.096				
1397500			0.207	0.020		
1398500	-0.218	0.014			-0.178	0.045
1399500	-0.198	0.026			-0.189	0.033
1408000	-0.368	0.000	-0.334	0.000	-0.315	0.000
1408500	-0.237	0.008	-0.264	0.003	-0.276	0.002
1411000	-0.242	0.006	-0.151	0.090		
1411500	-0.316	0.000	-0.301	0.001	-0.357	0.000
1413500	0.256	0.004	0.249	0.005	0.245	0.006
1414500	0.539	0.000	0.504	0.000	0.498	0.000
1420500			0.201	0.024		
1421000	0.304	0.001	0.319	0.000	0.285	0.001
1426500	0.285	0.001	0.221	0.013	0.259	0.003
1440000	0.178	0.045	0.213	0.016	0.208	0.019
1463500	0.247	0.005	0.227	0.011	0.204	0.022
1503000	0.369	0.000	0.328	0.000	0.360	0.000
1512500	0.252	0.005	0.231	0.009	0.270	0.002
1531000	0.203	0.022				

Table E.2, continued

Station Number	3-Month Lead		6-Month Lead		9-Month Lead	
	tau	p-value	tau	p-value	tau	p-value
1532000	0.249	0.005	0.281	0.002	0.225	0.011
1534000			0.227	0.011		
1538000			0.187	0.035		
1539000	0.296	0.001	0.315	0.000	0.262	0.003
1541000	-0.174	0.050	-0.213	0.016	-0.157	0.078
1548500	0.149	0.093				
1555000			0.160	0.072		
1555500	-0.177	0.046			-0.149	0.095
1556000	0.419	0.000	0.294	0.001	0.282	0.001
1560000			0.181	0.041		
1574000	-0.436	0.000	-0.359	0.000	-0.407	0.000
1580000			-0.163	0.066		
1599000	0.366	0.000	0.309	0.000	0.296	0.001
1604500			-0.155	0.081		
1610000	-0.349	0.000	-0.354	0.000	-0.345	0.000
1613000	-0.336	0.000	-0.362	0.000	-0.361	0.000
1614500	-0.345	0.000	-0.288	0.001	-0.325	0.000
1631000	-0.240	0.007	-0.189	0.033	-0.258	0.004
1634000	-0.205	0.021	-0.154	0.083	-0.228	0.010
1645000			-0.172	0.053		
2013000	-0.273	0.002	-0.183	0.040	-0.279	0.002
2016000	-0.181	0.042			-0.202	0.023
2035000	-0.327	0.000	-0.261	0.003	-0.329	0.000
2055000	-0.174	0.050			-0.149	0.095
2070000	-0.303	0.001	-0.246	0.006	-0.283	0.001
2083000			0.151	0.090		
2083500	0.353	0.000	0.276	0.002	0.283	0.001
2085500	0.173	0.051			0.156	0.079
2091500	0.198	0.026			0.162	0.068
2102000	0.303	0.001	0.255	0.004	0.238	0.007
2116500	-0.342	0.000	-0.387	0.000	-0.298	0.001
2118000	-0.231	0.009	-0.260	0.003	-0.207	0.020
2131000	-0.303	0.001	-0.348	0.000	-0.281	0.002
2132000	-0.363	0.000	-0.377	0.000	-0.326	0.000
2136000	-0.373	0.000	-0.370	0.000	-0.358	0.000
2138500			-0.167	0.060	-0.167	0.060
2154500			-0.167	0.061		
2156500	-0.259	0.004	-0.339	0.000	-0.289	0.001
2173500	-0.376	0.000	-0.408	0.000	-0.334	0.000
2177000	-0.253	0.004	-0.261	0.003	-0.237	0.008
2192000	-0.333	0.000	-0.340	0.000	-0.326	0.000
2198000	-0.337	0.000	-0.371	0.000	-0.293	0.001
2202500	-0.360	0.000	-0.378	0.000	-0.314	0.000
2203000	-0.389	0.000	-0.454	0.000	-0.361	0.000

Table E.2, continued

Station Number	3-Month Lead		6-Month Lead		9-Month Lead	
	tau	p-value	tau	p-value	tau	p-value
2213500	-0.289	0.001	-0.224	0.012	-0.224	0.012
2217500	-0.318	0.000	-0.346	0.000	-0.299	0.001
2225500	-0.403	0.000	-0.400	0.000	-0.327	0.000
2226000	-0.314	0.000	-0.288	0.001	-0.272	0.002
2226500	-0.327	0.000	-0.361	0.000	-0.289	0.001
2228000	-0.276	0.002	-0.308	0.001	-0.242	0.006
2231000			0.150	0.092	0.149	0.093
2256500	0.218	0.014	0.308	0.001	0.325	0.000
2296750	0.262	0.003	0.395	0.000	0.372	0.000
2298830	0.336	0.000	0.466	0.000	0.407	0.000
2301500	0.202	0.023	0.286	0.001	0.294	0.001
2303000			0.219	0.014	0.197	0.027
2313000	-0.207	0.020	-0.152	0.087	-0.160	0.071
2314500	-0.255	0.004	-0.320	0.000	-0.248	0.005
2317500	-0.151	0.089				
2320500	-0.340	0.000	-0.287	0.001	-0.259	0.003
2321500	-0.192	0.031	-0.215	0.015	-0.206	0.021
2329000	-0.301	0.001	-0.248	0.005	-0.263	0.003
2333500	-0.233	0.009	-0.208	0.019		
2337000	-0.192	0.031	-0.188	0.034	-0.157	0.078
2339500			-0.204	0.022		
2347500	-0.335	0.000	-0.366	0.000	-0.286	0.001
2353500	-0.316	0.000	-0.285	0.001	-0.263	0.003
2358000	-0.345	0.000	-0.374	0.000	-0.337	0.000
2361000	-0.221	0.013	-0.259	0.003	-0.213	0.016
2375500	-0.352	0.000	-0.308	0.001	-0.328	0.000
2392000	-0.166	0.063	-0.248	0.005	-0.164	0.065
2437000	0.254	0.004	0.239	0.007	0.202	0.023
2441000	-0.268	0.003	-0.297	0.001	-0.228	0.010
2448000	-0.168	0.058	-0.197	0.027	-0.202	0.023
2474500			-0.169	0.057	-0.163	0.067
2487500	0.183	0.039	0.221	0.013	0.158	0.076
3010500	0.214	0.016			0.150	0.092
3020500	0.169	0.057				
3032500	0.171	0.055	0.171	0.054		
3034500	0.193	0.030	0.229	0.010	0.289	0.001
3051000					-0.169	0.057
3109500	0.219	0.014			0.205	0.022
3118500			0.170	0.057		
3167000			-0.230	0.010		
3175500	0.172	0.053				
3183500	-0.259	0.004	-0.245	0.006	-0.288	0.001
3186500	0.195	0.028	0.281	0.002	0.199	0.025
3193000	0.223	0.012	0.151	0.090	0.154	0.083

Table E.2, continued

Station Number	3-Month Lead		6-Month Lead		9-Month Lead	
	tau	p-value	tau	p-value	tau	p-value
3198500	-0.337	0.000	-0.320	0.000	-0.297	0.001
3219500	-0.248	0.006	-0.189	0.035	-0.153	0.088
3230500	0.458	0.000	0.415	0.000	0.366	0.000
3262000	0.171	0.056			0.154	0.085
3265000	0.350	0.000	0.317	0.000	0.308	0.001
3266000	0.254	0.005	0.229	0.011	0.402	0.000
3269500	0.292	0.001	0.156	0.083	0.215	0.016
3274000	0.151	0.092			0.159	0.076
3275000	0.310	0.000	0.237	0.008	0.270	0.002
3281500			-0.194	0.030		
3294500			-0.213	0.018	-0.170	0.059
3301500	-0.451	0.000	-0.398	0.000	-0.392	0.000
3326500	0.193	0.030	0.207	0.020	0.221	0.013
3335500	0.192	0.031	0.185	0.038	0.197	0.026
3339500	0.376	0.000	0.306	0.001	0.361	0.000
3345500			0.150	0.092		
3360500	0.185	0.037	0.166	0.063	0.154	0.083
3363500	0.388	0.000	0.354	0.000	0.359	0.000
3373500	0.271	0.002	0.214	0.016	0.224	0.012
3374000	0.162	0.068	0.196	0.027	0.197	0.027
3379500			0.162	0.068	0.162	0.069
3381500					0.164	0.064
3434500	0.273	0.002	0.250	0.005	0.221	0.013
3438000			0.157	0.081		
3451500	-0.236	0.008	-0.302	0.001	-0.228	0.010
3465500			-0.147	0.097		
3473000			-0.209	0.019		
3479000	-0.181	0.042	-0.190	0.032		
3504000	-0.258	0.004	-0.227	0.011	-0.159	0.073
3528000	-0.218	0.014	-0.223	0.012		
3540500	0.168	0.059			0.155	0.082
3574500	-0.256	0.004	-0.276	0.002	-0.235	0.008
3604000	0.304	0.001	0.298	0.001	0.245	0.006
3612000	-0.153	0.089	-0.158	0.079		
4056500	-0.222	0.012	-0.184	0.039	-0.214	0.016
4079000	-0.265	0.003	-0.333	0.000	-0.338	0.000
4100500			0.147	0.097	0.156	0.079
4121500			-0.147	0.097		
4198000	-0.353	0.000	-0.228	0.010	-0.250	0.005
4214500	0.188	0.035				
4262500			0.186	0.036	0.169	0.057
4269000			0.173	0.051		
4275000			0.186	0.036	0.192	0.031
5053000	0.276	0.002	0.289	0.001	0.215	0.016

Table E.2, continued

Station Number	3-Month Lead		6-Month Lead		9-Month Lead	
	tau	p-value	tau	p-value	tau	p-value
5062000	0.211	0.018	0.262	0.003	0.271	0.002
5062500			0.177	0.047		
5078000	-0.155	0.082			-0.192	0.031
5082500			0.179	0.044		
5100000	0.150	0.092				
5112000	0.194	0.029	0.188	0.034		
5131500	-0.226	0.011	-0.300	0.001	-0.276	0.002
5133500	-0.288	0.001	-0.259	0.004	-0.236	0.008
5280000	0.233	0.009	0.276	0.002	0.181	0.042
5293000	0.157	0.077	0.147	0.097		
5313500	0.199	0.025	0.187	0.035		
5316500			0.175	0.049		
5317000	0.269	0.002	0.293	0.001	0.218	0.014
5330000	0.227	0.011	0.257	0.004	0.194	0.029
5331000	0.177	0.047	0.209	0.019		
5394500					-0.171	0.054
5399500	-0.218	0.014	-0.288	0.001	-0.256	0.004
5407000	-0.300	0.001	-0.247	0.006	-0.261	0.004
5419000					-0.159	0.074
5422000			0.240	0.007		
5426000			0.197	0.026	0.159	0.074
5430500			0.219	0.015	0.154	0.085
5435500	0.263	0.003	0.192	0.031	0.175	0.049
5436500	0.213	0.017			0.166	0.064
5440000			0.150	0.092		
5446500			0.228	0.010		
5451500			-0.158	0.076		
5455500	-0.160	0.071			-0.161	0.070
5459500	0.180	0.043	0.186	0.036	0.223	0.012
5464500			0.187	0.035		
5465500	0.181	0.042	0.222	0.012		
5470000	-0.209	0.019	-0.229	0.010		
5476000			0.188	0.034	0.153	0.086
5479000	0.244	0.006	0.224	0.012	0.264	0.003
5482500	0.360	0.000	0.348	0.000	0.308	0.001
5484000	0.208	0.020	0.224	0.012	0.204	0.022
5484500	0.262	0.003	0.259	0.004	0.151	0.090
5486490			-0.147	0.099		
5490500	0.234	0.009	0.207	0.020	0.233	0.009
5495000					0.150	0.091
5501000	-0.155	0.081				
5555300			0.173	0.051	0.182	0.041
5556500			0.186	0.036		
5572000	-0.167	0.060	-0.190	0.033		

Table E.2, continued

Station Number	3-Month Lead		6-Month Lead		9-Month Lead	
	tau	p-value	tau	p-value	tau	p-value
5593000	0.362	0.000	0.231	0.009	0.206	0.021
5597000	0.226	0.011			0.195	0.028
6019500	-0.301	0.001	-0.220	0.013		
6207500					-0.169	0.057
6214500					-0.160	0.072
6289000	-0.352	0.000	-0.372	0.000	-0.353	0.000
6441500	0.163	0.067				
6452000			0.155	0.082		
6478500	0.299	0.001	0.309	0.000	0.339	0.000
6485500	0.270	0.002	0.273	0.002	0.334	0.000
6606600					-0.171	0.054
6620000	-0.168	0.059	-0.235	0.008	-0.254	0.004
6630000	-0.220	0.013	-0.200	0.024	-0.162	0.068
6635000	-0.410	0.000	-0.445	0.000	-0.407	0.000
6800500	0.197	0.026	0.158	0.075	0.180	0.043
6809500	0.237	0.008	0.209	0.019		
6864500					-0.185	0.038
6869500	0.320	0.000	0.225	0.011	0.148	0.096
6889500	-0.187	0.035	-0.173	0.052		
6899500	-0.148	0.096	-0.203	0.022	-0.209	0.019
6933500	-0.193	0.030	-0.193	0.030		
7018500					0.148	0.096
7067000	-0.241	0.007	-0.247	0.005	-0.241	0.007
7069500	-0.244	0.006	-0.231	0.009	-0.198	0.026
7072000	-0.354	0.000	-0.385	0.000	-0.366	0.000
7096000					-0.159	0.074
7146500					0.157	0.078
7172000	0.171	0.054	0.163	0.067	0.184	0.039
7176000	0.280	0.002	0.212	0.017	0.173	0.051
7180500	-0.345	0.000	-0.351	0.000	-0.272	0.002
7187000	0.345	0.000	0.288	0.001	0.225	0.011
7196500	0.201	0.024	0.267	0.003	0.224	0.012
7203000	-0.215	0.017	-0.170	0.060	-0.255	0.005
7234000					-0.163	0.066
7252000			0.155	0.081		
7291000	-0.210	0.018			-0.177	0.047
7332500	-0.317	0.000	-0.256	0.004	-0.211	0.017
7340500	-0.170	0.057	-0.253	0.004	-0.287	0.001
7375500	-0.238	0.007	-0.186	0.036	-0.289	0.001
8032000	0.349	0.000	0.322	0.000	0.254	0.004
8033500	0.258	0.004	0.307	0.001	0.341	0.000
8041000	0.444	0.000	0.368	0.000	0.338	0.000
8041500	0.187	0.035	0.294	0.001	0.276	0.002
8070000	0.398	0.000	0.380	0.000	0.349	0.000

Table E.2, continued

Station Number	3-Month Lead		6-Month Lead		9-Month Lead	
	tau	p-value	tau	p-value	tau	p-value
8080500					-0.173	0.051
8088000					-0.182	0.041
8095000	0.200	0.024	0.210	0.018		
8128000	0.280	0.002	0.167	0.060		
8151500	-0.207	0.020	-0.158	0.075		
8153500	-0.197	0.027	-0.193	0.030	-0.155	0.082
8167000	-0.238	0.007	-0.326	0.000	-0.336	0.000
8167500	-0.341	0.000	-0.294	0.001	-0.228	0.010
8172000	0.159	0.073	0.171	0.055		
8189500	-0.176	0.047	-0.245	0.006	-0.265	0.003
8192000	-0.203	0.022				
8195000	-0.252	0.005	-0.330	0.000	-0.393	0.000
8205500	0.162	0.069				
8210000	-0.234	0.008	-0.200	0.024	-0.228	0.010
8276500	-0.252	0.005	-0.212	0.017		
9110000	0.151	0.090				
9119000	-0.204	0.022	-0.190	0.033		
9132500	-0.186	0.037	-0.234	0.008		
9147500			-0.173	0.052	-0.158	0.076
9239500	-0.153	0.086	-0.175	0.049		
9251000	-0.151	0.090				
9310500	-0.336	0.000	-0.342	0.000	-0.259	0.004
9379500					-0.152	0.087
9415000	-0.358	0.000	-0.331	0.000	-0.399	0.000
9430500	-0.258	0.004	-0.369	0.000	-0.297	0.001
9448500	-0.280	0.002	-0.332	0.000	-0.375	0.000
9508500	-0.386	0.000	-0.427	0.000	-0.456	0.000
10131000	-0.227	0.011	-0.184	0.038		
10174500	-0.374	0.000	-0.427	0.000	-0.323	0.000
10234500					0.157	0.077
10296000	0.356	0.000	0.368	0.000	0.320	0.000
10310000	0.350	0.000	0.311	0.000	0.259	0.004
10312000	0.147	0.099				
10322500	-0.225	0.011	-0.196	0.027		
10329500	-0.405	0.000	-0.391	0.000	-0.353	0.000
10396000	-0.221	0.013	-0.166	0.063	-0.236	0.008
11098000	-0.350	0.000	-0.328	0.000	-0.295	0.001
11152000	0.200	0.024	0.186	0.036	0.205	0.021
11160500	0.351	0.000	0.336	0.000	0.320	0.000
11237500	0.301	0.001	0.292	0.001	0.274	0.002
11264500	0.226	0.011	0.229	0.010	0.202	0.023
11266500	0.293	0.001	0.282	0.001	0.263	0.003
11381500	-0.164	0.064				
11425500	0.171	0.055	0.155	0.082	0.235	0.008

Table E.2, continued

Station Number	3-Month Lead		6-Month Lead		9-Month Lead	
	tau	p-value	tau	p-value	tau	p-value
11522500	-0.264	0.003	-0.210	0.018		
11525500	0.538	0.000	0.467	0.000	0.431	0.000
11532500	-0.203	0.022				
12010000	0.352	0.000	0.246	0.006	0.170	0.056
12020000	0.236	0.008				
12027500			-0.156	0.079	-0.214	0.016
12035000	0.280	0.002	0.206	0.021		
12039500	0.351	0.000	0.365	0.000	0.386	0.000
12048000	0.377	0.000	0.336	0.000	0.356	0.000
12054000	0.375	0.000	0.370	0.000	0.360	0.000
12056500	0.433	0.000	0.395	0.000	0.396	0.000
12134500	0.186	0.036				
12186000	0.270	0.002	0.218	0.014		
12322000	0.226	0.011				
12330000	-0.193	0.030	-0.221	0.013	-0.220	0.013
12354500					-0.148	0.096
12355500					-0.179	0.044
12358500	-0.192	0.031	-0.278	0.002	-0.332	0.000
12370000			-0.189	0.034	-0.216	0.015
12409000	0.430	0.000	0.369	0.000	0.296	0.001
12413000	0.361	0.000	0.284	0.001	0.227	0.011
12414500					-0.146	0.100
12488500	-0.294	0.001	-0.238	0.007	-0.177	0.046
13073000	-0.362	0.000	-0.468	0.000	-0.391	0.000
13082500	-0.252	0.005	-0.341	0.000	-0.289	0.001
13120500	-0.282	0.001	-0.275	0.002	-0.297	0.001
13185000	0.180	0.043				
13269000	-0.158	0.076	-0.187	0.035		
13302500					-0.227	0.011
13317000					-0.150	0.091
13336500					-0.172	0.053
14113000	-0.214	0.016	-0.171	0.055	-0.155	0.081
14137000	-0.368	0.000	-0.282	0.001	-0.336	0.000
14178000	0.219	0.014	0.185	0.038	0.157	0.078
14185000					0.162	0.069
14301000	-0.282	0.002	-0.292	0.001	-0.234	0.008
14306500	-0.223	0.012				
14325000	-0.207	0.020				
14359000	-0.261	0.003	-0.179	0.044		
14362000	-0.205	0.021				

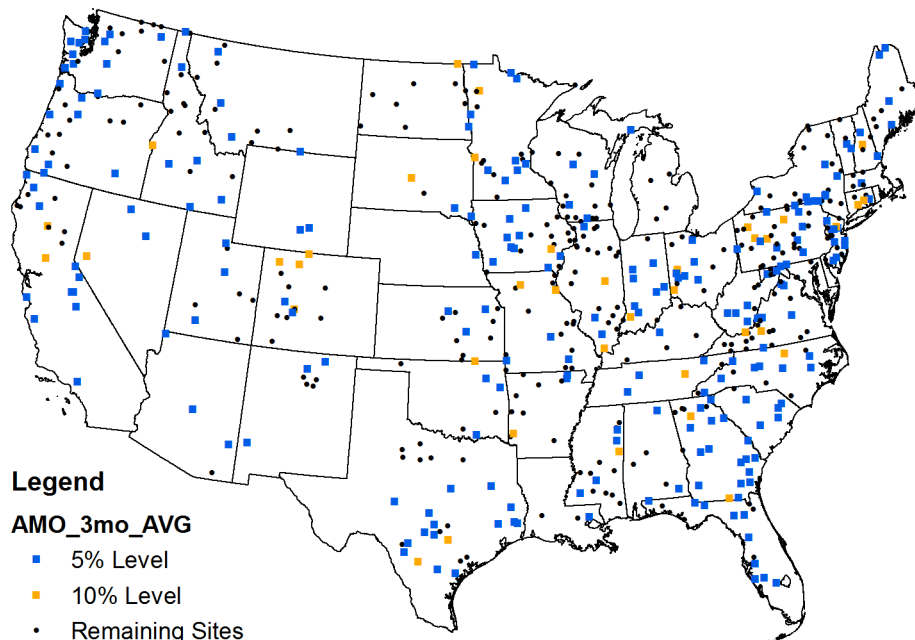


Figure E.1 Locations of sites with significant Kendall's tau correlation between 10-year moving average of log-transformed flood flows and 3-month average **AMO** anomalies with **3-month** lead.

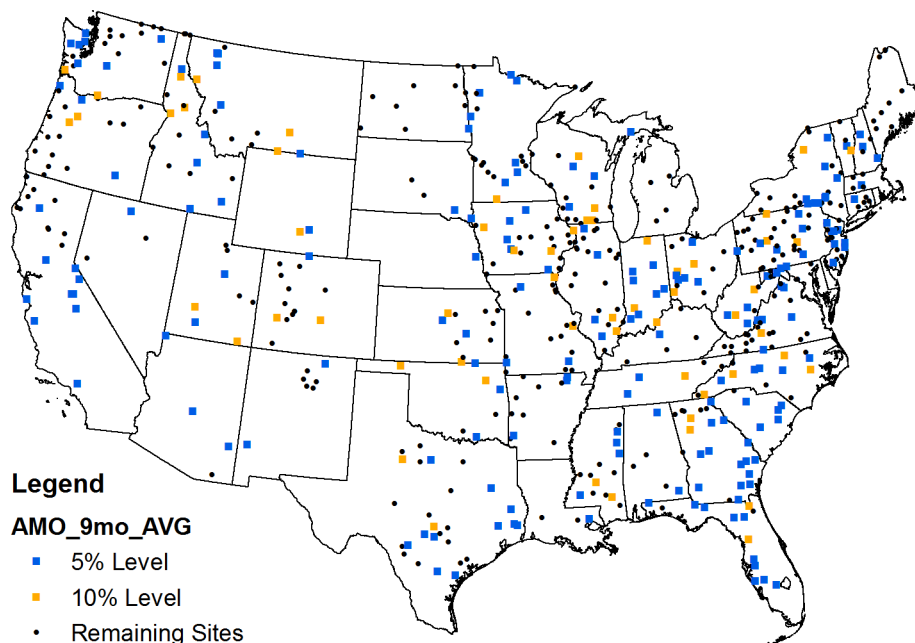


Figure E.2 Locations of sites with significant Kendall's tau correlation between 10-year moving average of log-transformed flood flows and 3-month average **AMO** anomalies with **9-month** lead.

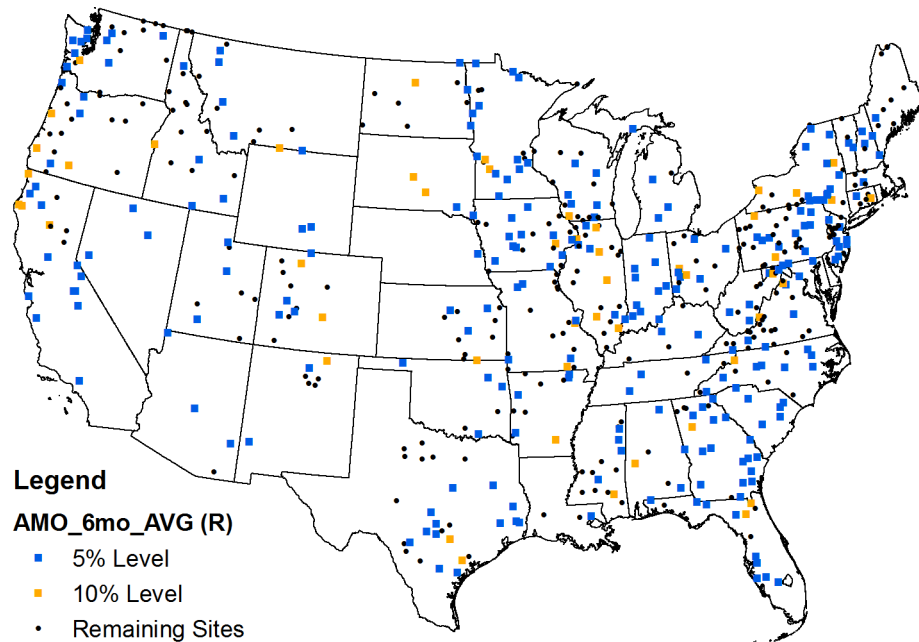


Figure E.1 Locations of sites with significant Pearson's r correlation between 10-year moving average of log-transformed flood flows and 3-month average AMO anomalies with **6-month** lead.

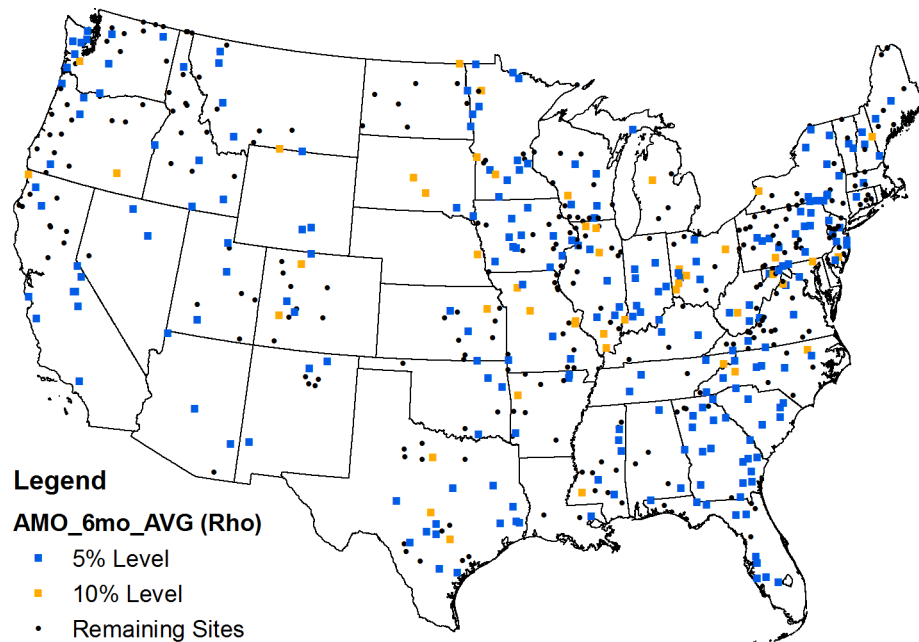


Figure E.2 Locations of sites with significant Spearman's ρ correlation between 10-year moving average of log-transformed flood flows and 3-month average AMO anomalies with **6-month** lead.

E.2 MEI Correlation Results

Table E.3

Results of Kendall's tau analyses (significant 10% level) between 10-year moving average of log-transformed flood flows and 3-month average MEI anomalies with 3-, 6-, and 9-month leads.

Station Number	3-Month Lead		6-Month Lead		9-Month Lead	
	tau	p-value	tau	p-value	tau	p-value
1011000					0.189	0.034
1014000					0.180	0.043
1038000	0.154	0.084	0.157	0.077	0.201	0.024
1047000					0.181	0.042
1055000					0.160	0.072
1057000					0.158	0.075
1064500	0.148	0.096	0.176	0.047	0.275	0.002
1073000					0.150	0.094
1078000					0.172	0.055
1127500					0.165	0.066
1169000					0.175	0.051
1196500			0.179	0.045	0.262	0.003
1350000					0.154	0.083
1365000					0.158	0.075
1381500			0.173	0.052	0.248	0.005
1396500					0.168	0.059
1397500					0.188	0.034
1398500					0.167	0.061
1410000					0.159	0.074
1411000					0.183	0.039
1420500			0.201	0.024	0.229	0.010
1426500					-0.147	0.097
1445500			0.158	0.075	0.147	0.097
1459500			-0.174	0.050	-0.160	0.072
1518000					-0.222	0.012
1520500					-0.238	0.007
1531000					-0.157	0.078
1560000			0.153	0.086	0.155	0.081
1601500					0.183	0.040
1604500					-0.224	0.012
1608500	0.169	0.057	0.169	0.057	0.176	0.048
1614500					0.195	0.028
1634000					0.157	0.078
1634500	0.155	0.082	0.195	0.028	0.259	0.003
1667500	0.221	0.013				
2016000					0.176	0.048
2018000			0.160	0.071	0.253	0.004
2045500	0.177	0.046	0.202	0.023	0.253	0.004

Table E.3, continued

Station Number	3-Month Lead		6-Month Lead		9-Month Lead	
	tau	p-value	tau	p-value	tau	p-value
2051500	0.159	0.074	0.181	0.041	0.249	0.005
2055000	0.175	0.049	0.193	0.030	0.238	0.007
2059500	0.267	0.003				
2061500					0.220	0.013
2074500	0.245	0.006	0.159	0.074	0.167	0.061
2083000					0.250	0.005
2118000			0.151	0.090	0.167	0.060
2126000					0.157	0.078
2138500			0.206	0.021		
2213500	0.186	0.036	0.204	0.022	0.237	0.008
2225500	0.159	0.073			0.173	0.051
2228000	0.149	0.093				
2231000	-0.258	0.004	-0.159	0.074	-0.169	0.057
2246000			-0.147	0.097		
2256500	-0.233	0.009	-0.149	0.095	-0.149	0.093
2296750	-0.259	0.003	-0.161	0.070	-0.150	0.091
2298830	-0.193	0.030	-0.154	0.083		
2301500	-0.209	0.019				
2303000	-0.157	0.078				
2313000	-0.220	0.013				
2317500	0.215	0.016	0.233	0.009	0.285	0.001
2320500	0.171	0.055	0.148	0.096	0.215	0.015
2321500	-0.172	0.053				
2329000	0.210	0.018	0.183	0.039	0.236	0.008
2333500			-0.156	0.079		
2339500					-0.226	0.011
2353500					0.160	0.072
2369000					0.170	0.056
2383500					-0.232	0.009
2387500					-0.206	0.020
2467000			0.188	0.035	0.162	0.069
2472500	0.172	0.053	0.207	0.020	0.244	0.006
2479000	0.180	0.043	0.233	0.009	0.275	0.002
2486000			0.174	0.050	0.162	0.069
2487500					0.159	0.074
2488500	0.173	0.052	0.226	0.011	0.304	0.001
3010500	-0.150	0.091	-0.155	0.082	-0.264	0.003
3011020	-0.160	0.071	-0.169	0.057	-0.249	0.005
3024000					-0.227	0.011
3049500					-0.237	0.008
3079000			-0.154	0.084	-0.246	0.006
3080000	-0.151	0.089	-0.165	0.063	-0.332	0.000
3102500			-0.168	0.058		
3106000					-0.167	0.061

Table E.3, continued

Station Number	3-Month Lead		6-Month Lead		9-Month Lead	
	tau	p-value	tau	p-value	tau	p-value
3118500	0.203	0.022	0.237	0.008	0.233	0.009
3144000	0.226	0.012	0.279	0.002	0.277	0.002
3164000			0.216	0.015	0.163	0.067
3167000					-0.206	0.020
3170000	0.156	0.079				
3182500					0.178	0.045
3186500					0.167	0.061
3234500					-0.247	0.006
3253500					-0.182	0.043
3262000			0.174	0.053		
3269500					-0.195	0.029
3294500					-0.192	0.032
3307000	0.161	0.073	0.216	0.016	0.244	0.007
3326500			0.197	0.027		
3379500					0.193	0.030
3380500	0.158	0.075	0.173	0.052	0.221	0.013
3381500			0.147	0.097	0.215	0.015
3434500			0.147	0.099	0.169	0.057
3438000			0.165	0.065	0.196	0.028
3479000					0.198	0.026
3524000					-0.164	0.064
3604000					0.163	0.066
4100500					0.154	0.084
4193500			0.158	0.076	0.167	0.060
4223000					-0.176	0.047
4262500					0.203	0.022
4264331			0.162	0.068	0.219	0.014
4275000					0.219	0.014
4293500					0.211	0.019
5084000	-0.147	0.099	-0.155	0.082	-0.267	0.003
5131500					-0.238	0.007
5286000					-0.151	0.089
5288500	-0.156	0.079	-0.155	0.082	-0.185	0.037
5304500					0.231	0.009
5316500			0.173	0.052	0.259	0.003
5340500					-0.172	0.053
5379500			-0.153	0.086		
5399500					-0.171	0.055
5408000			-0.164	0.065	-0.230	0.010
5410490	-0.162	0.069	-0.184	0.038	-0.253	0.004
5412500	-0.166	0.062	-0.164	0.065	-0.232	0.009
5414000					-0.179	0.044
5418500					-0.201	0.024
5432500	-0.155	0.082	-0.175	0.049	-0.257	0.004

Table E.3, continued

Station Number	3-Month Lead		6-Month Lead		9-Month Lead	
	tau	p-value	tau	p-value	tau	p-value
5434500	-0.163	0.067	-0.194	0.029	-0.272	0.002
5435500	-0.186	0.036	-0.186	0.036	-0.214	0.016
5436500	-0.160	0.075	-0.168	0.061	-0.234	0.009
5447500					0.162	0.068
5495000			0.160	0.071	0.202	0.023
5501000	0.155	0.081	0.180	0.043	0.211	0.017
5520500			0.150	0.092	0.219	0.014
5526000			0.158	0.075	0.237	0.008
5527500	0.159	0.073	0.201	0.024	0.302	0.001
5555300			0.179	0.045	0.252	0.005
5572000			0.159	0.073	0.195	0.028
5585000			0.153	0.086	0.184	0.038
6214500					-0.149	0.093
6335500	-0.165	0.063	-0.181	0.042	-0.272	0.002
6337000	-0.157	0.077	-0.171	0.055	-0.280	0.002
6340500					-0.235	0.008
6441500	-0.163	0.067	-0.182	0.041	-0.209	0.019
6864500	-0.153	0.086				
6889500					0.157	0.077
6908000					0.172	0.053
6933500					0.154	0.084
7016500			0.159	0.074	0.250	0.005
7019000					0.210	0.018
7067000	0.164	0.065	0.160	0.071		
7069500					-0.153	0.086
7072000	0.155	0.082				
7186000					0.156	0.079
7189000					0.174	0.055
7234000					-0.155	0.082
7247500					-0.217	0.015
7291000	0.224	0.012	0.233	0.009	0.303	0.001
7332500					0.149	0.093
7340000					-0.179	0.045
7340500					-0.205	0.021
7375500			0.149	0.093	0.234	0.008
7378500	0.157	0.077	0.186	0.036	0.307	0.001
8013500			0.183	0.040	0.241	0.007
8033500			0.148	0.096	0.211	0.017
8041500	0.147	0.099	0.164	0.065	0.258	0.004
8080500					-0.173	0.052
8082000					-0.199	0.025
8082500					-0.182	0.041
8088000					-0.156	0.079
8151500	0.160	0.071	0.164	0.065	0.186	0.036

Table E.3, continued

Station Number	3-Month Lead		6-Month Lead		9-Month Lead	
	tau	p-value	tau	p-value	tau	p-value
8153500	0.245	0.006	0.255	0.004	0.271	0.002
8158000	0.154	0.084	0.180	0.043	0.243	0.006
8167000	0.207	0.020	0.255	0.004	0.192	0.032
8167500	0.203	0.022	0.207	0.020	0.223	0.012
8171000	0.219	0.014	0.234	0.008	0.175	0.049
8195000	0.223	0.012	0.188	0.035		
8210000	-0.188	0.035				
8291000	0.264	0.003				
8378500			0.171	0.056	0.247	0.006
9110000			-0.165	0.063	-0.169	0.057
9180500					-0.155	0.082
9379500					-0.173	0.052
9430500	0.205	0.021				
9471000	-0.147	0.099				
11381500			-0.214	0.016		
11383500			-0.174	0.050		
11402000			-0.198	0.026		
11477000	-0.199	0.025	-0.272	0.002		
11478500	-0.179	0.045	-0.184	0.038		
11501000			-0.171	0.055	-0.188	0.035
11522500	-0.163	0.067	-0.189	0.033		
11530000	-0.175	0.049	-0.269	0.002		
11532500	-0.221	0.013	-0.218	0.014		
12035000			0.207	0.020		
12048000			0.152	0.087		
12134500	0.180	0.043	0.180	0.043		
12189500	0.159	0.073	0.158	0.076		
12306500	-0.179	0.045	-0.218	0.014	-0.284	0.001
12322000	-0.163	0.067	-0.193	0.030	-0.261	0.003
12332000			-0.151	0.089	-0.188	0.035
12354500			-0.163	0.067	-0.242	0.006
12355500			-0.167	0.061	-0.216	0.015
12358500					-0.164	0.065
12370000					-0.188	0.035
12409000					-0.169	0.057
12413000			-0.149	0.095	-0.193	0.030
12414500					-0.175	0.049
12422500			-0.184	0.038	-0.286	0.001
12442500			-0.156	0.079	-0.228	0.010
12445000					-0.203	0.022
12451000	-0.179	0.045	-0.214	0.016	-0.209	0.019
12459000	-0.185	0.037	-0.209	0.019	-0.182	0.041
13037500	-0.159	0.074	-0.208	0.019	-0.190	0.033
13185000			-0.163	0.066	-0.210	0.018

Table E.3, continued

Station Number	3-Month Lead		6-Month Lead		9-Month Lead	
	tau	p-value	tau	p-value	tau	p-value
13302500			-0.148	0.096	-0.168	0.058
13313000			-0.197	0.027	-0.271	0.002
13317000			-0.169	0.057	-0.246	0.006
13336500			-0.151	0.090	-0.239	0.007
13337000			-0.154	0.084	-0.233	0.009
13342500					-0.201	0.024
14044000					0.174	0.050
14105700					-0.168	0.058
14113000			-0.185	0.037		
14154500	-0.149	0.093	-0.220	0.013		
14178000	-0.190	0.033	-0.152	0.087		
14185000			-0.174	0.050		
14191000	-0.199	0.025	-0.327	0.000		
14301000	-0.175	0.049	-0.175	0.049		
14306500	-0.220	0.013	-0.250	0.005		
14308000	-0.180	0.043	-0.249	0.005		
14321000	-0.168	0.058	-0.264	0.003		
14325000	-0.224	0.012	-0.240	0.007		
14359000	-0.193	0.030	-0.253	0.004		
14362000	-0.210	0.018	-0.258	0.004		

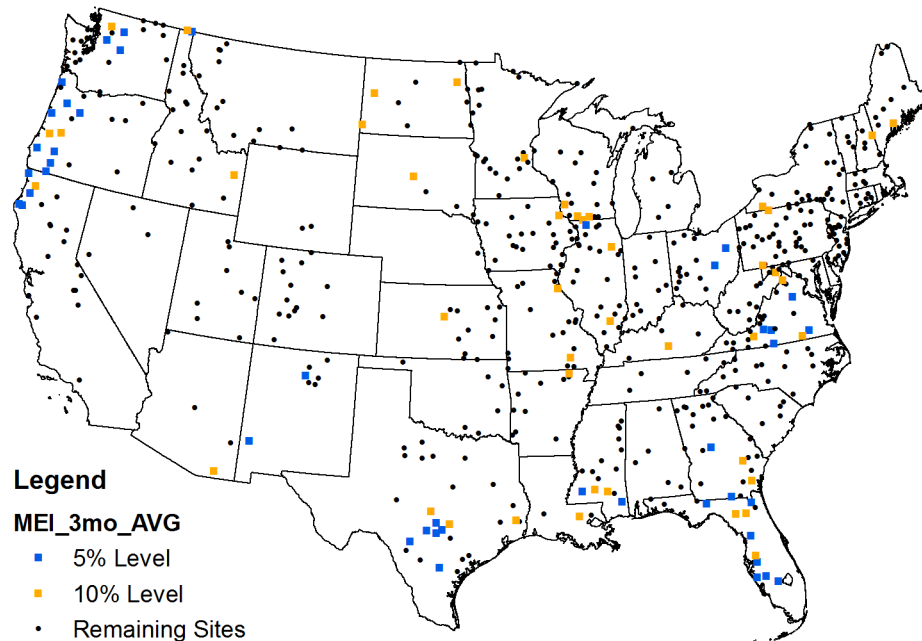


Figure E.3 Locations of sites with significant Kendall's tau correlation between 10-year moving average of log-transformed flood flows and 3-month average MEI anomalies with **3-month** lead.

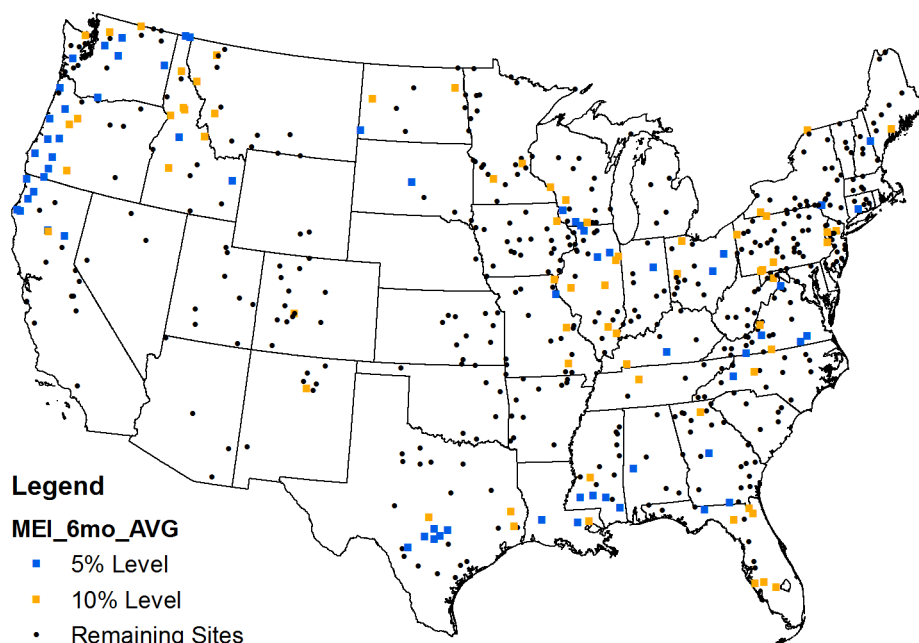


Figure E.4 Locations of sites with significant Kendall's tau correlation between 10-year moving average of log-transformed flood flows and 3-month average **MEI** anomalies with **6-month** lead.

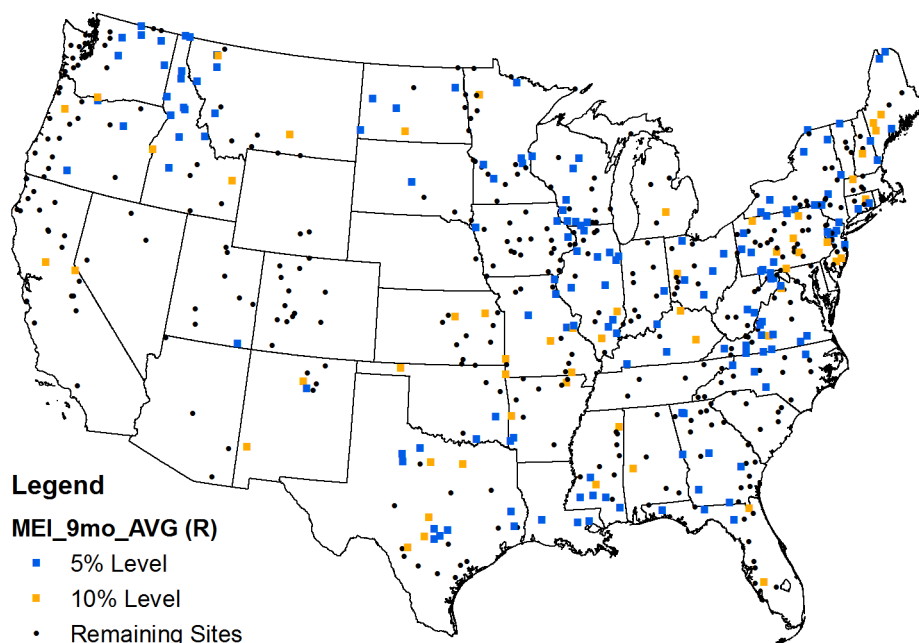


Figure E.5 Locations of sites with significant Pearson's r correlation between 10-year moving average of log-transformed flood flows and 3-month average **MEI** anomalies with **9-month** lead.

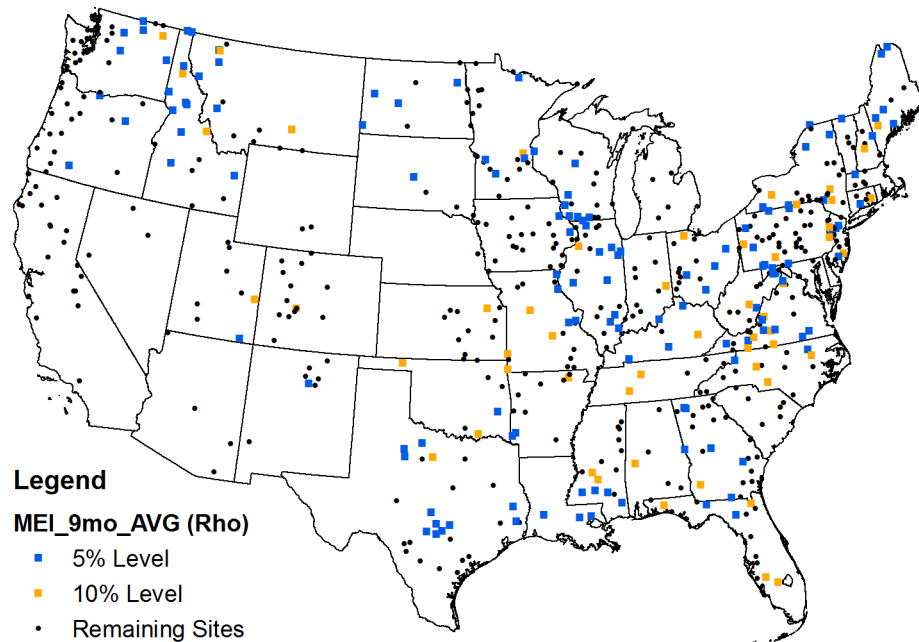


Figure E.6 Locations of sites with significant Spearman's rho correlation between 10-year moving average of log-transformed flood flows and 3-month average **MEI** anomalies with **9-month** lead.

E.3 NAO Correlation Results

Table E.4

Results of Kendall's tau analyses (significant 10% level) between 10-year moving average of log-transformed flood flows and 3-month average **NAO** anomalies with 3-, 6-, and 9-month leads.

Station Number	3-Month Lead		6-Month Lead		9-Month Lead	
	tau	p-value	tau	p-value	tau	p-value
1031500	0.228	0.010				
1038000	0.189	0.033				
1047000	0.246	0.006				
1055000	0.271	0.002				
1057000	0.323	0.000				
1064500	0.327	0.000				
1076500	0.154	0.085				
1078000	0.237	0.008				
1137500	0.185	0.039	-0.230	0.010		
1142500	0.152	0.090	-0.164	0.067	-0.189	0.035
1169000	0.275	0.002				
1181000	0.198	0.028				

Table E.4, continued

Station Number	3-Month Lead		6-Month Lead		9-Month Lead	
	tau	p-value	tau	p-value	tau	p-value
1321000					-0.160	0.072
1365000	0.184	0.039				
1379500			0.148	0.097		
1408500			0.149	0.095		
1411000	0.171	0.054				
1411500					0.190	0.033
1413500			-0.154	0.083		
1414500			-0.204	0.022		
1421000					-0.194	0.029
1426500			-0.153	0.085		
1532000					-0.182	0.041
1538000					-0.162	0.069
1541000			0.159	0.074		
1541500	0.154	0.083				
1548500					-0.178	0.046
1555500					-0.154	0.084
1567000	0.175	0.049				
1568000					-0.171	0.055
1574000			0.182	0.041		
1580000	-0.194	0.029				
1631000	0.146	0.100				
1667500			0.315	0.000		
2017500					-0.158	0.075
2018000	0.168	0.059				
2055000	0.211	0.018				
2059500			0.254	0.004		
2074500	0.154	0.084	0.287	0.001		
2102000	0.146	0.100				
2132000			0.193	0.030		
2198000			0.165	0.064		
2217500			0.180	0.043		
2231000			-0.288	0.001		
2256500			-0.315	0.000		
2296750			-0.360	0.000		
2298830			-0.222	0.012		
2301500			-0.231	0.009		
2303000			-0.252	0.005		
2313000			-0.213	0.016		
2321500					0.169	0.057
2331600					-0.230	0.010
2333500					-0.213	0.017
2337000			0.170	0.056		
2347500			0.150	0.091		
2358000			0.150	0.092		

Table E.4, continued

Station Number	3-Month Lead		6-Month Lead		9-Month Lead	
	tau	p-value	tau	p-value	tau	p-value
2369000			0.151	0.090		
2375500			0.162	0.069		
2398000					-0.186	0.036
2437000					-0.205	0.021
2441000					-0.179	0.044
2472500	0.162	0.068				
2475500					-0.215	0.016
2479000	0.154	0.083				
2487500					-0.216	0.015
2488500	0.177	0.047				
3020500					-0.182	0.041
3102500					-0.342	0.000
3170000	0.209	0.019				
3173000					-0.156	0.079
3234500	-0.247	0.006				
3253500					-0.258	0.004
3266000					-0.223	0.013
3275000			-0.159	0.074	-0.149	0.095
3301500			0.159	0.076		
3339500			-0.189	0.034		
3363500			-0.173	0.051		
3377500					-0.170	0.056
3379500	0.152	0.087				
3380500	0.146	0.100				
3381500	0.257	0.004				
3434500					-0.198	0.026
3488000					-0.215	0.016
3504000					-0.218	0.014
3528000					-0.290	0.001
3550000					-0.171	0.054
3604000					-0.218	0.014
4056500	0.172	0.053				
4073500	0.187	0.037				
4100500	0.202	0.023			-0.162	0.069
4112500			-0.174	0.050		
4191500					-0.175	0.051
4193500					-0.161	0.070
4264331	0.291	0.001				
4275000	0.215	0.015				
4287000	0.194	0.030				
4293500	0.165	0.066				
5062000			-0.178	0.045		
5082500	0.164	0.064				
5280000	0.151	0.090	-0.159	0.074	-0.151	0.089

Table E.4, continued

Station Number	3-Month Lead		6-Month Lead		9-Month Lead	
	tau	p-value	tau	p-value	tau	p-value
5304500	0.247	0.005				
5330000			-0.170	0.056		
5419000					-0.162	0.068
5420500	0.150	0.092				
5426000	0.202	0.023	-0.152	0.087		
5430500	0.170	0.059				
5446500					-0.149	0.095
5454500					-0.176	0.048
5459500			-0.149	0.095		
5465500					-0.172	0.053
5479000					-0.167	0.061
5484500	-0.162	0.068				
5495000	0.164	0.064				
5501000	0.321	0.000				
5520500	0.222	0.013				
5526000	0.188	0.035				
5527500	0.287	0.001				
5555300	0.176	0.048				
5570000	0.175	0.049				
5585000	0.178	0.046				
5593000	-0.214	0.016				
6019500	0.197	0.027			0.188	0.034
6354000	0.219	0.014				
6441500	-0.155	0.082				
6478500					-0.165	0.063
6485500					-0.163	0.066
6606600	-0.150	0.092				
6620000	-0.235	0.008				
6630000			0.228	0.010		
6809500	-0.192	0.031				
6864500	-0.258	0.004	-0.236	0.008		
6869500	-0.156	0.079				
6876900	-0.295	0.001				
6889500	0.389	0.000				
6897500	0.195	0.028				
6908000	0.227	0.011				
6933500	0.170	0.057				
7016500	0.225	0.011				
7018500	0.225	0.011				
7019000	0.204	0.022				
7056000					-0.158	0.075
7069500	0.241	0.007			-0.173	0.052
7096000	-0.251	0.005				
7146500	0.216	0.015				

Table E.4, continued

Station Number	3-Month Lead		6-Month Lead		9-Month Lead	
	tau	p-value	tau	p-value	tau	p-value
7176000	-0.170	0.056				
7183000	0.168	0.058				
7186000	0.354	0.000				
7187000	-0.174	0.051				
7203000			-0.229	0.011		
7218000	-0.258	0.004	-0.228	0.011		
7234000	-0.304	0.001				
7247500	-0.251	0.005				
7252000	0.199	0.025			-0.174	0.050
7261500	0.342	0.000				
7290000	0.190	0.032				
7331000	0.190	0.033				
7332500	0.181	0.042				
7340000	-0.196	0.028				
7340500	-0.151	0.089				
7363500	-0.172	0.053				
7375500			0.146	0.100		
8013500					0.212	0.017
8033500	0.251	0.005	-0.206	0.021		
8041500	0.249	0.005	-0.219	0.014		
8070000	-0.188	0.035				
8080500	-0.278	0.002				
8082000	-0.205	0.021	0.161	0.071		
8082500	-0.190	0.033				
8085500	-0.251	0.005				
8088000	-0.295	0.001				
8095000			-0.186	0.037		
8128000	-0.336	0.000				
8151500	0.151	0.089				
8153500					0.151	0.090
8164000	0.173	0.052	-0.155	0.082		
8167500	0.235	0.008			0.152	0.087
8190000					-0.205	0.022
8192000			-0.158	0.075	-0.272	0.002
8195000			0.165	0.063		
8205500	-0.200	0.024				
8210000			-0.256	0.004		
8276500	0.284	0.001				
8291000	0.190	0.035	0.226	0.012		
8378500	0.256	0.004	-0.168	0.061		
8380500	-0.228	0.011	-0.224	0.012		
9085000	-0.214	0.016	0.154	0.083		
9110000	-0.190	0.033				
9112500			0.155	0.081		

Table E.4, continued

Station Number	3-Month Lead		6-Month Lead		9-Month Lead	
	tau	p-value	tau	p-value	tau	p-value
9119000	0.155	0.082				
9124500			0.203	0.022		
9239500			0.200	0.024		
9251000	0.243	0.006				
9304500			0.178	0.046		
9315000	-0.216	0.015	0.174	0.051		
9361500			0.179	0.044		
9379500	-0.269	0.002				
9430500	0.201	0.024	0.251	0.005		
9471000			-0.215	0.016	0.176	0.047
10128500			0.236	0.011		
10131000	0.163	0.067				
10234500	0.242	0.006				
10296000					-0.189	0.034
11160500			-0.188	0.036		
11237500					-0.157	0.081
11477000			0.172	0.053	-0.260	0.003
11478500					-0.149	0.093
11501000					0.200	0.024
11522500					-0.379	0.000
11525500					-0.239	0.007
11530000			0.172	0.053	-0.314	0.000
11532500					-0.358	0.000
12010000					0.317	0.000
12020000			-0.156	0.079	0.319	0.000
12027500	0.168	0.059				
12035000					0.324	0.000
12056500					0.151	0.090
12134500					0.324	0.000
12186000					0.218	0.014
12189500					0.274	0.002
12306500	-0.235	0.008				
12322000	-0.331	0.000				
12332000	-0.312	0.000				
12354500	-0.241	0.007	0.171	0.055		
12355500	-0.215	0.015				
12358500	-0.179	0.045	0.156	0.079		
12370000	-0.261	0.003	0.164	0.065		
12404500			0.148	0.096		
12422500	-0.275	0.002	0.147	0.099		
12442500	-0.171	0.055	0.158	0.075		
13037500			0.163	0.066		
13073000					0.179	0.044
13139510			0.183	0.040		

Table E.4, continued

Station Number	3-Month Lead		6-Month Lead		9-Month Lead	
	tau	p-value	tau	p-value	tau	p-value
13185000	-0.152	0.087	0.148	0.097		
13302500	-0.308	0.001				
13313000	-0.278	0.002	0.191	0.032		
13317000	-0.243	0.006	0.173	0.052		
13336500	-0.263	0.003	0.171	0.054		
13337000	-0.259	0.004	0.182	0.041		
13342500	-0.289	0.001				
14044000	0.250	0.005				
14046500	0.280	0.002				
14105700	-0.369	0.000				
14137000	0.159	0.074	0.185	0.037		
14154500			0.164	0.065	-0.230	0.010
14185000					-0.178	0.046
14191000					-0.331	0.000
14301000	0.154	0.084			-0.157	0.077
14301500					-0.180	0.043
14306500					-0.377	0.000
14308000			0.149	0.093	-0.314	0.000
14321000					-0.354	0.000
14325000					-0.337	0.000
14359000					-0.429	0.000
14362000					-0.452	0.000

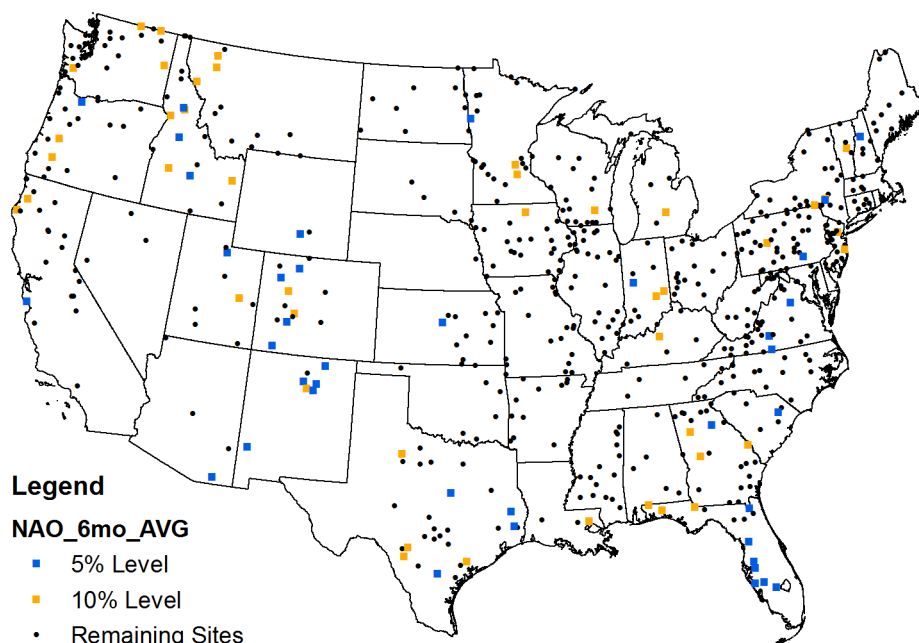


Figure E.7 Locations of sites with significant Kendall's tau correlation between 10-year moving average of log-transformed flood flows and 3-month average NAO anomalies with **6-month** lead.

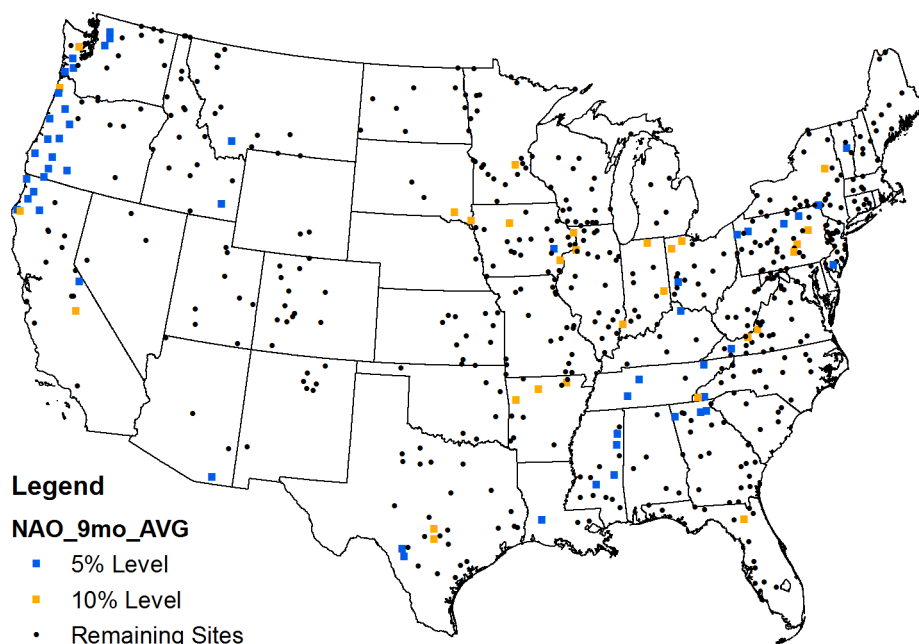


Figure E.8 Locations of sites with significant Kendall's tau correlation between 10-year moving average of log-transformed flood flows and 3-month average NAO anomalies with **9-month** lead.

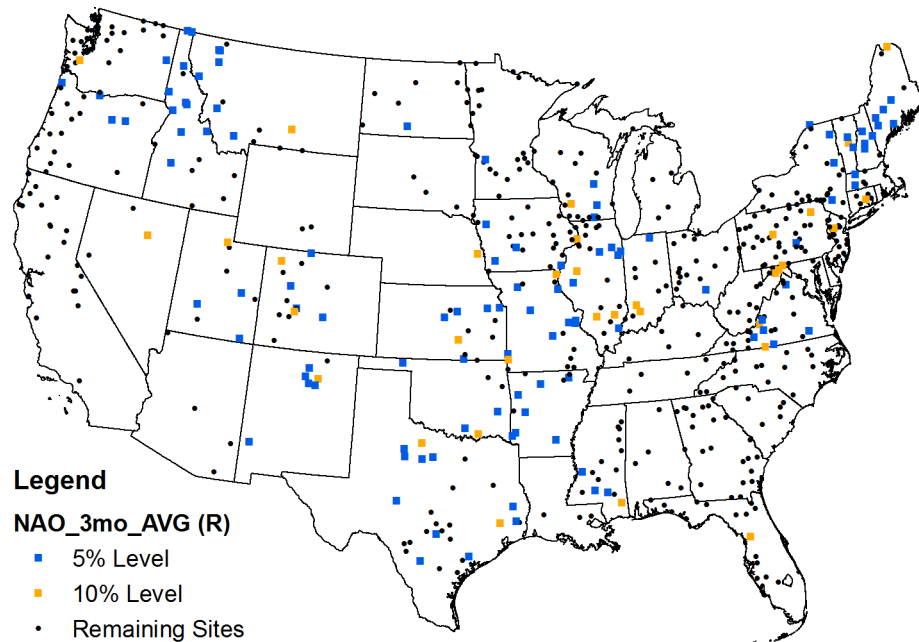


Figure E.9 Locations of sites with significant Pearson's r correlation between 10-year moving average of log-transformed flood flows and 3-month average NAO anomalies with **3-month** lead.

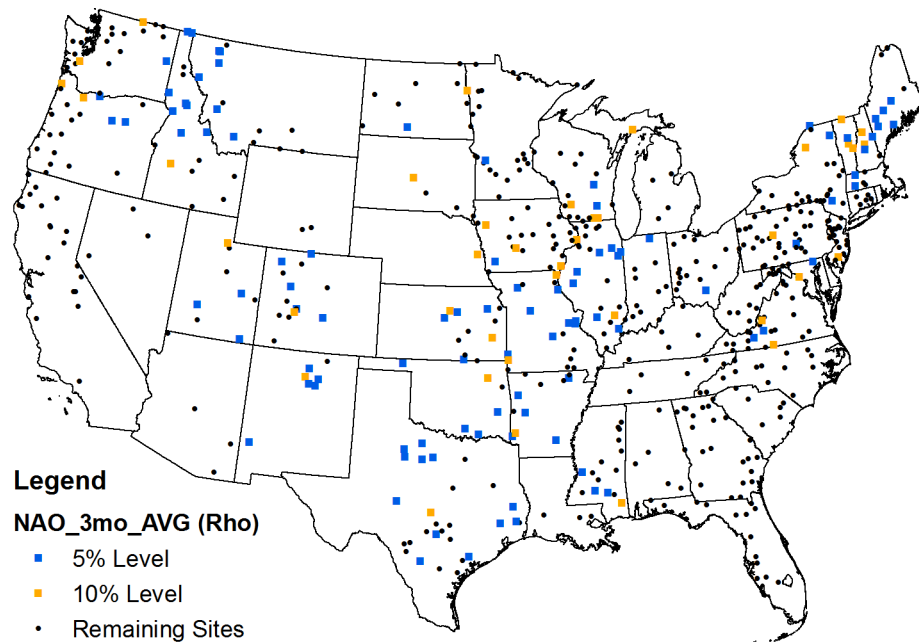


Figure E.10 Locations of sites with significant Spearman's ρ correlation between 10-year moving average of log-transformed flood flows and 3-month average NAO anomalies with **3-month** lead.

E.4 NINO 3.4 Correlation Results

Table E.5

Results of Kendall's tau analyses (significant at 10% level) between 10-year moving average of log-transformed flood flows and 3-month average **Nino3.4** anomalies with 3-, 6-, and 9-month leads.

Station Number	3-Month Lead		6-Month Lead		9-Month Lead	
	tau	p-value	tau	p-value	tau	p-value
1064500					0.154	0.083
1459500					-0.164	0.065
1520500					-0.149	0.093
2083000					0.148	0.096
2083500					0.175	0.049
2231000	-0.152	0.089				
2317500					0.170	0.056
3010500					-0.149	0.093
3080000					-0.218	0.014
3118500	0.150	0.091				
3144000			0.209	0.020	0.194	0.031
3326500			0.155	0.081		
3360500			0.161	0.070		
3373500			0.154	0.083		
3374000			0.150	0.092		
4112500			-0.153	0.086	-0.168	0.059
5084000					-0.206	0.020
5131500					-0.163	0.067
5288500					-0.151	0.090
5418500					-0.174	0.050
5419000			-0.151	0.090		
5432500			-0.155	0.081		
5434500			-0.161	0.070	-0.148	0.096
5435500			-0.149	0.095		
6214500					-0.179	0.044
6335500					-0.167	0.060
6337000					-0.174	0.050
6340500					-0.169	0.058
6354000					-0.152	0.089
6876900					-0.159	0.074
7050500	0.153	0.086				
7291000					0.155	0.082
7378500					0.161	0.071
8013500					0.215	0.015
8033500					0.161	0.070
8095000					0.155	0.081
8151500			0.148	0.096		
8153500			0.176	0.047		

Table E.5, continued

Station Number	3-Month Lead		6-Month Lead		9-Month Lead	
	tau	p-value	tau	p-value	tau	p-value
8158000			0.180	0.043	0.150	0.092
8167000	0.162	0.068	0.156	0.079		
8167500			0.157	0.077		
8171000	0.181	0.042	0.216	0.015	0.241	0.007
9239500					-0.149	0.095
9304500					-0.153	0.085
9310500					-0.153	0.085
9379500					-0.146	0.100
10131000					-0.212	0.017
11532500	-0.159	0.074				
12306500			-0.153	0.086		
12332000					-0.163	0.066
12404500					-0.150	0.092
12414500					-0.165	0.063
12442500					-0.168	0.059
12451000			-0.159	0.073		
12459000			-0.162	0.069	-0.176	0.048
12488500					-0.169	0.057
13037500			-0.175	0.049	-0.233	0.009
13269000					-0.198	0.026
13302500					-0.155	0.081
13317000					-0.151	0.090
14113000			-0.176	0.048		
14178000	-0.170	0.056	-0.214	0.016		
14191000			-0.195	0.028		
14301000			-0.151	0.090		

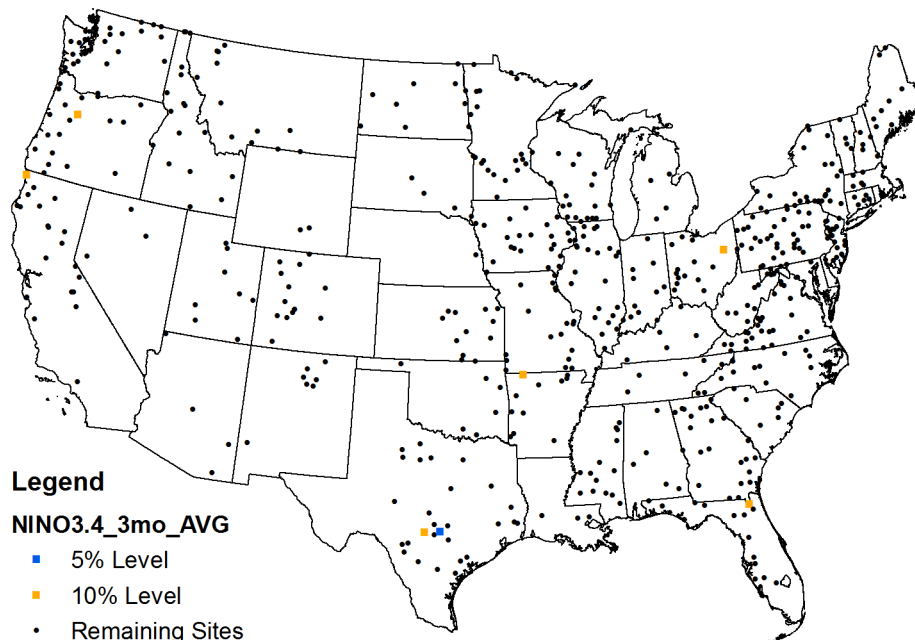


Figure E.11 Locations of sites with significant Kendall's tau correlation between 10-year moving average of log-transformed flood flows and 3-month average **Nino3.4** anomalies with **3-month** lead.

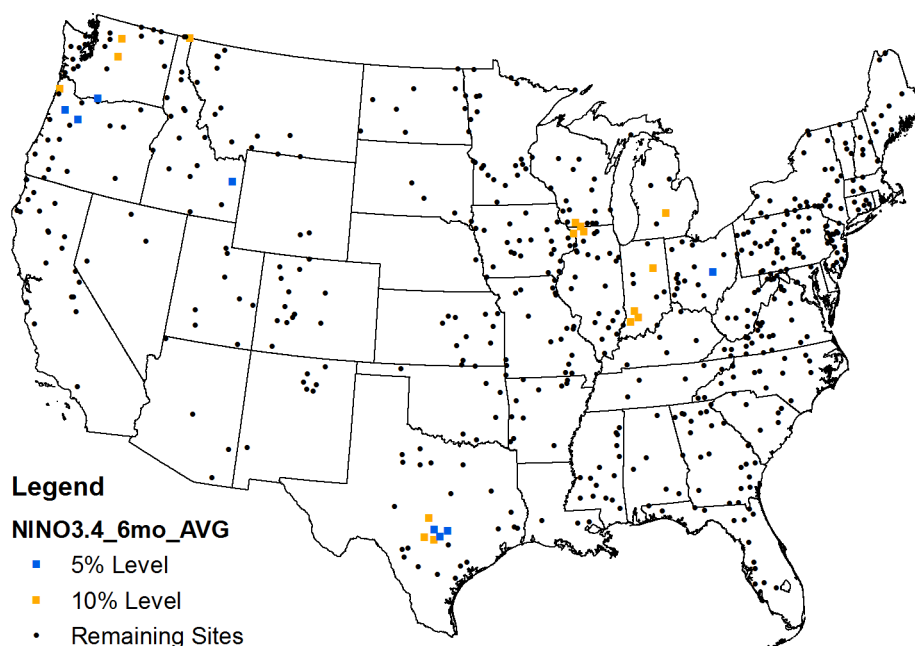


Figure E.12 Locations of sites with significant Kendall's tau correlation between 10-year moving average of log-transformed flood flows and 3-month average **Nino3.4** anomalies with **6-month** lead.

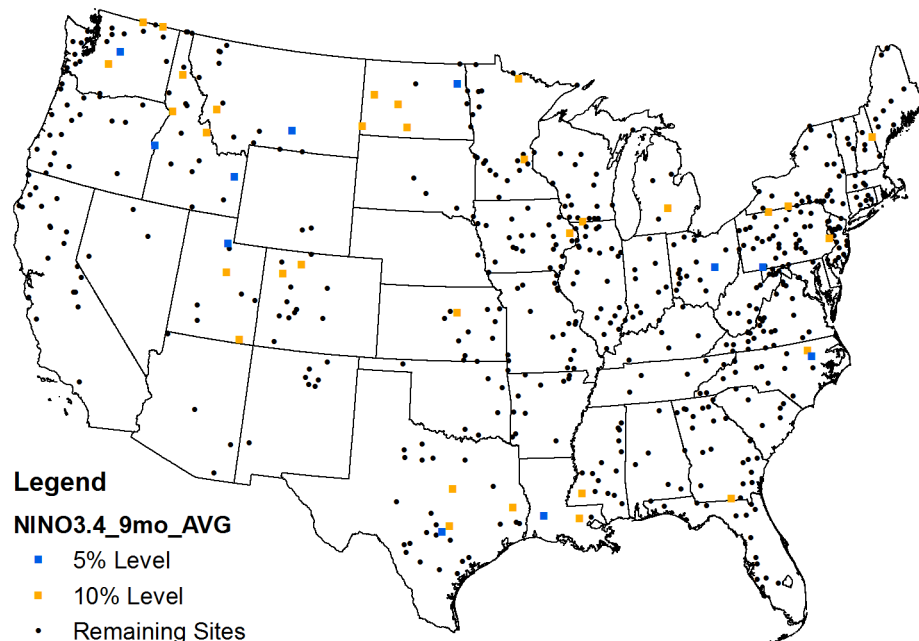


Figure E.13 Locations of sites with significant Kendall's tau correlation between 10-year moving average of log-transformed flood flows and 3-month average **Nino3.4** anomalies with **9-month** lead.

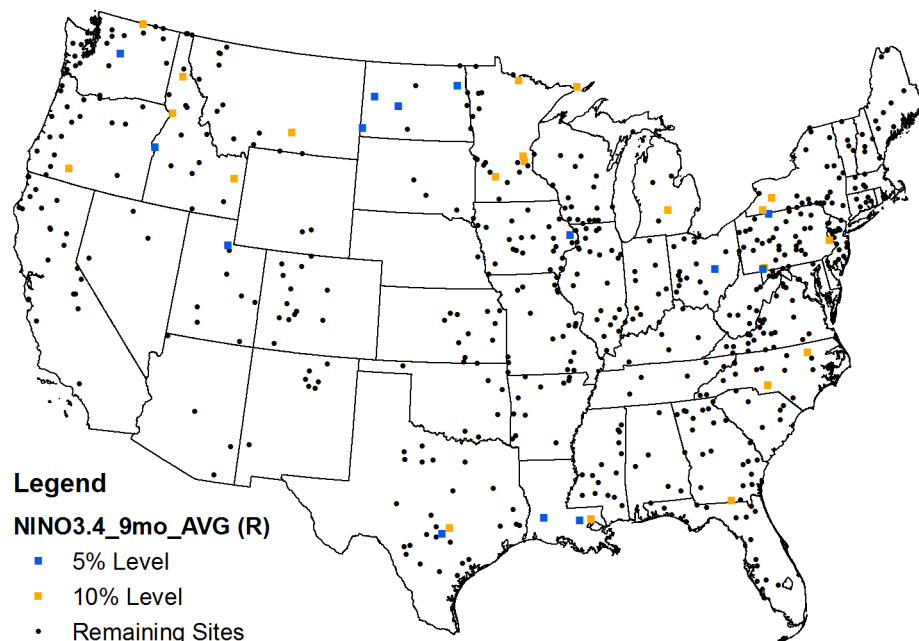


Figure E.14 Locations of sites with significant Pearson's r correlation between 10-year moving average of log-transformed flood flows and 3-month average **Nino3.4** anomalies with **9-month** lead.

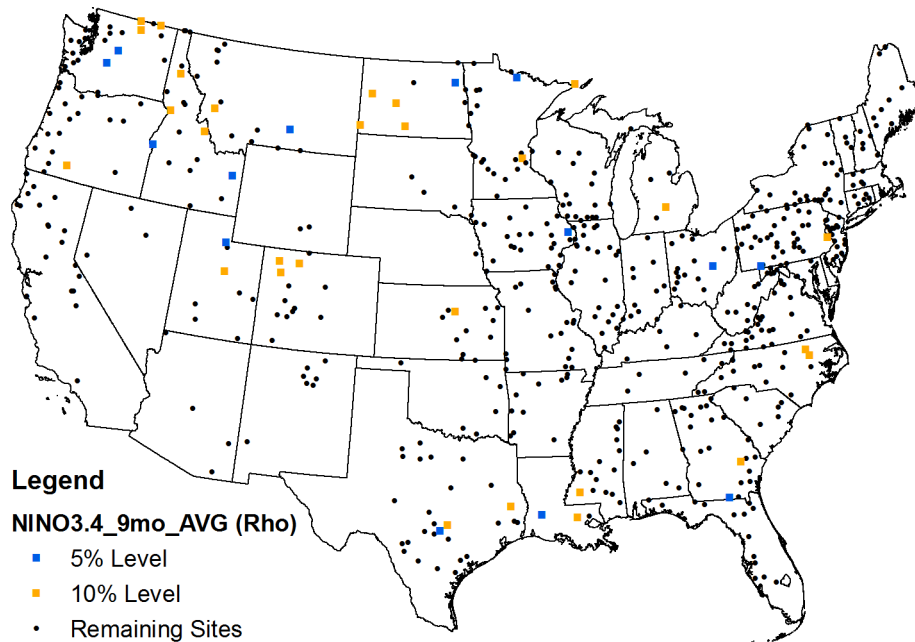


Figure E.15 Locations of sites with significant Spearman's rho correlation between 10-year moving average of log-transformed flood flows and 3-month average **Nino3.4** anomalies with **9-month** lead.

E.5 PDO Correlations Results

Table E.6

Results of Kendall's tau analyses (significant 10% level) between 10-year moving average of log-transformed flood flows and 3-month average **PDO** anomalies with 3-, 6-, 9-month leads.

Station Number	3-Month Lead		6-Month Lead		9-Month Lead	
	tau	p-value	tau	p-value	tau	p-value
1011000	0.234	0.008	0.226	0.011	0.150	0.092
1013500	0.239	0.007	0.176	0.048		
1014000	0.266	0.003	0.249	0.005	0.193	0.030
1031500			0.193	0.030	0.163	0.066
1038000	0.226	0.011	0.245	0.006	0.240	0.007
1047000	0.161	0.071			0.204	0.022
1055000					0.234	0.008
1057000	0.180	0.043	0.225	0.011	0.310	0.000
1064500	0.214	0.016	0.255	0.004	0.372	0.000
1073000	0.195	0.030			0.286	0.001
1076500	0.158	0.077			0.179	0.046
1078000	0.211	0.019	0.198	0.028	0.328	0.000

Table E.6, continued

Station Number	3-Month Lead		6-Month Lead		9-Month Lead	
	tau	p-value	tau	p-value	tau	p-value
1119500	0.166	0.064	0.157	0.080	0.264	0.003
1127500	0.233	0.009	0.274	0.002	0.261	0.004
1137500					0.165	0.066
1162500	0.205	0.022	0.211	0.019	0.196	0.028
1169000	0.266	0.003	0.222	0.013	0.282	0.002
1176000	0.160	0.074			0.185	0.039
1181000	0.218	0.015	0.247	0.006	0.254	0.005
1188000			0.161	0.073	0.220	0.014
1193500	0.192	0.032	0.205	0.022	0.202	0.024
1196500	0.249	0.005	0.334	0.000	0.401	0.000
1318500	0.181	0.042			0.181	0.041
1334500	0.205	0.021	0.248	0.005	0.211	0.017
1350000	0.213	0.016	0.202	0.023	0.309	0.001
1365000	0.278	0.002	0.211	0.017	0.253	0.004
1379500	0.147	0.097	0.171	0.055		
1381500	0.244	0.006	0.331	0.000	0.344	0.000
1387500	0.222	0.012	0.283	0.001	0.257	0.004
1396500	0.240	0.007	0.308	0.001	0.293	0.001
1397500			0.225	0.011	0.251	0.005
1398000					0.193	0.030
1398500	0.230	0.010	0.309	0.001	0.287	0.001
1399500			0.164	0.065		
1408000	0.215	0.016	0.161	0.070	0.169	0.057
1410000					0.149	0.093
1411000	0.201	0.024	0.220	0.013	0.175	0.049
1411500					0.162	0.068
1413500					0.148	0.096
1420500	0.186	0.036	0.275	0.002	0.305	0.001
1426500			-0.157	0.077		
1439500	0.146	0.100	0.157	0.077		
1445500	0.152	0.087	0.222	0.013	0.231	0.009
1518000			-0.198	0.026	-0.188	0.035
1520500			-0.240	0.007	-0.235	0.008
1531000			-0.173	0.052		
1532000					0.198	0.026
1534000			0.154	0.084		
1538000			0.194	0.029	0.220	0.013
1541000	0.173	0.051	0.182	0.041	0.149	0.093
1555000	0.188	0.034	0.180	0.043	0.295	0.001
1555500	0.221	0.013	0.263	0.003	0.230	0.010
1556000			-0.248	0.005		
1558000	0.159	0.074				
1560000	0.221	0.013	0.225	0.011	0.274	0.002
1574000	0.151	0.090	0.179	0.045		

Table E.6, continued

Station Number	3-Month Lead		6-Month Lead		9-Month Lead	
	tau	p-value	tau	p-value	tau	p-value
1601500	0.210	0.018	0.227	0.011	0.326	0.000
1604500	-0.154	0.083	-0.261	0.003	-0.277	0.002
1608500	0.222	0.012	0.300	0.001	0.272	0.002
1610000			0.211	0.017		
1614500	0.306	0.001	0.300	0.001	0.246	0.006
1631000	0.186	0.036	0.223	0.012	0.173	0.052
1632000	0.150	0.092	0.147	0.099	0.172	0.053
1634000	0.210	0.018	0.227	0.011	0.220	0.013
1634500	0.280	0.002	0.347	0.000	0.409	0.000
1645000	0.263	0.003	0.322	0.000	0.213	0.016
1667500	0.323	0.000	0.262	0.003	0.158	0.076
2013000	0.194	0.029	0.285	0.001	0.224	0.012
2016000	0.177	0.047	0.241	0.007	0.231	0.009
2017500	0.173	0.051	0.155	0.082	0.219	0.014
2018000	0.238	0.007	0.327	0.000	0.373	0.000
2035000	0.146	0.100	0.185	0.037		
2045500	0.245	0.006	0.285	0.001	0.341	0.000
2051500	0.213	0.017	0.280	0.002	0.335	0.000
2055000	0.244	0.006	0.304	0.001	0.319	0.000
2059500	0.361	0.000	0.152	0.087	0.178	0.045
2061500	0.205	0.021	0.278	0.002	0.312	0.000
2070000			0.227	0.011	0.171	0.055
2074500	0.323	0.000	0.202	0.023	0.170	0.057
2083000			0.150	0.091	0.271	0.002
2091500			-0.154	0.084		
2116500	0.166	0.062				
2118000	0.158	0.075			0.192	0.031
2126000					0.199	0.025
2138500	0.202	0.023			0.159	0.073
2154500			-0.175	0.049	-0.180	0.043
2213500	0.226	0.011	0.264	0.003	0.310	0.000
2225500			0.164	0.065	0.163	0.067
2231000	-0.354	0.000	-0.397	0.000	-0.233	0.009
2246000	-0.246	0.006	-0.277	0.002	-0.163	0.066
2256500	-0.289	0.001	-0.309	0.001	-0.199	0.025
2296750	-0.302	0.001	-0.256	0.004	-0.207	0.020
2298830			-0.153	0.086	-0.162	0.068
2301500	-0.244	0.006	-0.330	0.000	-0.201	0.024
2303000	-0.233	0.009	-0.280	0.002		
2313000	-0.227	0.011	-0.194	0.029		
2314500					-0.181	0.042
2317500			0.171	0.055	0.189	0.034
2320500			0.178	0.046	0.153	0.086
2321500	-0.196	0.028	-0.286	0.001		

Table E.6, continued

Station Number	3-Month Lead		6-Month Lead		9-Month Lead	
	tau	p-value	tau	p-value	tau	p-value
2329000			0.213	0.017	0.166	0.062
2333500			-0.195	0.028		
2339500	-0.167	0.060	-0.249	0.005	-0.305	0.001
2353500	0.163	0.066	0.162	0.069	0.194	0.029
2369000	0.153	0.085	0.192	0.031	0.312	0.000
2375500	0.194	0.029	0.235	0.008	0.161	0.070
2383500			-0.215	0.016	-0.265	0.003
2387500			-0.207	0.020	-0.261	0.003
2431000			-0.148	0.096	-0.174	0.050
2441000			-0.157	0.077	-0.201	0.024
2467000	0.160	0.072	0.216	0.015	0.294	0.001
2472500	0.179	0.045	0.275	0.002	0.322	0.000
2479000	0.214	0.016	0.264	0.003	0.296	0.001
2484500	0.151	0.090				
2486000	0.202	0.023	0.210	0.018	0.163	0.066
2487500			0.172	0.053	0.220	0.013
2488500	0.263	0.003	0.298	0.001	0.323	0.000
3010500	-0.189	0.033	-0.285	0.001	-0.298	0.001
3011020	-0.179	0.044	-0.282	0.002	-0.280	0.002
3015500	0.185	0.038	0.181	0.042	0.193	0.030
3024000			-0.226	0.011	-0.290	0.001
3034500			0.162	0.068	0.178	0.046
3049500			-0.233	0.009	-0.302	0.001
3079000			-0.217	0.015	-0.266	0.003
3080000	-0.218	0.014	-0.271	0.002	-0.392	0.000
3102500			-0.188	0.034	-0.190	0.033
3106000			-0.163	0.067	-0.161	0.071
3118500	0.279	0.002	0.336	0.000	0.338	0.000
3144000	0.157	0.081	0.264	0.003	0.347	0.000
3164000	0.176	0.047	0.216	0.015	0.341	0.000
3167000			-0.211	0.017	-0.274	0.002
3170000	0.197	0.026	0.218	0.014	0.207	0.020
3182500			0.219	0.014	0.272	0.002
3186500			0.168	0.058	0.257	0.004
3198500	0.147	0.097				
3219500			0.183	0.041		
3230500			-0.225	0.012		
3234500	-0.252	0.005	-0.261	0.004	-0.378	0.000
3253500	-0.207	0.021	-0.303	0.001	-0.257	0.004
3266000	-0.153	0.089				
3269500	-0.171	0.057	-0.264	0.003	-0.261	0.004
3274000	-0.167	0.062				
3275000	-0.223	0.012	-0.165	0.063	-0.296	0.001
3281500					-0.169	0.060

Table E.6, continued

Station Number	3-Month Lead		6-Month Lead		9-Month Lead	
	tau	p-value	tau	p-value	tau	p-value
3294500			-0.167	0.063	-0.256	0.004
3301500			0.148	0.099		
3307000	0.248	0.006	0.365	0.000	0.399	0.000
3326500					0.178	0.045
3339500	-0.194	0.029				
3360500	-0.167	0.061				
3363500	-0.215	0.015			-0.199	0.025
3373500	-0.197	0.026			-0.191	0.032
3380500			0.166	0.062	0.202	0.023
3381500	0.166	0.062			0.214	0.016
3434500					0.157	0.077
3438000	0.234	0.009	0.281	0.002	0.256	0.004
3465500					0.159	0.073
3479000	0.195	0.028	0.187	0.036	0.278	0.002
3524000			-0.165	0.063	-0.181	0.042
3528000			-0.168	0.058		
3604000					0.152	0.089
3612000					-0.157	0.080
4056500			0.235	0.008		
4087000	0.149	0.095				
4100500	0.190	0.033	0.173	0.052	0.306	0.001
4191500	0.148	0.098	0.195	0.030	0.206	0.021
4193500			0.215	0.015	0.220	0.013
4198000	0.177	0.047	0.164	0.065		
4223000			-0.183	0.040	-0.178	0.045
4234000					0.164	0.065
4262500	0.199	0.025			0.282	0.001
4264331	0.278	0.002	0.263	0.003	0.336	0.000
4269000					0.161	0.070
4275000	0.251	0.005	0.214	0.016	0.350	0.000
4287000	0.156	0.082	0.220	0.014	0.210	0.019
4293500	0.160	0.075	0.174	0.053	0.256	0.004
5078000					-0.189	0.034
5078500					-0.166	0.063
5084000	-0.194	0.029	-0.191	0.032	-0.340	0.000
5100000			-0.177	0.046	-0.170	0.056
5112000	-0.156	0.079	-0.208	0.019	-0.225	0.011
5131500					-0.161	0.071
5286000					-0.254	0.004
5288500	-0.147	0.099	-0.195	0.028	-0.283	0.001
5304500	0.185	0.037			0.214	0.016
5316500	0.167	0.061	0.231	0.009	0.283	0.001
5340500					-0.207	0.020
5379500			-0.158	0.075		

Table E.6, continued

Station Number	3-Month Lead		6-Month Lead		9-Month Lead	
	tau	p-value	tau	p-value	tau	p-value
5407000			0.220	0.014		
5408000			-0.213	0.017	-0.261	0.003
5410490			-0.242	0.006	-0.297	0.001
5412500	-0.207	0.020	-0.259	0.004	-0.336	0.000
5414000			-0.180	0.043	-0.185	0.037
5418500			-0.209	0.019	-0.282	0.002
5419000			-0.172	0.053	-0.231	0.009
5421000			-0.149	0.093	-0.215	0.016
5431486					-0.149	0.093
5432500	-0.146	0.100	-0.257	0.004	-0.265	0.003
5434500	-0.161	0.070	-0.241	0.007	-0.263	0.003
5435500	-0.207	0.020	-0.277	0.002	-0.240	0.007
5436500	-0.180	0.045	-0.267	0.003	-0.253	0.005
5447500			0.189	0.034	0.231	0.009
5459500			-0.167	0.060	-0.164	0.065
5474000	0.205	0.021	0.149	0.095		
5482500	-0.253	0.004	-0.198	0.026	-0.189	0.034
5484500	-0.270	0.002	-0.189	0.033	-0.182	0.041
5495000	0.261	0.003	0.165	0.063	0.177	0.047
5497000			0.151	0.096		
5501000	0.303	0.001	0.216	0.015	0.304	0.001
5520500	0.289	0.001	0.245	0.006	0.236	0.008
5526000	0.332	0.000	0.181	0.041	0.286	0.001
5527500	0.297	0.001	0.282	0.001	0.318	0.000
5555300	0.187	0.036	0.169	0.057	0.266	0.003
5570000	0.168	0.058	0.147	0.097		
5572000	0.215	0.015	0.207	0.020	0.169	0.057
5585000	0.240	0.007	0.198	0.026	0.203	0.022
5593000			-0.198	0.026	-0.163	0.067
5597000			-0.180	0.043	-0.205	0.021
6019500	0.221	0.013	0.202	0.023	0.193	0.030
6191500					-0.162	0.069
6214500					-0.170	0.057
6335500	-0.186	0.036	-0.303	0.001	-0.383	0.000
6337000	-0.180	0.043	-0.300	0.001	-0.387	0.000
6340500			-0.193	0.030	-0.275	0.002
6441500	-0.166	0.063	-0.225	0.011	-0.242	0.006
6600500			0.163	0.067	0.190	0.033
6606600	-0.180	0.043				
6809500	-0.218	0.014	-0.203	0.022	-0.206	0.021
6864500	-0.318	0.000	-0.227	0.011	-0.198	0.026
6876900	-0.214	0.016			-0.194	0.029
6889500	0.278	0.002	0.194	0.029	0.308	0.001
6899500					-0.148	0.097

Table E.6, continued

Station Number	3-Month Lead		6-Month Lead		9-Month Lead	
	tau	p-value	tau	p-value	tau	p-value
6933500			0.147	0.097	0.153	0.086
7016500	0.174	0.051	0.188	0.034	0.223	0.012
7019000					0.178	0.045
7067000			0.194	0.029		
7069500			-0.255	0.004	-0.384	0.000
7072000					-0.171	0.055
7074000	-0.224	0.012			-0.244	0.006
7096000	-0.249	0.005			-0.174	0.050
7144200	0.182	0.041				
7176000	-0.236	0.008	-0.193	0.030	-0.170	0.056
7186000	0.164	0.065			0.218	0.014
7187000			-0.199	0.025	-0.251	0.005
7203000	-0.171	0.059	-0.161	0.075		
7218000	-0.196	0.029	-0.184	0.040		
7234000	-0.285	0.001			-0.219	0.014
7247000	-0.249	0.005				
7247500	-0.199	0.025	-0.195	0.028	-0.292	0.001
7261500					0.149	0.095
7290000	0.185	0.037	0.231	0.009		
7291000	0.270	0.002	0.375	0.000	0.355	0.000
7331000					0.186	0.036
7332500			0.199	0.025	0.175	0.049
7340000	-0.280	0.002	-0.166	0.063	-0.259	0.004
7340500	-0.267	0.003			-0.276	0.002
7363500	-0.171	0.055			-0.157	0.078
7375500	0.247	0.005	0.259	0.004	0.271	0.002
7378500	0.183	0.040	0.320	0.000	0.334	0.000
8013500	0.228	0.010	0.340	0.000	0.150	0.092
8033500					0.190	0.033
8041500	0.213	0.017	0.191	0.032	0.311	0.000
8055500	-0.331	0.000	-0.207	0.020	-0.224	0.012
8080500	-0.257	0.004			-0.200	0.024
8082000	-0.246	0.006			-0.223	0.012
8082500	-0.238	0.007			-0.167	0.060
8128000			-0.183	0.040	-0.203	0.022
8151500	0.366	0.000	0.293	0.001	0.258	0.004
8153500	0.361	0.000	0.311	0.000	0.290	0.001
8158000	0.272	0.002			0.179	0.045
8164000	0.250	0.005				
8167000	0.255	0.004	0.289	0.001	0.227	0.011
8167500	0.317	0.000	0.302	0.001	0.287	0.001
8171000	0.179	0.044			0.169	0.057
8176500	0.173	0.051				
8189500			0.197	0.027		

Table E.6, continued

Station Number	3-Month Lead		6-Month Lead		9-Month Lead	
	tau	p-value	tau	p-value	tau	p-value
8195000	0.202	0.023	0.367	0.000	0.271	0.003
8210000	-0.229	0.010	-0.151	0.090		
8276500			0.188	0.035	0.190	0.032
8291000	0.345	0.000	0.269	0.003	0.227	0.011
8378500	0.256	0.004	0.170	0.059	0.247	0.006
8380500	-0.209	0.020	-0.156	0.083		
9085000	-0.196	0.028			-0.175	0.049
9110000	-0.217	0.015			-0.242	0.006
9180500	-0.147	0.097			-0.158	0.075
9379500	-0.274	0.002			-0.204	0.022
9430500	0.322	0.000	0.210	0.018	0.267	0.003
9448500	0.198	0.026	0.177	0.047	0.246	0.006
9471000	-0.176	0.048				
9508500					0.203	0.022
10174500			0.166	0.063		
10234500	0.157	0.078	0.146	0.100	0.180	0.043
10296000			-0.174	0.050		
10310000			-0.193	0.030		
10396000			0.163	0.067		
11160500	-0.165	0.066				
11381500					-0.155	0.082
11383500	-0.187	0.035	-0.171	0.055	-0.186	0.036
11413000	-0.168	0.061			-0.159	0.076
11425500	-0.188	0.034				
11477000	-0.221	0.013	-0.253	0.004	-0.265	0.003
11478500	-0.158	0.075	-0.205	0.021	-0.192	0.031
11522500			-0.196	0.028		
11525500			-0.227	0.011		
11530000	-0.153	0.086	-0.225	0.011	-0.259	0.004
11532500	-0.202	0.023	-0.254	0.004	-0.217	0.015
12035000	0.188	0.034	0.296	0.001	0.327	0.000
12039500					0.216	0.015
12048000			0.179	0.045	0.188	0.035
12054000					0.215	0.016
12056500					0.190	0.033
12134500	0.248	0.005	0.225	0.011	0.300	0.001
12186000	0.240	0.007	0.191	0.032	0.216	0.015
12189500	0.285	0.001	0.204	0.022	0.304	0.001
12306500	-0.308	0.001	-0.212	0.017	-0.292	0.001
12322000	-0.279	0.002	-0.257	0.004	-0.334	0.000
12332000	-0.200	0.024			-0.225	0.011
12354500	-0.198	0.026			-0.225	0.011
12355500	-0.239	0.007	-0.149	0.093	-0.267	0.003
12358500	-0.229	0.010			-0.208	0.019

Table E.6, continued

Station Number	3-Month Lead		6-Month Lead		9-Month Lead	
	tau	p-value	tau	p-value	tau	p-value
12370000					-0.225	0.011
12409000	-0.161	0.071	-0.284	0.001	-0.184	0.039
12413000	-0.196	0.027	-0.227	0.011	-0.204	0.022
12422500	-0.263	0.003	-0.161	0.070	-0.284	0.001
12442500	-0.259	0.003			-0.236	0.008
12445000	-0.273	0.002			-0.223	0.012
12451000	-0.270	0.002	-0.166	0.063		
12459000	-0.159	0.074				
12488500			0.163	0.066		
13185000	-0.187	0.036	-0.161	0.071	-0.209	0.019
13302500					-0.172	0.053
13313000	-0.266	0.003	-0.236	0.008	-0.311	0.000
13317000	-0.192	0.031			-0.247	0.005
13336500	-0.191	0.032			-0.249	0.005
13337000	-0.205	0.021			-0.238	0.007
13342500	-0.230	0.010			-0.261	0.003
14044000	0.147	0.099	0.164	0.065	0.185	0.038
14105700	-0.260	0.003	-0.167	0.061	-0.272	0.002
14185000					-0.151	0.089
14191000	-0.246	0.006	-0.268	0.003	-0.272	0.002
14301000			-0.236	0.008	-0.177	0.047
14301500	-0.167	0.060	-0.207	0.020		
14306500	-0.213	0.017	-0.298	0.001	-0.196	0.028
14308000	-0.164	0.065	-0.189	0.033	-0.213	0.017
14321000	-0.180	0.043	-0.219	0.014	-0.216	0.015
14325000	-0.189	0.034	-0.241	0.007		
14359000	-0.209	0.019	-0.294	0.001	-0.225	0.011
14362000	-0.235	0.008	-0.284	0.001	-0.190	0.033

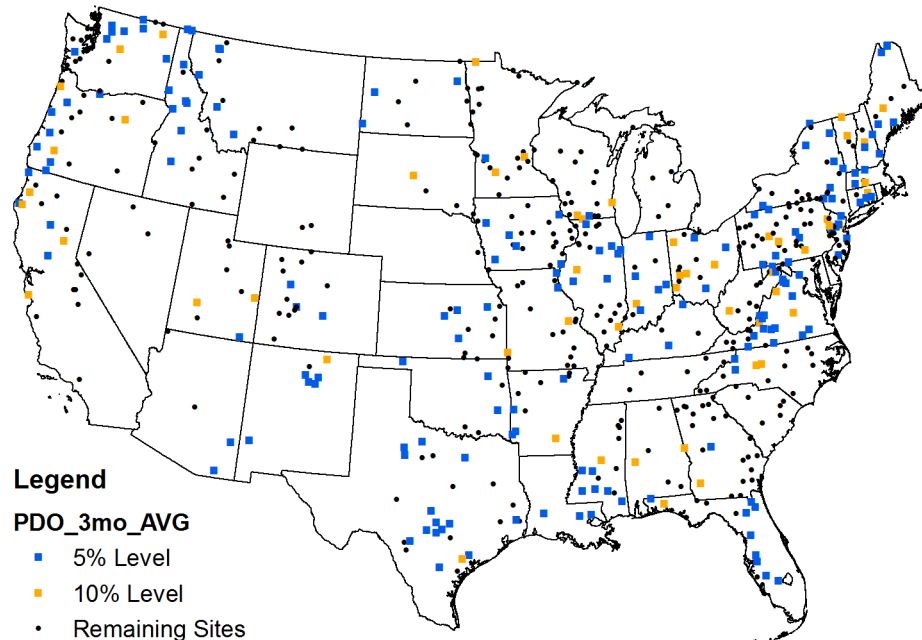


Figure E.16 Locations of sites with significant Kendall's tau correlation between 10-year moving average of log-transformed flood flows and 3-month average **PDO** anomalies with **3-month** lead.

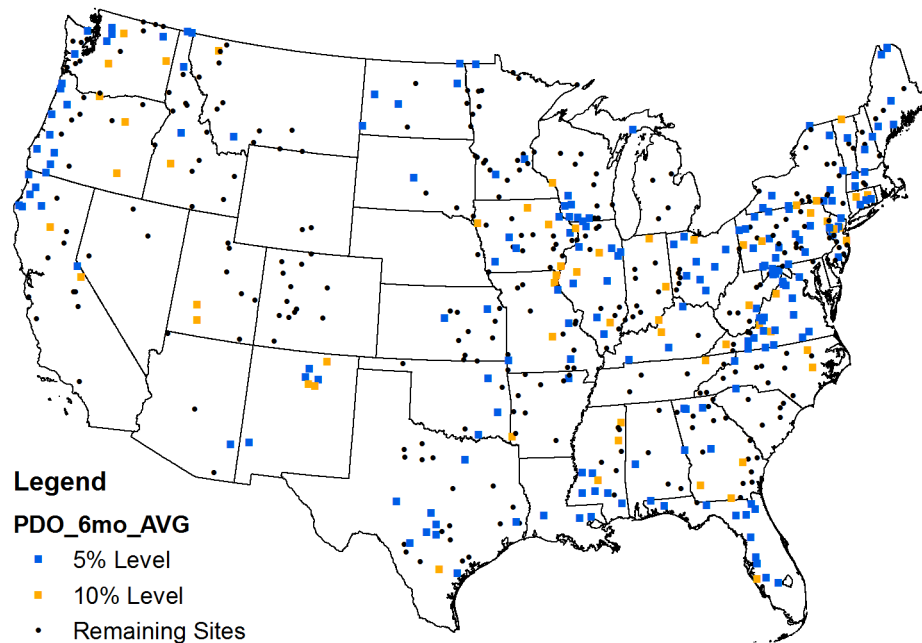


Figure E.17 Locations of sites with significant Kendall's tau correlation between 10-year moving average of log-transformed flood flows and 3-month average **PDO** anomalies with **6-month** lead.

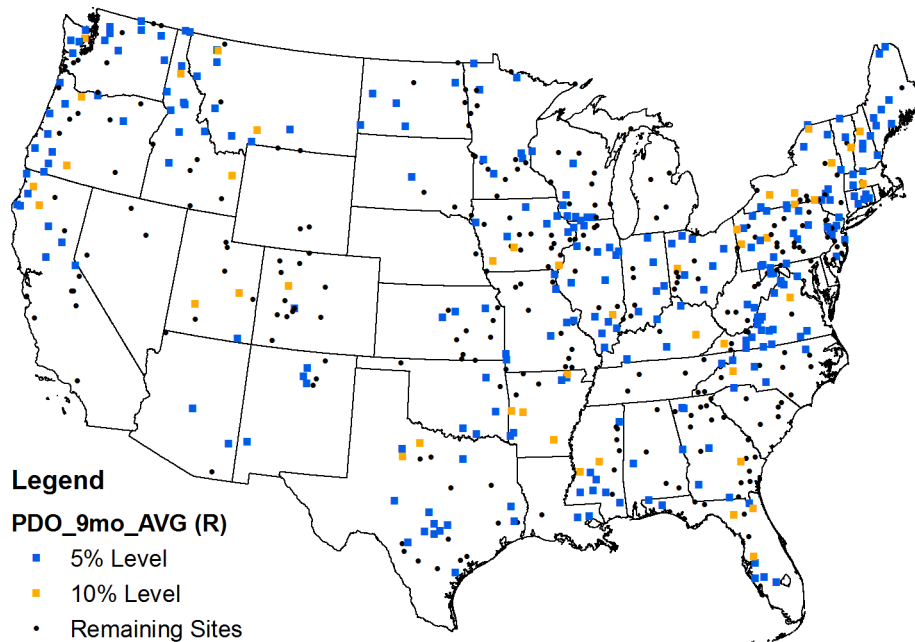


Figure E.18 Locations of sites with significant Pearson's r correlation between 10-year moving average of log-transformed flood flows and 3-month average **PDO** anomalies with **9-month** lead.

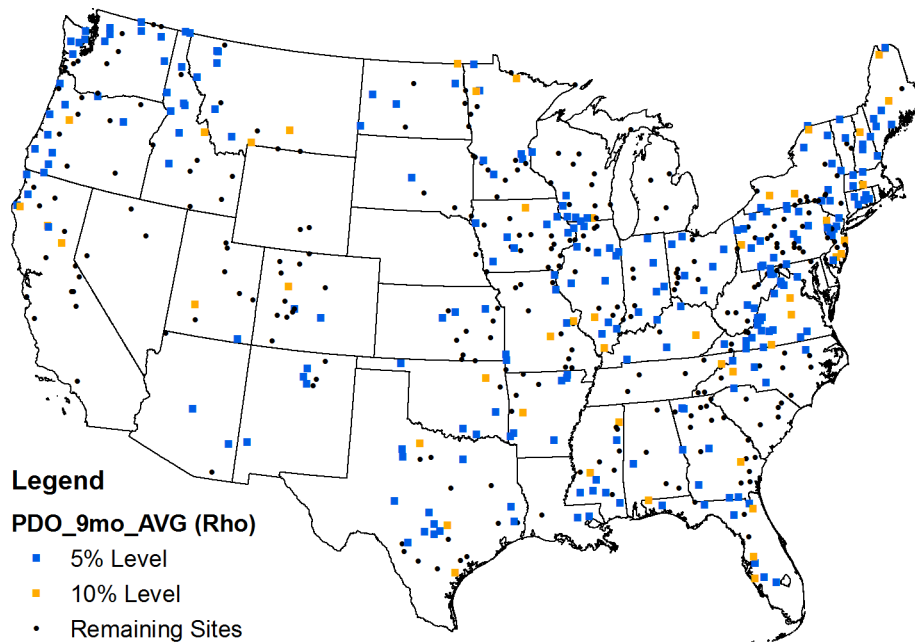


Figure E.19 Locations of sites with significant Spearman's ρ correlation between 10-year moving average of log-transformed flood flows and 3-month average **PDO** anomalies with **9-month** lead.

APPENDIX F CORRELATION ANALYSIS RESULTS BETWEEN 10 YEAR MOVING STANDARD DEVIATION OF LOGS OF FLOOD FLOWS AND CLIMATE ANOMALIES

This appendix contains tables and figures summarizing Kendall's tau correlation analyses between the 10-year moving standard deviation of log-transformed flood flows and 3-month average AMO, MEI, NAO, Nino3.4, and PDO anomalies with 3-, 6-, and 9-month leads. Tables include results only for sites with significant relationships on the 10% level (sites significant on the 5% level are in **bold**). Results are omitted (blank spaces) when p-values greater than 10% were obtained. Note that results of the Kendall's tau analyses for AMO, MEI, NAO, and PDO with lead times of 3-, 9-, 3-, and 9-months, respectively, are illustrated in Chapter 3. Figures for Pearson's r and Spearman's rho with the same lead times are included herein. The table below summarizes the number of sites where significant results were obtained using the Pearson's r and Spearman's rho analyses for all cases considered.

Table F.1
Number of sites with significant Pearson's r and Spearman's rho correlations (5 and 10% levels) between 10-yr moving standard deviation of log-transformed flood peaks and for AMO, MEI, NINO 3.4, NAO, and PDO indices with specified lead times.

Lead Time (months)	AMO		MEI		Nino 3.4		NAO		PDO	
	5%	10%	5%	10%	5%	10%	5%	10%	5%	10%
<i>Pearson's r Correlation</i>										
3	257	299	42	82	3	6	85	114	152	200
6	257	300	60	114	0	13	21	45	174	231
9	215	264	128	175	15	32	43	91	215	268
<i>Spearman's rho Correlation</i>										
3	234	287	41	77	3	11	77	104	155	206
6	230	283	55	94	5	18	29	48	178	223
9	201	244	109	152	14	33	39	78	204	248

F.1 AMO Correlation Results

Table F.2

Results of Kendall's tau analyses (significant 10% level) between 10-year moving standard deviation of log-transformed flood flows and 3-month average **AMO** anomalies with 3-, 6-, and 9-month leads.

Station Number	3-Month Lead		6-Month Lead		9-Month Lead	
	tau	p-value	tau	p-value	tau	p-value
1011000	-0.301	0.001	-0.279	0.002	-0.180	0.043
1013500	-0.168	0.058	-0.226	0.011	-0.165	0.063
1030500	-0.242	0.006	-0.185	0.037		
1038000	-0.315	0.000	-0.250	0.005	-0.183	0.039
1073000	0.274	0.002	0.299	0.001	0.233	0.009
1076500					-0.164	0.067
1078000	0.282	0.002	0.288	0.001	0.199	0.027
1127500			0.151	0.093		
1169000	0.188	0.036	0.167	0.062	0.148	0.099
1175500	0.196	0.028	0.217	0.015	0.258	0.004
1176000	0.171	0.056				
1181000	0.207	0.021	0.148	0.098	0.148	0.099
1188000	0.160	0.075				
1318500	0.159	0.074				
1321000	0.222	0.013	0.193	0.030		
1334500	-0.174	0.050	-0.219	0.014	-0.216	0.015
1350000	0.391	0.000	0.284	0.001	0.270	0.002
1365000	0.404	0.000	0.327	0.000	0.329	0.000
1381500	0.242	0.006	0.163	0.066		
1387500	0.166	0.062				
1396500	0.192	0.031	0.244	0.006	0.161	0.070
1398000	0.409	0.000	0.372	0.000	0.308	0.001
1398500	0.201	0.024	0.168	0.059		
1408000	0.299	0.001	0.373	0.000	0.340	0.000
1410000	-0.401	0.000	-0.287	0.001	-0.325	0.000
1411500	-0.277	0.002	-0.321	0.000	-0.328	0.000
1413500	0.421	0.000	0.464	0.000	0.360	0.000
1414500	0.497	0.000	0.485	0.000	0.441	0.000
1420500	0.271	0.002	0.242	0.006	0.199	0.025
1421000	0.369	0.000	0.320	0.000	0.287	0.001
1439500	0.246	0.006	0.179	0.044	0.199	0.025
1440000	0.240	0.007	0.279	0.002	0.212	0.017
1445500	0.186	0.036				
1459500	0.360	0.000	0.380	0.000	0.358	0.000
1463500	0.339	0.000	0.307	0.001	0.285	0.001
1514000	-0.293	0.001	-0.283	0.001	-0.270	0.002
1518000	-0.330	0.000	-0.384	0.000	-0.353	0.000
1520500	-0.279	0.002	-0.329	0.000	-0.284	0.001

Table F.2, continued

Station Number	3-Month Lead		6-Month Lead		9-Month Lead	
	tau	p-value	tau	p-value	tau	p-value
1531000	-0.261	0.003	-0.303	0.001	-0.279	0.002
1532000	-0.360	0.000	-0.261	0.003	-0.329	0.000
1538000			0.202	0.023		
1539000	-0.409	0.000	-0.334	0.000	-0.342	0.000
1548500	-0.163	0.067			-0.194	0.029
1558000	0.285	0.001	0.254	0.004	0.170	0.056
1560000	-0.236	0.008			-0.225	0.011
1564500	0.462	0.000	0.458	0.000	0.372	0.000
1570500	-0.271	0.002	-0.185	0.038	-0.246	0.006
1599000	0.240	0.007	0.245	0.006	0.175	0.049
1601500	0.189	0.034	0.281	0.002	0.179	0.044
1604500	0.210	0.018	0.214	0.016	0.218	0.014
1631000	0.153	0.086	0.273	0.002		
1632000			0.268	0.003	0.183	0.040
1634000			0.255	0.004	0.153	0.085
1645000	-0.355	0.000	-0.393	0.000	-0.359	0.000
1667500					0.156	0.079
2016000	0.175	0.049	0.287	0.001	0.173	0.051
2035000	-0.268	0.003	-0.190	0.032	-0.299	0.001
2045500					-0.162	0.068
2059500					0.173	0.052
2061500			0.213	0.016		
2074500	-0.301	0.001	-0.376	0.000	-0.341	0.000
2083500	0.164	0.065	0.294	0.001	0.218	0.014
2091500	0.288	0.001	0.324	0.000	0.280	0.002
2102000			0.246	0.006	0.162	0.068
2116500	-0.172	0.053				
2118000	-0.222	0.012	-0.176	0.047	-0.231	0.009
2126000	0.184	0.038	0.235	0.008		
2131000			0.195	0.028		
2132000	0.381	0.000	0.439	0.000	0.340	0.000
2134500	0.279	0.002	0.376	0.000	0.274	0.002
2138500	0.216	0.015	0.177	0.046		
2154500			0.155	0.081		
2173500	0.324	0.000	0.306	0.001	0.288	0.001
2192000	0.251	0.005	0.290	0.001	0.196	0.027
2198000	0.392	0.000	0.314	0.000	0.268	0.003
2202500	0.406	0.000	0.415	0.000	0.354	0.000
2203000	0.148	0.096	0.183	0.040		
2213500	0.223	0.012	0.163	0.067		
2217500	0.358	0.000	0.362	0.000	0.279	0.002
2226000	0.379	0.000	0.361	0.000	0.284	0.001
2226500	0.316	0.000	0.354	0.000	0.305	0.001
2228000	0.456	0.000	0.431	0.000	0.417	0.000
2231000	0.341	0.000	0.425	0.000	0.461	0.000

Table F.2, continued

Station Number	3-Month Lead		6-Month Lead		9-Month Lead	
	tau	p-value	tau	p-value	tau	p-value
2246000	0.238	0.007	0.284	0.001	0.288	0.001
2296750	0.343	0.000	0.322	0.000	0.366	0.000
2298830	0.214	0.016	0.200	0.025	0.202	0.023
2301500	0.412	0.000	0.491	0.000	0.492	0.000
2303000	0.393	0.000	0.344	0.000	0.380	0.000
2313000	0.417	0.000	0.525	0.000	0.481	0.000
2314500			0.149	0.095		
2320500	0.181	0.042	0.202	0.023		
2321500	0.301	0.001	0.378	0.000	0.416	0.000
2329000	0.202	0.023	0.212	0.017	0.167	0.061
2331600					-0.154	0.083
2333500			-0.180	0.043		
2337000			0.169	0.057		
2339500	0.553	0.000	0.518	0.000	0.471	0.000
2347500	0.436	0.000	0.427	0.000	0.336	0.000
2353500	0.240	0.007	0.258	0.004	0.193	0.030
2358000	0.524	0.000	0.499	0.000	0.409	0.000
2361000	0.258	0.004	0.319	0.000	0.216	0.015
2369000	0.318	0.000	0.361	0.000	0.242	0.006
2371500	0.165	0.063	0.166	0.063		
2375500	0.336	0.000	0.305	0.001	0.244	0.006
2387500			0.146	0.100		
2392000	-0.155	0.081				
2398000					-0.179	0.044
2436500	-0.173	0.052	-0.206	0.020	-0.169	0.057
2437000	-0.365	0.000	-0.327	0.000	-0.298	0.001
2467000	-0.210	0.018	-0.172	0.053		
2472500	-0.254	0.004	-0.255	0.004	-0.174	0.050
2474500	-0.149	0.095	-0.206	0.020	-0.151	0.089
2486000			-0.198	0.026	-0.150	0.091
2488500	-0.167	0.061	-0.152	0.087		
3011020			-0.178	0.045	-0.158	0.076
3015500	0.321	0.000	0.218	0.014	0.285	0.001
3020500	0.234	0.008			0.198	0.026
3034500	0.207	0.020	0.150	0.091		
3049500	0.185	0.037			0.154	0.083
3079000	0.286	0.001	0.289	0.001	0.253	0.004
3102500	0.202	0.023	0.180	0.043	0.319	0.000
3106000	0.408	0.000	0.375	0.000	0.354	0.000
3109500	0.335	0.000	0.223	0.013	0.298	0.001
3118500	0.167	0.061				
3164000					-0.245	0.006
3167000			0.188	0.034		
3170000	-0.200	0.024			-0.178	0.045
3173000			0.146	0.100		

Table F.2, continued

Station Number	3-Month Lead		6-Month Lead		9-Month Lead	
	tau	p-value	tau	p-value	tau	p-value
3182500	-0.193	0.030			-0.158	0.076
3183500	-0.172	0.053				
3186500	-0.199	0.025				
3193000	0.297	0.001	0.203	0.022	0.239	0.007
3198500			-0.187	0.035		
3230500	0.353	0.000	0.233	0.009	0.193	0.031
3234500	0.168	0.061				
3253500	0.353	0.000	0.342	0.000	0.375	0.000
3265000	0.206	0.022	0.161	0.072	0.178	0.047
3266000	0.246	0.006	0.225	0.012	0.348	0.000
3281500			-0.184	0.041		
3294500	0.337	0.000	0.237	0.008	0.265	0.003
3301500	-0.264	0.003	-0.148	0.098	-0.217	0.015
3307000	-0.181	0.044				
3326500					0.198	0.026
3360500	0.201	0.024				
3363500	0.181	0.042			0.239	0.007
3373500	0.360	0.000	0.289	0.001	0.325	0.000
3374000	0.413	0.000	0.368	0.000	0.328	0.000
3377500	0.427	0.000	0.370	0.000	0.327	0.000
3380500	-0.177	0.047	-0.188	0.034	-0.147	0.099
3381500	0.402	0.000	0.317	0.000	0.251	0.005
3434500	-0.215	0.016	-0.179	0.044		
3438000	0.150	0.094	0.198	0.028	0.154	0.085
3465500	-0.179	0.045			-0.189	0.033
3504000	0.240	0.007	0.151	0.089		
3524000	-0.202	0.023				
3528000	-0.183	0.039	-0.155	0.081		
3540500	-0.290	0.001	-0.236	0.008	-0.406	0.000
3604000	-0.233	0.009	-0.174	0.051	-0.184	0.039
4010500	0.236	0.008			0.165	0.063
4073500			-0.195	0.029		
4079000	0.311	0.001	0.233	0.009	0.182	0.043
4087000	0.426	0.000	0.391	0.000	0.315	0.000
4105000	-0.262	0.003	-0.283	0.001	-0.214	0.016
4112500	-0.276	0.002	-0.338	0.000	-0.216	0.015
4193500	-0.173	0.051	-0.149	0.093		
4214500	-0.237	0.008	-0.288	0.001	-0.228	0.010
4223000	-0.245	0.006	-0.243	0.006	-0.260	0.003
4234000	-0.218	0.014	-0.153	0.085		
4262500	-0.205	0.021	-0.258	0.004	-0.206	0.021
4264331					-0.155	0.081
4275000	0.285	0.001	0.294	0.001	0.255	0.004
4287000			-0.166	0.064	-0.160	0.075
5053000	-0.419	0.000	-0.351	0.000	-0.262	0.003

Table F.2, continued

Station Number	3-Month Lead		6-Month Lead		9-Month Lead	
	tau	p-value	tau	p-value	tau	p-value
5062000	-0.431	0.000	-0.418	0.000	-0.371	0.000
5062500	-0.228	0.010				
5066500	-0.212	0.017	-0.223	0.012		
5082500	-0.327	0.000	-0.309	0.000	-0.245	0.006
5084000	0.282	0.001	0.220	0.013	0.221	0.013
5131500			0.182	0.041		
5133500	0.211	0.018	0.191	0.032	0.190	0.032
5280000	-0.237	0.008	-0.262	0.003	-0.218	0.014
5286000	-0.255	0.004	-0.215	0.015	-0.155	0.082
5288500	-0.281	0.002	-0.262	0.003	-0.205	0.021
5291000	0.219	0.014	0.263	0.003	0.215	0.015
5293000			0.199	0.025	0.161	0.070
5313500	-0.237	0.008	-0.246	0.006	-0.198	0.026
5316500			-0.189	0.033		
5317000	-0.400	0.000	-0.359	0.000	-0.334	0.000
5330000	-0.153	0.085	-0.251	0.005	-0.231	0.009
5331000	-0.202	0.023	-0.210	0.018	-0.205	0.021
5340500			0.193	0.030	0.192	0.031
5362000	-0.237	0.008	-0.276	0.002	-0.251	0.005
5379500			-0.193	0.030		
5394500	-0.148	0.096	-0.283	0.001	-0.258	0.004
5399500	-0.187	0.035				
5408000	-0.159	0.073	-0.248	0.005	-0.152	0.087
5410490			-0.146	0.100		
5412500	0.260	0.003	0.323	0.000	0.266	0.003
5414000	0.314	0.000	0.324	0.000	0.256	0.004
5418500	0.344	0.000	0.319	0.000	0.329	0.000
5420500	-0.291	0.001	-0.383	0.000	-0.305	0.001
5422000			-0.162	0.068		
5426000	-0.241	0.007	-0.331	0.000	-0.245	0.006
5434500	-0.234	0.008	-0.265	0.003	-0.209	0.019
5435500	-0.224	0.012	-0.307	0.001	-0.205	0.021
5436500	0.272	0.002	0.157	0.081	0.200	0.026
5438500	0.298	0.001	0.194	0.029	0.245	0.006
5444000			0.158	0.076		
5447500	-0.151	0.089	-0.196	0.027		
5451500			-0.150	0.092	-0.185	0.037
5459500	-0.262	0.003	-0.285	0.001	-0.166	0.063
5465500			-0.149	0.095		
5470000	0.231	0.009	0.267	0.003	0.193	0.030
5474000			-0.160	0.071	-0.230	0.010
5476000	-0.201	0.024	-0.267	0.003	-0.249	0.005
5479000					-0.184	0.039
5486490					0.170	0.056
5500000	-0.260	0.003	-0.178	0.045	-0.229	0.010

Table F.2, continued

Station Number	3-Month Lead		6-Month Lead		9-Month Lead	
	tau	p-value	tau	p-value	tau	p-value
5501000	-0.203	0.022	-0.150	0.091		
5520500	-0.318	0.000	-0.301	0.001	-0.207	0.020
5527500	-0.254	0.004	-0.307	0.001	-0.255	0.004
5556500	-0.340	0.000	-0.365	0.000	-0.277	0.002
5592500	0.259	0.004	0.202	0.023	0.259	0.003
5593000	0.204	0.022				
6289000	0.169	0.057	0.191	0.032	0.263	0.003
6452000	0.165	0.064	0.169	0.057	0.223	0.012
6478500	-0.166	0.062	-0.192	0.031		
6485500	-0.224	0.012	-0.247	0.005	-0.310	0.000
6600500			-0.146	0.100		
6620000					0.152	0.087
6630000					0.146	0.100
6635000	-0.215	0.016	-0.201	0.024		
6710500	-0.289	0.002	-0.318	0.000	-0.350	0.000
6800500	-0.373	0.000	-0.410	0.000	-0.437	0.000
6809500	-0.237	0.008	-0.153	0.086		
6810000	-0.161	0.070				
6889500			0.179	0.045		
6892000	0.425	0.000	0.456	0.000	0.361	0.000
6897500	0.398	0.000	0.433	0.000	0.446	0.000
6899500	0.250	0.005	0.242	0.006	0.232	0.009
6908000	-0.149	0.095	-0.199	0.025		
6913500	0.370	0.000	0.379	0.000	0.282	0.001
6933500	0.364	0.000	0.379	0.000	0.374	0.000
7018500	-0.236	0.008	-0.208	0.019	-0.172	0.053
7019000	-0.168	0.059	-0.206	0.020		
7050500	-0.166	0.063	-0.197	0.026		
7056000	-0.361	0.000	-0.367	0.000	-0.296	0.001
7067000	-0.149	0.095				
7069500	-0.146	0.100				
7074000	-0.313	0.000	-0.205	0.021	-0.180	0.043
7096000					0.203	0.022
7144200	0.234	0.009	0.215	0.016	0.192	0.031
7146500	0.157	0.078				
7147800	0.277	0.002	0.216	0.015		
7176000	0.158	0.076				
7180500	0.376	0.000	0.359	0.000	0.219	0.014
7183000	0.453	0.000	0.467	0.000	0.385	0.000
7186000	0.364	0.000	0.394	0.000	0.360	0.000
7187000	0.148	0.097				
7189000	-0.219	0.017	-0.236	0.010		
7196500			-0.192	0.031		
7218000	0.174	0.053	0.178	0.048	0.163	0.070
7234000					0.158	0.076

Table F.2, continued

Station Number	3-Month Lead		6-Month Lead		9-Month Lead	
	tau	p-value	tau	p-value	tau	p-value
7247000			-0.217	0.015	-0.289	0.001
7252000	-0.406	0.000	-0.378	0.000	-0.273	0.002
7261500	-0.222	0.012	-0.175	0.049		
7291000	0.151	0.089	0.172	0.053		
7331000	0.163	0.067	0.241	0.007	0.263	0.003
7332500	0.193	0.030	0.214	0.016	0.234	0.008
7340000	-0.161	0.071	-0.220	0.013	-0.277	0.002
7340500	-0.374	0.000	-0.344	0.000	-0.325	0.000
7363500	-0.210	0.018	-0.169	0.057	-0.197	0.027
8013500	0.210	0.018	0.198	0.026	0.248	0.005
8041000	0.212	0.017				
8055500	-0.168	0.058	-0.215	0.016	-0.149	0.093
8070000	0.394	0.000	0.302	0.001	0.267	0.003
8080500	-0.168	0.059	-0.179	0.045	-0.219	0.014
8082500			0.149	0.093		
8085500	-0.431	0.000	-0.423	0.000	-0.328	0.000
8128000	-0.313	0.000	-0.280	0.002	-0.251	0.005
8153500	0.376	0.000	0.374	0.000	0.342	0.000
8158000	0.216	0.015	0.156	0.079	0.172	0.053
8164000	0.329	0.000	0.424	0.000	0.349	0.000
8167500	0.283	0.001	0.365	0.000	0.360	0.000
8171000	0.253	0.004	0.321	0.000	0.206	0.021
8172000	0.182	0.041	0.211	0.017	0.254	0.004
8176500	0.191	0.032	0.270	0.002	0.295	0.001
8189500	0.168	0.058			0.213	0.018
8195000	0.290	0.001	0.204	0.022	0.276	0.002
8276500	0.466	0.000	0.437	0.000	0.353	0.000
8378500	0.431	0.000	0.414	0.000	0.296	0.001
9085000	0.167	0.061				
9124500	0.264	0.003	0.292	0.001	0.287	0.001
9310500	-0.259	0.004	-0.221	0.013		
9415000					0.174	0.050
9430500	0.181	0.041	0.153	0.086	0.275	0.002
9448500			-0.159	0.073		
9471000	0.164	0.064			0.164	0.065
9508500	-0.146	0.100	-0.217	0.015		
10174500			0.203	0.022	0.163	0.067
10296000	0.160	0.072	0.169	0.057	0.167	0.061
10310000	0.236	0.008	0.234	0.008	0.159	0.073
10312000	-0.150	0.091				
11098000	0.302	0.001	0.301	0.001	0.174	0.052
11152000	-0.182	0.041	-0.200	0.024	-0.158	0.076
11160500	-0.341	0.000	-0.286	0.001	-0.290	0.001
11237500	0.243	0.007	0.252	0.005	0.202	0.024
11381500	-0.265	0.003	-0.245	0.006	-0.327	0.000

Table F.2, continued

Station Number	3-Month Lead		6-Month Lead		9-Month Lead	
	tau	p-value	tau	p-value	tau	p-value
11383500	-0.238	0.007	-0.223	0.012	-0.274	0.002
11402000	-0.148	0.096	-0.157	0.077	-0.206	0.020
11413000	-0.206	0.021	-0.168	0.061		
11425500	-0.206	0.021	-0.154	0.084	-0.253	0.004
11525500	-0.389	0.000	-0.488	0.000	-0.459	0.000
12020000	0.190	0.032				
12035000					0.157	0.077
12039500	0.353	0.000	0.322	0.000	0.312	0.000
12056500	0.166	0.063				
12134500	0.292	0.001	0.329	0.000	0.360	0.000
12186000	0.448	0.000	0.385	0.000	0.314	0.000
12189500	0.409	0.000	0.352	0.000	0.290	0.001
12306500	0.231	0.009	0.235	0.008	0.228	0.010
12330000	-0.299	0.001	-0.258	0.004		
12332000					0.183	0.040
12358500	-0.180	0.043	-0.233	0.009	-0.262	0.003
12401500	0.148	0.096	0.150	0.091		
12409000	-0.211	0.018	-0.209	0.019	-0.159	0.073
12413000	-0.161	0.071				
12422500	-0.164	0.065				
12451000	0.232	0.009	0.293	0.001	0.293	0.001
12459000			0.168	0.058	0.157	0.077
13037500	0.224	0.012	0.232	0.009	0.246	0.006
13082500	-0.250	0.005	-0.338	0.000	-0.275	0.002
13120500			0.159	0.073	0.199	0.025
13185000	-0.312	0.000	-0.267	0.003	-0.211	0.018
13269000			0.201	0.024	0.182	0.041
13313000	-0.174	0.050				
13317000	-0.215	0.016				
13342500	-0.192	0.031	-0.252	0.005	-0.261	0.003
14020000	-0.188	0.034				
14046500	-0.343	0.000	-0.359	0.000	-0.344	0.000
14137000	-0.161	0.070	-0.189	0.034	-0.217	0.015
14325000	0.201	0.024				
14359000	0.185	0.038	0.166	0.063	0.209	0.019
14362000	0.168	0.059				

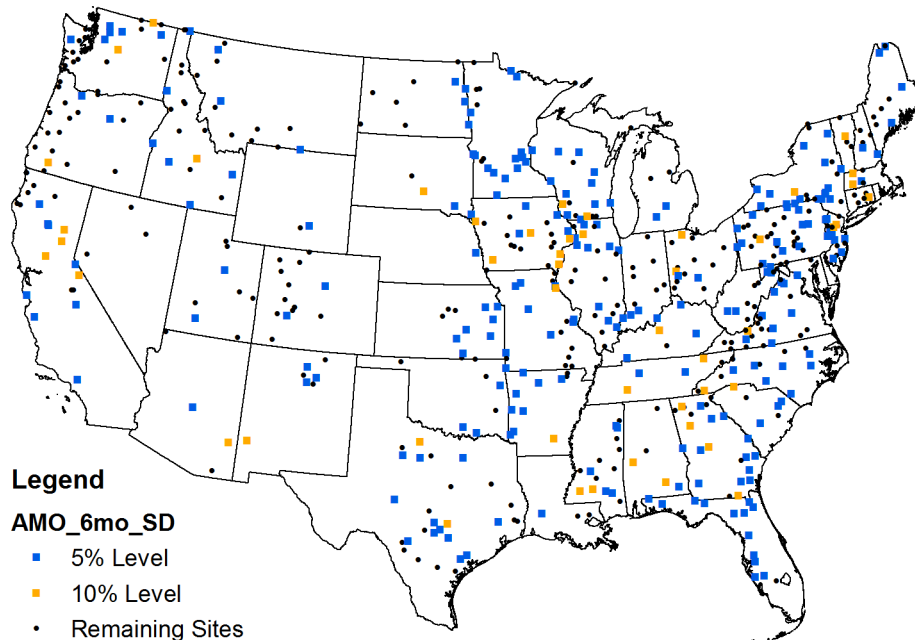


Figure F.1 Locations of sites with significant Kendall's tau correlation between 10-year moving standard deviation of log-transformed flood flows and 3-month average **AMO** anomalies with **6-month** lead.

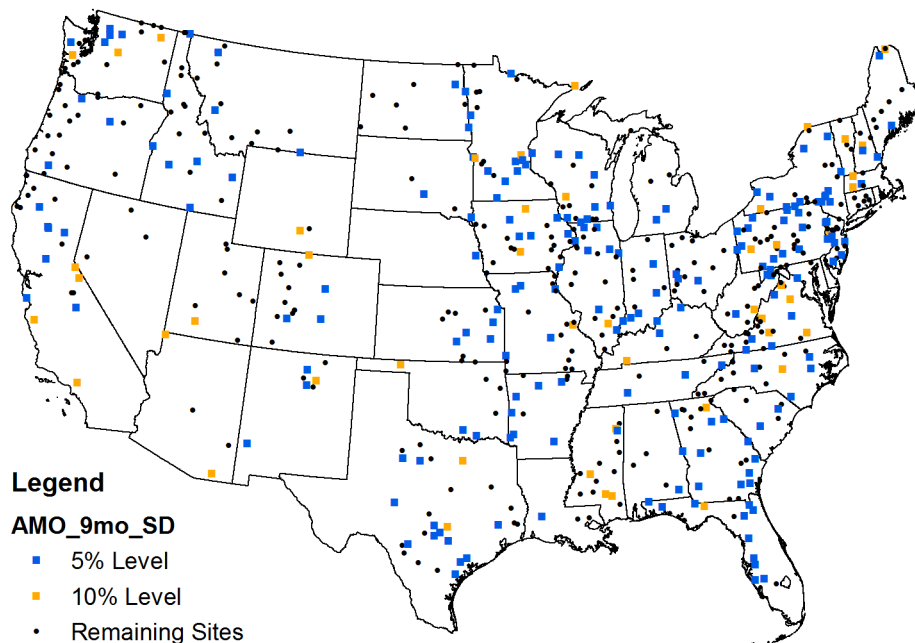


Figure F.2 Locations of sites with significant Kendall's tau correlation between 10-year moving standard deviation of log-transformed flood flows and 3-month average **AMO** anomalies with **9-month** lead.

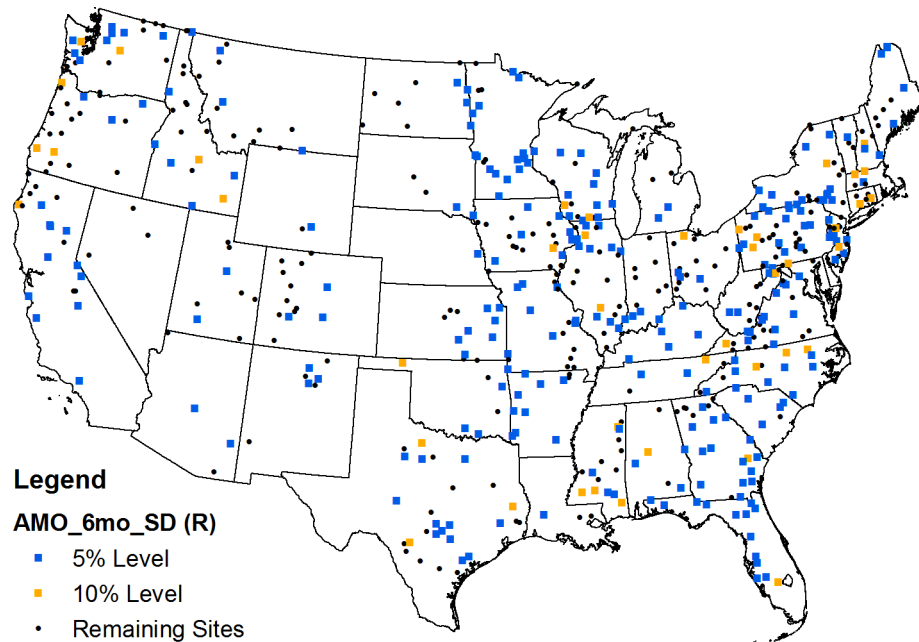


Figure F.3 Locations of sites with significant Pearson's r correlation between 10-year moving standard deviation of log-transformed flood flows and 3-month average AMO anomalies with **6-month** lead.

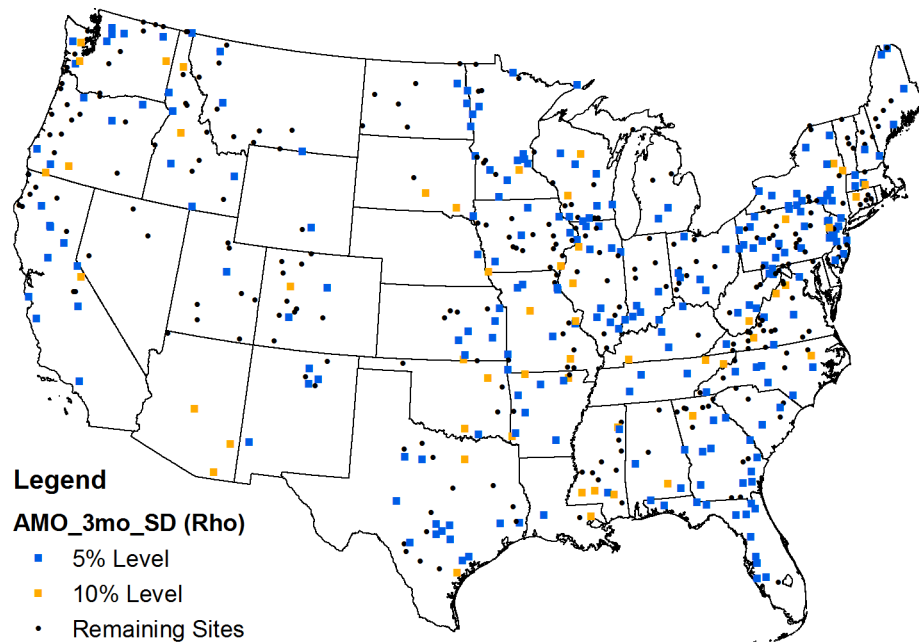


Figure F.4 Locations of sites with significant Spearman's ρ correlation between 10-year moving standard deviation of log-transformed flood flows and 3-month average AMO anomalies with **3-month** lead.

F.2 MEI Correlation Results

Table F.3

Results of Kendall's tau analyses (significant at 10% level) between 10-year moving standard deviation of log-transformed flood flows and 3-month average **MEI** anomalies with 3-, 6-, and 9-month leads.

Station Number	3-Month Lead		6-Month Lead		9-Month Lead	
	tau	p-value	tau	p-value	tau	p-value
1013500					-0.150	0.091
1055000					-0.154	0.083
1064500					-0.164	0.065
1127500					0.186	0.038
1137500					-0.155	0.084
1169000			-0.169	0.060	-0.170	0.058
1181000			-0.181	0.044	-0.182	0.043
1188000	-0.232	0.010	-0.219	0.014	-0.198	0.028
1196500	-0.158	0.077	-0.178	0.047		
1334500					-0.179	0.044
1372500			-0.149	0.093	-0.163	0.066
1381500	-0.251	0.005	-0.215	0.016	-0.227	0.011
1387500	-0.162	0.069				
1397500	-0.147	0.099				
1398500	-0.181	0.042	-0.165	0.063	-0.176	0.048
1399500	-0.174	0.050	-0.158	0.075	-0.152	0.087
1408500	0.154	0.084	0.173	0.052	0.249	0.005
1410000	0.148	0.096			0.212	0.017
1439500	-0.228	0.010	-0.219	0.014	-0.216	0.015
1440000					-0.154	0.084
1518000					-0.199	0.025
1520500					-0.172	0.053
1531000					-0.183	0.040
1541500					-0.159	0.074
1543500	-0.186	0.036	-0.207	0.020	-0.268	0.003
1560000					0.146	0.100
1580000	0.231	0.009	0.152	0.087		
1601500					0.196	0.027
1634000					0.147	0.097
2018000					0.183	0.040
2051500					0.157	0.077
2055000	0.156	0.079	0.161	0.071	0.202	0.023
2059500	0.232	0.009				
2061500					0.173	0.051
2074500	0.149	0.095				
2083000					0.188	0.034
2083500					0.173	0.051
2085500			0.202	0.023	0.199	0.025

Table F.3, continued

Station Number	3-Month Lead		6-Month Lead		9-Month Lead	
	tau	p-value	tau	p-value	tau	p-value
2102000			0.165	0.063	0.228	0.010
2131000			0.155	0.082		
2134500					0.183	0.040
2138500			0.162	0.069		
2154500					0.186	0.036
2156500	0.195	0.030	0.214	0.017	0.276	0.002
2213500			-0.152	0.087		
2320500	-0.181	0.042	-0.181	0.042	-0.253	0.004
2329000	-0.180	0.043	-0.186	0.036	-0.247	0.005
2333500			-0.214	0.016		
2361000					0.199	0.025
2431000					0.228	0.010
2474500					-0.212	0.017
2479000					-0.267	0.003
2486000					-0.189	0.034
3010500	-0.188	0.035	-0.212	0.017	-0.233	0.009
3011020	-0.179	0.045	-0.212	0.017	-0.274	0.002
3015500	-0.154	0.084	-0.185	0.037	-0.261	0.003
3020500					-0.179	0.044
3118500					-0.148	0.096
3164000			0.166	0.062		
3167000			0.211	0.017	0.221	0.013
3175500					0.161	0.070
3182500					0.231	0.009
3183500					0.152	0.087
3186500					0.240	0.007
3193000					-0.229	0.010
3198500					-0.196	0.027
3234500			-0.154	0.087	-0.255	0.004
3269500			-0.160	0.093	-0.206	0.030
3272000			-0.149	0.097	-0.227	0.011
3274000	-0.163	0.069	-0.174	0.053	-0.191	0.034
3275000	-0.160	0.071	-0.219	0.014	-0.189	0.034
3281500					-0.182	0.042
3294500	-0.176	0.050	-0.158	0.077	-0.199	0.027
3301500					0.207	0.021
3307000			-0.162	0.071		
3345500					-0.194	0.029
3360500					-0.152	0.087
3363500	-0.216	0.015	-0.234	0.008	-0.246	0.006
3379500					-0.171	0.055
3438000			0.174	0.053	0.235	0.009
3473000			0.180	0.043	0.201	0.024
3524000	0.150	0.091	0.184	0.038	0.160	0.072
3540500			0.159	0.073	0.147	0.099

Table F.3, continued

Station Number	3-Month Lead		6-Month Lead		9-Month Lead	
	tau	p-value	tau	p-value	tau	p-value
3550000	0.155	0.082	0.225	0.011	0.228	0.010
4105000					-0.161	0.071
4223000			-0.163	0.066	-0.168	0.058
4262500					-0.203	0.022
5053000					0.188	0.035
5062500	0.205	0.021	0.215	0.016	0.302	0.001
5082500					0.198	0.026
5112000	0.240	0.007	0.232	0.009	0.303	0.001
5131500					0.166	0.063
5133500			0.166	0.062	0.195	0.028
5286000	0.164	0.065				
5288500	0.168	0.058	0.156	0.079		
5293000					0.151	0.090
5316500			-0.147	0.099	-0.183	0.040
5394500			-0.167	0.061	-0.238	0.007
5399500	0.168	0.058	0.224	0.012	0.277	0.002
5412500	0.158	0.075	0.188	0.035	0.285	0.001
5418500					0.150	0.092
5436500					-0.226	0.012
5593000					-0.232	0.009
5597000			-0.153	0.086	-0.153	0.085
6191500	0.159	0.074	0.179	0.045	0.190	0.033
6192500	0.177	0.047	0.199	0.025	0.192	0.031
6214500	0.159	0.074	0.199	0.025	0.194	0.029
6289000			0.148	0.096	0.148	0.096
6335500					0.249	0.005
6337000					0.245	0.006
6340500					0.210	0.018
6478500			0.167	0.061	0.167	0.061
6600500			-0.149	0.093	-0.220	0.013
6606600			-0.162	0.069	-0.173	0.052
6620000	0.153	0.085	0.148	0.096	0.171	0.055
6630000	0.179	0.044	0.147	0.099	0.147	0.099
6635000	0.176	0.047	0.194	0.029	0.169	0.057
6864500	0.214	0.016	0.174	0.050	0.186	0.036
6889500	-0.146	0.100	-0.172	0.053	-0.172	0.053
7013000					0.147	0.099
7018500	0.149	0.093			0.186	0.036
7061500					0.177	0.046
7096000	0.204	0.022	0.183	0.039	0.206	0.021
7203000	0.288	0.002	0.180	0.053		
7247000					-0.216	0.015
7340000					-0.179	0.045
7375500			-0.167	0.060	-0.241	0.007
7378500					-0.157	0.078

Table F.3, continued

Station Number	3-Month Lead		6-Month Lead		9-Month Lead	
	tau	p-value	tau	p-value	tau	p-value
8032000					-0.150	0.091
8033500	-0.157	0.077	-0.194	0.029	-0.251	0.005
8041000	-0.227	0.011	-0.231	0.009	-0.324	0.000
8041500	-0.158	0.075	-0.159	0.073	-0.246	0.006
8070000	-0.183	0.039	-0.160	0.071	-0.171	0.055
8082000					0.176	0.047
8095000					0.214	0.016
8167000	0.193	0.030				
8167500					0.185	0.037
9110000	0.185	0.038	0.153	0.086	0.166	0.062
9112500	0.195	0.028	0.176	0.047	0.199	0.025
9119000					0.162	0.069
9132500	0.178	0.046	0.174	0.050	0.244	0.006
9147500	0.184	0.039			0.147	0.099
9180500	0.183	0.039	0.166	0.062	0.241	0.007
9251000	0.167	0.061	0.157	0.078	0.242	0.006
9304500	0.252	0.005	0.253	0.004	0.323	0.000
9310500	0.188	0.035	0.195	0.028	0.270	0.002
9315000	0.184	0.039	0.188	0.035	0.190	0.033
9448500	0.197	0.027				
9471000	0.189	0.034				
10128500	0.183	0.047	0.187	0.043	0.196	0.033
10131000	0.201	0.024	0.207	0.020	0.268	0.003
10234500	0.193	0.030	0.190	0.033	0.249	0.005
10312000					0.167	0.060
10329500	0.154	0.084				
10396000					0.160	0.072
11266500					-0.155	0.081
11383500			0.149	0.093	0.164	0.065
11402000	0.165	0.063	0.194	0.029	0.175	0.049
11413000	0.155	0.084				
11425500			0.193	0.030	0.167	0.060
11478500	0.224	0.012	0.275	0.002		
11501000					0.238	0.007
11530000	0.167	0.060	0.173	0.052		
12010000			0.171	0.054		
12020000	0.166	0.062	0.216	0.015		
12027500			0.250	0.005		
12039500			0.173	0.051		
12048000	0.245	0.006	0.205	0.021		
12054000	0.166	0.062	0.162	0.068		
12189500			0.155	0.081		
12306500					0.153	0.086
12413000					0.212	0.017
12459000					0.176	0.047

Table F.3, continued

Station Number	3-Month Lead		6-Month Lead		9-Month Lead	
	tau	p-value	tau	p-value	tau	p-value
13185000					0.215	0.015
13269000					0.272	0.002
13313000					0.188	0.035
13317000					0.195	0.028
14301000			0.208	0.019		
14301500	0.147	0.099	0.195	0.028		

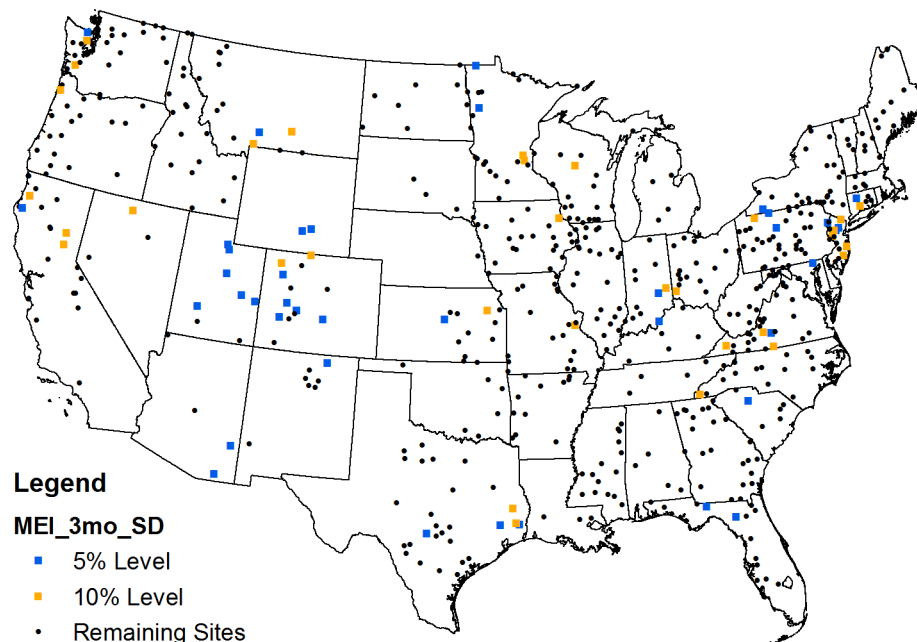


Figure F-5 Locations of sites with significant Kendall's tau correlation between 10-year moving standard deviation of log-transformed flood flows and 3-month average **MEI** anomalies with **3-month** lead.

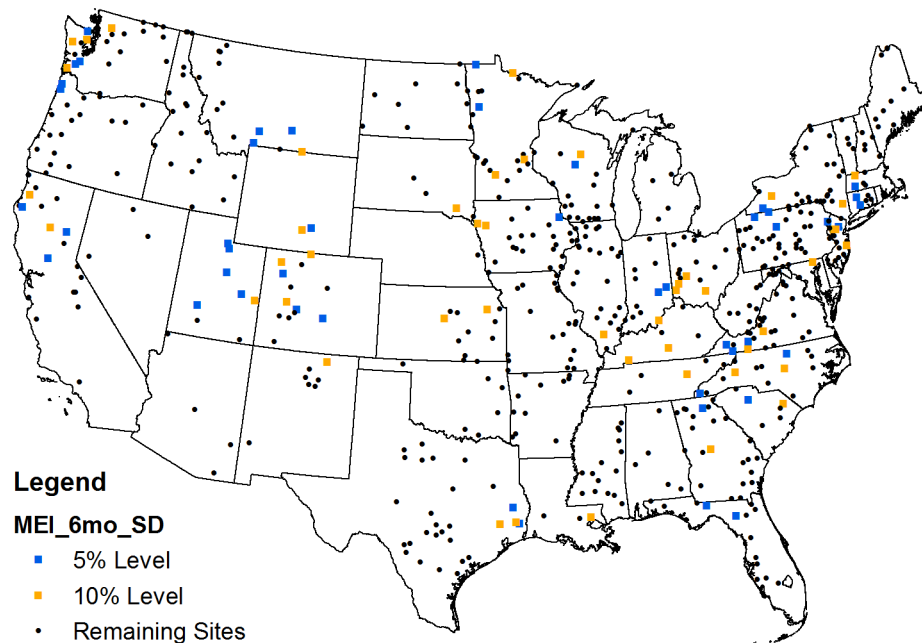


Figure F-6 Locations of sites with significant Kendall's tau correlation between 10-year moving standard deviation of log-transformed flood flows and 3-month average **MEI** anomalies with **6-month** lead.

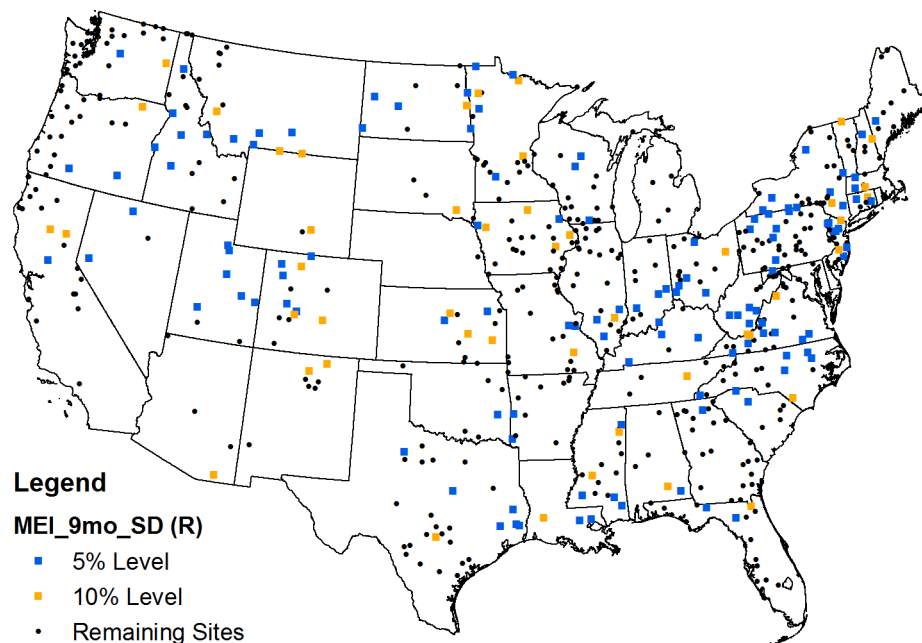


Figure F.7 Locations of sites with significant Pearson's r correlation between 10-year moving standard deviation of log-transformed flood flows and 3-month average **MEI** anomalies with **9-month** lead.

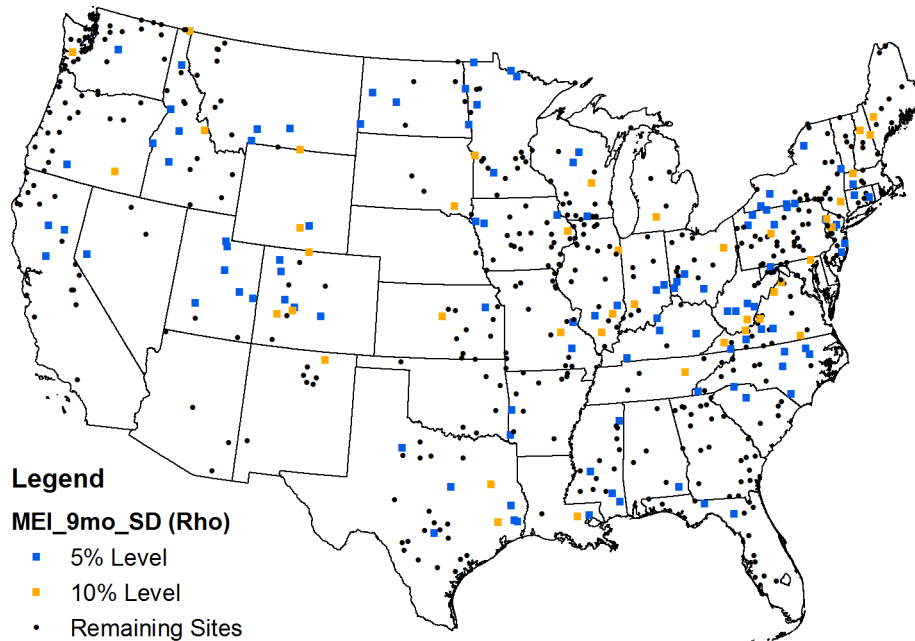


Figure F.8 Locations of sites with significant Spearman's rho correlation between 10-year moving standard deviation of log-transformed flood flows and 3-month average **MEI** anomalies with **9-month** lead.

F.3 NAO Correlation Results

Table F.4

Results of Kendall's tau analyses (significant at 10% level) between 10-year moving standard deviation of log-transformed flood flows and 3-month average **NAO** anomalies with 3-, 6-, and 9-month leads.

Station Number	3-Month Lead		6-Month Lead		9-Month Lead	
	tau	p-value	tau	p-value	tau	p-value
1038000	0.242	0.006				
1064500	-0.219	0.014			0.148	0.096
1137500	-0.267	0.003				
1142500			-0.181	0.044		
1144000					0.151	0.093
1334500	0.162	0.068				
1357500					0.149	0.093
1408500	0.190	0.032				
1414500			-0.179	0.044		
1514000			0.210	0.018		

Table F.4, continued

Station Number	3-Month Lead		6-Month Lead		9-Month Lead	
	tau	p-value	tau	p-value	tau	p-value
1538000					-0.150	0.091
1541000					-0.154	0.084
1555500					-0.188	0.035
1560000			0.171	0.054		
1567000					-0.198	0.026
1580000			0.313	0.000		
2059500			0.263	0.003		
2070000	0.183	0.040				
2074500			0.174	0.051		
2083000	0.170	0.056				
2126000					-0.158	0.075
2132000			-0.175	0.049		
2138500					0.318	0.000
2192000			-0.160	0.072		
2217500			-0.221	0.013		
2226000			-0.167	0.061		
2231000			-0.222	0.012		
2256500			-0.147	0.100		
2298830					-0.168	0.059
2303000			0.148	0.097		
2321500					-0.154	0.083
2333500					-0.252	0.005
2339500			-0.195	0.029		
2353500	-0.150	0.092				
2358000			-0.161	0.070		
2398000					0.165	0.064
2474500	-0.178	0.045				
2479000	-0.189	0.033				
2486000	-0.152	0.087				
2487500	0.165	0.064				
3032500	-0.186	0.036				
3102500					-0.153	0.086
3164000					0.317	0.000
3230500	-0.241	0.007				
3234500	-0.240	0.007				
3272000	-0.256	0.004				
3275000					-0.160	0.072
3301500			0.225	0.012		
3335500					0.155	0.082
3363500					-0.193	0.030
3379500	-0.154	0.083				
3381500	-0.191	0.032			-0.214	0.016
3434500					0.163	0.067
3540500					0.286	0.001
3550000					0.226	0.011

Table F.4, continued

Station Number	3-Month Lead		6-Month Lead		9-Month Lead	
	tau	p-value	tau	p-value	tau	p-value
4010500	-0.246	0.006				
4087000			-0.165	0.064		
4198000					0.147	0.099
4234000			0.167	0.061		
4262500					0.188	0.035
4275000			-0.185	0.038		
5062000			0.172	0.053		
5078000	-0.231	0.009				
5078500	-0.196	0.027				
5120500					-0.157	0.078
5280000					0.205	0.021
5286000					0.150	0.091
5288500					0.192	0.031
5291000					0.166	0.062
5300000					0.167	0.060
5313500					0.165	0.063
5317000			0.161	0.070	0.168	0.058
5330000	-0.231	0.009			0.197	0.027
5331000					0.184	0.038
5394500	-0.314	0.000			0.160	0.072
5399500	0.162	0.068				
5420500	-0.168	0.059				
5421000					0.153	0.086
5422000	-0.146	0.100	0.159	0.074		
5434500			0.158	0.076	0.194	0.029
5455500	-0.193	0.030				
5476000	-0.215	0.015			0.167	0.060
5484000	0.269	0.002				
5484500	0.400	0.000				
5486490	0.175	0.049				
5497000	0.328	0.000			0.204	0.028
5501000	0.257	0.004				
5527500			0.226	0.011		
5555300	-0.155	0.081	0.158	0.076		
5570000	0.246	0.006				
5585000	0.167	0.060				
5593000	-0.291	0.001				
6019500	0.191	0.032				
6191500	0.352	0.000				
6192500	0.346	0.000				
6207500	0.300	0.001				
6214500	0.239	0.007				
6289000	0.225	0.012				
6441500	0.298	0.001				
6478500	0.243	0.006				

Table F.4, continued

Station Number	3-Month Lead		6-Month Lead		9-Month Lead	
	tau	p-value	tau	p-value	tau	p-value
6485500					0.166	0.063
6630000	0.177	0.047				
6635000	0.191	0.032				
6710500	0.168	0.067				
6800500	-0.147	0.100			0.158	0.076
6809500	0.225	0.012				
6864500	0.305	0.001	0.230	0.010		
6869500	-0.168	0.058				
6889500	-0.269	0.002				
6933500					-0.185	0.038
7013000	0.240	0.007				
7061500	0.272	0.002				
7067000	0.206	0.020				
7068000	0.242	0.006				
7071500	0.175	0.049				
7074000			0.148	0.097		
7096000	0.180	0.043				
7144200					-0.194	0.029
7146500					-0.182	0.041
7176000	-0.148	0.097				
7180500	-0.278	0.002			-0.175	0.049
7183000					-0.201	0.024
7186000					-0.154	0.083
7187000	-0.195	0.028				
7196500	-0.153	0.086				
7203000	0.161	0.085	0.187	0.045		
7234000	0.153	0.085				
7247000	-0.327	0.000				
7331000					-0.239	0.007
7340000	-0.263	0.003				
7340500					0.184	0.039
8032000	-0.211	0.017				
8070000					-0.204	0.022
8082000	0.209	0.019				
8082500					-0.151	0.090
8085500			0.150	0.091		
8095000	0.324	0.000				
8153500					-0.160	0.072
8158000					-0.152	0.087
8167000			0.258	0.004	0.150	0.095
8195000			0.187	0.036	0.205	0.022
8205500	0.284	0.001				
8210000					-0.181	0.042
8276500					-0.151	0.089
8380500	-0.155	0.085	-0.163	0.069		

Table F.4, continued

Station Number	3-Month Lead		6-Month Lead		9-Month Lead	
	tau	p-value	tau	p-value	tau	p-value
9110000	0.243	0.006				
9119000	0.168	0.058				
9147500	0.217	0.015				
9180500	0.172	0.053				
9251000	0.146	0.100				
9304500	0.179	0.045				
9315000	0.229	0.010				
9379500	-0.214	0.016				
9415000			0.235	0.008		
9430500			0.234	0.008		
9448500	0.195	0.028	0.320	0.000		
9471000			0.173	0.052		
9508500			0.208	0.019		
10128500	0.305	0.001				
10131000	0.225	0.011				
10234500	0.171	0.055				
10312000	0.151	0.089				
10329500					0.163	0.067
11098000			-0.151	0.093		
11152000					-0.159	0.074
11160500			0.178	0.048		
11237500	-0.175	0.051				
11264500	-0.201	0.024				
11266500	-0.214	0.016				
11381500			0.166	0.062		
11383500			0.187	0.035		
11425500					0.162	0.068
11478500					0.167	0.060
11525500	-0.164	0.065			0.186	0.036
12010000					0.229	0.010
12020000					0.393	0.000
12027500					0.340	0.000
12048000					0.227	0.011
12054000					0.260	0.003
12056500					0.148	0.097
12134500	-0.211	0.018				
12186000	-0.210	0.018	-0.206	0.021		
12189500	-0.222	0.012	-0.175	0.049	0.205	0.021
12321500			-0.147	0.099		
12330000	0.326	0.000				
12332000	0.264	0.003				
12355500			-0.182	0.041		
12414500			-0.182	0.041		
12422500	0.148	0.096				
12451000					-0.169	0.057

Table F.4, continued

Station Number	3-Month Lead		6-Month Lead		9-Month Lead	
	tau	p-value	tau	p-value	tau	p-value
12459000	0.200	0.024				
13073000					0.153	0.085
13082500					0.239	0.007
13120500	0.223	0.012				
13139510	0.260	0.003				
13185000					0.206	0.021
13302500	0.309	0.000				
13313000	0.190	0.033				
13317000	0.220	0.013				
14113000	-0.176	0.047				
14301000					0.309	0.001
14301500					0.297	0.001
14306500					0.167	0.061
14325000					0.204	0.022

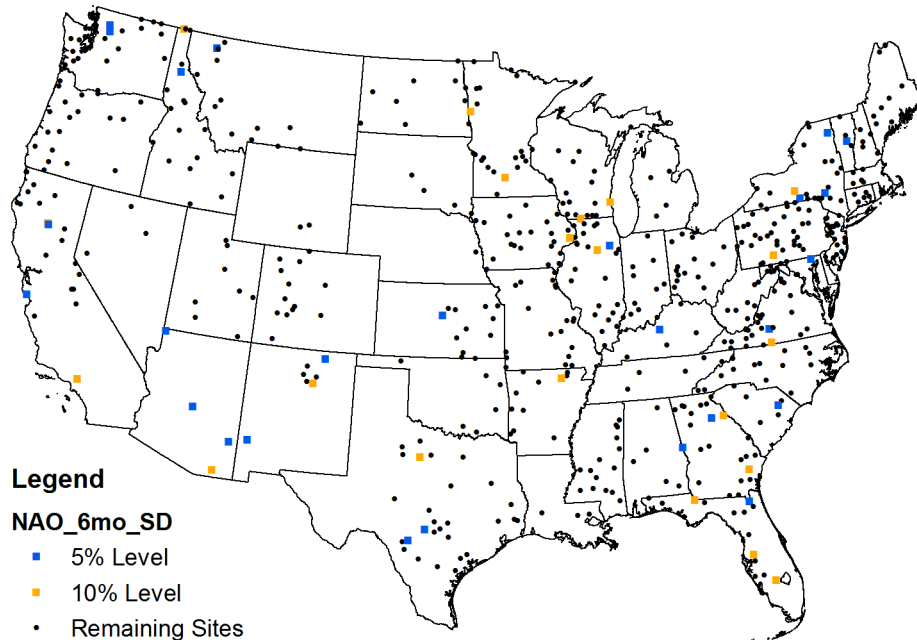


Figure F-9 Locations of sites with significant Kendall's tau correlation between 10-year moving standard deviation of log-transformed flood flows and 3-month average **NAO** anomalies with **6-month** lead.

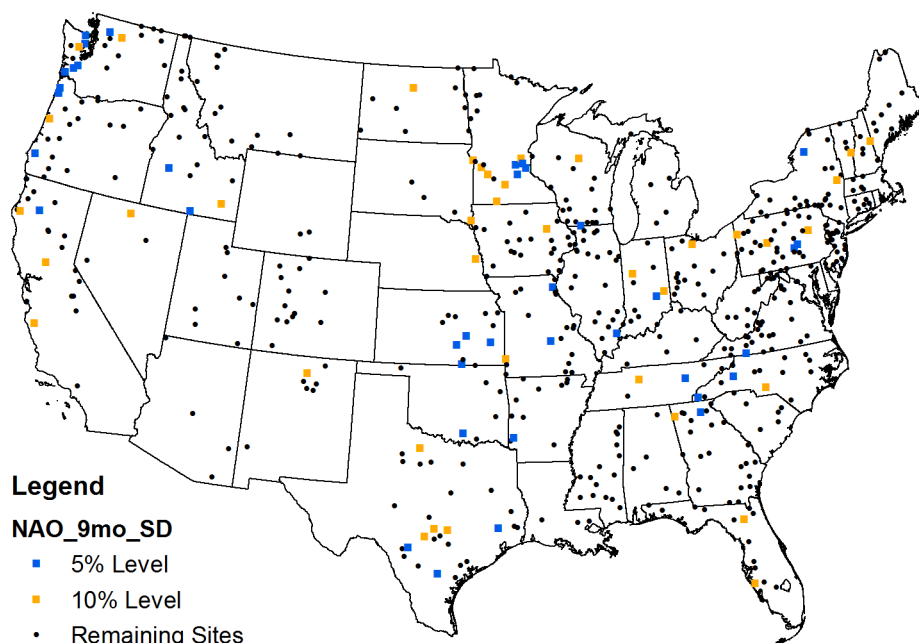


Figure F-10 Locations of sites with significant Kendall's tau correlation between 10-year moving standard deviation of log-transformed flood flows and 3-month average NAO anomalies with **9-month** lead.

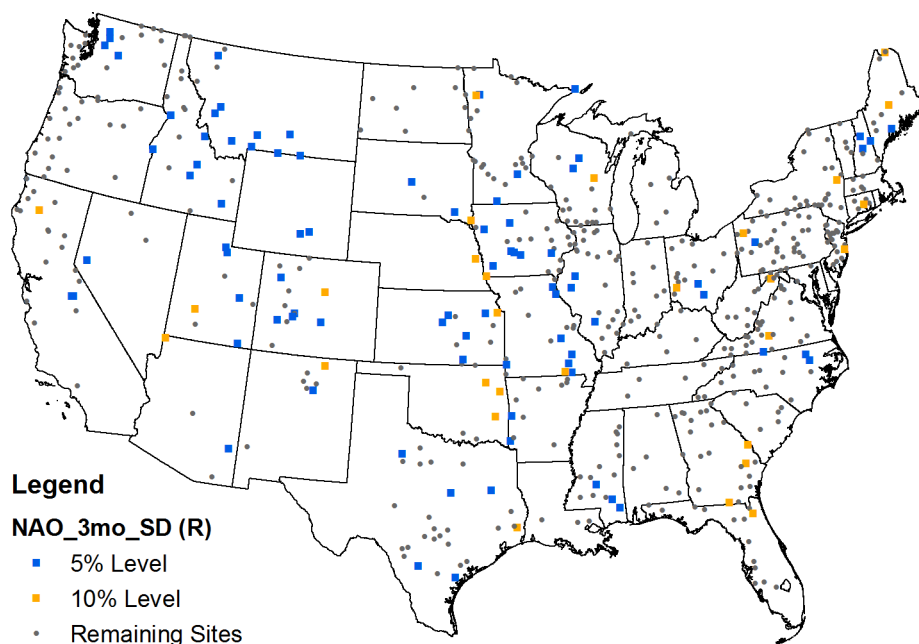


Figure F.11 Locations of sites with significant Pearson's r correlation between 10-year moving standard deviation of log-transformed flood flows and 3-month average NAO anomalies with **3-month** lead.

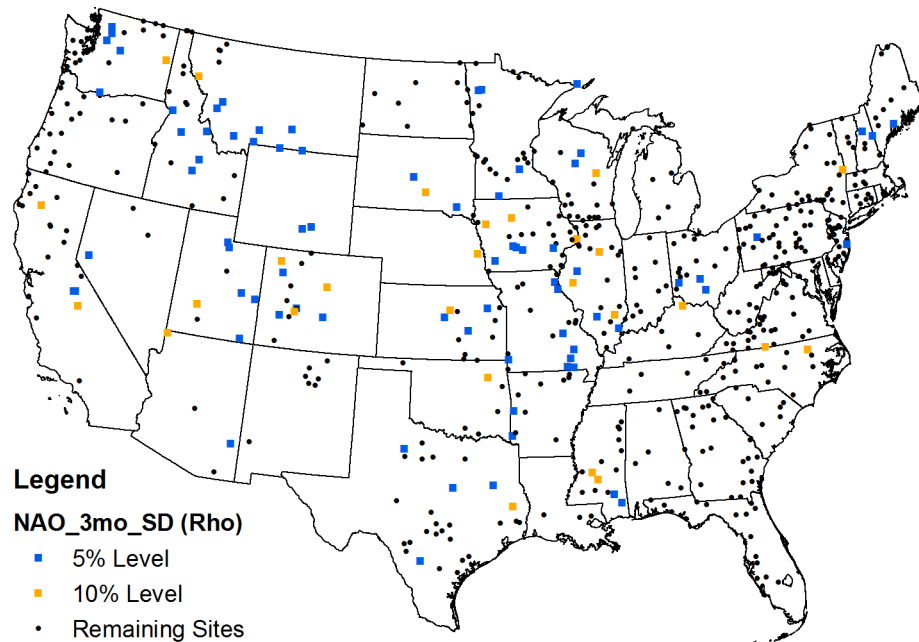


Figure F.12 Locations of sites with significant Spearman's rho correlation between 10-year moving standard deviation of log-transformed flood flows and 3-month average **NAO** anomalies with **3-month** lead.

F.4 NINO 3.4 Correlation Results

Table F.5

Results of Kendall's tau analyses (significant at 10% level) between 10-year moving standard deviation of log-transformed flood flows and 3-month average Nino3.4 anomalies with 3-, 6-, and 9-month leads.

Station Number	3-Month Lead		6-Month Lead		9-Month Lead	
	tau	p-value	tau	p-value	tau	p-value
1196500	-0.156	0.083	-0.184	0.041	-0.169	0.060
1381500	-0.155	0.081				
1541500					-0.161	0.071
1543500					-0.201	0.024
1548500					-0.147	0.099
2156500			0.173	0.054	0.160	0.075
2217500			0.192	0.031		
2320500					-0.190	0.033
2329000					-0.188	0.035
3010500			-0.202	0.023	-0.236	0.008
3011020			-0.157	0.078	-0.202	0.023
3262000			0.178	0.048	0.152	0.090
3488000	0.162	0.068				

Table F.5, continued

Station Number	3-Month Lead		6-Month Lead		9-Month Lead	
	tau	p-value	tau	p-value	tau	p-value
4223000					-0.154	0.083
5062500					0.147	0.097
5078500					0.147	0.097
5112000	0.187	0.036	0.169	0.057	0.219	0.014
5133500			0.177	0.047	0.185	0.038
5280000					0.151	0.090
5412500					0.196	0.028
5418500					0.155	0.082
5431486			-0.147	0.097		
6214500			0.167	0.061	0.168	0.059
6289000					0.171	0.054
6620000			0.149	0.095	0.216	0.015
6630000			0.170	0.056	0.213	0.016
6635000			0.156	0.079	0.165	0.063
7096000			0.170	0.056	0.179	0.044
7203000	0.221	0.018				
7375500					-0.166	0.063
8033500			-0.160	0.071	-0.201	0.024
8041000			-0.148	0.097	-0.186	0.036
8041500					-0.177	0.047
8070000					-0.165	0.064
8167000	0.154	0.083				
8167500					0.162	0.068
9180500					0.153	0.085
9304500			0.190	0.033	0.160	0.072
9315000					0.175	0.049
10329500			0.161	0.070		
10396000					0.158	0.075
12035000	0.158	0.075			-0.149	0.093
12048000	0.192	0.031				
13269000					0.206	0.020

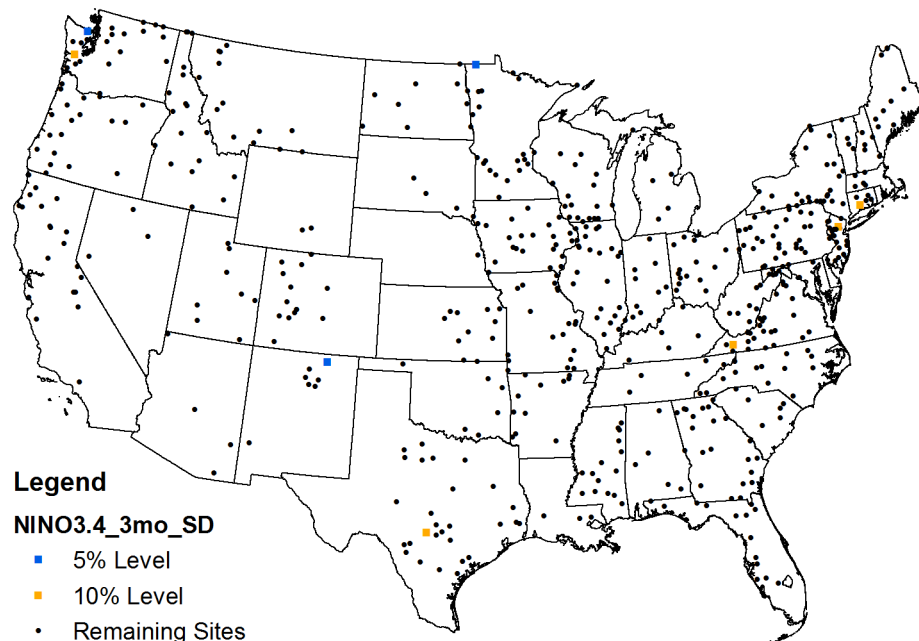


Figure F-13 Locations of sites with significant Kendall's tau correlation between 10-year moving standard deviation of log-transformed flood flows and 3-month average **Nino3.4** anomalies with **3-month** lead.

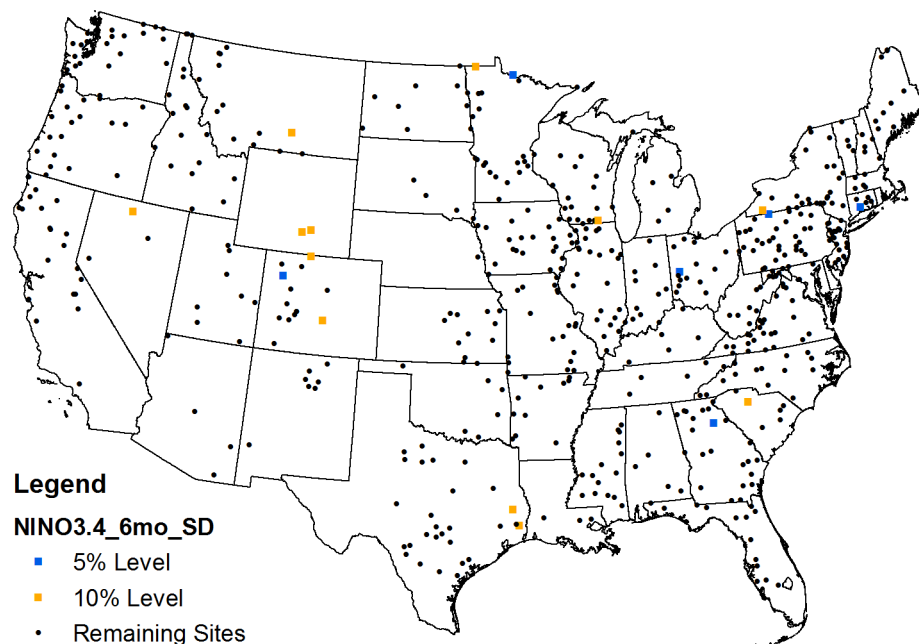


Figure F-14 Locations of sites with significant Kendall's tau correlation between 10-year moving standard deviation of log-transformed flood flows and 3-month average **Nino3.4** anomalies with **6-month** lead.

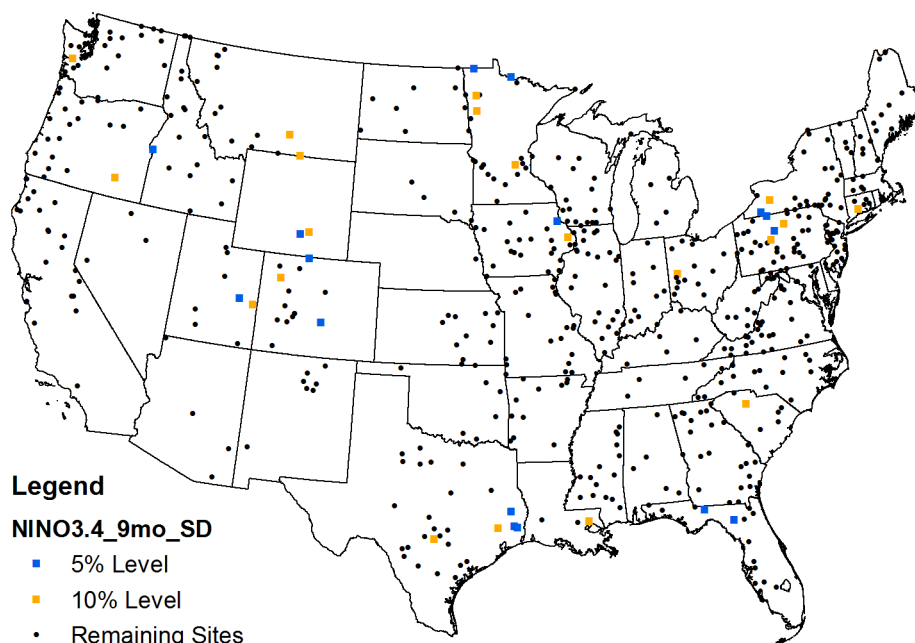


Figure F-15 Locations of sites with significant Kendall's tau correlation between 10-year moving standard deviation of log-transformed flood flows and 3-month average **Nino3.4** anomalies with **9-month** lead.

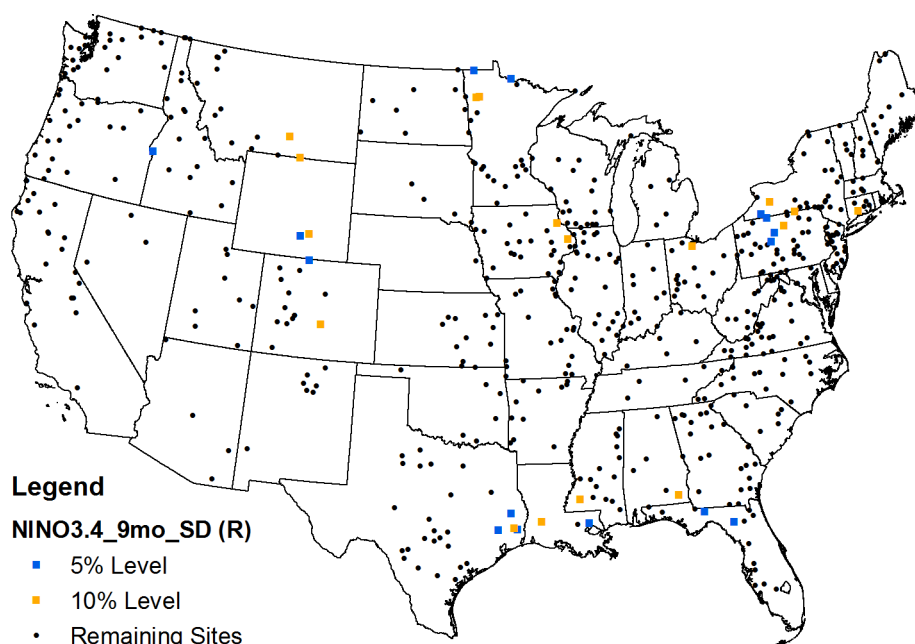


Figure F.16 Locations of sites with significant Pearson's r correlation between 10-year moving standard deviation of log-transformed flood flows and 3-month average **Nino3.4** anomalies with **9-month** lead.

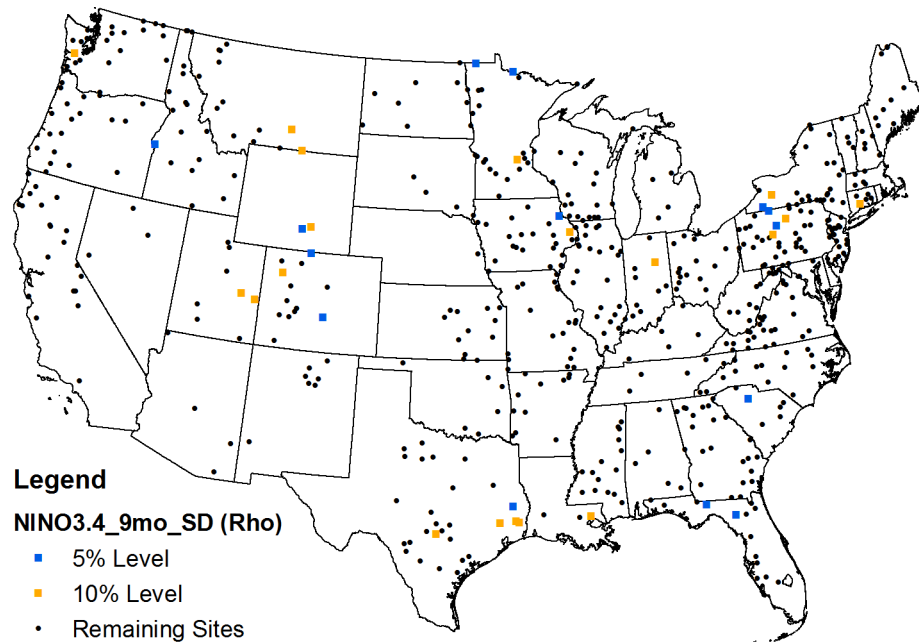


Figure F.17 Locations of sites with significant Spearman's rho correlation between 10-year moving standard deviation of log-transformed flood flows and 3-month average **Nino3.4** anomalies with **9-month** lead.

F.5 PDO Correlations Results

Table F.6

Results of Kendall's tau analyses (significant at 10% level) between 10-year moving standard deviation of log-transformed flood flows and 3-month average PDO anomalies with 3-, 6-, and 9-month leads.

Station Number	3-Month Lead		6-Month Lead		9-Month Lead	
	tau	p-value	tau	p-value	tau	p-value
1030500					0.187	0.036
1038000	0.175	0.049	0.277	0.002	0.231	0.009
1055000	-0.196	0.027	-0.167	0.061		
1057000					0.173	0.051
1064500			-0.160	0.071	-0.189	0.033
1073000			-0.171	0.056		
1127500	0.157	0.081	0.220	0.014	0.301	0.001
1137500					-0.210	0.019
1142500					-0.186	0.038
1169000	-0.223	0.013	-0.182	0.043	-0.156	0.083
1175500					0.164	0.068
1176000	-0.154	0.085				
1181000	-0.260	0.004	-0.226	0.012	-0.159	0.076

Table F.6, continued

Station Number	3-Month Lead		6-Month Lead		9-Month Lead	
	tau	p-value	tau	p-value	tau	p-value
1188000	-0.223	0.013	-0.237	0.008	-0.206	0.021
1334500					-0.296	0.001
1350000	-0.210	0.018	-0.206	0.021	-0.201	0.024
1372500			-0.178	0.046	-0.235	0.008
1381500	-0.229	0.010	-0.319	0.000	-0.276	0.002
1387500					-0.147	0.099
1397500			-0.179	0.045		
1398000	-0.153	0.086	-0.151	0.090		
1398500	-0.195	0.028	-0.235	0.008	-0.226	0.011
1399500			-0.149	0.093	-0.164	0.065
1408500	0.296	0.001	0.261	0.003	0.262	0.003
1410000	0.283	0.001	0.343	0.000	0.294	0.001
1411000	0.167	0.060				
1411500					0.187	0.035
1420500	-0.150	0.092	-0.151	0.089		
1421000	-0.170	0.056	-0.171	0.055		
1439500	-0.238	0.007	-0.292	0.001	-0.208	0.019
1440000			-0.175	0.049		
1445500					-0.176	0.047
1459500					0.176	0.047
1518000					-0.218	0.014
1520500					-0.215	0.016
1531000					-0.262	0.003
1532000	0.179	0.044	0.187	0.036		
1541500					-0.234	0.008
1543500	-0.203	0.022	-0.251	0.005	-0.374	0.000
1548500					-0.192	0.031
1560000			0.223	0.012	0.182	0.041
1568000			0.252	0.005		
1580000	0.276	0.002	0.282	0.002	0.159	0.074
1599000	-0.147	0.097			-0.159	0.073
1601500			0.209	0.019	0.250	0.005
1632000			0.205	0.021	0.172	0.053
1634000			0.198	0.026	0.193	0.030
2013000					-0.155	0.082
2018000			0.167	0.060	0.174	0.050
2045500			0.213	0.017		
2051500			0.196	0.027	0.180	0.043
2055000			0.288	0.001	0.221	0.013
2059500	0.285	0.001	0.194	0.029	0.184	0.039
2061500			0.210	0.018	0.172	0.053
2070000	0.167	0.061	0.226	0.011		
2074500	0.240	0.007	0.161	0.071	0.257	0.004
2083000	0.202	0.023	0.279	0.002	0.313	0.000
2083500	0.153	0.085	0.222	0.013	0.279	0.002

Table F.6, continued

Station Number	3-Month Lead		6-Month Lead		9-Month Lead	
	tau	p-value	tau	p-value	tau	p-value
2085500	0.179	0.045	0.265	0.003	0.292	0.001
2102000	0.168	0.059	0.252	0.005	0.269	0.002
2116500			0.192	0.031		
2131000			0.149	0.093		
2134500					0.198	0.026
2138500			0.199	0.025	0.208	0.019
2154500			0.189	0.034	0.208	0.019
2156500	0.160	0.074	0.272	0.002	0.291	0.001
2198000	-0.190	0.032	-0.180	0.043		
2202500	-0.152	0.087				
2213500	-0.220	0.013	-0.278	0.002	-0.201	0.024
2226000	-0.197	0.026	-0.192	0.031	-0.176	0.047
2228000	-0.149	0.095	-0.183	0.039		
2231000	-0.192	0.031	-0.159	0.073	-0.188	0.034
2301500			-0.190	0.033	-0.193	0.030
2313000					-0.158	0.076
2320500	-0.168	0.059	-0.211	0.017	-0.322	0.000
2321500					-0.207	0.020
2329000	-0.180	0.043	-0.226	0.011	-0.302	0.001
2333500	-0.156	0.079	-0.327	0.000	-0.275	0.002
2339500	-0.193	0.030				
2347500	-0.180	0.043				
2358000	-0.155	0.081				
2361000					0.187	0.036
2371500					-0.210	0.018
2375500	-0.237	0.008	-0.252	0.005	-0.201	0.024
2431000	0.192	0.031	0.284	0.001	0.360	0.000
2437000	0.176	0.048	0.226	0.011	0.231	0.009
2441000			0.162	0.069		
2474500	-0.156	0.079	-0.164	0.065	-0.283	0.001
2479000	-0.267	0.003	-0.272	0.002	-0.374	0.000
2488500			0.179	0.045	0.207	0.020
3010500			-0.171	0.055	-0.260	0.003
3011020	-0.175	0.049	-0.232	0.009	-0.332	0.000
3015500	-0.320	0.000	-0.344	0.000	-0.352	0.000
3020500	-0.164	0.064	-0.213	0.017	-0.235	0.008
3024000			-0.188	0.034		
3049500	-0.187	0.035				
3102500	-0.228	0.010			-0.149	0.093
3106000	-0.168	0.059				
3109500	-0.253	0.005	-0.210	0.019		
3118500			-0.226	0.011	-0.222	0.012
3144000			-0.150	0.094		
3164000	0.188	0.035	0.209	0.019	0.220	0.013
3167000	0.196	0.027	0.241	0.007	0.249	0.005

Table F.6, continued

Station Number	3-Month Lead		6-Month Lead		9-Month Lead	
	tau	p-value	tau	p-value	tau	p-value
3170000			0.165	0.063		
3175500			0.159	0.073	0.172	0.053
3182500	0.216	0.015	0.337	0.000	0.305	0.001
3183500	0.152	0.087	0.275	0.002	0.207	0.020
3186500	0.224	0.012	0.347	0.000	0.352	0.000
3193000	-0.178	0.045	-0.266	0.003	-0.302	0.001
3198500	-0.175	0.049	-0.208	0.019	-0.267	0.003
3230500			-0.237	0.008	-0.189	0.035
3234500	-0.211	0.019	-0.274	0.002	-0.309	0.001
3266000					-0.148	0.099
3269500			-0.183	0.054	-0.209	0.028
3272000					-0.202	0.024
3274000			-0.185	0.039	-0.217	0.016
3275000			-0.261	0.003	-0.314	0.000
3281500					-0.181	0.044
3294500	-0.174	0.052	-0.307	0.001	-0.258	0.004
3301500	0.249	0.005	0.316	0.000	0.274	0.002
3339500					-0.191	0.032
3345500			-0.174	0.050	-0.261	0.003
3360500	-0.209	0.019	-0.260	0.003	-0.256	0.004
3363500	-0.255	0.004	-0.319	0.000	-0.375	0.000
3374000			-0.164	0.065		
3377500			-0.166	0.063		
3379500			-0.158	0.075		
3381500			-0.163	0.067		
3438000	0.224	0.012	0.233	0.009	0.341	0.000
3465500					0.181	0.042
3473000	0.191	0.032	0.224	0.012	0.273	0.002
3504000	-0.162	0.069	-0.177	0.047	-0.154	0.084
3524000	0.230	0.010	0.312	0.000	0.226	0.011
3540500	0.294	0.001	0.189	0.033	0.174	0.050
3550000	0.155	0.081	0.231	0.009	0.346	0.000
3604000			0.188	0.035		
4073500			-0.156	0.082	-0.208	0.021
4079000			-0.176	0.050		
4087000	-0.167	0.061	-0.201	0.024		
4105000					-0.179	0.044
4121500	-0.161	0.071				
4142000	-0.151	0.090				
4198000			0.186	0.037	0.183	0.039
4214500					-0.193	0.030
4223000					-0.234	0.009
4234000			0.178	0.046		
4264331	-0.165	0.063			-0.172	0.053
4293500	0.155	0.084				

Table F.6, continued

Station Number	3-Month Lead		6-Month Lead		9-Month Lead	
	tau	p-value	tau	p-value	tau	p-value
5053000	0.242	0.006	0.313	0.000	0.290	0.001
5062500	0.345	0.000	0.373	0.000	0.336	0.000
5066500	0.194	0.029	0.246	0.006	0.232	0.009
5082500	0.204	0.022	0.249	0.005	0.203	0.022
5100000	0.243	0.006	0.175	0.049		
5112000	0.293	0.001	0.342	0.000	0.290	0.001
5131500	0.177	0.047				
5133500	0.263	0.003			0.148	0.096
5286000	0.151	0.089	0.215	0.016	0.185	0.038
5288500	0.215	0.016	0.269	0.002	0.149	0.095
5293000			0.178	0.046	0.194	0.029
5316500	-0.168	0.059	-0.219	0.014	-0.208	0.019
5394500	-0.154	0.083	-0.180	0.043	-0.291	0.001
5399500	0.284	0.001	0.323	0.000	0.323	0.000
5408000					-0.179	0.045
5410490					-0.170	0.057
5412500			0.204	0.022	0.336	0.000
5418500					0.207	0.020
5420500			0.164	0.065		
5426000					-0.167	0.060
5436500	-0.219	0.015	-0.316	0.000	-0.293	0.001
5454500	-0.216	0.015			-0.219	0.014
5459500			0.178	0.046	0.165	0.063
5464500	-0.207	0.020	-0.178	0.046	-0.171	0.055
5482500	0.232	0.009			0.153	0.086
5484000	0.261	0.003			0.148	0.096
5484500	0.258	0.004			0.250	0.005
5490500	-0.161	0.071				
5497000					0.217	0.020
5500000			0.171	0.055		
5501000					0.161	0.071
5520500			0.193	0.030		
5555300					-0.177	0.047
5572000	-0.186	0.036	-0.196	0.027	-0.216	0.015
5593000	-0.249	0.005	-0.198	0.026	-0.271	0.002
5597000			-0.219	0.014	-0.182	0.041
6019500					0.181	0.042
6191500	0.313	0.000	0.159	0.074	0.295	0.001
6192500	0.286	0.001	0.177	0.047	0.302	0.001
6207500	0.348	0.000	0.173	0.051	0.251	0.005
6214500	0.352	0.000	0.159	0.074	0.256	0.004
6289000	0.185	0.037			0.164	0.065
6335500	0.263	0.003	0.313	0.000	0.380	0.000
6337000	0.223	0.012	0.309	0.001	0.376	0.000
6340500			0.179	0.045	0.157	0.077

Table F.6, continued

Station Number	3-Month Lead		6-Month Lead		9-Month Lead	
	tau	p-value	tau	p-value	tau	p-value
6441500	0.167	0.061	0.195	0.028	0.288	0.001
6452000	0.254	0.004	0.263	0.003	0.266	0.003
6478500	0.326	0.000	0.220	0.013	0.291	0.001
6600500			-0.234	0.008	-0.283	0.001
6606600	-0.179	0.045	-0.183	0.040	-0.214	0.016
6620000	0.235	0.008			0.155	0.082
6630000	0.178	0.046			0.216	0.015
6635000	0.230	0.010	0.168	0.058	0.263	0.003
6864500	0.345	0.000	0.213	0.017	0.227	0.011
6869500	-0.211	0.018	-0.149	0.095		
6889500	-0.180	0.043			-0.202	0.023
6892000	-0.207	0.020	-0.171	0.054	-0.151	0.089
6913500	-0.303	0.001	-0.254	0.004	-0.225	0.011
7013000	0.247	0.005	0.188	0.034	0.175	0.049
7016500	0.151	0.090			0.205	0.021
7018500	0.322	0.000	0.289	0.001	0.271	0.002
7019000			0.168	0.058		
7061500	0.263	0.003	0.228	0.010	0.222	0.012
7074000			0.260	0.003		
7096000	0.306	0.001	0.190	0.032	0.239	0.007
7146500	-0.251	0.005			-0.223	0.012
7180500	-0.274	0.002	-0.237	0.008	-0.291	0.001
7183000	-0.180	0.043	-0.220	0.013		
7187000	-0.206	0.021				
7203000	0.248	0.008	0.183	0.049	0.194	0.037
7218000					-0.178	0.047
7234000	0.182	0.041				
7247000	-0.267	0.003	-0.167	0.061	-0.310	0.000
7247500	-0.240	0.007				
7252000			0.223	0.012		
7261500	0.223	0.012	0.234	0.008		
7291000			-0.159	0.073	-0.163	0.067
7340000	-0.180	0.043			-0.272	0.002
7375500	-0.175	0.049	-0.223	0.012	-0.187	0.035
7378500					-0.211	0.017
8013500	-0.149	0.095				
8032000	-0.249	0.005	-0.192	0.031	-0.246	0.006
8033500	-0.275	0.002	-0.179	0.044	-0.254	0.004
8041000	-0.327	0.000	-0.357	0.000	-0.314	0.000
8041500					-0.166	0.063
8055500			0.189	0.033	0.181	0.042
8070000	-0.258	0.004	-0.202	0.023	-0.203	0.022
8082000					0.159	0.073
8082500	0.210	0.018			0.147	0.099
8085500	0.168	0.059	0.289	0.001	0.210	0.018

Table F.6, continued

Station Number	3-Month Lead		6-Month Lead		9-Month Lead	
	tau	p-value	tau	p-value	tau	p-value
8088000			0.184	0.039	0.175	0.049
8095000	0.279	0.002	0.203	0.022	0.249	0.005
8128000			0.219	0.014		
8167000	0.185	0.038	0.271	0.002	0.163	0.069
8167500	0.155	0.081			0.159	0.073
8171000			-0.194	0.029		
8189500			-0.321	0.000	-0.220	0.014
8190000			-0.252	0.005		
8205500	0.163	0.066			0.220	0.013
8210000			-0.153	0.085		
8276500			-0.159	0.073		
8291000	0.219	0.015	0.194	0.030		
9085000	0.170	0.057				
9110000	0.366	0.000	0.196	0.027	0.283	0.001
9112500	0.465	0.000	0.285	0.001	0.272	0.002
9119000	0.306	0.001	0.232	0.009	0.305	0.001
9132500	0.345	0.000	0.266	0.003	0.303	0.001
9147500	0.243	0.006	0.231	0.009	0.284	0.001
9180500	0.297	0.001	0.219	0.014	0.312	0.000
9239500	0.277	0.002	0.210	0.018	0.197	0.027
9251000	0.347	0.000	0.249	0.005	0.355	0.000
9304500	0.391	0.000	0.299	0.001	0.363	0.000
9310500	0.328	0.000	0.255	0.004	0.301	0.001
9315000	0.272	0.002	0.152	0.087	0.258	0.004
9379500					-0.162	0.069
9430500	0.163	0.066				
9448500	0.293	0.001	0.154	0.083	0.180	0.043
9471000	0.389	0.000	0.361	0.000		
9508500	0.359	0.000	0.280	0.002	0.204	0.022
10128500	0.299	0.001	0.168	0.068	0.304	0.001
10131000	0.342	0.000	0.273	0.002	0.416	0.000
10234500	0.291	0.001	0.215	0.015	0.236	0.008
10296000	0.201	0.024				
10310000			-0.223	0.012	-0.153	0.086
10312000	0.205	0.021	0.166	0.063	0.236	0.008
10329500					0.157	0.077
11264500			-0.183	0.040	-0.168	0.058
11367500					0.168	0.058
11381500	0.190	0.033	0.161	0.070	0.259	0.004
11383500	0.206	0.020	0.218	0.014	0.337	0.000
11402000	0.188	0.034	0.214	0.016	0.306	0.001
11413000	0.160	0.074			0.221	0.014
11425500	0.250	0.005	0.242	0.006	0.343	0.000
11477000					0.216	0.015
11478500	0.201	0.024	0.206	0.020	0.370	0.000

Table F.6, continued

Station Number	3-Month Lead		6-Month Lead		9-Month Lead	
	tau	p-value	tau	p-value	tau	p-value
11501000	0.208	0.019	0.197	0.027	0.209	0.019
11522500					0.168	0.058
11530000					0.259	0.004
12010000			0.148	0.096		
12020000	0.217	0.015	0.227	0.011	0.157	0.077
12027500	0.174	0.050	0.220	0.013	0.208	0.019
12039500			0.260	0.003	0.192	0.031
12048000	0.262	0.003	0.219	0.014	0.168	0.058
12054000	0.286	0.001	0.271	0.002	0.251	0.005
12056500	0.164	0.065				
12186000	0.167	0.060	0.213	0.017		
12189500			0.200	0.024		
12306500	0.190	0.032				
12330000	0.284	0.001	0.257	0.004	0.326	0.000
12332000	0.217	0.015			0.159	0.073
12354500	0.178	0.045				
12401500	-0.227	0.011	-0.252	0.005	-0.285	0.001
12404500	-0.183	0.040	-0.229	0.010	-0.293	0.001
12413000	0.240	0.007	0.239	0.007	0.210	0.018
12422500	0.226	0.011	0.154	0.083		
12459000	0.189	0.033			0.157	0.077
12488500	0.256	0.004				
13037500	0.269	0.002				
13185000	0.271	0.002	0.232	0.009	0.178	0.045
13269000	0.153	0.086			0.246	0.006
13302500	0.245	0.006			0.223	0.012
13313000	0.275	0.002	0.197	0.026	0.193	0.030
13317000	0.236	0.008	0.214	0.016	0.206	0.021
13342500					-0.175	0.049
14020000			0.156	0.079		
14105700	0.191	0.032				
14113000					0.193	0.030
14154500					0.191	0.032
14185000					0.184	0.038
14301000	0.189	0.033	0.228	0.010	0.230	0.010
14301500	0.222	0.013	0.204	0.022	0.248	0.005
14308000					0.207	0.020
14325000			0.150	0.091	0.206	0.021
14359000					0.182	0.041

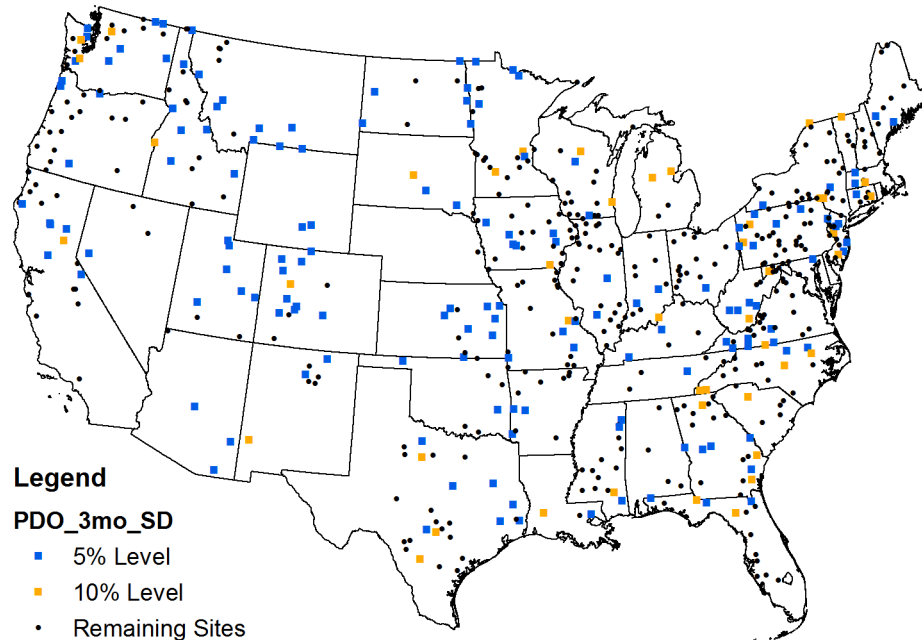


Figure F-18 Locations of sites with significant Kendall's tau correlation between 10-year moving standard deviation of log-transformed flood flows and 3-month average **PDO** anomalies with **3-month** lead.

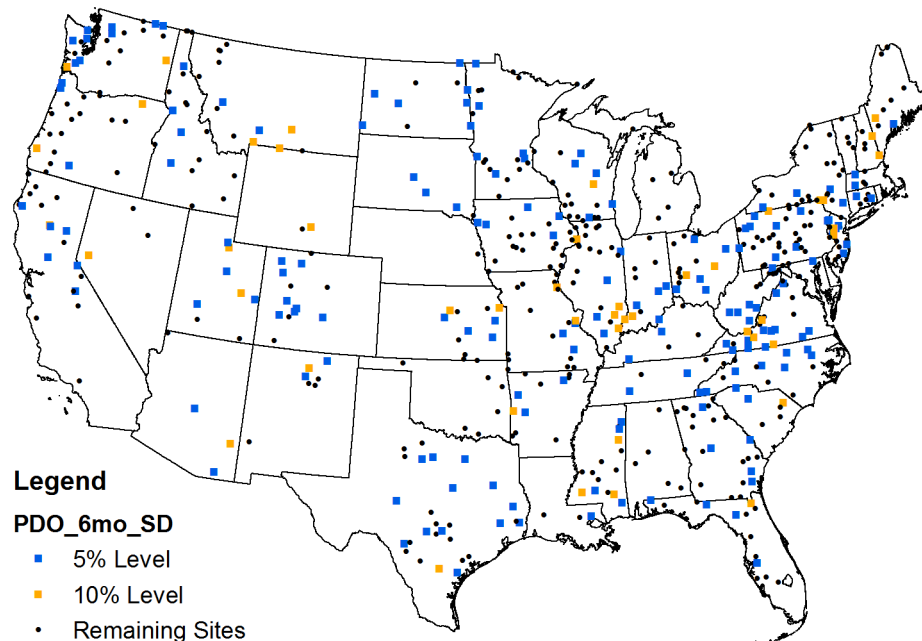


Figure F-19 Locations of sites with significant Kendall's tau correlation between 10-year moving standard deviation of log-transformed flood flows and 3-month average **PDO** anomalies with **6-month** lead.

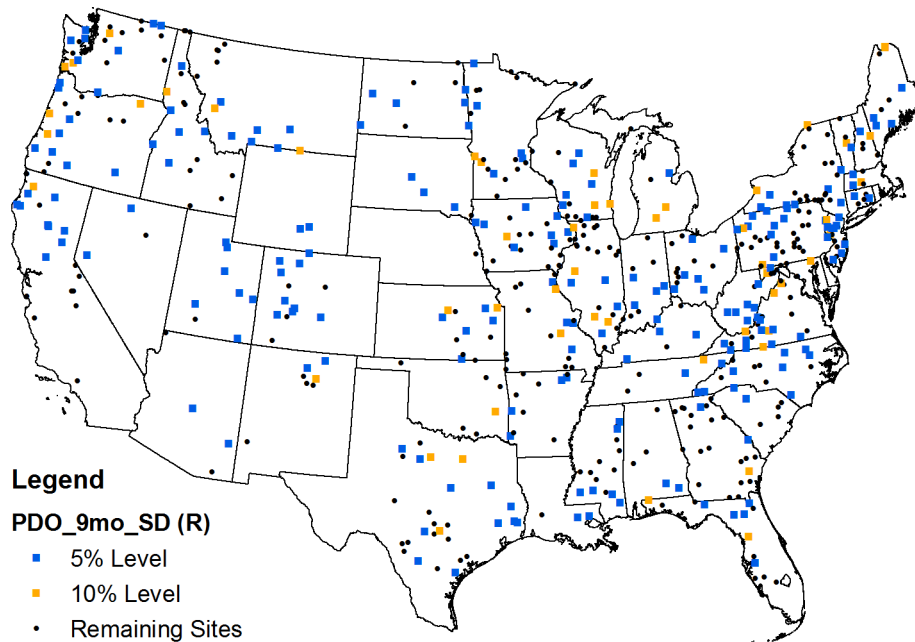


Figure F.20 Locations of sites with significant Pearson's r correlation between 10-year moving standard deviation of log-transformed flood flows and 3-month average **PDO** anomalies with **9-month** lead.

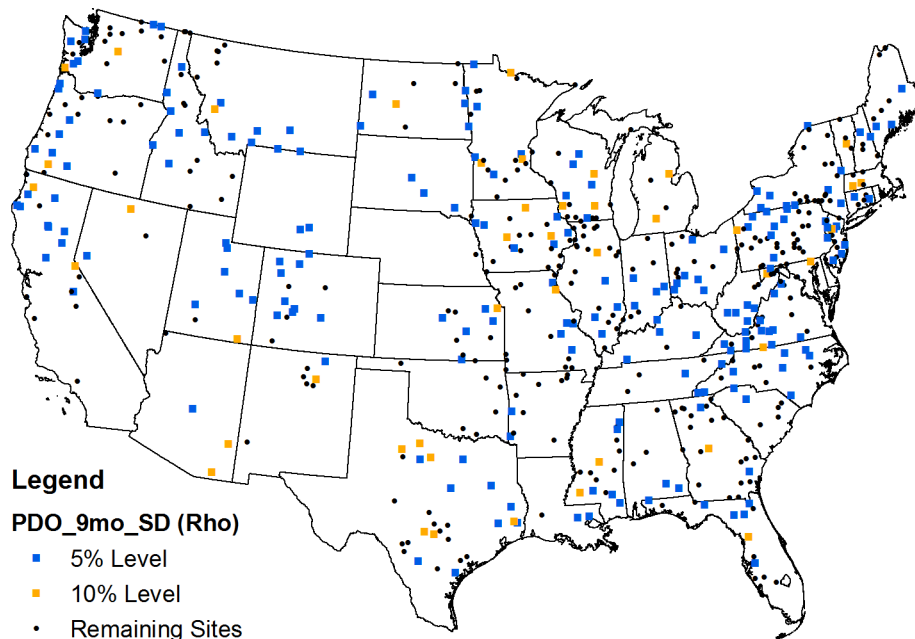


Figure F.21 Locations of sites with significant Spearman's ρ correlation between 10-year moving standard deviation of log-transformed flood flows and 3-month average **PDO** anomalies with **9-month** lead.

APPENDIX G CORRELATION ANALYSIS RESULTS BETWEEN ANNUAL MAXIMUM FLOOD SERIES AND FLOOD GENERATING HYDROCLIMATIC SERIES

This appendix summarizes results of Pearson's correlation analyses between annual maximum flood (AMF) series and the associated flood generating precipitation and temperature series constructed using 1/8 degree gridded data and the best X-day lead time as described in Chapter 3. The association between temperature and AMF series is assessed with respect to both the magnitude and timing of AMF peaks. Only sites for which results are significant on the 10% level are included in the following tables (results significant on the 5% level are in **bold**). Results are omitted (blank spaces) when p-values greater than 10% level were obtained.

Table G.1
Results of Pearson's correlation analyses between magnitude of AMF peaks and associated flood generating hydroclimatic series with best lead times.

Site Number	Precipitation			Maximum Temperature			Minimum Temperature		
	Lead Time (days)	r	p-value	Lead Time (days)	r	p-value	Lead Time (Days)	r	p-value
1011000	2	0.545	0.000	7	0.272	0.041	2	0.299	0.024
1013500	4	0.399	0.002				3	0.401	0.002
1030500	5	0.402	0.002				7	0.410	0.002
1031500	2	0.709	0.000						
1038000	4	0.631	0.000						
1047000	4	0.612	0.000						
1055000	2	0.519	0.000						
1057000	4	0.644	0.000						
1064500	4	0.617	0.000						
1073000	3	0.774	0.000				2	0.369	0.005
1076500	4	0.543	0.000						
1078000	4	0.618	0.000	7	0.389	0.003	6	0.473	0.000
1119500	7	0.770	0.000	7	0.284	0.032	6	0.372	0.004
1127500	7	0.770	0.000	7	0.244	0.067			
1137500	7	0.479	0.000	4	-0.307	0.020	4	-0.262	0.049
1142500	3	0.570	0.000	6	0.532	0.000	7	0.487	0.000
1144000	7	0.455	0.000	7	0.362	0.006	7	0.348	0.008
1162500	7	0.463	0.000						

Table G.1, continued

Site Number	Precipitation			Maximum Temperature			Minimum Temperature		
	Lead Time (days)	r	p-value	Lead Time (days)	r	p-value	Lead Time (Days)	r	p-value
1169000	5	0.705	0.000	5	0.256	0.055	6	0.243	0.069
1175500	7	0.450	0.000						
1176000	4	0.761	0.000	5	0.284	0.032	3	0.396	0.002
1181000	7	0.773	0.000	6	0.234	0.080	5	0.271	0.042
1188000	7	0.839	0.000				7	0.328	0.013
1193500	6	0.683	0.000						
1196500	7	0.665	0.000						
1318500	2	0.302	0.023						
1321000	2	0.530	0.000				2	0.265	0.046
1334500	2	0.619	0.000						
1350000	2	0.669	0.000						
1365000	2	0.642	0.000	6	0.221	0.099	7	0.226	0.091
1372500	2	0.687	0.000	2	0.306	0.021	7	0.330	0.012
1379500	4	0.615	0.000	7	0.306	0.021	2	0.350	0.008
1381500	7	0.717	0.000						
1387500	2	0.798	0.000	5	0.335	0.011	2	0.342	0.009
1396500	2	0.521	0.000						
1398000	2	0.779	0.000	3	0.323	0.014	2	0.273	0.040
1398500	5	0.833	0.000	3	0.280	0.035	2	0.264	0.047
1399500	5	0.676	0.000				2	0.229	0.087
1408000	4	0.524	0.000						
1408500	3	0.725	0.000				2	0.316	0.017
1410000	7	0.658	0.000	7	0.350	0.008	2	0.428	0.001
1411000	4	0.548	0.000						
1411500	5	0.655	0.000	7	0.236	0.078	4	0.308	0.020
1413500	2	0.590	0.000						
1414500	2	0.538	0.000						
1420500	4	0.654	0.000				2	0.249	0.061
1421000	4	0.633	0.000				2	0.259	0.052
1426500	4	0.518	0.000				2	0.261	0.050
1439500	7	0.799	0.000	2	0.431	0.001	7	0.407	0.002
1440000	2	0.641	0.000						
1445500	6	0.509	0.000						
1459500	7	0.610	0.000	4	0.453	0.000	3	0.433	0.001
1463500	5	0.600	0.000	2	0.410	0.002	3	0.371	0.005
1467000	4	0.615	0.000	7	0.251	0.059	2	0.364	0.005
1503000	4	0.559	0.000	2	0.375	0.004	2	0.396	0.002
1512500	4	0.398	0.002	6	0.282	0.034	4	0.313	0.018
1514000	3	0.449	0.000						
1518000	2	0.768	0.000	7	0.242	0.070	3	0.288	0.030
1520500	3	0.677	0.000				4	0.235	0.079
1531000	4	0.677	0.000	4	0.329	0.013	4	0.351	0.007
1532000	3	0.671	0.000				2	0.229	0.086

Table G.1, continued

Site Number	Precipitation			Maximum Temperature			Minimum Temperature		
	Lead Time (days)	r	p-value	Lead Time (days)	r	p-value	Lead Time (Days)	r	p-value
1534000	2	0.691	0.000	6	0.235	0.078	6	0.285	0.032
1538000	5	0.594	0.000	2	0.343	0.009	2	0.257	0.053
1539000	4	0.734	0.000	2	0.375	0.004	7	0.412	0.001
1541000	3	0.663	0.000	6	0.401	0.002	7	0.412	0.001
1541500	3	0.638	0.000						
1543500	4	0.701	0.000						
1548500	3	0.787	0.000				3	0.238	0.075
1555000	4	0.707	0.000						
1555500	2	0.852	0.000	2	0.241	0.071	3	0.277	0.037
1556000	2	0.653	0.000						
1558000	3	0.780	0.000						
1560000	2	0.630	0.000	2	0.394	0.002	5	0.353	0.007
1564500	2	0.665	0.000						
1567000	3	0.765	0.000				6	0.221	0.099
1568000	3	0.690	0.000				4	0.221	0.098
1574000	5	0.825	0.000	7	0.266	0.046	7	0.337	0.010
1580000	2	0.450	0.000						
1599000	2	0.754	0.000	2	0.279	0.036	2	0.381	0.003
1601500	3	0.292	0.028						
1604500	2	0.662	0.000						
1608500	3	0.779	0.000						
1610000	3	0.776	0.000				4	0.236	0.077
1613000	4	0.651	0.000						
1614500	3	0.770	0.000				5	0.261	0.050
1631000	5	0.877	0.000				2	0.353	0.007
1632000	4	0.720	0.000						
1634000	5	0.761	0.000				2	0.241	0.070
1634500	4	0.652	0.000	4	0.360	0.006	2	0.407	0.002
1645000	2	0.618	0.000	7	0.289	0.029	7	0.328	0.013
1667500	3	0.825	0.000	3	0.344	0.009	2	0.415	0.001
2013000	2	0.702	0.000				6	0.347	0.008
2016000	3	0.793	0.000	2	0.302	0.022	2	0.388	0.003
2017500	2	0.561	0.000						
2018000	2	0.599	0.000						
2035000	7	0.754	0.000	4	0.236	0.077	3	0.332	0.012
3010500	2	0.847	0.000				4	0.226	0.091
3011020	4	0.676	0.000						
3015500	3	0.277	0.037						
3020500	3	0.529	0.000						
3024000	2	-0.246	0.065	2	-0.225	0.092	2	-0.253	0.058
3032500	7	0.713	0.000	7	0.415	0.001	7	0.460	0.000
3034500	2	0.570	0.000	7	0.319	0.016	6	0.336	0.011
3051000	3	0.770	0.000						

Table G.1, continued

Site Number	Precipitation			Maximum Temperature			Minimum Temperature		
	Lead Time (days)	r	p-value	Lead Time (days)	r	p-value	Lead Time (Days)	r	p-value
3069500	2	0.700	0.000	5	0.355	0.007	4	0.420	0.001
3079000	2	0.488	0.000						
3080000	2	0.730	0.000						
3102500	6	0.453	0.000						
3106000	3	0.661	0.000						
3109500	6	0.684	0.000	2	0.331	0.012	2	0.337	0.010
3118500	2	0.631	0.000						
3144000	3	0.766	0.000						
3164000	2	0.718	0.000						
3167000	3	0.491	0.000						
3170000	2	0.672	0.000	7	0.276	0.037	7	0.349	0.008
3173000	2	0.678	0.000						
3175500	2	0.569	0.000						
3182500	2	0.711	0.000						
3183500	3	0.577	0.000						
3186500	2	0.546	0.000	2	0.276	0.037	2	0.297	0.025
3193000	2	0.650	0.000						
3198500	3	0.667	0.000						
3219500	5	0.446	0.001						
3230500	5	0.584	0.000						
3234500	4	0.762	0.000	2	-0.384	0.003	2	-0.380	0.004
3253500	4	0.716	0.000						
3262000	6	0.603	0.000						
3265000	2	0.626	0.000						
3266000	7	0.525	0.000						
3269500	2	0.537	0.000	5	-0.331	0.013	4	-0.337	0.011
3272000	3	0.662	0.000						
3274000	3	0.684	0.000						
3275000	3	0.543	0.000						
3281500	6	0.718	0.000						
3301500	6	0.856	0.000	2	0.276	0.038	2	0.324	0.014
3307000	3	0.781	0.000						
3326500	5	0.537	0.000						
3335500	7	0.517	0.000						
3339500	3	0.693	0.000						
3345500	4	0.737	0.000	3	-0.304	0.022	5	-0.280	0.035
3360500	7	0.792	0.000						
3363500	3	0.735	0.000						
3373500	7	0.451	0.000						
3374000	7	0.502	0.000						
3379500	4	0.746	0.000	7	-0.243	0.068			
3380500	6	0.884	0.000						
3381500	7	0.369	0.005						

Table G.1, continued

Site Number	Precipitation			Maximum Temperature			Minimum Temperature		
	Lead Time (days)	r	p-value	Lead Time (days)	r	p-value	Lead Time (Days)	r	p-value
3434500	3	0.705	0.000				3	0.269	0.043
3438000	2	0.754	0.000						
3612000	5	0.834	0.000						
4056500	3	0.484	0.000						
4073500	2	0.225	0.092				2	0.230	0.085
4079000	7	0.371	0.004						
4087000	7	0.351	0.007						
4100500	2	0.428	0.001						
4105000	4	0.544	0.000				2	0.298	0.025
4112500	6	0.304	0.022						
4191500	4	0.301	0.023						
4193500							7	-0.232	0.083
4214500	4	0.581	0.000						
4223000	5	0.724	0.000						
4234000	3	0.508	0.000						
4262500	2	0.552	0.000	5	-0.230	0.085	2	-0.273	0.040
4269000	6	0.304	0.021						
4275000	3	0.412	0.001						
4287000	2	0.546	0.000						
5291000	3	0.360	0.006						
5293000									
5300000	3	0.239	0.073						
5304500	2	0.245	0.067						
5313500	3	0.399	0.002						
5316500	4	0.373	0.004						
5317000	7	0.278	0.037						
5340500	4	0.332	0.012						
5362000	2	0.264	0.048						
5379500	3	0.240	0.072	3	0.244	0.068	5	0.235	0.078
5399500	3	0.504	0.000						
5408000	2	0.539	0.000						
5412500	3	0.478	0.000						
5414000	4	0.360	0.006	6	0.312	0.018	7	0.286	0.031
5419000	3	0.450	0.000						
5421000	3	0.519	0.000						
5422000	5	0.348	0.008						
5432500	2	0.546	0.000	2	0.388	0.003	2	0.388	0.003
5434500	4	0.392	0.003						
5436500	3	0.312	0.018						
5438500	3	0.280	0.035						
5440000	3	0.322	0.014						
5444000	5	0.500	0.000						
5446500	6	0.387	0.003						

Table G.1, continued

Site Number	Precipitation			Maximum Temperature			Minimum Temperature		
	Lead Time (days)	r	p-value	Lead Time (days)	r	p-value	Lead Time (Days)	r	p-value
5447500	2	0.443	0.001	3	-0.241	0.071	4	0.229	0.086
5451500	4	0.301	0.023						
5454500	2	0.229	0.087						
5455500	4	0.528	0.000						
5459500	2	0.339	0.010						
5464500	7	0.312	0.018						
5465500	2	0.352	0.007						
5470000	4	-0.256	0.055						
5479000	5	0.452	0.000						
5482500	7	0.375	0.004						
5484000	5	0.452	0.000						
5484500	5	0.444	0.001						
5486490	4	0.468	0.000						
5490500	2	0.235	0.079						
5495000	5	0.489	0.000						
5497000	4	0.482	0.000						
5500000	7	0.594	0.000	2	0.235	0.079	3	0.267	0.045
5501000	2	0.647	0.000						
5520500	5	0.262	0.049						
5526000	7	0.344	0.009						
5527500	4	0.418	0.001						
5555300	4	0.425	0.001						
5556500	3	0.469	0.000						
5570000	5	0.429	0.001						
5572000	4	0.664	0.000						
5585000	7	0.624	0.000						
5592500	3	0.791	0.000						
5593000	7	0.699	0.000						
5597000	7	0.694	0.000						
7013000	3	0.713	0.000						
7016500	5	0.820	0.000				4	0.225	0.092
7018500	7	0.763	0.000				5	0.225	0.092
7019000	6	0.817	0.000						

Table G.2
Results of Pearson's correlation analyses between timing of AMF peaks and associated flood generating temperature (minimum and maximum) series with best lead times.

Site Number	Minimum Temperature		Maximum Temperature	
	Lead Time (days)	p-value	Lead Time (days)	p-value
01011000			7	0.000
01013500	3	0.013	7	0.000
01030500	2	0.002	2	0.000
01031500	6	0.000	7	0.000
01038000	5	0.000	6	0.000
01047000	5	0.000	7	0.000
01055000	7	0.000	7	0.000
01057000	6	0.000	5	0.000
01064500	7	0.000	7	0.000
01073000	4	0.000	7	0.000
01076500	7	0.000	7	0.000
01078000	3	0.000	6	0.000
01119500	7	0.000	6	0.000
01127500	5	0.001	7	0.001
01137500	7	0.000	7	0.000
01142500	4	0.000	4	0.000
01144000	5	0.000	5	0.000
01162500	5	0.000	7	0.000
01169000	3	0.000	5	0.000
01175500	2	0.000	3	0.000
01176000	3	0.000	6	0.000
01181000	7	0.000	2	0.000
01188000	6	0.000	5	0.000
01193500	7	0.000	4	0.000
01196500	7	0.000	5	0.000
01318500	7	0.005	7	0.000
01321000	4	0.002	4	0.000
01334500	5	0.000	6	0.000
01350000	2	0.000	3	0.000
01365000	3	0.000	3	0.000
01372500	7	0.000	4	0.000
01379500	2	0.000	3	0.000
01381500	7	0.000	7	0.000
01387500	2	0.000	3	0.000
01396500	7	0.000	3	0.000
01398000	7	0.000	4	0.000
01398500	7	0.000	4	0.000
01399500	7	0.000	7	0.000
01408000	2	0.000	2	0.000

Table G.2, continued

Site Number	Minimum Temperature		Maximum Temperature	
	Lead Time (days)	p-value	Lead Time (days)	p-value
01408500	4	0.000	3	0.000
01410000	3	0.000	3	0.000
01411000	4	0.000	5	0.000
01411500	4	0.000	4	0.000
01413500	7	0.000	3	0.000
01414500	7	0.000	2	0.000
01420500	7	0.000	3	0.000
01421000	7	0.000	3	0.000
01426500	5	0.000	7	0.000
01439500	7	0.000	4	0.000
01440000	2	0.000	3	0.000
01445500	7	0.000	2	0.000
01459500	7	0.000	4	0.000
01463500	2	0.000	4	0.000
01467000	4	0.000	7	0.000
01503000	5	0.000	4	0.000
01512500	4	0.000	5	0.000
01514000	2	0.000	5	0.000
01518000	7	0.009	2	0.024
01520500	7	0.000	7	0.000
01531000	7	0.000	7	0.000
01532000	7	0.000	7	0.000
01534000	2	0.000	7	0.000
01538000	7	0.000	7	0.000
01539000	7	0.000	2	0.000
01541000	2	0.000	2	0.000
01541500	2	0.000	6	0.000
01543500	7	0.000	5	0.000
01548500	7	0.000	7	0.000
01555000	2	0.000	2	0.000
01555500	7	0.000	7	0.000
01556000	2	0.000	7	0.000
01558000	2	0.000	7	0.000
01560000	2	0.000	2	0.000
01564500	6	0.003	2	0.008
01567000	3	0.003	6	0.008
01568000	4	0.000	7	0.000
01574000	5	0.000	7	0.000
01580000	7	0.000	4	0.000
01599000	7	0.000	7	0.000
01601500	5	0.000	7	0.000
01604500	6	0.000	3	0.000

Table G.2, continued

Site Number	Minimum Temperature		Maximum Temperature	
	Lead Time (days)	p-value	Lead Time (days)	p-value
01608500	7	0.000	7	0.000
01610000	7	0.000	7	0.000
01613000	7	0.000	7	0.000
01614500	7	0.002	7	0.008
01631000	2	0.000	5	0.000
01632000	6	0.000	7	0.000
01634000	7	0.000	7	0.000
01634500	4	0.000	7	0.000
01645000	7	0.000	7	0.000
01667500	7	0.000	2	0.000
02013000	2	0.000	2	0.000
02016000	7	0.000	7	0.000
02017500	7	0.000	7	0.000
02018000	7	0.000	5	0.000
02035000	3	0.000	2	0.000
03010500	6	0.000	6	0.000
03011020	2	0.000	5	0.000
03015500	7	0.000	7	0.000
03020500	6	0.000	7	0.000
03024000	2	0.000	7	0.000
03032500	5	0.000	5	0.000
03034500	2	0.000	3	0.000
03051000	2	0.000	3	0.000
03069500	7	0.000	7	0.000
03079000	7	0.000	7	0.000
03080000	7	0.000	7	0.000
03102500	2	0.000	3	0.000
03106000	2	0.000	6	0.000
03109500	2	0.000	6	0.000
03118500	2	0.000	7	0.000
03144000	2	0.000	4	0.000
03164000	2	0.000	3	0.000
03167000	6	0.000	6	0.000
03170000	2	0.000	7	0.000
03173000	7	0.000	5	0.000
03175500	6	0.000	7	0.000
03182500	2	0.001	3	0.000
03183500	5	0.000	5	0.000
03186500	6	0.000	3	0.000
03193000	6	0.000	6	0.000
03198500	7	0.000	7	0.000
03219500	3	0.000	3	0.000

Table G.2, continued

Site Number	Minimum Temperature		Maximum Temperature	
	Lead Time (days)	p-value	Lead Time (days)	p-value
03230500	2	0.000	6	0.000
03234500	3	0.000	3	0.000
03253500	2	0.000	2	0.000
03262000	7	0.000	7	0.000
03265000	7	0.000	3	0.000
03266000	3	0.000	3	0.000
03269500	3	0.000	3	0.000
03272000	2	0.000	2	0.000
03274000	2	0.000	4	0.000
03275000	2	0.000	7	0.000
03281500	3	0.000	5	0.000
03301500	4	0.000	4	0.000
03307000	2	0.000	2	0.000
03326500	2	0.000	2	0.000
03335500	4	0.000	7	0.000
03339500	2	0.000	2	0.000
03345500	2	0.000	2	0.000
03360500	4	0.000	3	0.000
03363500	7	0.000	7	0.000
03373500	3	0.000	7	0.000
03374000	3	0.000	5	0.000
03379500	4	0.000	6	0.000
03380500	5	0.000	6	0.000
03381500	5	0.000	5	0.000
03434500	7	0.000	7	0.000
03438000	7	0.000	2	0.000
03612000	4	0.000	4	0.000
04056500	3	0.045	7	0.008
04073500	6	0.000	6	0.000
04079000	7	0.000	5	0.000
04087000	4	0.000	5	0.000
04100500	6	0.000	7	0.000
04105000	2	0.000	6	0.000
04112500	6	0.000	6	0.000
04121500	7	0.000	7	0.000
04142000	2	0.000	6	0.000
04191500	7	0.000	7	0.000
04193500	2	0.000	7	0.000
04198000	2	0.000	7	0.000
04214500	7	0.000	5	0.000
04223000	7	0.000	7	0.000
04234000	7	0.010	7	0.004

Table G.2, continued

Site Number	Minimum Temperature		Maximum Temperature	
	Lead Time (days)	p-value	Lead Time (days)	p-value
04262500	7	0.054	7	0.000
04269000	7	0.000	7	0.000
04275000	7	0.000	5	0.000
04287000	4	0.000	5	0.000
05280000	7	0.000	7	0.000
05286000	7	0.000	7	0.000
05291000	5	0.000	7	0.000
05293000	4	0.000	7	0.000
05300000	7	0.000	7	0.000
05304500	7	0.000	7	0.000
05313500	7	0.000	6	0.000
05316500	7	0.000	7	0.000
05317000	5	0.000	7	0.000
05340500	4	0.000	7	0.000
05362000	3	0.000	4	0.000
05379500	6	0.000	7	0.000
05394500	4	0.000	7	0.000
05399500	3	0.000	4	0.000
05408000	4	0.000	7	0.000
05412500	2	0.000	2	0.000
05414000	7	0.000	7	0.000
05418500	3	0.000	5	0.000
05419000	3	0.000	3	0.000
05421000	6	0.000	6	0.000
05422000	7	0.000	7	0.000
05426000	7	0.000	7	0.000
05430500	7	0.000	7	0.000
05432500	3	0.000	4	0.000
05434500	7	0.000	7	0.000
05435500	5	0.000	7	0.000
05436500	2	0.000	2	0.000
05438500	7	0.000	7	0.000
05440000	7	0.000	7	0.000
05444000	7	0.000	7	0.000
05446500	7	0.000	2	0.000
05447500	7	0.000	7	0.000
05451500	7	0.000	7	0.000
05454500	7	0.000	7	0.000
05455500	7	0.000	2	0.000
05459500	4	0.000	4	0.000
05464500	6	0.000	7	0.000
05465500	7	0.000	6	0.000

Table G.2, continued

Site Number	Minimum Temperature		Maximum Temperature	
	Lead Time (days)	p-value	Lead Time (days)	p-value
05470000				
05474000	5	0.000	6	0.000
05476000	7	0.000	7	0.000
05479000	6	0.000	6	0.000
05482500	4	0.000	7	0.000
05484000	2	0.000	5	0.000
05484500	7	0.000	7	0.000
05486490	4	0.000	6	0.000
05490500	7	0.000	6	0.000
05495000	4	0.000	5	0.000
05497000	2	0.000	5	0.000
05500000	3	0.000	4	0.000
05501000	3	0.000	4	0.000
05520500	7	0.000	7	0.000
05526000	3	0.000	2	0.000
05527500	6	0.000	7	0.000
05555300	5	0.000	6	0.000
05556500	7	0.000	7	0.000
05570000	6	0.000	6	0.000
05572000	5	0.000	6	0.000
05585000	7	0.000	7	0.000
05592500	2	0.000	2	0.000
05593000	5	0.000	5	0.000
05597000	7	0.000	3	0.000
07013000	6	0.000	7	0.000
07016500	2	0.000	2	0.000
07018500	2	0.000	2	0.000
07019000	3	0.000	2	0.000